IAEA-TECDOC-1448

Use of isotope techniques to trace the origin of acidic fluids in geothermal systems

IAEA
International Atomic Energy Agency

April 2005

IAEA-TECDOC-1448

Use of isotope techniques to trace the origin of acidic fluids in geothermal systems

IAEA
International Atomic Energy Agency

April 2005

The originating Section of this publication in the IAEA was:

Isotope Hydrology Section
International Atomic Energy Agency
Wagramer Strasse 5
P.O. Box 100
A-1400 Vienna, Austria

USE OF ISOTOPE TECHNIQUES TO TRACE THE ORIGIN OF
ACIDIC FLUIDS IN GEOTHERMAL SYSTEMS
IAEA, VIENNA, 2005
IAEA-TECDOC-1448
ISBN 92–0–102805–9
ISSN 1011–4289

Printed by the IAEA in Austria
April 2005

FOREWORD

Geothermal energy is an indigenous source of energy and, if used properly, also a renewable one. Many IAEA Member States are currently using these resources either for electric power generation or for direct use of the heat. However, geothermal development involves high risks due to its geological uncertainty, intensive drilling investment and other technical difficulties.

Natural waters with pH values lower than 5 found in geothermal areas are called 'acidic fluids'. The presence of these fluids constrains the development of geothermal resources in many geothermal systems around the globe. Acid wells are either plugged or abandoned. Limited understanding of their origin prevents effective management of many high temperature geothermal reservoirs.

This issue was identified as a major problem encountered in geothermal development and management during an advisory group meeting organized by the IAEA and held in Vienna from 29 May to 1 June 1995. At that meeting, the state of the art on this subject was reviewed and research needs identified by a group of 19 experts from 13 Member States. It was suggested that a research project be supported by the IAEA to promote the application of isotope techniques, in particular, isotopes of sulphur compounds, to study the origin of acidic fluids in geothermal reservoirs.

Based on the recommendations of the meeting, the IAEA implemented a Coordinated Research Project (CRP) on The Use of Isotope Techniques in Problems Associated with Geothermal Exploitation (1997–2000). Research groups from China, Indonesia, Italy, Japan, Mexico, the Philippines, the Russian Federation, Turkey and the United States of America participated in and contributed to the project. The current publication is a compilation of final reports on ten individual studies carried out under the CRP.

The IAEA would like to thank A. Truesdell and H. Ferrer for reviewing the manuscripts. The IAEA officer responsible for this publication was Zhonghe Pang of the Division of Physical and Chemical Sciences.

EDITORIAL NOTE

The papers in these proceedings are reproduced as submitted by the authors and have not undergone rigorous editorial review by the IAEA.

The views expressed do not necessarily reflect those of the IAEA, the governments of the nominating Member States or the nominating organizations.

The use of particular designations of countries or territories does not imply any judgement by the publisher, the IAEA, as to the legal status of such countries or territories, of their authorities and institutions or of the delimitation of their boundaries.

The mention of names of specific companies or products (whether or not indicated as registered) does not imply any intention to infringe proprietary rights, nor should it be construed as an endorsement or recommendation on the part of the IAEA.

The authors are responsible for having obtained the necessary permission for the IAEA to reproduce, translate or use material from sources already protected by copyrights.

CONTENTS

SUMMARY OF THE COORDINATED RESEARCH PROJECT

Background and objectives

Natural waters with pH values lower than 5 found in geothermal areas are called 'acidic fluids'. These fluids occur in geothermal well discharges, especially in geothermal areas associated with recent volcanism such as the geothermal areas in Central America, Japan and the Philippines. Acidic fluids cause serious damage to production wells. Their origin needs to be understood in order to design appropriate preventive or treatment measures.

Previous research has mainly aimed at determination of geological occurrence and chemical characterization of acidic fluids. Two major types of acidity had been identified, sulphate acidity and HCl acidity. The former was believed to be the result of oxidation of H_2S or SO_2 from a deep source to SO_4. The latter was hypothesed as resulting from the reaction of feldspar with superheated steam.

Realizing the potential contribution of stable isotopes of the water molecule and those of sulphur compounds in tracing the sources of acidic fluids, especially the sulphate type of acidity in geothermal well discharges, the IAEA organized a Coordinated Research Project (CRP) with the objectives of integrating isotope techniques, in particular the isotopes of sulphur compounds, into:

(1) identification of the origin of the water component in acidic fluids;
(2) identification of the origin of sulphur compounds in acidic fluids and;
(3) study on mixing of waters from different sources to form acidic fluids.

In addition to these objectives, the CRP was also to test isotope geothermometry based on sulphur compounds in geothermal fluids.

Ten research groups from China, Indonesia, Italy, Japan, Mexico, the Philippines, the Russian Federation, Turkey and the United States of America participated in the CRP and carried out field and laboratory investigations on twenty geothermal fields. Samples of geothermal waters, gases and minerals were collected and analyzed for the following isotopes: $\delta^{18}O$, $\delta^{2}H$, ^{3}H of water, $\delta^{34}S$ in H_2S gas, $\delta^{34}S$ in aqueous sulphate (SO_4), $\delta^{18}O$ in aqueous sulphate (SO_4), $\delta^{34}S$ in anhydrite and pyrite and $\delta^{18}O$ in anhydrite as required by the individual research projects.

Table I provides an overview of geothermal fields investigated, main technical issues involved and isotope methodologies used and major findings of the project. Results of the research can be summarized as follows.

Origin of water in acidic fluids

In this CRP, isotopic composition of oxygen-18 and deuterium in waters sampled from acidic wells indicates that these waters are mixtures of meteoric and magmatic waters. Examples of this type of geothermal systems are Miravalles in Costa Rica, Onikobe in Japan, Los Humeros in Mexico and Several fields in the Philippines. It has further shown that acidic fluids are isotopically heavier in some systems, implying a larger fraction of magmatic inputs. This isotopic evidence confirms the hypothesis that some acidic fluids are un-neutralized magmatic water.

Origin of sulphur compounds in acidic fluids

There are three possible origins for the aqueous sulphate in geothermal well discharges of a volcanic geothermal system:

a. oxidation of H_2S gas similar to that producing acidic hot springs and ponds at the surface,
b. hydrolysis of magmatic SO_2 gas,
c. hydrolysis of native sulphur at shallow depth.

$\delta^{34}S$ in aqueous sulphate (SO_4) formed by the first process is close to 0 ‰ VCDT, similar to those found in surface thermal manifestations. However, $\delta^{34}S$ (SO_4) is enriched (up to 30‰ VCDT) in acidic well discharges. Isotopically enriched fluids are found to be also higher in SO_4 concentration, such as those in Kyushu, Japan. This $\delta^{34}S$ (SO_4) enrichment has been interpreted by different authors as either from hydrolysis of native sulphur at a shallow depth or as hydrolysis of deep magmatic SO_2. If there were additional evidence on the origin of the water component in the respective well discharges, it would have been possible to distinguish the two origins.

Some studies in this CRP report data of $\delta^{34}S$ in H_2S and in SO_4 samples from both acidic and neutral wells of the same geothermal field. In neutral wells, they are identical, with $\delta^{34}S$ values in the range of ±5 ‰ deviation from 0 ‰ VCDT that was accepted for un-altered magmatic H_2S. In acidic wells, fractionation of ^{34}S between H_2S and SO_4 has been recognized. Furthermore, there is a negative correlation between pH of water and $\delta^{34}S$ (H_2S) but positive correlation with that in SO_4, implying an isotope exchange between the two.

Application of geothermometers based on isotopes in sulphur compounds

Isotope geothermometry based on $\delta^{34}S$ (H_2S) provides estimates of reservoir temperatures that are compatible to measured temperature values for the acidic wells, but not for neutral pH wells. This suggests that fractionation equilibrium is more easily attained in acidic wells as compared to neutral pH wells.

Isotope geothermometer based on $\delta^{18}O$ in water and aqueous sulphate was found to be generally not applicable to low temperature (<100ºC) formation waters in sedimentary basins, but gave agreeable results for saline thermal waters of marine origin at reservoir temperature of 150ºC.

Future research needs

Results of the CRP have improved the understanding of acidic fluids in terms of the origin of water and sulphur compounds in the fluids. Existing theories have been tested including geothermometry methodologies. However, isotope data collected for sulphur compounds are still rather limited. Extended sampling and measurements on isotopes will further verify the findings of this project. Research on gaseous tracers, such as carbon gases and noble gases in geothermal systems, will increase the knowledge on the origin of geothermal fluids in general.

Table I. Overview of research carried out in the geothermal fields under the coordinated research project on acidic fluids in geothermal reservoirs

Principal investigator	**Name of geothermal field**	**Technical issues**	**Isotopes or other tools used**	**Main findings and conclusions**
Pang, Z. (China)	Thermal waters of Southern Fujian and Eastern Hebei Provinces, China	Origin of thermal water and aqueous sulphate, applicability of aqueous sulphate oxygen isotope geothermometry	$\delta^{18}O$, $\delta\ ^{2}H$, $\delta\ ^{34}S\ (SO_4)$, $\delta^{18}O\ (SO_4)$	In Southern Fujian, thermal water is a mixture of meteoric water and seawater and the sulphate is marine origin. In Eastern Hebei, aqueous sulphate is non-marine in origin. Isotope geothermometry temperature estimates are compatible to reference temperatures in the former case but not in the latter.
Zhou, W. (China)	Los Azufres, Mexico	Chemistry of Water Rock interactions in an active geothermal system	Water and rock chemistry, reaction experiments, numerical modelling	Water-rock interactions in the geothermal field have two stages producing different assemblages of secondary minerals. Acidic fluids may be produced by oxidation of H_2S gas.
Abidin, Z. (Indonesia)	Sibayak, Sumatra, Indonesia	Origin of geothermal water, possible linkage to a nearby volcano	$\delta^{18}O$, $\delta\ ^{2}H$, $\delta^{34}S(H_2S)$, $\delta\ ^{34}S\ (H_2S)$, $\delta\ ^{34}S\ (SO_4)$, $\delta^{18}O\ (SO_4)$	The system doesn't seem to gain magmatic inputs of the nearby Sibayak volcano.
Panichi, C. (Italy)	Miravalles, Costa Rica	Origin of acidic fluids in production wells	$\delta^{18}O$, $\delta\ ^{2}H$	Acidic fluids found in production wells may originate from inflow of immature volcanic waters or oxidation of H_2S near the surface.
Matsuda, K. (Japan)	Hatchobaru, Takigami, Shiramizugoe, and yamagawa, Kyushu, Japan	Origin of acidic fluids in production wells	$\delta\ ^{34}S\ (H_2S)$, $\delta\ ^{34}S\ (SO_4)$, $\delta^{18}O\ (SO_4)$	Origin of acidic fluids in the production wells is from shallow low temperature SO_4-rich waters.
Tello, E. (Mexico)	Los Humeros, Mexico	Origin of HCl acidity	$\delta^{18}O$, $\delta\ ^{2}H$, Tritium	High HCl in the steam phase is produced by reactions between NaCl and Rock minerals.
Bayon, B. (Philippines)	Mt. Apo, Bacman, Mahanagdong, Palinpino, Philippines	Origin of acidic fluids in production wells and isotope geothermometry	$\delta^{18}O$, $\delta^{34}S(H_2S)$, $\delta\ ^{34}S\ (SO_4)$, $\delta^{18}O\ (SO_4)$, $\delta\ ^{34}S$ (Anhydrite), $\delta^{34}S$(Pyrite), $\delta^{18}O$ (Anhydrite)	H_2S in acid wells is magmatic origin. Isotopically light acid sulphate waters are formed by oxidation of H_2S at shallower depth, heavier ones reflect equilibrium with H_2S in the reservoir or deeper hotter environment. Aqueous sulphate isotope geothermometry gives similar temperature estimates to measured ones in lower pH environments but not in neutral pH environments.

Principal investigator	Name of geothermal field	Technical issues	Isotopes or other tools used	Main findings and conclusions
Karpov, G.	Karymsky, Kamchatka, Russia	Origin of salinity and acidity in a caldera lake	$\delta^{18}O$, $\delta D^{2}H$	Water is meteoric. Acidity comes from oxidation of sulphur compounds (H_2S) and halides (HF and HCl) from magmatic degassing.
Simsek, S. (Turkey)	Denizli-Kizildere, Aydin-Germencik, Afyon and Soeke, Turkey	Origin of water and reservoir temperatures of geothermal fields	$\delta^{18}O$, $\delta^{2}H$, ^{3}H	Water from the four areas is meteoric in origin. Deep temperatures are in the ranges of 230-260 °C for Kizidere and Germenick areas but <110 °C for the other two fields.
Truesdell, A. (USA)	Onikobe, Honshu, Japan	Origin of acidic fluids in production wells	$\delta^{18}O$, $\delta^{2}H$	Acidic fluids have two origins: one is shallow oxidation of H_2S, the other HCl formed by superheated steam at depth. They are located in certain areas of the field and can be avoided by selecting drilling sites.

ORIGIN OF SULPHUR COMPOUNDS AND APPLICATION OF ISOTOPE GEOTHERMOMETRY IN SELECTED GEOTHERMAL SYSTEMS OF CHINA

Zhonghe Pang[*]

Institute of Geology and Geophysics,
Chinese Academy of Sciences,
Beijing,
China

Abstract. Geothermal and groundwater samples from East of Hebei (EH) Province in the North China Basin and South of Fujian (SF) Province in Southeast of China were studied using sulphur and water isotopes. EH is located in a Mesozoic-Cenozoic sedimentary basin while SF is composed of small fault-block basins formed in Quaternary period. These systems belong to non-volcanic geothermal environments. Samples were collected from exploratory and production geothermal wells: 11 wells in EH and 17 wells in SF. The samples were analyzed for oxygen-18 ($\delta^{18}O$) and deuterium ($\delta^{2}H$) in water, sulfur-34 ($\delta^{34}S$) and oxygen-18 ($\delta^{18}O$) in aqueous sulphate (SO_4). Chemical composition of the water samples was also determined. Results show that aqueous sulphate in the saline thermal waters of SF is of marine origin. The aqueous sulphate in EH waters is of non-marine origin. Reservoir temperature estimated using the oxygen isotope geothermometer is not compatible to those by chemical geothermometers or by down-hole measurements in the sedimentary environment for EH, different from that for the SF samples where aqueous sulphate seems to have reached equilibrium with thermal waters in the main up-flow zone.

1. Introduction

Origin of water and solute is an important issue in geothermal development. Stable isotopes of water and dissolved sulphur compounds have found application in geothermal studies in term of source identification and isotope geothermometry [1]. Lloyd [2], Mizutani and Rafter [3] measured the equilibrium fractionation factors of the oxygen isotope exchange reaction between aqueous sulphate and water, which laid the foundation for isotope geothermometry based on the SO_4-H_2O pair.

The two equations they have calibrated are as follows:

$$1000\ln\alpha = 3.251 \times 10^6/(T^2) - 5.6 \qquad (1)$$
$$1000\ln\alpha = 2.88 \times 10^6/(T^2) - 4.1 \qquad (2)$$

The applicable temperature ranges given in their papers are 0–500°C and 110–200°C for the two equations, respectively. In the overlapping temperature range, the difference between the two equations is less than 10°C.

Oxygen isotope geothermometry based on the SO_4-H_2O pair is considered as one of the most reliable isotope geothermometry methods [4] and has been used in the investigation of geothermal fields in many countries such as Greece [5], Italy [6], Japan [6], New Zealand [1], and USA [8]. This geothermometry method is used especially when chemical geothermometers are hampered by unfavorable water chemistry.

However, its applicability to non-volcanic, low to intermediate temperature geothermal areas has so far not been sufficiently understood.

[*] Present address: Isotope Hydrology Section, International Atomic Energy Agency, P. O. Box 100, Wagramer-strasse 5, A–1400, Vienna, Austria, e-mail: z.pang@iaea.org.

This study attempts to apply stable isotopes of water and aqueous sulphate in geothermal waters in the above temperature range and geological environments. The focus of this study is on sulphur isotopic signatures and source of sulphur compounds, oxygen isotope geothermometry based on SO_4-H_2O equilibrium fractionation.

Two areas were selected for this study: East of Hebei and South of Fujian Provinces. Each of the two geothermal areas is representative of systems found in low to medium temperature ranges (<150°C), not related to recent volcanic activities, that are widely found in large sedimentary basins and in fault basins in crystalline rocks in China and other parts of the world.

2. Sampling and analyses

Samples collected from SF area included geothermal wells in the central part of the Zhangzhou geothermal field (ZGF) (t >90°C) which represent water coming directly from the deep geothermal reservoir; geothermal wells in the outer part (90 >t >30°C) of the geothermal field and in the shallow geothermal aquifer which may involve mixing with cold water (Figure 1a). Samples from groundwater wells were also collected for the purpose of comparison (t<30°C). Xinlin (XL) Bay hot spring (Sample 17), and Shitou (ST) Village hot spring (Sample 16) were sampled. They are geologically similar to Zhangzhou geothermal system but located closer to the sea. Quepu hot spring (Sample 15) discharges dilute water in the eastern area but obviously without seawater involvement (Table I).

Thermal and non-thermal waters were collected from different formations in EH area (Figure 1b). The sample sites include shallow wells for domestic drinking water supply, oil production wells and two oil exploration wells now used for supplying hot water. The results have enabled us to establish a reference column for the chemistry of different formations in both age and depth sequences (Table II).

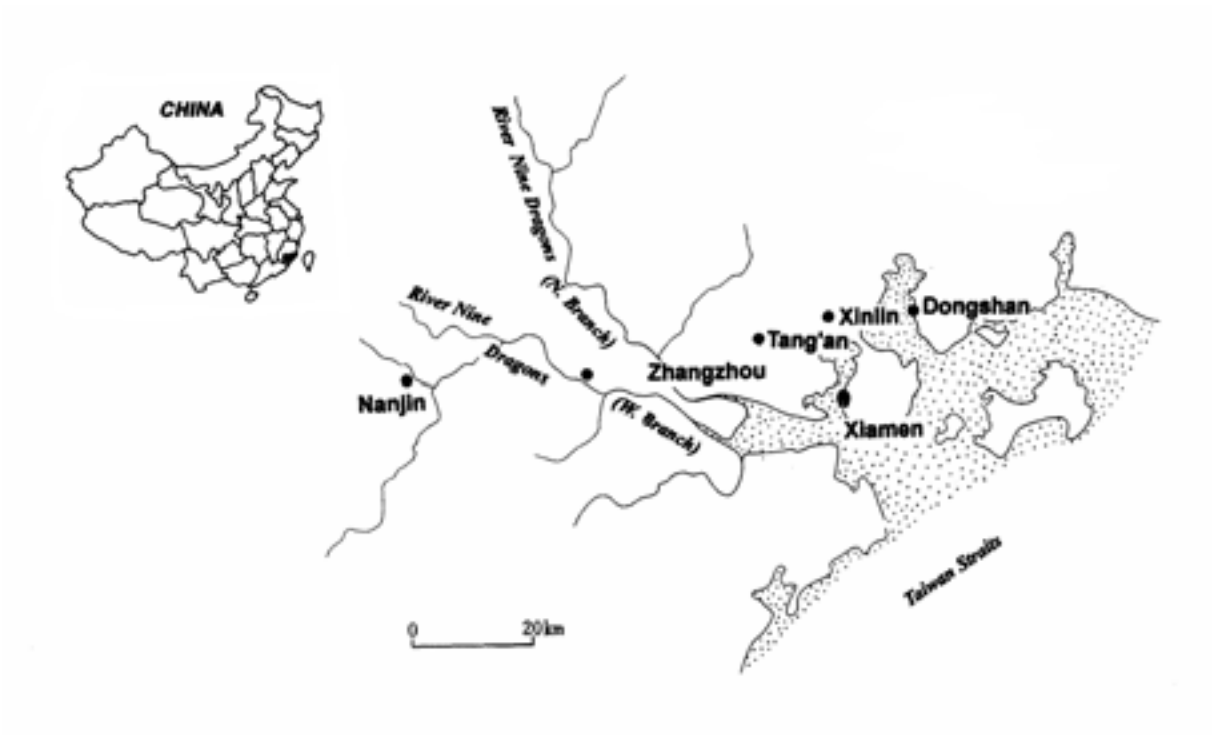

Figure 1a. Location of sampling sites in the South of Fujian Province, Southeast of China.

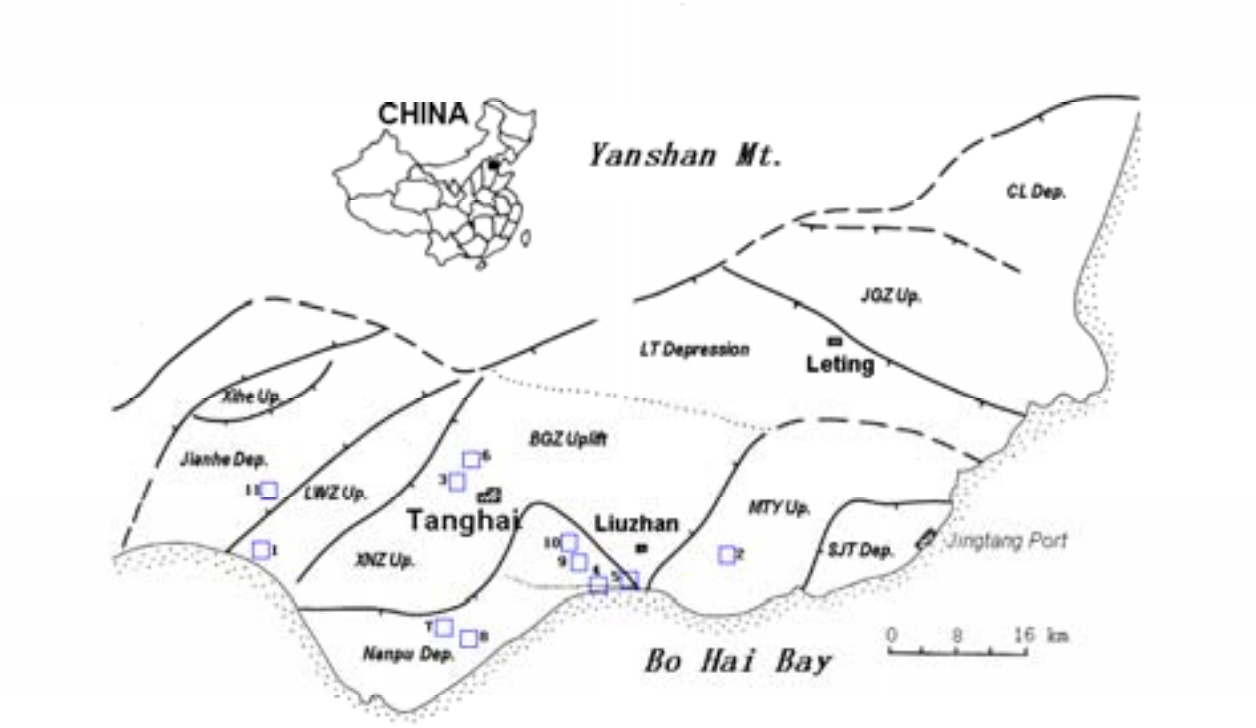

Figure 1b. Location of sampling sites in the East of Hebei Province, North China Basin.

The samples were analyzed for deuterium (δ^2H) and oxygen-18 ($\delta^{18}O$) in water, sulfur-34 ($\delta^{34}S$) and oxygen-18 ($\delta^{18}O$) in dissolved sulphate (SO_4). Measurements of the isotopes on S. Fujian samples were made at the Laboratory for Isotope Hydrology and Geochemistry, University of Paris in Orsay. The rest of the measures, including chemical and isotope compositions of the waters were carried out in the Institute of Geology and Geophysics, Chinese Academy of Sciences (IGG-CAS) in Beijing. The cations were analyzed using ICP-MS. Ion chromatography and titration methods were used for the analysis of anions. Samples from oil production wells went through filtration to remove the oil before analysis.

The remaining samples from East of Hebei Province were measured at the Institute of Geology and Geophysics, Chinese Academy of Sciences in Beijing.

Aqueous sulfate was extracted by precipitating it as $BaSO_4$ from the water after acidification. The precipitate was then reacted with graphite to produce CO_2, the $\delta^{18}O$ of which was then measured on the mass spectrometer. SO_2 was prepared by oxidizing BaS and then $\delta^{34}S$ was measured on the mass spectrometer.

3. Origin of water and aqueous sulphate

3.1. South of Fujian Province

Zhangzhou geothermal field (ZGF) is formed in a Quaternary fault basin (~ 500 km^2) by deep circulation of ground water in the Mesozoic granite basement. It has the record of the highest temperature ever measured in southeast of China (114°C at the well-head and 122°C at a depth of 90 meters from surface). The occurrence of geothermal waters in the basin is controlled by the major fracture systems. The thermal water from the system is saline with total dissolved solids of 12 g/l [9].

Table I. Chemical composition of geothermal waters from South of Fujian Province, China

Code	Site Name	Sample Type	Rock type	T_s (°C)	pH	SiO_2	Na	K	Mg	Ca	Li (mg/L)	Al	Fe	Cl	SO_4	HCO_3	TDS (g/L)	Chem. type
1	V05Q	GTB	Q, sand	28	7.4	62.5	170.2	28.7	3	110.8	0.3	0.136	2.567	215	48.5	293.7	0.79	Na-Ca-Cl-HCO3
2	V02Q	GTB	Q, sand	40	7.9	54.7	711.7	42.9	5.2	341.8	0.982	0.214	6.367	1526	65.2	275.2	2.89	Ca-Cl
3	Gongliao	GTB	Q, sand	62	7.5	106.3	1784.8	91.8	8.1	1022.4	2.17	0.315	0.717	4466	135	115.6	7.67	Na-Ca-Cl
4	ZR2	GTB	Granite	26	7.3	22.7	1057.6	14.2	32.3	927.2	0.735	0.247	1.739	3008	150	15	5.22	Ca-Na-Cl
5	ZR34	GTB	Granite	26	7.2	21	655.9	21.3	28.1	124.6	0.015	0.136	9.35	1272	19.9	34.7	2.16	Na-Cl
6	ZR12	GTB	Granite	30	7.2	39.1	2086.4	48.1	11	740.9	3.377	0.253	2.723	4682	120	26.6	7.74	Na-Ca-Cl
7	V05G	GTB	Granite	31	6.8	22.7	2287.4	83.4	15.6	1210.4	2.893	0.3	2.98	5368	121	11.6	9.11	Na-Ca-Cl
8	ZR26	GTB	Granite	40	6.9	45.1	1845.6	48.6	6.1	1272	1.614	0.3	1.419	5500	123	21.8	8.85	Na-Ca-Cl
9	ZR35	GTB	Granite	41	7.1	85.9	2323.2	104	5.4	1208	3.334	0.281	7.472	5463	165	42.8	9.38	Na-Ca-Cl
10	ZR16	GTB	Granite	41	7	88.3	2172	93.6	3.6	1097.6	2.792	0.283	7.99	5275	198	34.7	8.95	Na-Ca-Cl
11	ZR17	GTB	Granite	47	6.8	37.1	2140	57.7	17.7	1242.4	2.192	0.296	1.609	5369	182	13.9	9.05	Na-Ca-Cl
12	V02G	GTB	Granite	62	7.3	96.1	2161.6	83.8	4.5	984.8	3.026	0.35	7.117	4688	181	52	8.23	Na-Ca-Cl
13	V04	GTB	Granite	93	7.2	131.9	2480	105	3.2	1390.4	3.373	0.315	0.507	5744	199	41.6	10.07	Na-Ca-Cl
14	S044	GTB	Granite	97	7.1	121.9	2401.6	115	3.3	1251.2	3.517	0.293	0.495	5775	200	42.8	9.89	Na-Ca-Cl
15	Quepu	GTB	Granite	57	7.6	36.7	460.6	12	0.3	102.1	0.326	0.12	0.018	747	70.1	38.2	1.45	Na-Ca-Cl
16	Shitou	GTH	Granite	52	7.3	52.7	7062.4	174	337	2293.6	3.605	0.436	10.82	14200	1203.9	219.7	25.43	Na-Ca-Cl
17	Xinlin	GTH	Granite	80	7.4	100	3387.6	97.8	99.3	1375.2	1.991	0.355	0.55	7971	578	71.7	13.65	Na-Ca-Cl

Note: Ts = sampling temperature;
GWB = Groundwater borehole; GTB = Geothermal borehole;

Table II. Chemical composition of geothermal waters in East of Hebei Province, China

Code	Site name	Sample type	Formation	Depth (m)	T_s (°C)	T_f (°C)	pH	SiO_2	Na	K	Mg	Ca	Li	Al	Fe	Cl	SO_4	HCO_3 (mg/L)	Water chem type
1	TN-2	GWB	Nm, sand	383	22	25	7.9	17.46	145	0.25	0.62	6.10	0.007	0.027	0.03	28.8	85.44	248.1	Na-Cl-HCO3
2	XG-3	GWB	Nm, sand	500	22	25	7.5	15.21	109	0.25	0.25	5.70	0.005	0.116	0.05	19.6	66.90	205.0	Na-HCO3-Cl
3	QY-1	GWB	Nm, sand	350	25	30	7.4	16.92	238	0.42	1.24	7.12	0.015	0.042	0.01	81.5	120.05	375.4	Ca-Na-SO4
4	N34x1	GTB	Ng, sand	1128	52	55	7.2	29.49	252	3.74	2.10	20.95	0.060	0.044	0.07	92.2	336.23	183.0	Na-HCO3
5	L21x10	GTB	Nm, sand	1816	70	79	7.3	54.01	338	3.98	1.61	3.05	0.043	0.019	0	196.0	6.69	555.6	Na-HCO3-Cl
6	L25x13	OPW	Ng, sand	1994	75	88	7.2	51.70	366	4.73	0.99	3.05	0.078	0.039	0.18	163.7	4.83	686.3	Na-HCO3-Cl
7	M2-3	OPW	Ed, sand	2700	80	88	6.8	50.92	442	7.97	1.85	8.14	0.619	0.014	0	325.2	0.00	649.4	Na-HCO3-Cl
8	M16x1	OPW	Ed, sand	2872	85	94	6.9	71.37	1289	17.93	2.72	11.80	0.619	0.014	0	345.9	0.00	2838.6	Na-SO4-HCO3-Cl
9	L20x2	OPW	Es, sand	3400	95	116	7.1	113.81	516	17.93	20.02	71.19	1.170	0.078	0.22	547.7	171.38	548.2	Na-SO4-HCO3-Cl
10	L90x2	OPW	Es, sand	3057	96	110	8.2	78.32	382	7.72	3.09	7.12	0.282	0.136	0.53	149.9	114.84	661.8	Na-HCO3-SO4
11	HC-1	GTB	O, limestone	3075	96	112	7.1	83.05	246	112.07	19.16	220.69	3.827	0.106	0.18	140.7	809.73	296.9	Na-HCO3-SO4

Note: Ts = sampling temperature; Tf = measured formation temperature;
GWB = Groundwater borehole; GTB = Geothermal borehole; OPW = Oil production well.

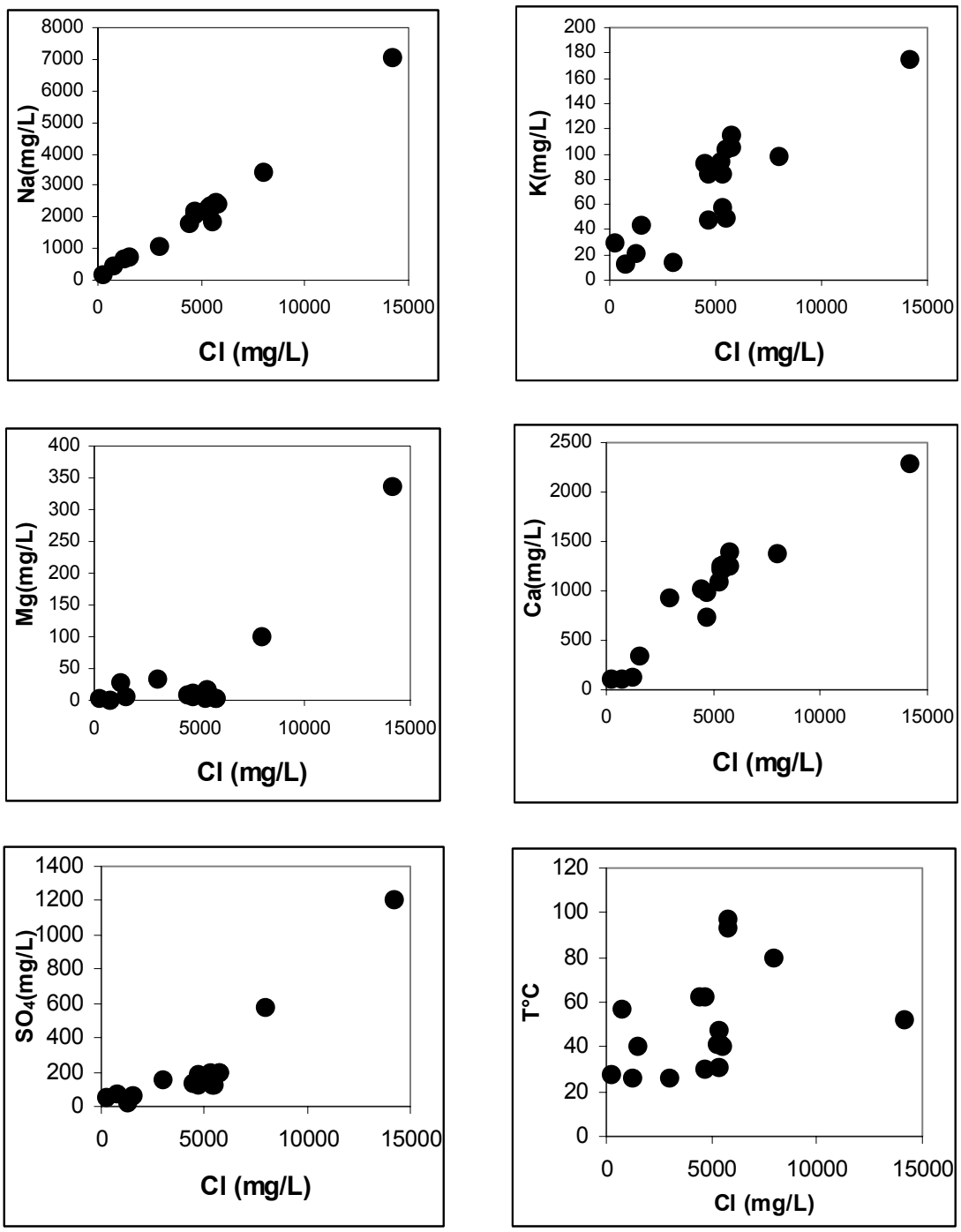

Figure 2. Correlation of Chloride with SO_4 and temperature-dependent cations in Zhangzhou geothermal field and its surroundings.

Figure 2 shows the correlations of Cl with cations and other anions, pointing to a mixing with seawater. The correlation of Cl with temperature differs from one system to another. Isotopic composition of the thermal waters, as shown in Figure 3 and Table III, confirms the seawater involvement. Thermal waters approximate to but plot slightly away from the global meteoric water line on a $\delta^{2}H$ versus $\delta^{18}O$ diagram. A linear correlation between $\delta^{2}H$ and Cl^- or $\delta^{18}O$ and Cl^- indicates that the thermal water is a mixture of meteoric and sea water.

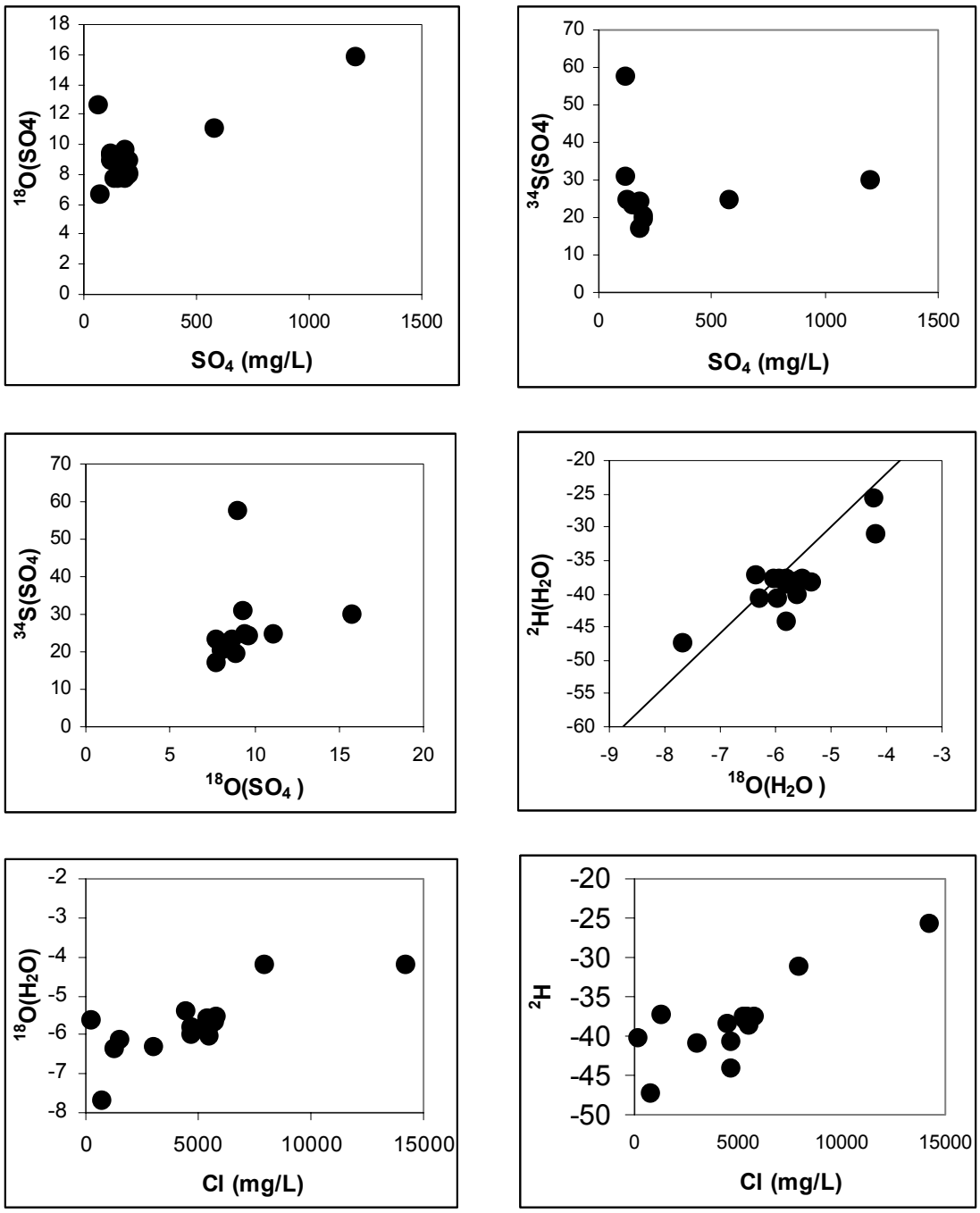

Figure 3. Correlation of Chloride and SO_4 with isotopes and isotope cross plotsfor samples from Zhangzhou geothermal field and its surrounding areas.

Also in Figure 3, the $\delta\ ^{34}S$ values of most of the samples are quite consistent with increase SO_4 concentration, between 20–30, with one exception of a very high value for sample 6 (ZR12), which might have been affected by shallow processes.

Table III. Isotope composition of water and dissolved sulphate in South of Fujian Province, China

Code	Site Name	Sample Type	Rock type	T_s (°C)	$\delta^{18}O(SO_4)$ (‰VSMOW)	$\delta^{34}S(SO_4)$ (‰VCDT)	$\delta^{18}O(H_2O)$ (‰VSMOW)	$\delta^{2}H(H_2O)$ (‰VSMOW)
1	V05Q	GTB	Q, sand	28			-5.60	-40.2
2	V02Q	GTB	Q, sand	40	12.60		-6.11	
3	Gongliao	GTB	Q, sand	62	7.70		-5.37	-38.3
4	ZR2	GTB	Granite	26	7.70	23.1	-6.29	-40.8
5	ZR34	GTB	Granite	26			-6.37	-37.2
6	ZR12	GTB	Granite	30	9.00	57.6	-5.80	-44.2
7	V05G	GTB	Granite	31	9.30	31.0	-5.95	-37.6
8	ZR26	GTB	Granite	40	9.40	24.7	-5.80	-38.6
9	ZR35	GTB	Granite	41	8.70	23.3	-6.02	-37.6
10	ZR16	GTB	Granite	41	8.10		-5.80	-37.6
11	ZR17	GTB	Granite	47	9.60	24.3	-5.57	-38.0
12	V02G	GTB	Granite	62	7.70	17.3	-5.97	-40.7
13	V04	GTB	Granite	93	8.00	20.6	-5.68	
14	S044	GTB	Granite	97	8.90	19.5	-5.53	-37.6
15	Quepu	GTB	Granite	57	6.70		-7.67	-47.3
16	Shitou	GTH	Granite	52	15.80	29.8	-4.22	-25.6
17	Xinlin	GTH	Granite	80	11.10	25.0	-4.19	-31.1

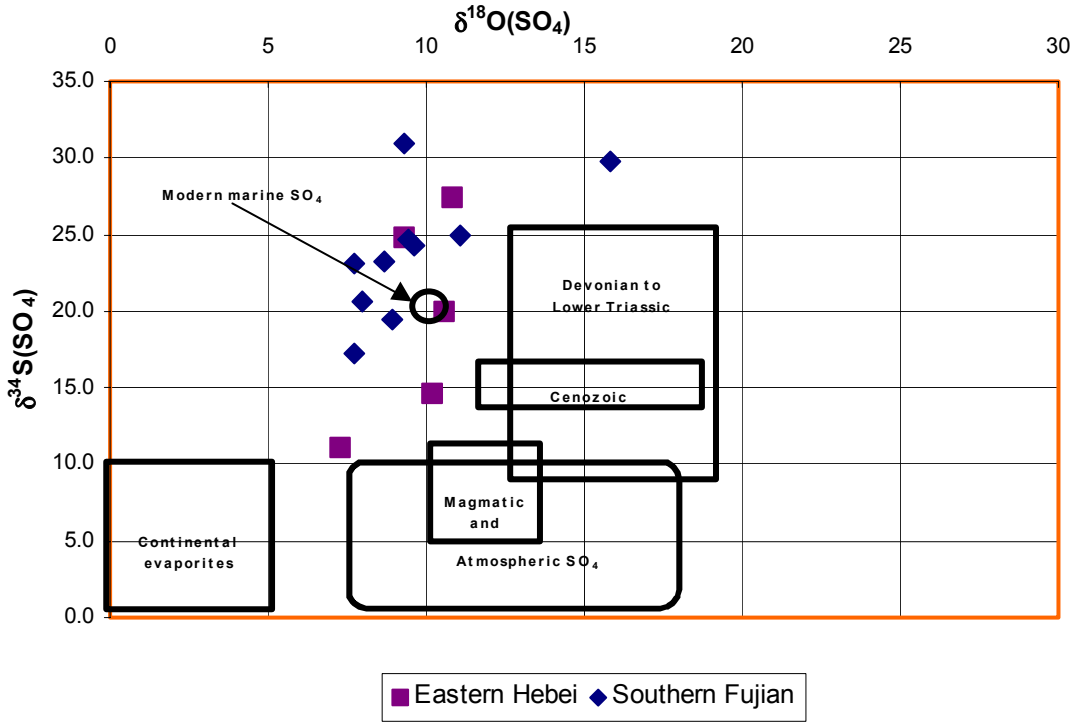

Figure 4. Sulphur isotope composition and origin of sulphur in Eastern Hebei and Zhangzhou geothermal systems as compared to other systems.

The isotope composition of marine sulfate, $\delta\ ^{34}S$ = +20‰, $\delta\ ^{18}O$ = +9.5‰ SMOW [10] has been constant for several million years [11]. If the SO_4 in the geothermal waters for this study is of a marine origin, but the original S-isotopic composition has been modified by processes such as: 1, mixing; 2, precipitation of sulfate minerals (mainly gypsum and anhydrite); 3, reduction from sulfate to sulfide and, for ^{18}O alone, 4, O-isotope exchange between SO_4 and water.

Despite of all these processes, exchange of ^{18}O between water and aqueous sulphate seems to have reached equilibrium in the system.

Figure 4 confirms the marine origin of sulphur in this area. Data for the Eastern of Hebei are also plotted in this diagram but will be discussed later.

3.2. Easter Hebei Province

North China Basin is a Mesozoic-Cenozoic basin rich in geothermal resources. More than half of geothermal resources found in sedimentary basins in China is stored in this basin. Geothermal waters are usually hit by oil exploration drilling. In major cities, such as Beijing and Tianjin, however, many wells have been drilled solely for geothermal development.

The genesis of the geothermal systems in North China Basin has been studied [12]. Most geothermal anomalies are related to the relief of the pre-Cenozoic basement; positive anomalies (higher thermal gradient) correspond to basement uplift. These geothermal systems belong to low-medium temperature conductive geothermal systems, which don't need a magmatic heat source.

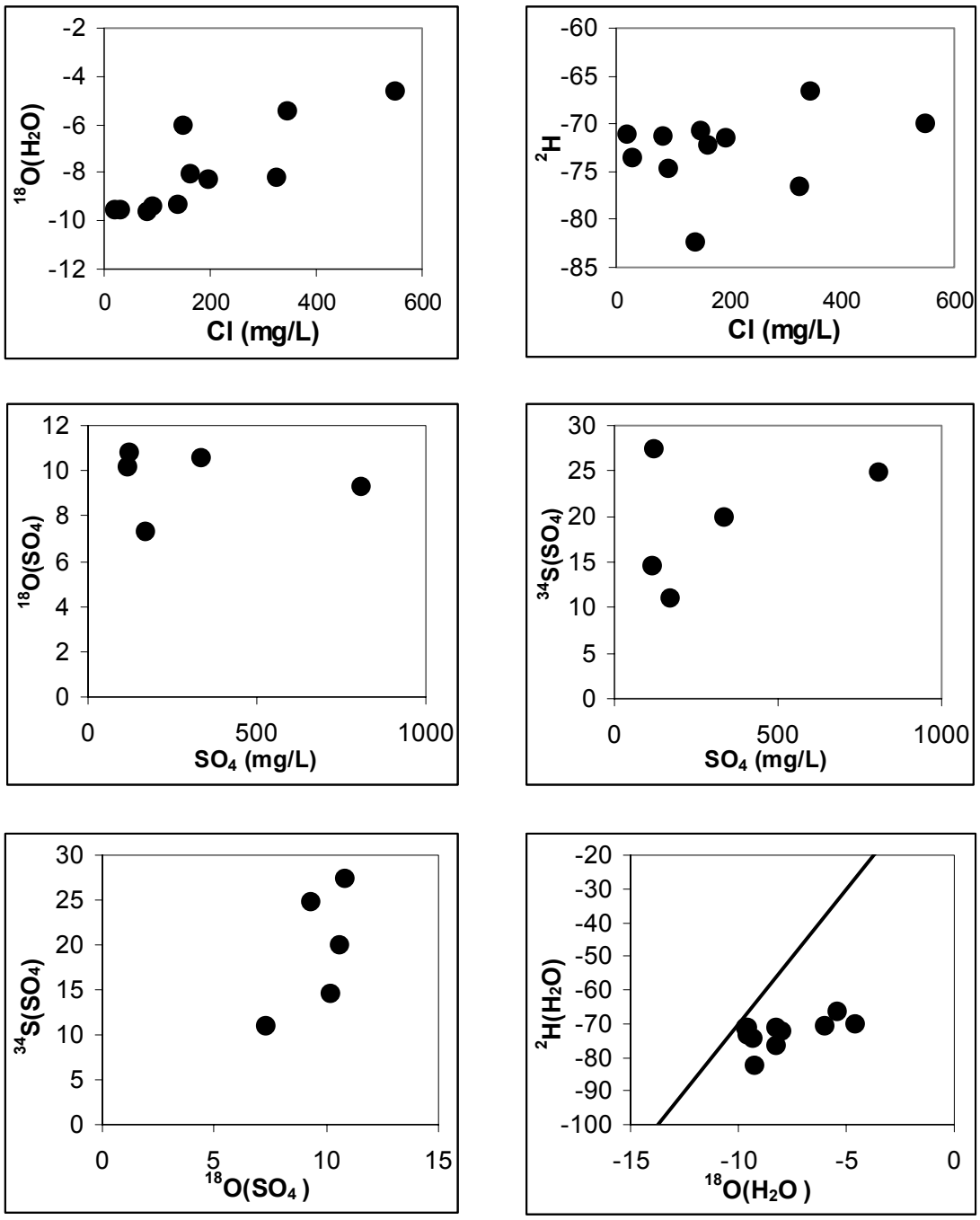

Figure 5. Correlation of Chloride and SO_4 with isotopes and isotope cross plots for samples from East of Hebei geothermal area.

In Figure 5, $\delta^{18}O$, but not $\delta^{2}H$, is enriched with increased Cl concentration. The O-18 versus H-2 plot further indicates a trend of O-18 enrichment alone. The slope of this trend line is not in the normal range of an evaporation line that is usually between 3 and 7. The isotopic composition represents exchange with the formation matrix or mixing between different aquifers.

Water sample HC-1 has a much depleted deuterium values, implying recharge to the Paleozoic limestone aquifer from higher altitudes as compared to the Upper Tertiary aquifers. The relatively lower salinity also indicates a better hydraulic circulation condition than that in the sandstone aquifers.

In addition to these, only 5 out of the 11 samples produced a result for isotopes of SO_4 mainly due to the low sulphate concentration of the thermal waters.

Figure 4 shows that the thermal waters from different aquifers plot very scattered and they are unlikely from a unique marine origin (Table IV).

Table IV. Isotope composition of water and aqueous sulphate in East of Hebei Province, China

Code	Site name	Sample type	Formation	Depth (m)	T_s (°C)	T_f (°C)	$\delta^{18}O(SO_4)$ (‰VSMOW)	$\delta^{34}S(SO_4)$ (‰VCDT)	$\delta^{18}O(H_2O)$ (‰VSMOW)	$\delta^{2}H(H_2O)$ (‰VSMOW)
1	TN-2	GWB	Nm, sand	383	22	25			-9.56	-73.6
2	XG-3	GWB	Nm, sand	500	22	25			-9.57	-71.1
3	QY-1	GWB	Nm, sand	350	25	30	10.8	27.4	-9.63	-71.3
4	N34x1	GTB	Ng, sand	1128	52	55	10.6	19.9	-9.37	-74.6
5	L21x10	GTB	Nm, sand	1816	70	79			-71.40	-8.3
6	L25x13	OPW	Ng, sand	1994	75	88			-8.01	-72.2
7	M2-3	OPW	Ed, sand	2700	80	88			-8.21	-76.6
8	M16x1	OPW	Ed, sand	2872	85	94			-5.44	-66.6
9	L20x2	OPW	Es, sand	3400	95	116	7.3	11.1	-4.60	-69.9
10	L90x2	OPW	Es, sand	3057	96	110	10.2	14.6	-6.04	-70.8
11	HC-1	GTB	O, limestone	3075	96	112	9.3	24.8	-9.28	-82.3

4. Isotope geothermometry

The oxygen isotope geothermometer based on isotope equilibration between dissolved sulfate and the water was used and results listed in Tables III, IV, V and VI together with those by chemical geothermometers for comparison. Figure 6 shows the isothermal lines and data points for samples from the two areas.

A comparison was then made with the reference temperatures for each of the areas. In Figures 7a and 7b, direct comparison of temperature estimates shows that closer approximation is evident for samples higher than 80°C. Oxygen-18 temperatures are close to the deep temperatures worked out by mixing models from earlier studies that have also showed that the deeper water is saturated with sulphate [13 14], probably reflecting isotopic equilibrium in the deeper part of the system.

The main influencing processes are therefore mixing with shallow groundwater and missing chemical equilibrium with sulphate minerals as shown by low SO_4 concentration in the water samples. This can be further verified when more data become available for the EH area.

5. Conclusions

Sulfate isotope study, integrated with water chemistry, confirms the marine origin of aqueous sulfate in the thermal water from South of Fujian Province. For the East of Hebei Province, thermal waters from Upper Tertiary and Lower Paleozoic aquifers are low in SO_4 and limited results on sulphur isotopes doesn't allow firm discrimination of sulphur sources, but they are unlikely of marine origin.

The estimated temperatures by oxygen geothermometry are compatible to those by chemical geothermometry and fluid-mineral chemical equilibrium calculations. This implies that oxygen isotope exchange equilibrium has probably been attained between aqueous sulfate and water at a reservoir temperature of 150ºC in the central part of Zhangzhou geothermal field. In the case of East of Hebei Province, isotope geothermometry failed to give a reasonable temperature estimate.

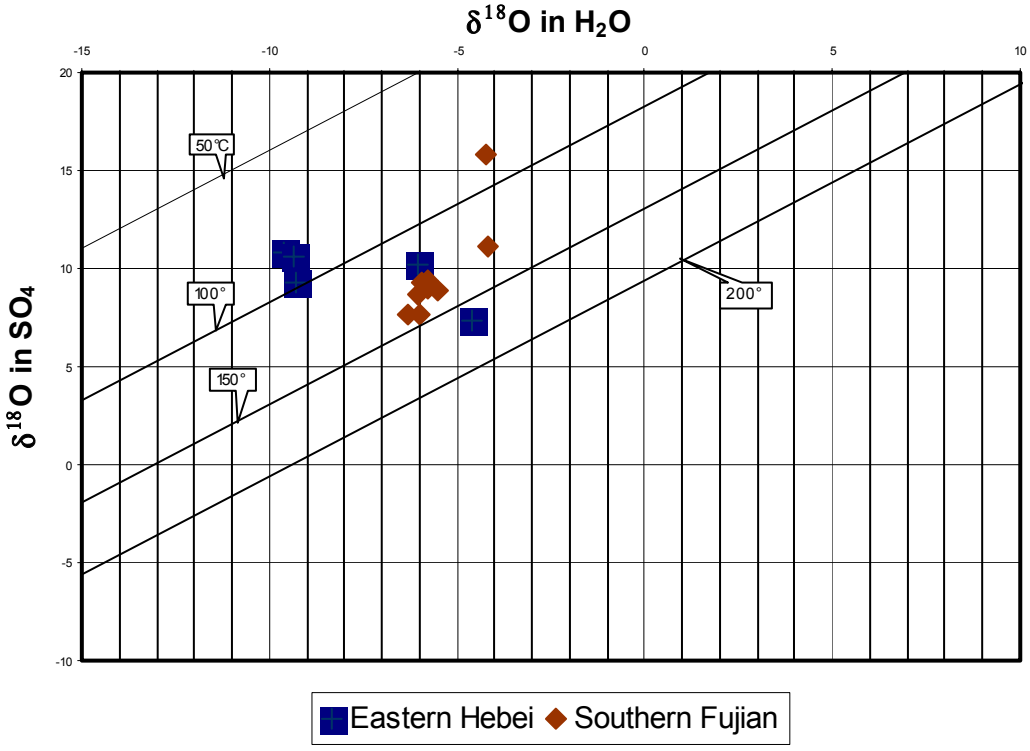

Figure 6. Reservoir temperature estimates according to Oxygen-18 equilibrium in Zhangzhou (South of Fujian) and East of Hebei (East of Hebei) geothermal areas.

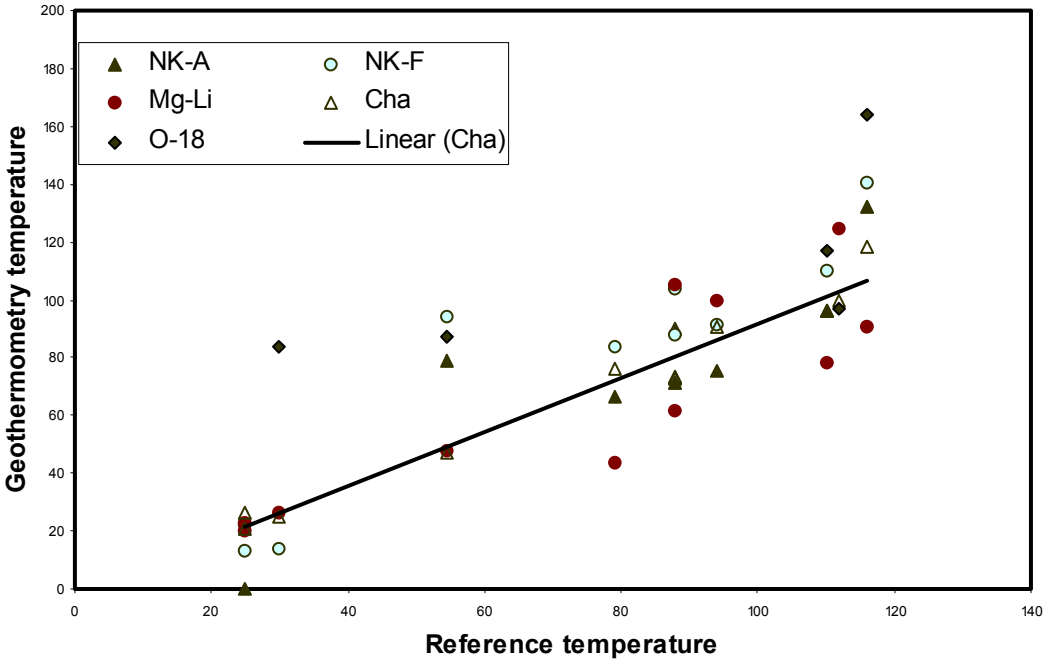

Figure 7a. Comparison of temperature estimates from different methods (East of Hebei area).

Table V. Temperature estimates based on chemical and isotopic geothermometers for samples of South of Fujian Province, China

Code	Site name	Sample type	Rock type	T_s	NK-G	NK-A	NK-F	K-Mg	Mg-Li	Q-nsl	Chal	T(^{18}O)
								(°C)				
1	V05Q	GTB	Q, sand	28	278	289	266	17	80	113	83	
2	V02Q	GTB	Q, sand	40	195	176	177	16	104	106	76	
3	Gongliao	GTB	Q, sand	62	184	162	166	11	121	141	114	
4	ZR2	GTB	Granite	26	111	73	90	33	73	68	36	139
5	ZR34	GTB	Granite	26	156	127	136	29	1	65	33	
6	ZR12	GTB	Granite	30	137	104	117	18	130	91	60	131
7	V05G	GTB	Granite	31	163	135	143	15	119	68	36	126
8	ZR26	GTB	Granite	40	144	113	124	15	116	97	67	127
9	ZR35	GTB	Granite	41	175	151	156	9	141	129	101	132
10	ZR16	GTB	Granite	41	173	148	154	8	142	130	103	
11	ZR17	GTB	Granite	47	146	114	126	18	109	88	58	127
12	V02G	GTB	Granite	62	167	140	147	10	141	135	108	143
13	V04	GTB	Granite	93	172	146	153	7	150	153	128	
14	S044	GTB	Granite	97	180	156	161	6	151	149	123	135
15	Quepu	GTB	Granite	57	144	112	124	14	113	88	57	
16	Shitou	GTH	Granite	52	141	109	121	21	83	104	75	87
17	Xinlin	GTH	Granite	80	149	119	129	21	83	137	110	126

Note: NK-G = Giggenbach, 1988; NK-A = Arnorsson, 1983; NK-F = Fournier, 1991; K-Mg = Giggenbach, 1988; Kharaka & Mariner, 1989, Qz = Quartz temperature, Arnorsson, 1983; Cha = Chalcedony temperature, Arnorsson, 1983; T^{18}O = Oxygen-18 geothermometer, Mizutani & Rafter, 1969

Table VI. Reservoir temperature estimated by geothermometers for sampled geothermal wells in East of Hebei Province, China

Code	Site name	Sample type	Formation	Depth (m)	Ts	T_f	NK-G	NK-A	NK-F	K-Mg	Mg-Li	Qz	Cha	T(^{18}O)
										(°C)				
1	TN-2	GWB	Nm, sand	383	22	25	35	-9	13	66	20	58	26	
2	XG-3	GWB	Nm, sand	500	22	25	43	0	22	56	23	53	21	
3	QY-1	GWB	Nm, sand	350	25	30	36	-8	14	62	26	57	25	84
4	N34x1	GTB	Ng, sand	1128	52	55	115	79	94	24	48	79	47	87
5	L21x10	GTB	Nm, sand	1816	70	79	105	67	83	21	44	105	76	
6	L25x13	OPW	Ng, sand	1994	75	88	109	71	88	14	62	103	74	
7	M2-3	OPW	Ed, sand	2700	80	88	125	90	104	11	105	103	73	
8	M16x1	OPW	Ed, sand	2872	85	94	112	75	91	1	100	119	91	
9	L20x2	OPW	Es, sand	3400	95	116	160	132	141	17	90	145	119	164
10	L90x2	OPW	Es, sand	3057	96	110	130	96	110	15	78	124	96	117
11	HC-1	GTB	O, limestone	3075	96	112	392	471	394	-11	125	127	99	97

Note: NK-G = Giggenbach, 1988; NK-A = Arnorsson, 1983; NK-F = Fournier,1991; K-Mg = Giggenbach, 1988; Kharaka & Mariner, 1989.
Qz = Quartz temperature, Arnorsson, 1983; Cha = Chalcedony temperature, Arnorsson, 1983; T^{18}O=Oxygen-18 geothermometer, Lloyd, 1968

Table VII. Reservoir temperature estimated using the oxygen isotope geothermometer based on aqueous sulphate

Site name	T-ref	$\delta^{18}O(H_2O)$	$\delta^{18}O(SO_4)$	1000Lnα	T-^{18}O
Qy-1	29.8	-9.63	10.8	20.43	73
N34x1	54.5	-9.37	10.6	19.97	76
L90x2	110	-6.04	10.2	16.24	108
Hc-1	112	-9.28	9.3	18.58	87
L20x3	116	-4.6	7.3	11.9	158
ZR2	36	-6.29	7.7	13.99	131
V05G	36	-5.95	9.3	15.25	118
ZR17	58	-5.57	9.6	15.17	119
ZR12	60	-5.8	9	14.8	122
ZR26	67	-5.8	9.4	15.2	118
Shitou	75	-4.22	15.8	20.02	76
ZR35	101	-6.02	8.7	14.72	123
V02G	108	-5.97	7.7	13.67	135
Xinlin	110	-4.19	11.1	15.29	117
S044	123	-5.53	8.9	14.43	127

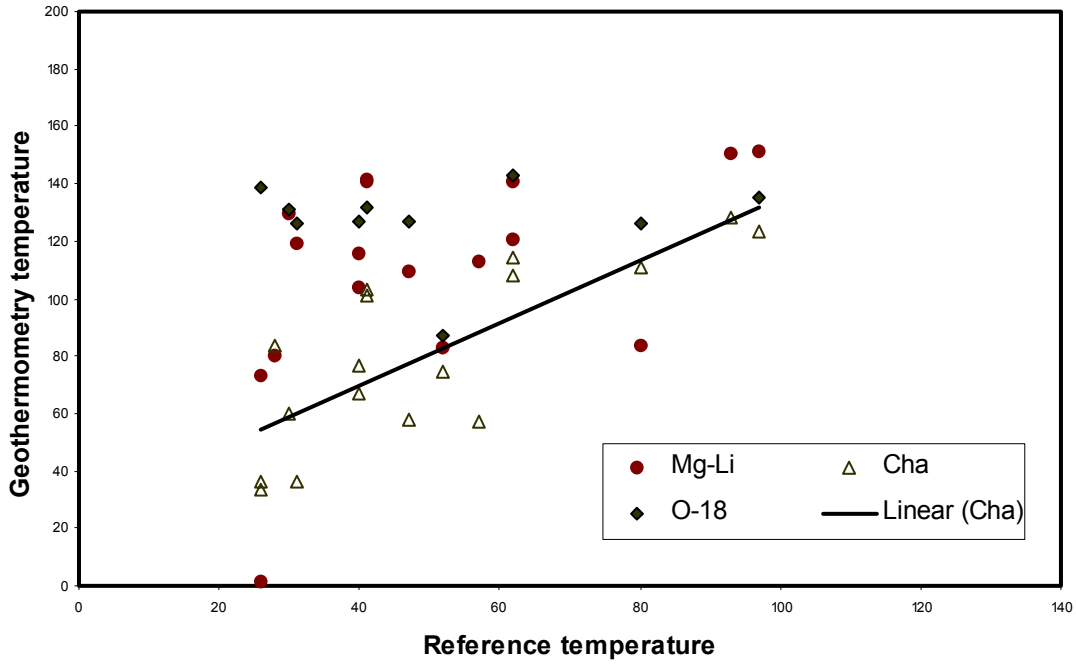

Figure 7b. Comparison of temperature estimates from different methods (Southern Fujian area).

Acknowledgements

This study was financed jointly by the International Atomic Energy Agency through Research Contract 9180/RB and the National Natural Science Foundation of China through research grant Earth Science 49372156. Thanks are due to S. Arnorsson who reviewed and commented an earlier version of the manuscript.

REFERENCES

[1] ROBINSON, B.W., 1987, Sulphur and sulphate-oxygen isotopes in New Zealand geothermal systems and volcanic discharges, in: Studies on sulphur isotope variations in nature, Proc. of an advisory group meeting, International Atomic Energy Agency, Vienna, ISBN 92-0-141087-5, 31–48.

[2] LLOYD, R.M., 1968, Oxygen isotope behavior in the sulfate-water system, J. Geophys. Res., 73:6099–6110.

[3] MIZUTANI, Y., RAFTER, T.A., 1969, Oxygen isotope composition of sulfates, 3. Oxygen isotopic fractionation in the bisulfate ion-water system, N. Z. J. Sci., 12:54–59.

[4] GIGGENBACH, W., GONFIANTINI, R., PANICHI, C., 1983, geothermal systems, in: Guidebook on Nuclear techniques in hydrology, International Atomic Energy Agency, Vienna.

[5] MICHELOT, J-L, DOTSIKA, E., FYTIKAS, M., 1993, A hydrochemical and isotopic study of thermal waters on Lesbos Island (Greece), Geothermics, 22: 91–99.

[6] CORTECCI, G., NOTO, P., PANICHI, C., 1978, Environmental isotopic study of the Campi Flegrei (Naples, Italy) geothermal field, J. of Hydrl., 36, 143.

[7] KUSAKABE, M., 1974, Sulphur isotope variations in nature, Part 10: Oxygen and sulphur isotope study of Wairakei geothermal well discharges, NZ J. Sci., 17, 183.

[8] MCKENZIE, W.F., TRUESDELL, A., 1977, Geothermal reservoir temperatures estimated from the oxygen isotope compositions of dissolved sulphate and water from hot springs and shallow drill holes, geothermics, Vol. 5.

[9] PANG, Z., 1987, Zhangzhou geothermal system: genesis analysis and thermal energy potential, Ph.D thesis (in Chinese with a summary in English), Academia Sinica, Beijing, China.

[10] Longinelli, A., 1989, Oxygen-18 and sulfate-34 in dissolved oceanic sulfate and phosphate. Chapter 7 in Handbook of Environmental Isotope Geochemistry (Fritz, P. and Fontes, J. Ch., eds), 3: pp219-255, Elsevier Amsterdam.

[11] CLAYPOOL, G. E., HOLSER, W. T., KAPLAN, I. R., SAKAI, H. AND ZAK, I., 1980, The age curve of sulfur and oxygen isotopes in marine sulfate and their mutual interpretation, Chem. Geol., 28, 199–260.

[12] CHEN M. (ED.), 1988, Geothermics of North China, Science Press, Beijing, 218 (In Chinese with an English abstract).

[13] PANG, Z.H., FAN, Z.C., WANG J.Y., 1990, Calculation of reservoir temperature of the Zhangzhou Geothermal Field by using a SiO_2 mixing model, Chinese Science Bulletin (English Edition), 1:57–59.

[14] PANG, Z. and REED, M., 1998, Theoretical chemical geothermometry on geothermal waters: problems and methods, Geochimica et Cosmochimica Acta, 62(6), 1083–1091.

EXPERIMENTAL STUDY AND MODELLING OF WATER-ROCK INTERACTION IN ACTIVE GEOTHERMAL FIELDS: LOS AZUFRES, MEXICO

Wenbin Zhou*, Zhanshi Zhang

East China Institute of Technology, Fuzhou,
Jiangxi, China

Abstract. The Los Azufres Geothermal Field in Mexico is a typical high temperature hydrothermal system along convergent plate boundaries. Models of high-temperature and high-pressure experiments and geochemical simulation calculations of it have been set up. Natural rock samples that were cut and polished into small rock cylinders with a diameter around 4.0 mm were used as the solid phase in high-temperature-pressure experiments. Mineral alteration and evolution of the equilibrium solution composition due to WRI processes have been explored in this study. A conceptual model of the origin and evolution of the fluids in Los Azufres hydrothermal system is presented.

1. Introduction

Water-rock interaction (WRI) is among the most important and extensive of natural processes. An active hydrothermal system is an open or partially open geochemical system where various kinds of water-rock interaction are taking place. Isotope exchange and chemical alteration of geothermal fluids and rocks result largely from water-rock interaction. Therefore, experimental study of interaction between geothermal water and rock will help to (1) determine the origin of geothermal fluids; (2) explore the mechanism of many complicated geochemical reactions in geothermal systems; (3) provide useful information to the exploitation and utilization of the geothermal resources.

This report was focused on an active geothermal field. The Los Azufres geothermal field in Mexico, a famous active geothermal field along convergent plate boundaries, had been selected as example of active geothermal fields. The main results were given below.

2. Methodology

2.1. Experimental study

2.1.1. Experimental model

The experiment was designed to simulate water-rock interaction and chemical evolution of thermal fluids in geothermal systems. The distinguishing feature of the experimental study was that rock samples which, cut and polished into small rock cylinders of about 4 mm diameter, were used rather than the rock powders used in most experiments. The advantage of this method was that water-rock interactions took place on the mineral surface especially at the interface of different minerals, which was helpful in the study of surface interactions and alteration of minerals. At the same time, it had the disadvantage that it was very difficult to interpret the chemical composition of the resulting fluid, as the rocks were usually heterogeneous materials [1].

2.1.2. Experimental facilites

The experiments were carried out in the National Key Laboratory on Mineral Deposit Research, Nanjing University. The reactions took place within the internally cooled Rapid Quenching Vessel (RQV). The temperature of the reaction was measured by thermal and controlled by XTMA-1000 digital regulator with accuracy of $\pm$1 ºC. The pressure of the RQV was adjusted by a hydraulic pressure device with accuracy of

* Present address: Nachang University, Jiangxi, China.

1MPa. The reaction tube was made of pure gold, 4.2 mm in diameter and 100 mm long with an effective volume of some 1.3 ml after being sealed.

2.1.3. Procedures

First, a certain number of rock cylinders were put in the reaction tube and a water sample was added. Then melting sealed the open end of the tube. The tube was placed at the bottom of the high-pressure vessel, with a steel bar added to reduce the free space. The vessel was filled with distilled water and closed. The vessel was heated in a tubular electric heater and kept at the temperature desired. No leakage from the vessel was observed after being under pressure for 2 hours. When the reaction time was completed, the vessel was removed from the stove and quenched. After cooling to room temperature, the reaction tube was removed from the vessel under some negative pressure. Then, the tube was examined to find whether or not there was any leakage by means of surface observation and weighting. A successful experiment was one with no weight difference or a weight difference less than 0.5mg before and after experiment [2]. Then, the reaction products were separated into solid and liquid phases using a centrifuge, the liquid phase was transferred into a small plastic sample bottle with injector, in preparation for chemical analysis. The surface of the rock cylinder was cleaned by leaching, washing and drying, and then sectioned in preparation for further mineralogical study and electron microprobe analysis.

2.2. Modelling

The aim of the modelling was to simulate the water-rock interaction and the evolution thermal fluids in geothermal system. Like the water-rock interaction experiment, the modelling study of water-rock interaction should first select the sample. The same samples as the experimental study were used in the modelling in order to verify the experimental study.

The EQ3/6 geochemical software package was run on a SUN Spark 20 workstation in ECIT to simulate the interaction under different temperature conditions. The calculation models were the reaction path calculation in a closed system, with the direct results of the modelling were in OUTPUT and TAB data files, and the data of interest were selected and plotted using Microsoft EXCEL.

2.3. Analysis

The major-element compositions had been measured by the analysis centre in ECIT. The compositions of solutions from the experiments were measured by an Elan 6000 ICP-MS in Institute of Geochemistry, Chinese Academy of Sciences, Guangzhou. The mineral compositions before and after experiments were measured by a JEOL JXA-8800M Electronic Probe X-Ray Micro-analyzer (EPMA) in the National Key Laboratory on Mineral Deposit Research, Nanjing University. The measured conditions of the EPMA included accelerating voltage —12~ 15KV, beam current — 2×10-8A, and beam spot — 0~ 2μm. ZAF correction was employed.

3. Case studies

Los Azufres in Mexico, a famous active geothermal field along convergent plate boundaries, was selected for the case studies.

3.1. Geological setting

Los Azufres geothermal field is located in central Mexico, approximately 200 km Northwest of Mexico City. It is one of several Pleistocene silicic volcanic centres with active geothermal systems in the Mexico Volcanic Belt (MVB). With an electricity production of 98 MW, it is the first geothermal field in Mexico that generates electricity from fluids in volcanic rocks, and represents the second most important geothermal field in Mexico after Cerro Prieto [3]. Geologically, the volcanic rock at Los Azufres could be divided into two principal units [4]. (1) A silicic sequence of rhyodacites, rhyolites and

dacites with ages between 1.0 and 0.15 m.y. and a thickness up to 1000 m. (2) A 2700 m thick interstratification of lava flows and pyroclastic rocks, of andesitic to basaltic composition with ages between 18 and 1 m.y., forming the local basement. This unit provided the main aquifer with flow through fractures and faults. Three different fault systems, NE-SW, E-W and N-S could be distinguished in the field. The E-W system was the most important one form geothermal fluid circulation (Fig. 1).

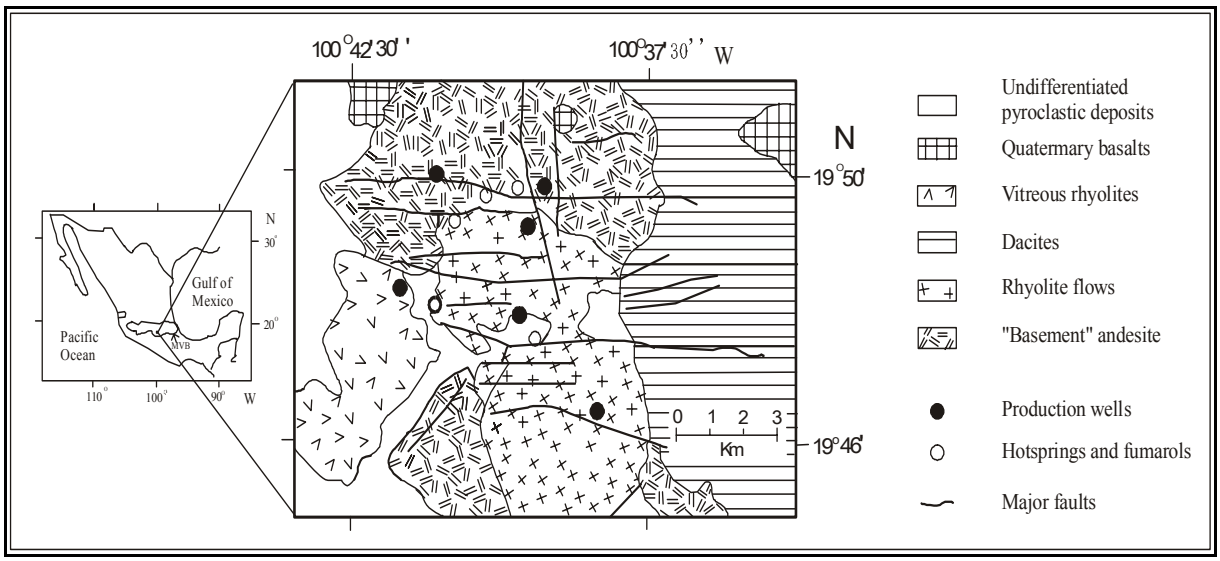

Figure 1. Simplified geological map of the los azufres geothermal field (after dobsonand mahood[5], 1985).

3.2. Geochemistry of the Geothermal Fluid

Almost all waters from Los Azufres geothermal field production wells were the neutral sodium-chloride geothermal types, with TDS ranging between 5 and 8 g/L. Only the well Az-14 produced sodium-bicarbonate geothermal water because it was fed by shallow water [4]. At Los Azufres geothermal field, CO_2 was the predominant gas followed by H_2S and N_2, as expected in a geothermal environment.

In most production wells in Los Azufres geothermal field, typical $\delta^{18}O$ varies from -2‰ to -6‰ (average -5‰), δD ranges from -62‰ to -57‰ (average -60‰), which indicated that the geothermal fluid was enriched in $\delta^{18}O$ and δD relative to local meteoric waters ($\delta^{18}O$= -10‰, δD=-70‰,[7]). This could be interpreted to result from high-temperature water-rock interaction between infiltered local meteoric water and andesitic rock. Mixing of waters also caused shifts to the compositions of $\delta^{18}O$ and δD [6].

3.3. Geochemistry of Volcanic Rock

A brief field investigation was carried out by Mr. Wenbin Zhou during the field trip of the Workshop on Geothermal Utilization held in Los Azufres Geothermal Field, Mexico November 1998. During the field trip, the geology, surface geothermal manifestations, and production wells of geothermal field were investigated. Both fresh (M1, M2) and altered rock (M3, M4, M6, M7, M8) samples were collected for the experimental study. The chemical compositions of the rocks were shown in Table I.

Both fresh volcanic and altered rocks collecting from Los Azufres geothermal fields had been sliced and examined by means of microscopy in order to assess the composition, texture, structure and

hydrothermal alteration of the minerals of them. The typical volcanic rock in Los Azufres geothermal field was described as andesite (M2), with a typical porphyritic texture, and the minerals of porphyritic crystals were usually dark pyroxene and plagioclase, and with a crystalline plagioclase and glassy matrix with a flow orientation around the porphyritic pyroxene crystals. Common alteration minerals, chlorite and epidote could be found in the altered rock (M3) around pyroxene crystallized at an early stage. Near surface alteration products of andesite included CT-Opal (M6, M7), cristobalite and well crystallized kaolinite (M8) (according to the X-diffraction analysis, Fig.2).

3.4. Water-Rock Reaction Equilibrium and Geothermometry

The state of equilibrium and temperatures at which water-rock interactions took place could be indicated on a Giggenbach diagram [6]. Fig.3 indicated the relative Na-K-Mg content in water from produced water of the Los Azufres reservoir. Except for well Az-14 that fed by shallow water, and wells Az-49 and 32, they were found in the area of partial equilibrium, all well waters fall on the line of total equilibrium at temperature between 300-340°C [3].

The field investigation and geochemical study of samples were helpful in constructing the experimental model.

Table I. Major-element chemistry of rock sample from Los Azufres geothermal field unit: wt%*

	M1	M2	M3	M4	M6	M7	M8
SiO_2	51.98	59.8	55.92	77.24	93.77	89.33	70.94
Al_2O_3	18.05	16.73	17.96	10.78	0.82	0.52	19.69
TiO_2	1.12	0.8	0.88	0.064	0.056	0.152	0.08
Fe_2O_3	8.18	6.69	6.81	0.858	0.502	0.3711	0.15
MnO	0.132	0.15	0.15	0.054	0.002	0.001	0.23
MgO	5.36	3.72	3.32	0.056	0.009	0.009	0.002
CaO	6.4	7.2	6	0.110	0.040	0.022	0.002
Na_2O	3.74	3.38	5.66	0.210	0.028	0.148	0.164
K_2O	1.28	1.16	2.54	1.92	0.044	0.032	0.108
P_2O_5	0.506	0.38	0.36	0.0003	0.015	0.024	-
Total	96.748	100.01	99.6	91.292	95.286	90.609	91.366

* Measured by East China Institute of Technology

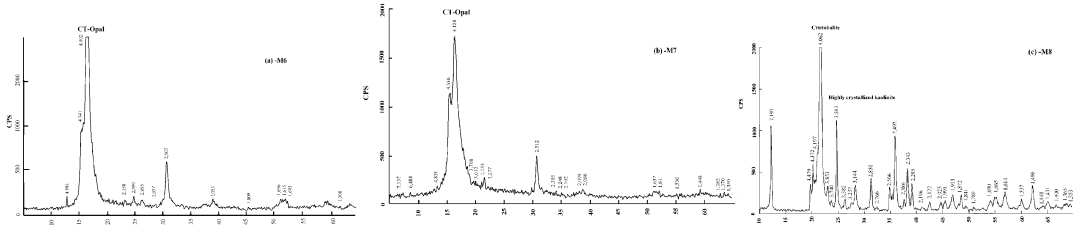

Figure 2. X-diffraction analysis of M6, M7, M8 rock samples from Los Azufres.

**Measured by the moden analysis centre in Nanjing University.*

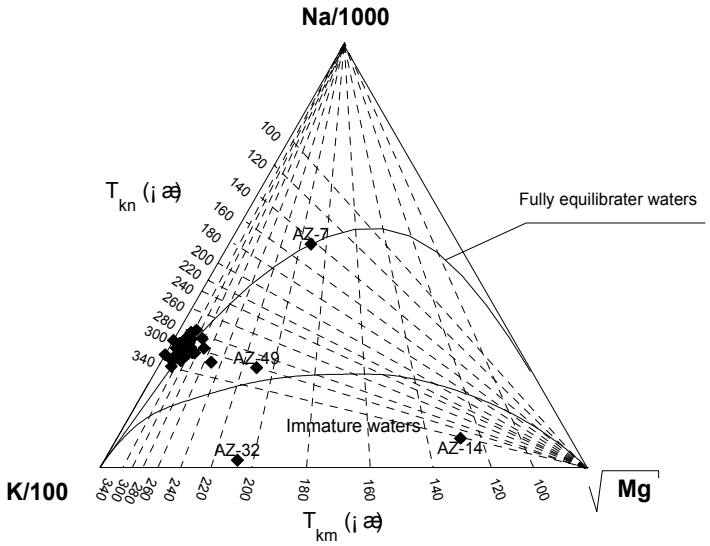

Figure 3. The relative Na-K-Mg content diagram.

3.5. Experimental results and discussions

The rock cylinders of M2 andesite from Los Azufres geothermal field had been selected as the solid phase of the reaction. The liquid phase MF was prepared according to the composition of water from wells in Los Azufres. The Water/Rock ratio (W/R) was determined around to 1, the temperature and pressure had chosen as 350°C and 50 MPa separately, and the duration of the reaction had been designed from 48 to 720 hrs (See Table II).

Table II. Parameters for the Experiments

No:	Rock	Fluid	W/R	T(°C)	P(Mpa)	Duration (hours)
SY-02	M2	MF	1	350	50	144
SY-04	M2	MF	1	350	50	720
SY-08	M2	MF	1	350	50	48
SY-09	M2	MF	1	250	50	48
SY-10	M2	MF	1	150	50	48
SY-12	M2	pure water	1	350	50	48
SY-17	M2	MF	1	350	50	480

M2: rock sample; MF = 0.1M NaCl + 0.02M KCl

3.5.1. Characteristic of solid phase before and after experiment

After slicing, the solid phase (rock cylinder) before and after experimentation had been studied by means of microscope and electron microprobe analysis. Using a microscope, an obvious discoloured alteration of feldspar and lots of little secondary crystals around the porphyritic crystals of pyroxene were observed in the rock slice after the experiment. More detailed electron microprobe analysis results were described below.

3.5.2. Feldspar before and after experiment

In the M2 rock cylinder from Los Azufres, two kinds of feldspar, porphyritic crystal and micro-crystal in matrix, can be distinguished. The An component of feldspar in the matrix varies from 48.5 to 51.9%, and from 36 to 42% in the porphyritic crystal, showing andesine to laboratories and andesine respectively. Both feldspars have normal girdle banding. In the M3 natural altered rock sample, there are two kinds of feldspars, K-feldspar and albite, which are the products of water-rock interaction of andesine in the

original andesite rock with fluid enriched in Na and K. After the experiment, the secondary feldspar crystals around the porphyritic crystals are K-feldspar and albite, just like the natural altered rock sample. But in the leaked sample, the An component of feldspar increased and the Ab component decreased. The classification of feldspar before and after experiment is shown in Fig.4.

3.5.3. Pyroxene before and after experiment

In the M2 rock sample most pyroxenes were augite before the experiment, but during the experiment, most of them changed into diopside, actinolite and actinolite-Hb (Fig.5. and Fig.6) and epidote. In the natural altered rock sample M3, all augite had changed into epidote and actinolite.

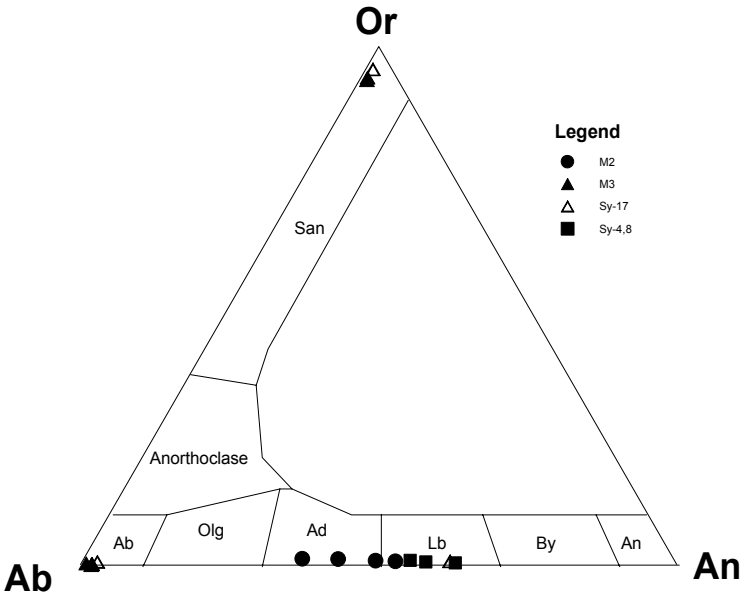

Figure 4. The classification of feldspar before and after experiment.

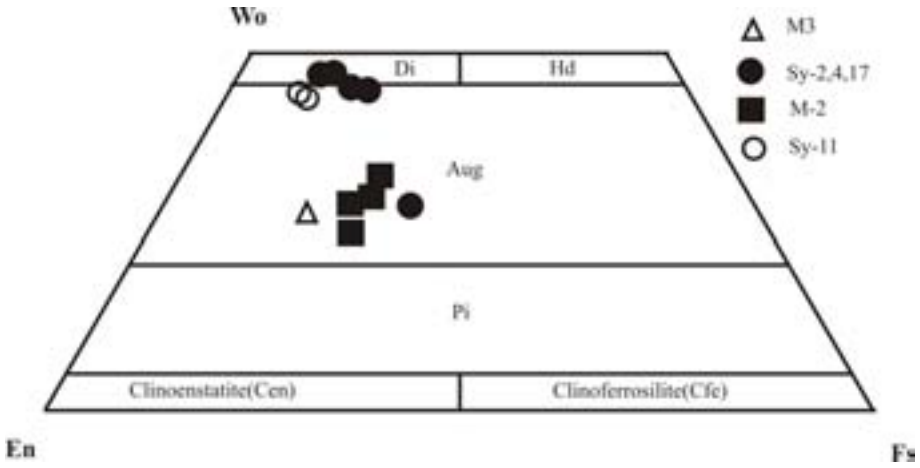

Figure 5. The classsification of pyroxene before and after experiment.

**Measured by jxa-8800 m EMA in the national key laboratory on mineral deposit research, Nanjing university. The classification according to the IMA guideline, morimoto, 1989. The no: 2,3,4,5 - m2 rock cylinder before experiment; 9,10 - the remainder of sy-4 and m3; 1,6,7,8,11,12 - from sy-2,17.*

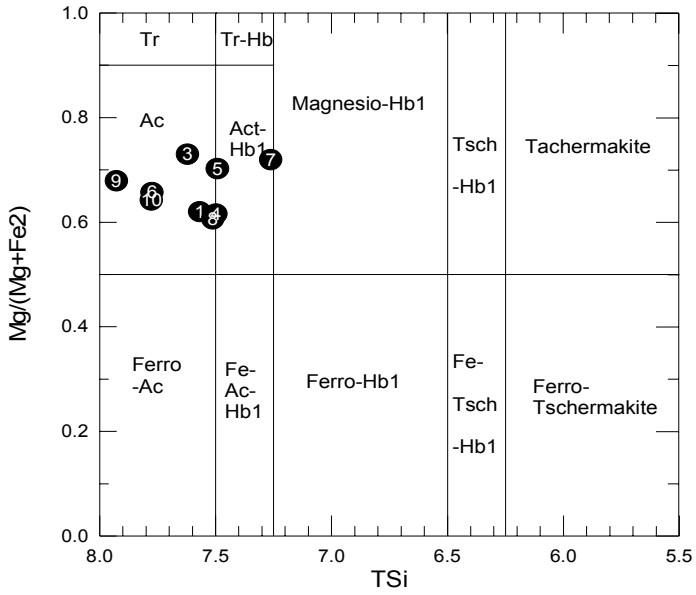

Fig.6. The classification of amphibole after experiment.

**Measured by JXA-8800 M EMA in the National Key Laboratory on Mineral Deposit Research, Nanjing University, the classification according to Hawthorne, 1981. The No.:1 ,2 from M3 rock, 3-10 from sy-4;*

Expect that, electron microprobe analysis found some very little secondary minerals around the porphyritic crystal, there are hematite, chlorite, sphene, ilmentite, SiO_2 and calcite. The typical mineral paragenesis is actinolite + epidote + chlorite + albite.

3.5.4. Factors affecting the water-rock interaction

The analytical results of the solution after water-rock interaction experiment are listed in Table III. In spite of the fact that it was affected by the heterogeneous rock cylinder, we can also get some knowledge from it.

Table III. Chemical composition of solution after experiment

Element	Sy-9	Sy-10	Sy-12	Sy-17	Element	Sy-9	Sy-10	Sy-12	Sy-17
Li	2.403	1.114	1.422	18.124	Mn	0.164	0.286	0.353	0.717
Na	2887.89	2958.96	71.07	2425.37	Fe	0.395	1.541	16.939	1.272
Mg	0.571	1.22	23.155	3.643	Co	0.005	0.007	0.018	0.004
Al	0.234	0.949	23.633	0.497	Ni	0.212	0.385	0.246	0.469
Si	3.005	7.133	29.449	3.809	Cu	0.475	0.186	0.136	0.169
P	0.114	0.237	1.457	0.321	Zn	0.146	0.062	0.31	0.246
K	789.78	736.48	30.767	624.48	Rb	0.154	0.252	0.052	0.704
Ca	8.137	24.598	7.852	28.157	Sr	0.175	0.497	0.074	0.716
Ti	0.013	0.402	0.989	0.026	Mo	0.033	0.051	0.012	0.041
V	0.023	0.069	0.164	0.032	Sn	0.001	0	0.003	0.001
Cr	0.023	0.021	0.5	0.088	Pb	0.041	0.007	0.016	0.028

Measured by Elan 6000 ICP-MS in Institute of Geochemistry, Chinese Academy of Sciences, Guangzhou

3.5.5. Temperature

Temperature had an important effect on the water-rock interaction. The evolution of the elements when the interaction between MF and M2 andesite cylinder at different temperature (Fig. 7.) infer that high-temperature (350°C) is more favourable for the water-rock interaction. When 350°C, most major-elements content are less than 250°C and 150°C, expect Mg and Ca, but minor-elements were

inverse. That was because the dominant process was the rock dissolving at low-temperature, but at high-temperature along the rock dissolving (which was more strong than low-temperature), some secondary minerals may precipitate.

3.3.6. The fluid composition

After the interaction between distilled water with M2 andesite cylinder, Na, K, Si, Al, Ca, Fe enriched solution (Fig.8.) was formed, much liked the well water from the geothermal field above. Those indicated that the local meteoric water had added into the fluid after water-rock interaction when infiltration into the andesite rocks zone.

3.6. Modelling results and discussions

The MF had been used as the water samples for the modelling (expect K, Na, Cl, HCO_3^-, other elements content as the pickup file required adept were 1.000E-12mol/L). M2 andesite from Los Azufres geothermal field had been used as rock sample for the modelling.

The rock-forming minerals that settled according to the electron microprobe analysis and CIPW calculation were augite, pigeonite, orthoclase, plagioclase, quartz and little magnetite and ilmenite. The interaction between MF and andesite under different temperature and pH value condition.

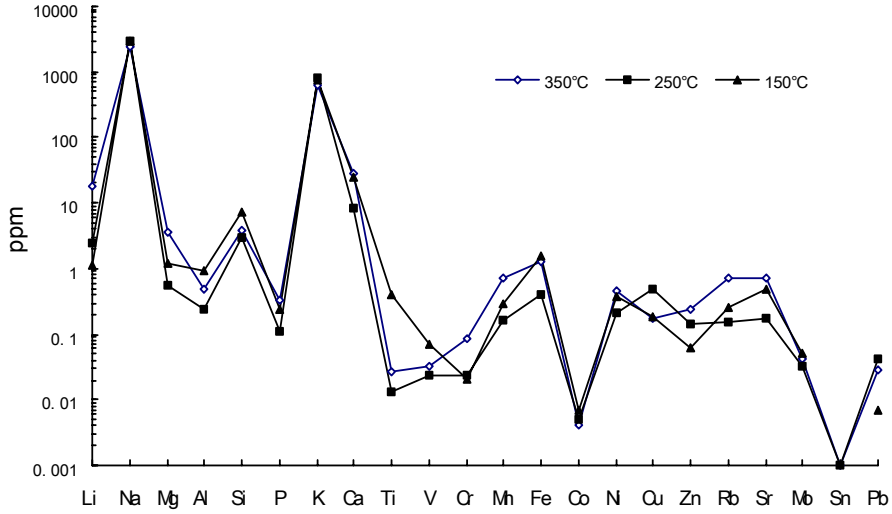

Figure 7. Experimental study of mf-m2 interaction: temperature on the evolution of elements.

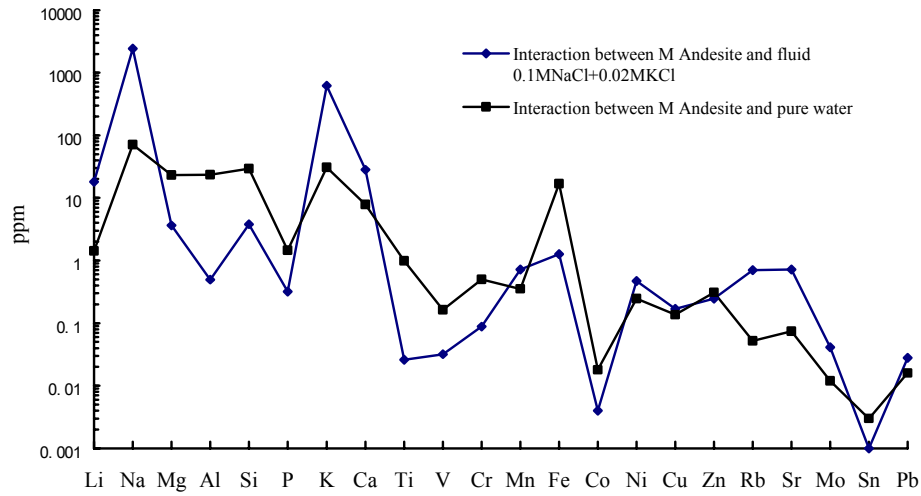

Figure 8. Experimental study of water-m2 interaction: evolution of elements in the solution.

3.6.1. The evolution of the solution

In the processes of water-rock interaction between MF and M2 andesite, the content of Na, Si, Ca in the solution increased continuous, Cl, B, C, Li, Ti almost fixed, Mg, Fe decreased. The content of K and Al reached the peak during 1–10 days, and then declined 10 days later (showed in Fig. 9). The regular pattern of K, Na, Ca accorded with the experimental studying. This regularity due to the rock dissolving and secondary minerals precipitated in the processes of water-rock interaction. Fig.10 revealed the formation processes of the secondary minerals when MF-M2 interaction. Only hematite precipitated throughout the reaction, epidote, hydroxyl-apatite, clinozoisite, mesolite, chlorite, amesite-14A, albite, diopside and muscovite precipitated from 1 days later to the end of the reaction. The products of the modelling were accord with the experimental studying and the natural altered products.

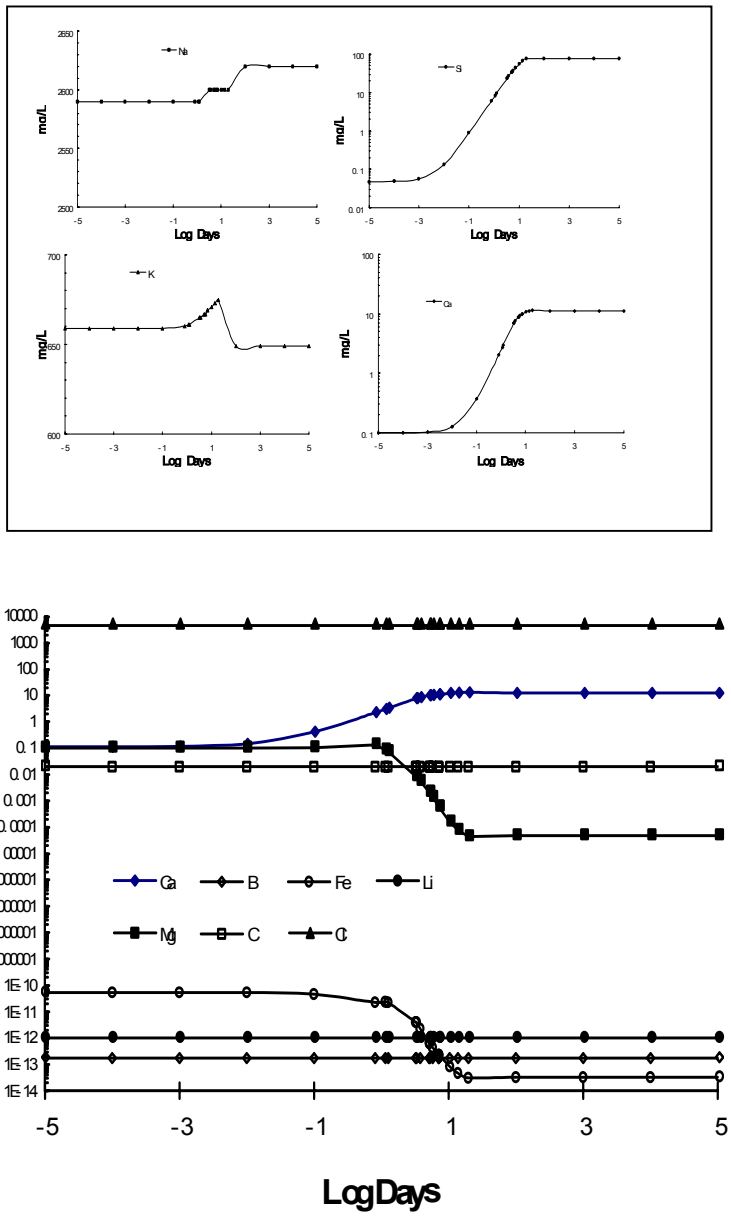

Figure 9. Modelling study of MF-M2 interaction: Evolution of elements in the solution.

3.6.2. Temperature

Temperature has a different effect on various elements in MF-M2 interaction (Fig.11). Temperature has no obvious influence on the content of the elements in the solution when temperature higher than 250°C. While content of Fe, Mg, Ca, Ti, Al, Si were affected when temperature lower than 250°C. The content of Fe in the solution decreased with the temperature between 200-150°C, but increased inversely with temperature when temperature was lower than 150°C. The content of Mg and Ca increased when temperature declined, but Ti, Al, Si decreased with decline in temperature.

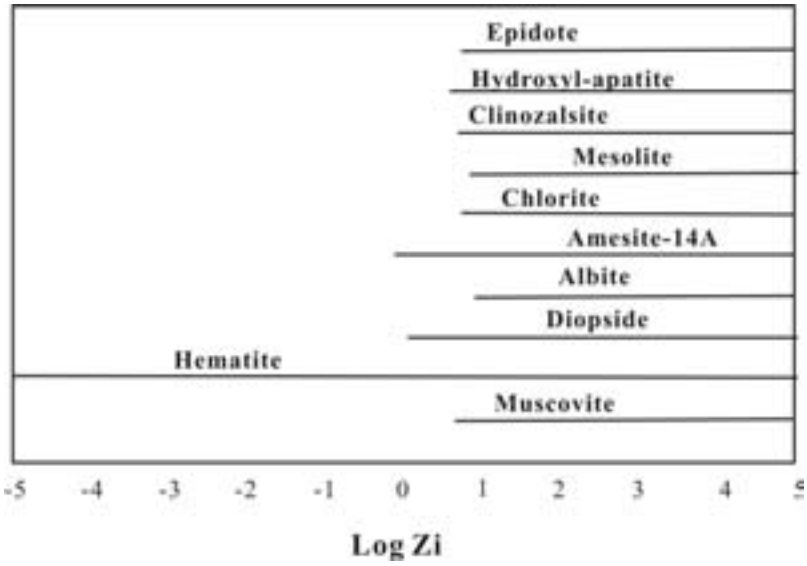

Figure 10. Modelling study of mf-m2 interaction: precipitated of the secondary minerals.

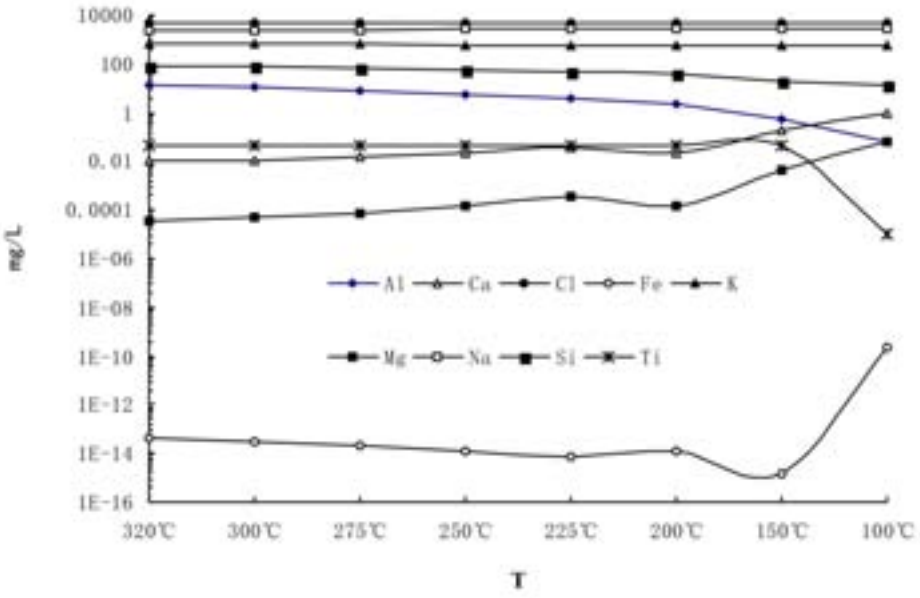

Figure 11. Modelling study of mf-m2 interaction: temperature on the elements content.

3.6.3. Formation of the geothermal fluids

The fluids samples used in the modelling and experimental studying are the Na, Cl, K enriched fluids which were the products of the long time water-rock interaction, not the original water of the water-rock interaction. To verify if the local meteoric water could evolve into the geothermal fluid through the water-rock interaction, the modelling study of distilled water –andesite interaction had been carried out. The evolution of elements and precipitation of secondary minerals is shown in Fig.12. and Fig.13. At the early stage of the water-rock interaction, the element contents were very low and increased slowly. In the later stage, some elements had obviously changed. For instance, the content of Si, K, Na and Al in the solution slowly increased at the early stage and then increased sharply. At the later stage of the water-rock interaction, the content of Ca, Mg and Fe in the solution decreased sharply with the precipitated of the secondary minerals such as hydroxyl-apatite, amesite-14A, chlorite, muscovite, hematite, phlogopite, clinozoisite, biotite and epidote. But the content of Ti, C, B, Li, S, Cl were almost fixed throughout the water-rock interaction processes.

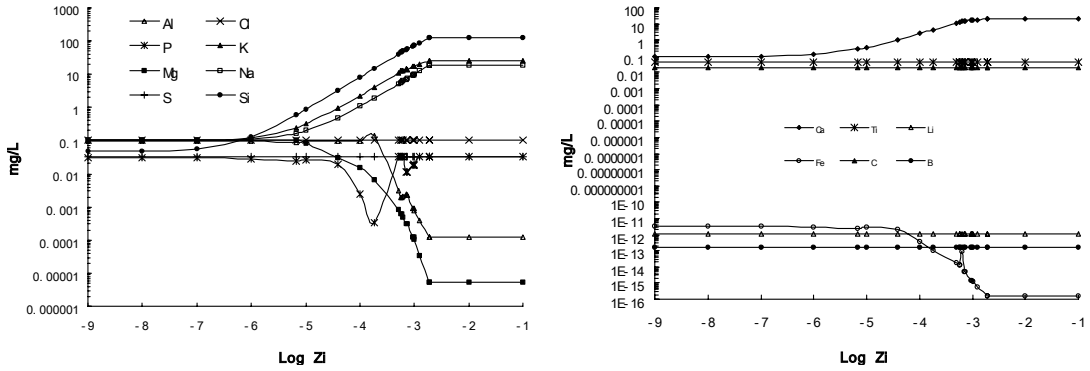

Figure 12. Modelling study of distilled water-M2 interaction: The evolution of elements in the solution.

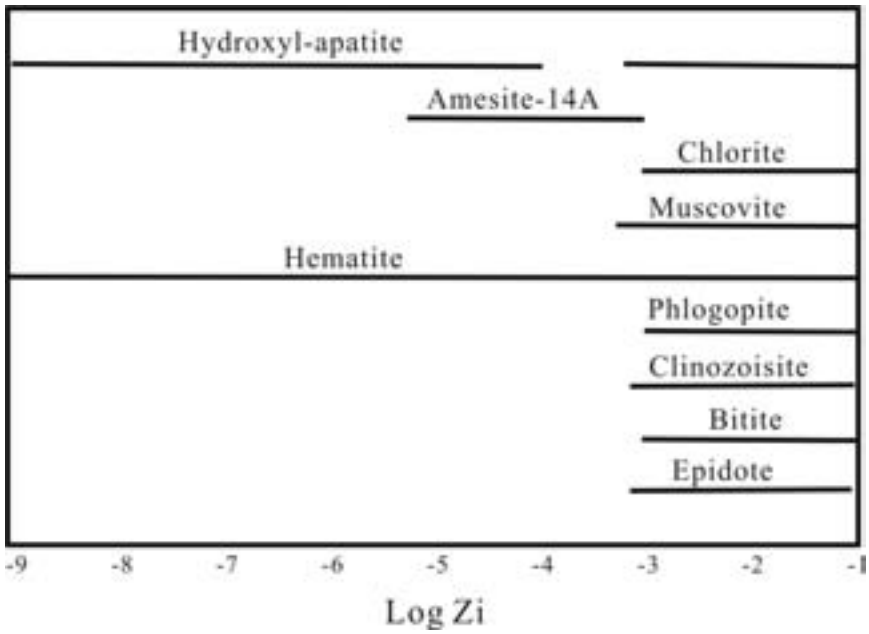

Figure 13. Modelling study of distilled water-M2 interaction: precipitated of the secondary minerals.

4. Origin and evolution of the geothermal fluid

Based on the experimental and modelling studying, the origin and evolution of the acid geothermal fluid might could be deduced as follows:

4.1. Formation of the acid geothermal fluid

It was believed that water-rock interaction was one of the major factors in the formation of the acid geothermal fluid. In this section, the authors focus on the water-rock interaction in the studied hydrothermal system. Based on the field study, rock geochemistry study, and experimental and modelling studies, water-rock interaction in Los Azufres could be divided into two stages: a deeper high-temperature stage and a near-surface stage. They had different characteristics and different products.

4.1.1. Deeper high-temperature WRI

Microscope and electron microprobe analyses revealed that the rock-forming minerals in fresh andesite from the Los Azufres geothermal field include augite, andesine and labradorite, biotite and other minerals. The secondary minerals in altered rock M3 and the experiment product formed by water-rock interaction were actinolite, diopside, epidote, chlorite, albite, hematite, muscovite, calcite and quartz. This data indicated that the following water-rock interaction took place in the K, Na, CO_2 enriched geothermal fluid at high-temperatures (250-350°C). The typical reactions were:

$$2(Ca,Mg,Fe,Al)_2[(Si,Al)_2O_6] + H_2O = Ca_2FeAl_2Si_2O_{12}OH + H^+ \quad (1)$$

augite epidote

$$5Ca(Fe,Mg)[Si_2O_6] + H_2O = Ca_2(Fe,Mg)_5[Si_8O_{22}](OH)_2 + 3Ca^{2+} + 2SiO_2 \quad (2)$$

diopside actinolite

$$2NaCaAl_3Si_5O_8 + 2SiO_2 + H_2O = Ca_2Al_3Si_3O_{12}(OH) + 3NaAlSi_3O_8 + H^+ \quad (3)$$

andesine clinozoisite albite

$$2K(Mg,Fe)_3AlSi_3O_{10} + 4\,H^+ = (Mg,Fe)_5Al_2Si_3O_{10}(OH)_8 + 2K^+ + (Mg,Fe)^{2+} + 3SiO_2 \quad (4)$$

biotite chlorite

$$2Na_{0.5}Ca_{0.5}AlSi_3O_8 + Na^+ + K^+ = NaAlSi_3O_8 + KAlSi_3O_8 + 0.5Na + Ca^{2+} \quad (5)$$

feldspar albite potash feldspar

The reactions above represented the typical reactions between andesite with K, Na, CO_2 enriched thermal fluid in Los Azufres, and form the main paragenesis: actinolite + epidote + chlorite + albite; moreover, H^+, Ca^{2+}, CO_2 increased in the fluid. This H^+, Ca^{2+}, CO_2 enriched fluid flowed up and was involved in near-surface low-temperature interactions.

4.1.2. Near-surface low-temperature WRI

The main reactions were the incongruent reactions at low-temperature in Los Azufres. The minerals formed were calcite, kaolinite and amorphous silicoide. H_2S in the fluid changed into sulphur or SO_4^{2-} by the oxidation. The represent reactions were:

$$Na_{0.5}Ca_{0.5}AlSi_3O_8 + 6H_2CO_3 + 11H_2O = 2Na^+ + 2Ca^{2+} + 4H_2SiO_4 + 6HCO_3^- + 3Al_2Si_2O_5(OH)_4 \quad (6)$$

Andesine kaolinite

$$3Ca^{2+} + 3H_2CO_3 = 3\ CaCO_3 + 6H^+ \quad (7)$$

$$Al_2Si_2O_5(OH)_4 + 5\ H_2O = 2H_2SiO_4 + Al_2O_3 \cdot 3H_2O \quad (8)$$

$$H_4SiO_4 = SiO_2 + 2\ H_2O \quad (9)$$

$$2H_2S + O_2 = 2\ H_2O + S \quad (10)$$

$$2S + 3O_2 + H_2O = 4H^+ + 2SO_4^{2-} \quad (11)$$

Thus cristobalite and well-crystallized kaolinite (in M8 rock sample) and CT-Opal (in M6 and M7 rock samples) were formed through the indicated water-rock interactions. At the same time some acid species such as H^+, H_2SiO_4, SO_4^{2-}, HCO_3^- were formed. This might be one of the major factors of the formation of acid fluid in the surface.

4.2. Origin and evolution of the geothermal fluid

The origin and evolution of the thermal fluid in a geothermal system was always one of the most important but also most disputed questions. Through the study of rock geochemistry along with experimental and model study, combined with the isotopic data, a conceptual model of the origin and evolution of the thermal fluid in Los Azufres geothermal system had been set up as following (Fig. 14). First heat, Na, Cl, H_2S, and CO_2, contained in andesitic water and magmatic water ascended from a magma chamber. Local meteoric water infiltrated through the faults in pyroclastic rock and mixed with the andesitic water flowing up in the andesitic rock zone, and formed the original thermal fluid. Then interaction between this original fluid and andesite took place, and oxygen isotopes exchanged between the water and rock, resulting in $\delta^{18}O$ decrease in rocks and $\delta^{18}O$ increase in water. At the same time the main paragenesis: actinolite + epidote + chlorite + albite formed in the altered rock, which made the contents of Si and Ca decrease in the altered rocks, but increase in the fluids. Silica precipitated in sequence as cristobalite and CT-opal as the temperature declined. H_2S in the fluid changed into sulfur or SO_4^{2-} by oxidation forming an acid fluid.

5. Conclusions

(1) Water-rock interactions of the studied geothermal fields reached equilibrium under deep high-temperature conditions. The equilibrium temperatures are between 300–340°C. An oxygen isotope shift of 3.5–6‰ was found in water from production wells and $\delta^{18}O$ decreased in andesite due to high-temperature water-rock interaction.

(2) Water-rock interactions at Los Azufres can be divided into two stages: a deeper high-temperature water-rock interaction stage and a near-surface water-rock interaction stage. These interactions

have different characteristics and different products. During the deeper high-temperature water-rock interactions, porphyritic crystals of pyroxene and feldspar were changed into diopside, actinolite, epidote, actinolite-Hb, K-feldspar and albite, the contents of SiO_2 and CaO in the altered rock decreased, and Al_2O_3, Fe_2O_3, K_2O, Na_2O, TiO_2 increased. In the near-surface water-rock interactions, the influential factors may be more complex than those of the deeper high-temperature interactions, but the products are simpler, these include complex mixtures of CT-opal and cristobalite, and well-crystallized kaolinite.

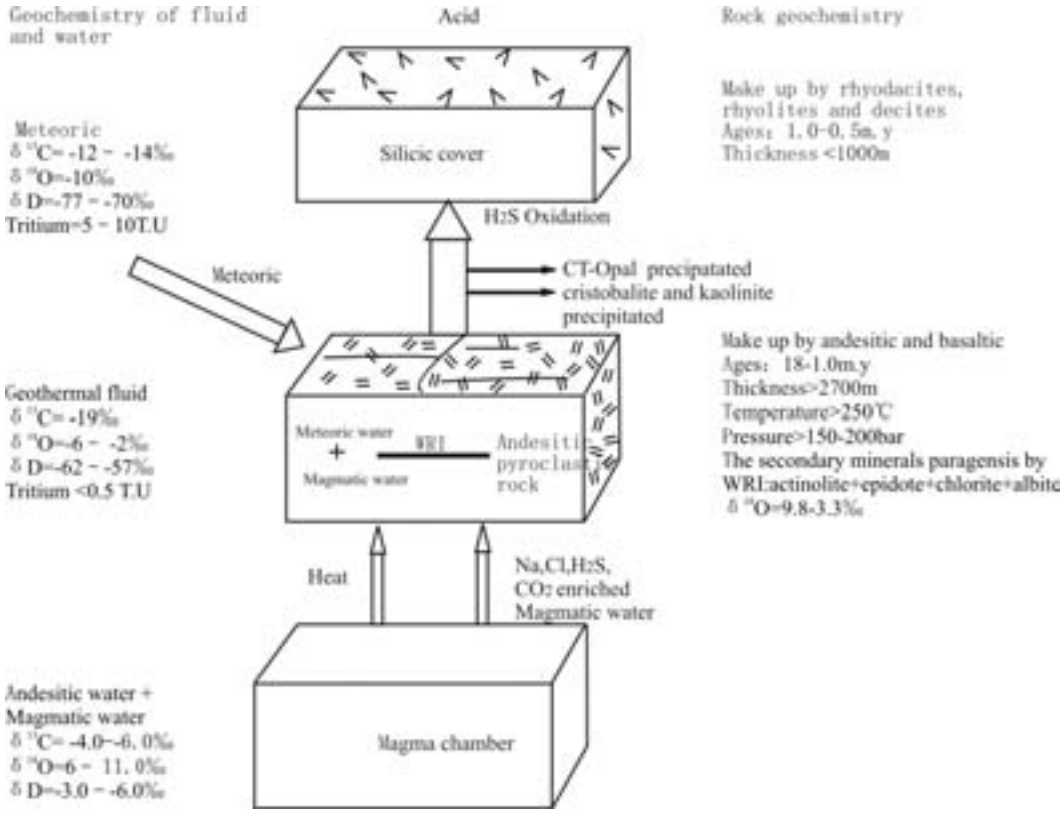

Figure 14. Model of origin and evolution of the geothermal fluid in Los Azufres geothermal field.

(3) Electron microprobe analysis indicated that the main dark porphyritic crystals in the original experimental rock sample from the Los Azufres geothermal field are augite and hematite, light porphyritic crystals are andesine or andesine to labradorite having normal girdle banding. But in the rock cylinder after experimental the main very little altered minerals around the porphyritic crystals are diopside, actinolite, epidote, albite, K-feldspar, hematite, chlorite, sphene, SiO_2 and actinolite-Hb.

(4) The modelling study of MF-M2 andesite interaction indicated that the evolution of the elements in the solution is different. Contents of Na, Si, Ca increased continuously, Cl, B, C, Li, Ti were almost fixed, and Mg, Fe decreased. The contents of K and Al reached the peak during 1-10 days, and then declined 10 days later. The regular pattern of K, Na, Ca was in accord with the experimental study.

Acknowledgements

This project is financially supported by the International Atomic Energy Agency Research Contract No. CPR-9716. Special thanks are due to our Mexican colleagues of the IIE for providing the water samples. The authors greatly appreciate the help and support from the National Key Laboratory on Mineral Deposit Research at Nanjing University, China. The authors would like to thank Alfred Truesdell for reviewing the manuscript and for constructive comments that have helped to greatly improve the contents and the language.

REFERENCES

[1] ZHANG ZHANSHI, 2000. Study of water-rock interaction in active hydrothermal system--with case study of Los Azufres in Mexico and Tongonan in the Philippines. Thesis for Master Degree of East China Geological Institute.

[2] XIONG XIAOLIN, 1998. Experiment on the fluid/melt partition of fluorine in the system albite granite-H_2O-HF. *Geochemistry,*Vol.27,66–73 (in Chinese)

[3] TELLO, H., E. 1997, Geochemical model update of the Los Azufres, Mexico, Geothermal Reservoir. GRC Transactions, Vol.21, 441–448

[4] TORRES-ALVARADO, I.S., 2000. Mineral chemical of hydrothermal silicates in Los Azufres geothermal field, Mexico. *Proceedings world geothermal congress*, 2000, Kyushu-Tohoku, Japan, May 28–June 10. 1861–1866

[5] DOBSON P. F. and MAHOOD G.A., 1985. Volcanic stratigraphy of the Los Azufres geothermal area, Mexico. *Journal of Volcanology and Geothermal Research* 25,273–287

[6] GIGGENBACH W. F., 1992, Isotopic shifts in waters from geothermal and volcanic systems along convergent plate boundaries and their origin. *Earth and planetary science letters*, 113, 495–510

[7] GIGGENBACH, W. F., 1988: Geothermal solute equilibria. Derivation of Na-K-Mg-Ca geoindicators. *Geochim. Cosmochim. Acta, 52*, 2749–2765.

ENVIRONMENTAL ISOTOPES OF GEOTHERMAL FLUIDS IN SIBAYAK GEOTHERMAL FIELD

Z. Abidin[1], D. Alip[1], L. Nenneng[1], P.I. Ristin[1], A. Fauzi[2]

[1]Centre for Research and Development of Isotopes and Radiation Technology, BATAN, Jakarta, Indonesia
[2]PERTAMINA Geothermal Indonesia, Jakarta, Indonesia

Abstract. Sibayak is located in a young volcanic area of North Sumatra, Indonesia. The surface manifestations such as acid springs, fumaroles and acid alterations indicate that Sibayak geothermal field is probably associated with the volcanic system. The aims of this study are to define the origin of the geothermal fluids, reservoir temperature and interactions between the volcanic system and the geothermal reservoir. Chemical composition, stable isotopes $^{18}O_{H2O}$, $^{18}O_{SO4}$, D_{H2O}, $^{34}S_{H2S}$, and $^{34}S_{SO4}$ of water and gas samples from the geothermal surface manifestations and exploration wells are analyzed. $\delta^{18}O$ and δD values show that the reservoir fluids of Sibayak geothermal field come from meteoric water that is recharged at an elevation of 1300–1500 masl. Geothermometers based on $\delta^{18}O_{H2O-SO4}$, water chemistry ($T_{Na-K-Ca}$) and gas chemistry (T_{H2-Ar}) show similar reservoir temperatures that range from 250 to 280°C. $\delta^{18}O$, δD isotope composition of the steam vents at the cone of Sibayak mountain, having the value of -2.9 $^{o}/_{oo}$ for $\delta^{18}O$ and –44.9 $^{o}/_{oo}$ for δD, shows magmatic inputs.

1. Introduction

Sibayak geothermal field is situated in Brastagi highland, North Sumatra. Sibayak complex consists of caldera's rim called Singkut caldera with some volcanic cones such as Sibayak, Pintou and Prategtekan. There are ten production wells with a capacity of 25 MWe.

The study was conducted to assess the origin of acidic fluids based on isotope and geochemical investigations. Surface manifestations including acid springs, magmatic gas trace and acid alteration indicate that Sibayak geothermal field is probably associated with the volcanic system. The study of fluid origin and geothermometer is very important to know the influence of the magmatic system on the neutral reservoir and geochemical process occurring in the system. Isotopes of ^{18}O and D from water samples (rain and reservoir waters), ^{18}O and ^{34}S from aqueous sulphate, ^{34}S from H_2S gas, chemistry (cation and anion) of water and gas samples from surface manifestations and geothermal wells. Fluid sampling of wells is conducted using a Weber separator or from the Weir box.

2. Geological setting

Plate movement of Indian-Australia in Sumatra trench is oblique. It is not relatively vertical as occurred in Java trench causing strike slip fault and volcanic arc in Sumatra. The process causes possible crustal magmatic heat sources becoming shallow, and secondary permeability as a geothermal reservoir occurred. Physiographically, Sibayak geothermal field is located in the Brastagi highlands, North Sumatra. The old Sibayak activity was started in 0.5 Ma, then the caldera of Sibayak collapsed in 0.1 Ma, and finally volcanic activity appeared such as Prategtekan and young Sibayak. The morphology seems to be a rims caldera that is called Singkut. Inside, the caldera is occupied by volcanic cones of Sibayak, Pintou and Prategtekan.

Stratigraphically, according to the drilling in Sibayak field, it can be divided into four kinds of rock (from bottom to upper part). Those are meta sediment, andesite, andesite brecia and tuff. The sediment rock acts as the geothermal reservoir. Bedrock of Sibayak geothermal field consists of meta sediment intercalation with sandstone and claystone. This rock is covered by volcanic rock of Sibayak, Singkut,

Prategtekan and Simpul Angin activity consisting of andesite lava, andesite brecia, tuff brecia and tuff (Figure 1).

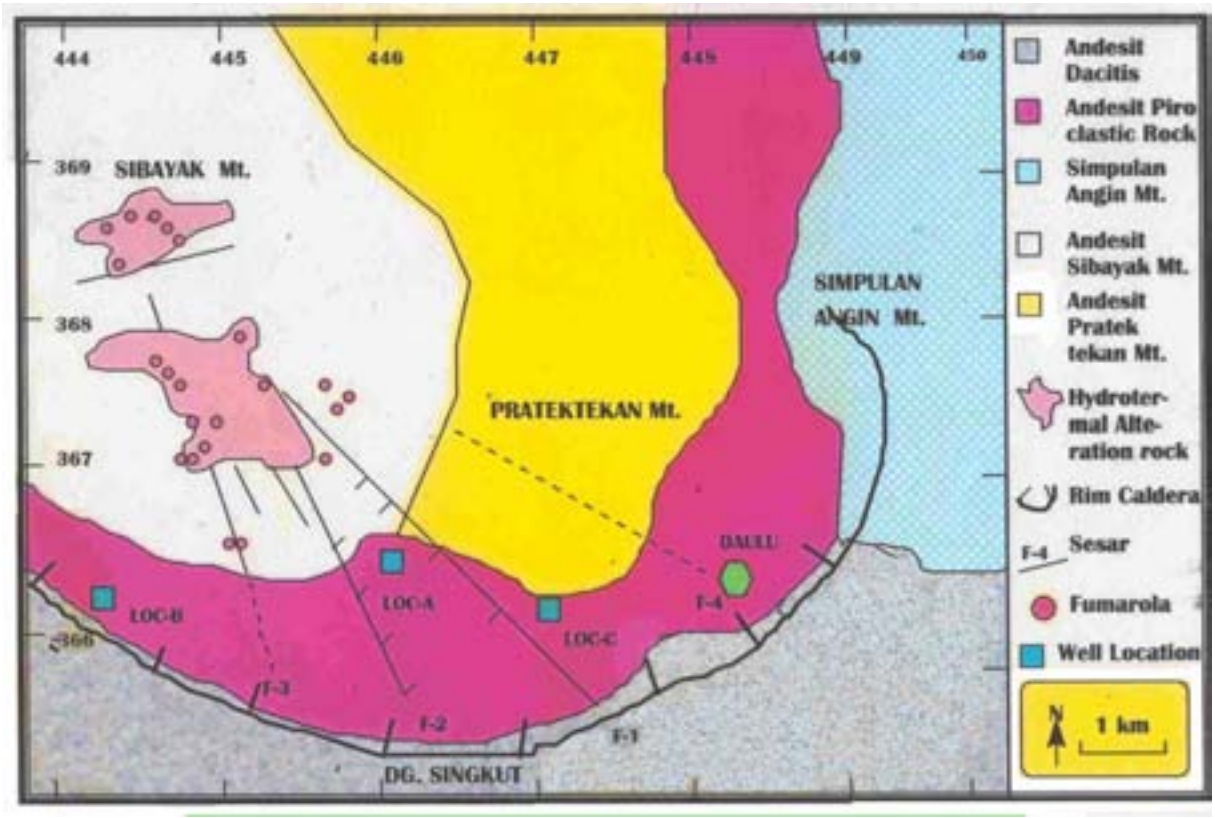

Figure 1. Geological map of Sibayak Geothermal Field.

Structural geology that has developed in Sibayak area is normal fault with west-north southeast direction. The fault structure has formed a valley that has a radial pattern with the centre located in Sibayak Mountain. Geothermal manifestations in the valley are fumaroles, solfatara and hot springs.

Hydrothermal alterations as argilisation, silification and chloritisation are found in Sibayak wells number one, two and three, while propilisation alteration is characterized by epidotic mineral that is only found in Sibayak wells number one and three. Epidotic mineral is found at the depth of 50 meters under sea level and 200 meters above sea level. The formation temperature exchange at the wells of Sibayak one and three is higher (T = 247 ^{o}C) at the deeper location according to quantity/amount of alteration mineral. While Sibayak well number two at the depth 230 m, the alteration rock is still argilisation, chloritisation and silisification and the existing identity of high temperature mineral of above 150 ^{o}C is not yet found. From the three locations of wells, it is clear that the temperature is higher to the north direction (Sibayak mountain).

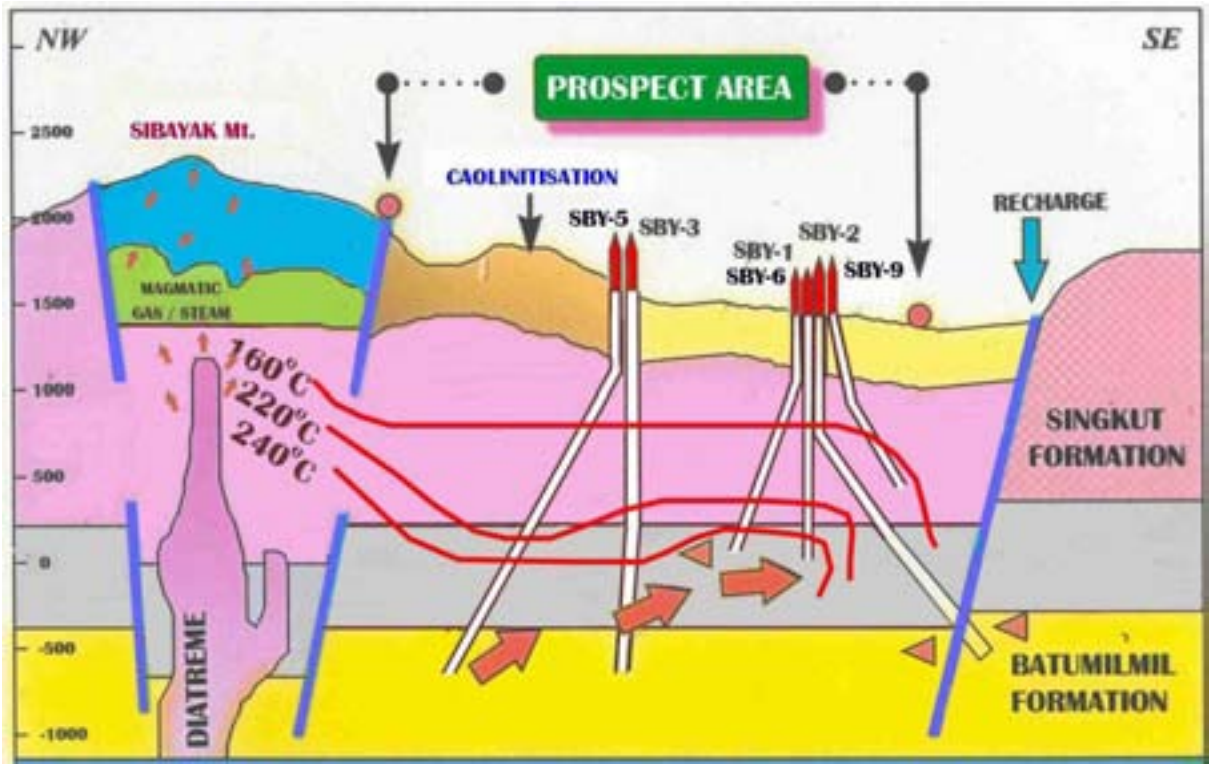

Figure 2. A geological cross section of Sibayak geothermal field.

3. Methodology

3.1. Sample collection

Sampling of fluids is divided into 2 groups, i.e. surface manifestations and wells.

3.1.1. Surface manifestations

Samples of acid springs, steam vent and hot springs were taken at the surface for the following analyses:

Samples of acid springs for chemistry, ^{18}O and ^{34}S in sulphate, ^{18}O and D in H_2O

Samples of steam vents were taken using stainless steel pipe connected to special gas bottle filled by NaOH 4 N solution using silicon rubber tube. The sample was analyzed for gases (CO_2, H_2S, He, H_2, Ar, N_2, CH_4 and SO_2) as well as ^{34}S isotope in H_2S, in sulphate ion. A volume of 20 ml was taken for analysis of H_2O

Samples of hot springs were taken from the location with volume of two litres for analysis of chemical and ^{18}O and ^{34}S in sulphate. A volume of 20 ml was taken for analysis of ^{18}O and D.

3.1.2. Deep wells

Samples of three deep wells SBY-3, 5 and 6 were taken using a Weber separator with a pressure gauge and a thermometer. Sample from separator and weir box was used for analyzing its isotope composition as follows:

SPW sample for analyzing chemical, ^{18}O and ^{34}S in sulphate and ^{18}O and D in H_2O.

SCS sample for analyzing chemical, ^{18}O and D, gas and ^{34}S isotope in H_2S

Sample of weir box for analyzing chemical, ^{18}O and D.

3.2. Chemical analysis

Na, K, Ca, Mg and Li cations are analyzed using atomic absorption spectrometer
SO_4, CO_3 and Cl anions are analyzed using UV-Vis
Non-condensable gases of He, H_2, CH_4, Ar and N_2 are analyzed using Gas Chromatography
Condensable gases of CO_2 and H_2S are analyzed using titration method

3.3. Stable isotope analysis

3.3.1. ^{18}O and Deuterium in H^2O

^{18}O and D is analysed using Epstein-Mayeda method through exchange reaction:

$$H2\,^{18}O + C^{16}O_2 \leftrightarrow H_2\,^{16}O + C^{18}O_2$$

2 ml of water sample is reacted by CO_2 gas during 6 hour in isoprep analyzer until reach equilibrium. The CO_2 gas was passed through to the mass spectrometer.

Deuterium in H_2O is analyzed using Zn (BDH) method through redox reaction as below:

$$Zn + H_2O \xrightarrow[\text{Vacuum}]{480\,^\circ C} ZnO + H_2$$

0.3 grams of Zn reacts with 10 ul of water sample and is heated to 480 °C in vacuum condition. H_2 gas then is passed through to the mass spectrometer.

3.3.2. ^{18}O and ^{34}S in SO_4

Sample was precipitated as $BaSO_4$. ^{18}O in $BaSO_4$ is analyzed using Mizutani-Rafter method through reaction:

$$SO_4^{=} + 2\,C \leftrightarrow S^{=} + 2CO_2$$

^{34}S in BaSO4 is analyzed using Kusakabe-Robinson method through reaction:

$$S^{=} + Ag^{+} \leftrightarrow Ag_2S$$
$$S + 2CuO \leftrightarrow 4Cu + SO_2$$

CO_2, H_2 and SO_2 gases from the reactions above are then measured using the mass spectrometer for $^{18}O/^{16}O$, D/H, and $^{34}S/^{32}S$ ratios.

3.4. Data Reduction

3.4.1. Mass Spectrometer Calculation

The measurement result of Mass Spectrometer is expressed in terms of (δ) in per mill deviation of the isotope ratio from that of the standard.

$$\delta = \frac{Rx - Rs}{Rs} * 1000\text{o/oo} \qquad (1)$$

Where: Rx = isotope ratio of sample, Rs = isotope ratio of standard.

For ^{18}O in H_2O, the standards SMOW, ^{34}S are CDT and ^{18}O in SO4 are PDB. For calculating of geothermometer, $\delta\ ^{18}O$ in PDB is converted into $\delta\ ^{18}O$ SMOW according to the formula:

$$\delta\ ^{18}O\ SMOW = 1.04143 * (\delta\ ^{18}O \text{ in PDB}) + 41.43 \qquad (2)$$

3.4.2. Isotope Geothermometers

T $^{18}O_{H2O\text{-}SO4}$ and T $^{18}O_{SO4\text{-}H2S}$ geothermometers have different ranges of temperatures. T $^{18}O_{H2O\text{-}SO4}$ is 100–300 °C while T $^{18}O_{SO4\text{-}H2S}$ is 250–500°C.

Calculation of those geothermometers is as follows:

For T $^{18}O_{H2O\text{-}SO4:}$

$$1000 Ln\alpha_1 = \frac{2.88 * 10^6}{T^2} - 4.1 \quad (3)$$

$$1000 Ln\alpha_2 = \frac{6.02 * 10^6}{T^2} - 2.6 \quad (4)$$

Where,

$$Ln\alpha_1 = \frac{1000 + \delta^{18}O_{SO_4}}{1000 + \delta^{18}O_{H_2O}} \qquad (5)$$

$$Ln\alpha_2 = \frac{1000 + \delta^{18}O_{SO_4}}{1000 + \delta^{18}O_{H_2O}} \qquad (6)$$

4. Isotope data of ^{18}O and D from meteoric water

Table I shows ^{18}O and D isotopes data and amount of rainwater observed during rainy season between 1997 and 1998. It also shows the average rainwater isotope content that was calculated using amount effect. Data show that the isotopes ^{18}O and D content of the meteoric water at elevation 700 m asl, have δ value is –8.1 $^{o}/_{oo}$ and -50.1 $^{o}/_{oo}$ respectively, while isotope ^{18}O and D content at the higher elevation 1310 m asl, is -10.99 $^{o}/_{oo}$ and -73.29 $^{o}/_{oo}$ respectively. Isotope and elevation data in Table I, and figures 3,4 and 5 show the relationship between ^{18}O Vs D of meteoric water, ^{18}O Vs elevation and D Vs elevation respectively.

Table I. Isotopes ^{18}O and D of rain water in difference elevation in Sibayak Field

Station and Elevation	Date	Rain (mm)	^{18}O ($^{o}/_{oo}$ VSMOW)	D ($^{o}/_{oo}$ VSMOW)
Sibolangit	November 1997	305.9	-10.97	-72.1
720 m ASL	December 1997	119.3	-5.57	-33.1
	January 1998	250.1	-5.79	-32.2
	WT AVE		-8.1	-50.1
PABUM	November 1997	224.6	-12.56	-86.2
1320 m ASL	December 1997	105.1	-7.35	-46.1
	January 1998	87.5	-7.48	-45.9
	WT AVE		-10.18	-67.65
BASECAMP	November 1997	336.7	-12.45	-83.3
1310 m ASL	December 1997	123.1	-8.56	-56.1
	January 1998	109.5	-9.23	-59.1
	WT AVE		-10.99	-73.24
BERASTAGI II	November 1997	269.4	-12.11	-80.9
1510 m ASL	December 1997	104.7	-8.7	-56.2
	January 1998	93.5	-7.69	-48.3
	WT AVE		-10.97	-68.85

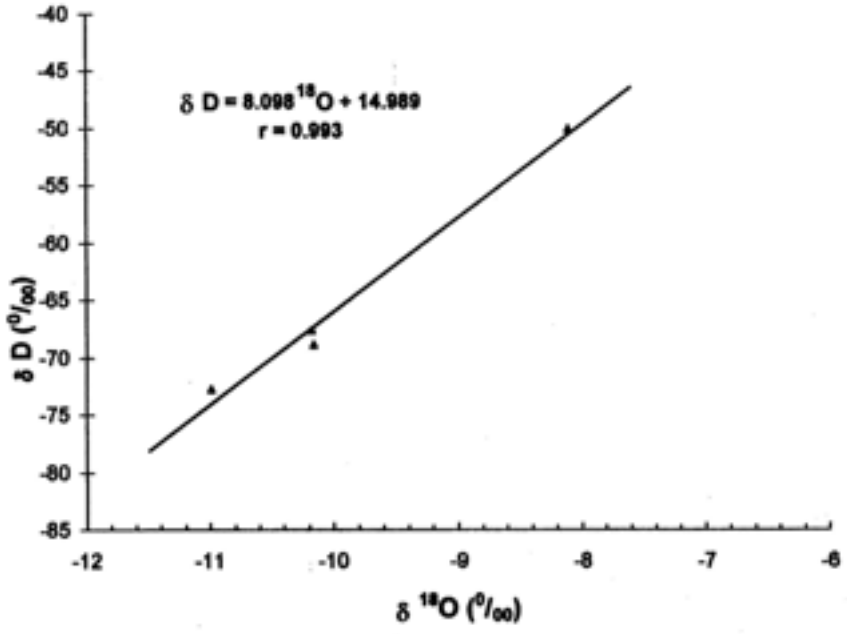

Figure 3. $\delta^{18}O$ versus δD and the local meteoric water line.

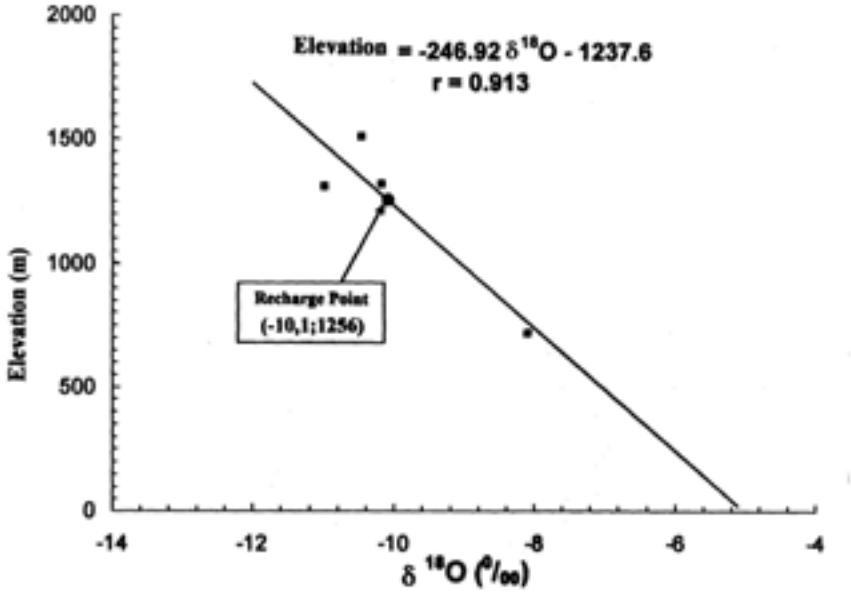

Figure 4. Correlation between δ18O and elevations of sample sites.

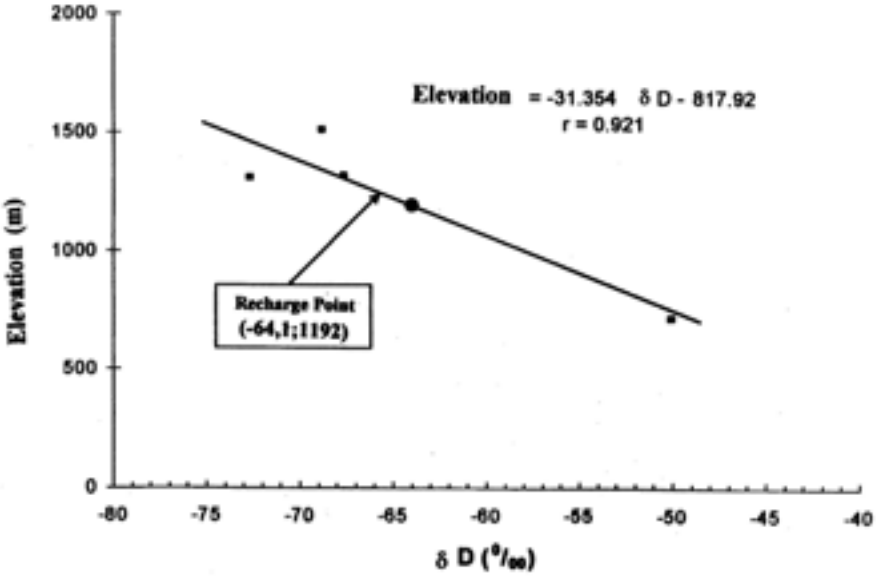

Figure 5. Correlation between δD and elevations of sample sites.

Local meteoric water line is based on the isotope content of the meteoric water from four stations at the elevation from 720 m to 1320 m asl.

$\delta D = 8.1*\delta^{18}O + 15$ (7)

The regression coefficient (r) is 0.95.

Linear regression equation ^{18}O Vs Elevation (H) of the local found is as follows,

$H = -246.92*\delta^{18}O - 1273.6$ (8)

Linear regression equation D versus Elevation (H) of the local meteoric found is as follows:

$$H = -31.354\ \delta D + 817.92 \qquad (9)$$

The regression coefficient (r) is 0.9.

The third equation mentioned above is useful to determine recharge area and origin of the Sibayak geothermal field.

5. Surface manifestations

5.1. Water chemistry

Table II shows that the chemical contents of hot springs and fumaroles in Sibayak show different values from the reservoir chemistry. Magnesium and bicarbonate ion of the hot springs have a high value ranging from 60 to 70 ppm and 120 to 300 ppm, respectively. Those are indicators of dilution effect with local groundwater, while ratio of Na/K still indicating the reservoir temperature with value 3 to 5. High sulphate content of the hot springs with range 200 to 700 ppm indicates there are oxidation processes of the H_2S gas in the near surface. Fumaroles located in the cone of the Sibayak mountain discharge acid fluids with pH >1. The fluids have very high sulphate concentrations about 7500 ppm, while chloride content is about 300 ppm.

5.2. Stable Isotopes

Table III shows ^{18}O and D isotope data of hot springs, fumaroles and steam vents. The isotope contents of hot springs located around geothermal field are close to meteoric line. ^{18}O and D isotope contents of the steam vents discharging near Sibayak crater at an elevation of 2200 m asl show enriched values of -3.0 $^{o}/_{oo}$ and -45.0 $^{o}/_{oo,}$ respectively. The average $\delta^{34}S$ value of the H_2S from steam vent discharge is + 1.67 $^{o}/_{oo.}$ It is more depleted than production wells and supposing that value is close to the ^{34}S magmatic or influenced by magmatic sources.

6. Deep geothermal wells

6.1. Water Chemistry

Chemical analytical results from monitoring wells are presented in Table IV. Cation and anion of Na, K and Ca are important parameters that have played a role in chemical geothermometer. The Na/K ratio of the third well is around 3 to 5 value, while Ca concentration that has value around 60 ppm, will influence the reservoir temperature. Concentration of chloride end sulphate anions of the wells show significant value. The Chloride content of the SBY-3, 5 and 6 wells are 1333.6 ppm, 1212.0 ppm and 887.0 ppm respectively. Higher sulphate content are shown by acid spring that has concentration of 7748 ppm.

Table II Chemical data of the hot springs and Fumaroles

No	Site name	Sample code	Chemical concentration (ppm)									
			Na	K	Ca	Mg	Li	Rb	Cs	Cl	HCO_3	SO_4
4	Smg.Gn_1	MAP	93.1	25.8	31.1	67	00.7	0.07	ttd	89.0	121.6	631.4
	Smg.Gn_2	MAP	78.7	26.9	32.6	55	00.8	0.05	ttd	81.0	112.5	600.5
	Smg.Gn_3	MAP	85.6	26.1	29.8	60	00.7	0.05	ttd	85.0	115.1	620.0
5	L-Debuk$^2_1$	MAP	71.8	15.8	27.1	58.7	0.04	0.05	ttd	55.8	369.1	199.0
	L-Debuk$^2_2$	MAP	60.2	15.4	20.3	42.7	0.04	ttd	ttd	58.2	345.0	182.1
	L-Debuk$^2_3$	MAP	65.7	16.2	23.4	56.6	0.04	ttd	ttd	52.1	132.4	188.5
6	Antara A-B_1	MAP	103.7	26.5	123	72.6	0.07	0.07	ttd	84.8	132.4	711.9
	Antara A-B_2	MAP	93.2	25.6	113.5	64.9	0.08	ttd	0.07	81.2	125.6	692.0
	Antara A-B_3	MAP	96.7	25.1	120.6	68.3	0.07	ttd	0.08	79.8	135.8	701.9
7	Lokasi C_1	MAP	15.3	8.5	0.6	1.2	0.01	0.04	ttd	11.0	0.0	597.5
	Lokasi C_2	MAP	17.8	10.5	0.9	3.2	0.02	ttd	ttd	12.2	0.0	560.3
	Lokasi C_3	MAP	16.1	9.7	0.7	1.9	0.01	ttd	ttd	11.9	0.0	575.2
8	Kawah$_1$	Fum	25.9	13.9	0.8	6.5	Ttd	ttd	ttd	331	0.0	7963
	Kawah$_2$	Fum	29.3	24.4	0.7	10.2	ttd	ttd	ttd	295	0.0	7688
	Kawah$_3$	Fum	26.7	17.6	0.8	7.9	ttd	ttd	ttd	301	0.0	7595

6.2. Gas chemistry

Condensable and non-condensable gas data from wells can be seen in Table V. The concentration unit is expressed in mmol/mol steam. CO_2 gas content of the Sibayak wells is higher than 80 % of the total gas, while H_2S gas content is approximately 10 % of the total gas. The non-condensable gas such as N2, He, Ar and CH_4 concentration is very small i.e. less than 1 % of the total gas. He gas is the highest one having concentration of 0.03 mmol/mol.

6.3. Stable isotope

Analysis result of ^{18}O and D isotope three wells can be seen in Table VI which consists of separated water sample (spw), separator steam condensate (scs) and weir box. Concentration of $\delta^{18}O$ and δ D of SCS sample of the three wells is -11.0 $^{o}/_{oo}$ and - 70.0 $^{o}/_{oo}$ respectively, while isotope concentration of SPW sample is more enriched, i.e. around –8.6 $^{o}/_{oo}$ for ^{18}O and -58.0 $^{o}/_{oo}$ for D isotopes. Weir box samples have the most enrichment of $\delta^{18}O$ and δ D comparing with SCS and SPW samples. That is due to atmospheric evaporation processes through steam separation with steam fraction about 30 %. The $\delta^{18}O$ and δ D content of three production wells of weir box samples is around -7.5 $^{o}/_{oo}$ and - 55.0 $^{o}/_{oo}$ respectively. Table VI shows isotopes data of ^{18}O and ^{34}S in sulphate ion and ^{34}S in H_2S gas from three sampling periods. Average of $^{18}O_{SO4}$ concentration for SBY-3,5 and 6 production wells corresponds to SMOW standard is isotope -3.62 $^{o}/_{oo}$, -3.67 $^{o}/_{oo}$ and - 3.82 $^{o}/_{oo}$ respectively, while its isotope $^{34}S_{SO4}$ for those production wells corresponding to CDT standard are -18.13 $^{o}/_{oo}$, -17.13 $^{o}/_{oo}$ and -17.87 $^{o}/_{oo}$ respectively. Isotope ^{34}S concentration of H_2S gas from three production wells, shows average value i.e. -3.31 $^{o}/_{oo}$, -3.72 $^{o}/_{oo}$ and -4.30 $^{o}/_{oo}$ respectively.

Table III. Isotope data for surface manifestations in Sibayak geothermal field

Source	Date	Type	^{18}O (H_2O)	^{2}H ($^{o}/_{oo}$ VSMOW)	^{18}O (SO_4)	^{34}S ($^{o}/_{oo}$ VCDT)	Elevation (m)
Kawah	Nov.97	FUM	-6.1	-42.6	+2.63	+3.31	2000
Kawah	Mar.98	FUM	-6.2	-43.2	+2.66	+3.60	
Kawah	Nov.98	FUM	-5.3	-39.5	+2.63	+3.49	
Loc. B	Nov.97	HS	-9.6	-58.2	-7.12	+3.90	1310
Loc. B	Mar.98	HS	-9.5	-57.0	-7.24	+4.10	
Loc. B	Nov.98	HS	-9.3	-56.1	-7.08	+4.0	
Loc. C	Nov.97	HS	-10.1	-64.7	-8.43	+4.47	1310
Loc. C	Mar.98	HS	-10.3	-65.0	-8.64	+4.81	
Loc. C	Nov.98	HS	-10.2	-65.0	-8.57	+4.60	
L. Debuk	Nov.97	HS	-10.6	-67.6	-7.85	+3.82	1300
L. Debuk	Mar.98	HS	-10.7	-67.0	-7.33	+3.93	
L. Debuk	Nov.98	HS	-10.6	-67.1	-7.32	+3.91	
S. Gunung	Nov.97	HS	-9.8	-62.3	NA	NA	1300
S. Gunung	Mar.98	HS	-9.6	-61.5	NA	NA	
S. Gunung	Nov.98	HS	-9.6	-61.5	NA	NA	
S. Vent	Nov.97	SV	-3.0	-45.7	NA	NA	2200
S. Vent	Mar.98	SV	-2.9	-45.1	NA	NA	
S. Vent	Nov.98	SV	-2.7	-43.8	NA	NA	

7. General discussions

7.1. ^{18}O and D isotope composition of the reservoir fluid

^{18}O and D isotope content of the reservoir can be calculated based on the total discharge equation from separator of well influenced by steam fraction and separation temperature. ^{18}O and D isotopes from calculation result of the SBY-3, 5 and 6 wells are (-9.2 $^{o}/_{oo}$ and -64.3 $^{o}/_{oo}$), (-9.15 $^{o}/_{oo}$ and -65.1 $^{o}/_{oo}$) and (-1.2 $^{o}/_{oo}$ and -63.0 $^{o}/_{oo}$) respectively. Average of the D value from those wells is -64.1 $^{o}/_{oo,}$ it represents value of the meteoric water that recharges to the reservoir.

Figure 6 shows the isotope composition of the reservoir constructed from weirbox, SPW and SCS. The ^{18}O isotope composition in reservoir calculated from three wells is relatively similar having the value of about -9.1 $^{o}/_{oo}$. The value shows that Sibayak geothermal fluids have relatively small ^{18}O shift which is about 1 $^{o}/_{oo}$. The ^{18}O shift reflects insensitive reaction between water and the rocks. It may be due to rock alteration or water dilution in the reservoir.

^{18}O and D isotopes composition of the Sibayak fluids reservoir is not influenced by andesitic water or volcanic system, although ^{18}O and D isotopes composition of the steam vent exhales at the cone of Sibayak Mountain showing andesitic water as shown in Figure 4.

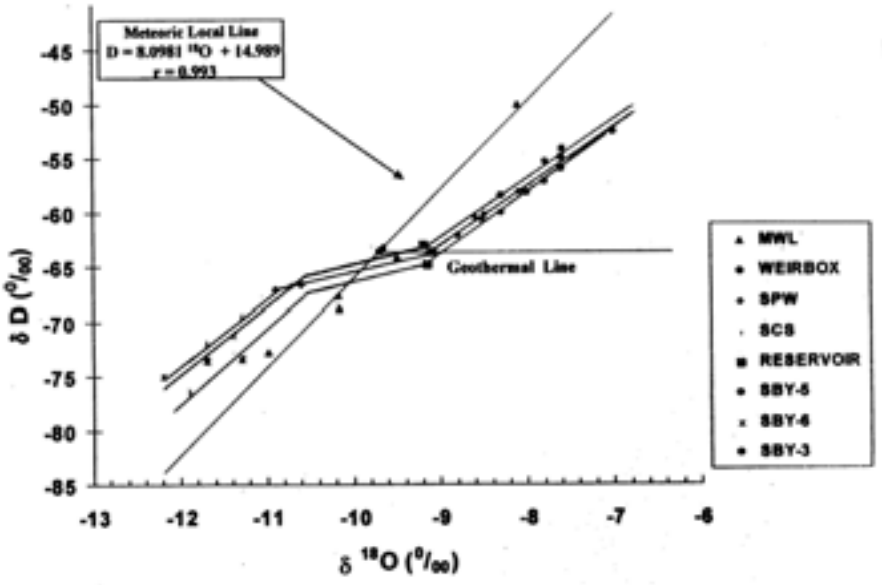

Figure 6. Isotopic composition of geothermal fluids from production wells.

Table IV Chemical data for the production wells in Sibayak geothermal field

No	Production Wells	Source	Chemical Concentration (ppm)										Ionic Balance
			Na	K	Ca	Mg	Li	Rb	Cs	Cl	HCO_3	SO_4	(%)
1.	SBY-3	SPW_1	18.3	7.3	1.4	0.08	0.05	0.04	Ttd	40	0.0	18.5	-
		SPW_2	969	196	69.5	0.30	1.80	0.80	1.67	1542	19.5	55.2	2.58
		SPW_3	1012	212	74.2	0.25	1.87	0.76	1.59	1616	18.9	53.4	5.88
		SCS_1	11.7	1.9	ttd	ttd	ttd	ttd	ttd	21.5	0.0	10.8	21.1
		SCS_2	10.8	ttd	ttd	ttd	ttd	ttd	ttd	18.6	0.0	7.9	19.03
		SCS_3	9.4	ttd	ttd	ttd	ttd	ttd	ttd	18.0	0.0	7.1	23.65
		WBX_1	1285	276	87.3	0.5	2.08	0.94	1.96	1925	23.8	62.8	8.83
		WBX_2	1136	259	79.8	0.66	2.74	1.29	1.77	1897	30.1	58.5	3.89
		WBX_3	1205	265	82.6	0.42	2.15	1.05	1.82	1910	27.6	65.1	6.06
		Reservoir	830.50	178.49	58.38	0.31	1.29	0.71	130	1333.56	17.67	43.8	-
2.	SBY-5	SPW_1	740	269	91.8	0.75	225	0.03	1.96	1410	25.0	64	2.49
		SPW_2	731	238	87.4	0.63	228	1.17	1.56	1463	35.1	60.2	0.92
		SPW_3	745	251	88.2	0.40	219	0.95	1.67	1442	29.8	59.8	0.92
		SCS_1	11.2	6.8	ttd	ttd	ttd	ttd	ttd	18.3	10.3	1.4	11.63
		SCS_2	2.31	ttd	ttd	ttd	ttd	ttd	ttd	2.0	1.0	1.2	42.86
		SCS_3	5.4	ttd	ttd	ttd	ttd	ttd	ttd	3.5	2.1	2.0	15.90
		WBX_1	919	339.8	111.3	0.66	2.72	1.19	2.39	1783	50.7	50.0	1.77
		WBX_2	935	300.1	98.7	0.46	2.49	1.29	1.84	1801	55.8	56.2	0.16
		WBX_3	901	295.8	101.2	0.58	2.52	1.10	1.96	1792	49.3	49.8	0.76
		Reservoir	621.8	211.9	72.6	0.45	1.81	0.71	143	1212.04	30.36	43.16	-
3.	SBY-6	SPW_1	601	208	208	68.4	1.0	1.0	1.96	1090	54.9	45.4	3.08
		SPW_2	625	196	196	64.5	1.03	0.92	1.13	1123	51.0	43.8	2.61
		SPW_3	611	202	202	66.7	0.97	1.05	1.58	1109	50.2	46..3	3.56
		SCS_1	8.8	4.6	4.6	ttd	ttd	ttd	ttd	14.4	0.0	17.6	21.88
		SCS_2	3.3	ttd	ttd	ttd	ttd	ttd	ttd	5.6	0.0	5.2	31.70
		SCS_3	5.0	2.2	2.2	ttd	ttd	ttd	ttd	7.2	0.0	6.8	12.90
		WBX_1	665	246	246	103	1.2	0.84	1.52	1257	59.9	48.2	3.46
		WBX_2	640	224	224	98.7	1.0	1.04	1.21	1232	56.1	50.2	2.08
		WBX_3	653	235	235	99.2	0.98	0.92	1.36	1260	58.4	51.0	2.04
		Reservoir	460.5	158.81	60.3	0.75	1.02	0.70	107	857.07	40.07	34.55	-

Table V Chemical data on gas samples for production wells and steam vents in Sibayak geothermal field

No	Well	Chemical concentration (mmol/mol of steam)						
		CO_2	H_2S	H_2	CH_4	Ar	He	N_2
1	SBY-3							
	Nov. 97	8.7134	0.9666	0.0174	0.0212	0.00084	0.0316	0.0324
	Mar.98	8.9434	1.0381	0.0199	0.0187	0.00078	0.0472	0.0345
	Nov. 98	9.4054	1.0021	0.0305	0.0347	0.00119	0.0964	0.0410
2	SBY-5							
	Nov.97	10.9015	1.1383	0.0628	0.0145	0.00127	0.0302	0.0414
	Mar.98	12.1908	1.4790	0.0939	0.0611	0.00153	0.0519	0.0589
	Nov.98	8.3745	1.4135	0.0827	0.0326	0.00256	0.0295	0.0900
3	SBY-6							
	Nov.97	11.5255	1.6899	0.0521	0.0167	0.00159	0.0295	0.0492
	Mar.98	12.1908	1.7334	0.0527	0.0251	0.00158	0.0932	0.0527
	Nov.98	8.3745	1.2184	0.0351	0.0110	0.00182	0.0137	0.0351
4	Steam vent							
	Nov.97	99.102	6.8648	0.6674	0.0219	0.0088	0.5440	0.6674
	Mar.98	51.807	2.8883	0.5915	0.0024	0.0076	0.3101	0.5915
	Nov. 98	102.98	6.0632	0.3799	0.0039	0.0056	0.5712	0.3799

Table VI Isotope data for well samples in Sibayak geothermal field collected using a mini separator or the weir box.

Well	Date	Source	Sampling Press. (Barg)	^{18}O H_2O (‰)	^{2}H	^{18}O Cond. (‰)	^{2}H	^{18}O Res (‰)	^{2}H	^{18}O SO_4	^{34}S	^{34}S H_2S
SBY-3	Nov.97	Separator	7.0	-10.9	-67.1	-11.3	-67.8	-11.0	-67.2	-	-	-3.35
SBY-3	Mar.98	Separator	7.8	-9.5	-64.3	-11.7	-68.0	-9.9	-65.0	-	-	-3.24
SBY-3	Nov.98	Separator	7.0	-10.6	-66.5	-11.4	-68.2	-10.8	-66.8	-	-	-3.34
SBY-3	Nov.97	WBX	ATM	-8.3	-58.0	-	-	-9.8	-66.4	-3.18	-18.5	-
SBY-3	Mar.98	WBX	ATM	-7.6	-55.0	-	-	-9.1	-63.4	-3.08	-18.0	-
SBY-3	Nov.98	WBX	ATM	-7.0	-52.6	-	-	-8.5	-61.0	-3.98	-17.9	-
SBY-5	Nov.97	Separator	10.0	-8.8	-61.3	-11.3	-73.4	-9.2	-63.2	-	-	-4.04
SBY-5	Mar.98	Separator	8.7	-8.5	-60.3	-11.9	-75.4	-9.1	-63.0	-	-	-3.4
SBY-5	Nov.98	Separator	4.0	-8.3	-60.0	-11.3	-73.2	-9.0	-63.0	-	-	-3.72
SBY-5	Nov.97	WBX	ATM	-8.0	-58.2	-	-	-9.2	-66.6	-3.5	+17.5	-
SBY-5	Mar.98	WBX	ATM	NA	NA	NA	NA	NA	NA	-3.3	+16.8	-
SBY-5	Nov.98	WBX	ATM	NA	NA	NA	NA	NA	NA	-4.2	+17.1	-
SBY-6	Nov.97	Separator	3.0	-8.6	-60.5	-11.7	-73.6	-9.4	-63.7	-		+4.7
SBY-6	Mar.98	Separator	3.8	-8.5	-60.5	-12.2	-75.0	-9.4	-64.0	-		+4.2
SBY-6	Nov.98	Separator	3.0	-8.1	-58.1	-11.7	-73.4	-9.0	-61.8	-		+4.0
SBY-6	Nov.97	WBX	ATM	-7.6	-54.1	-	-	-9.1	-62.5	-4.06	+17.9	-
SBY-6	Mar.98	WBX	ATM	-7.8	-55.2	-	-	-9.3	-63.5	-3.8	+18.0	-
SBY-6	Nov.98	WBX	ATM	-7.6	-54.1	-	-	-9.1	-62.5	-3.7	+17.7	-

Table VII Reservoir temperatures calculated using chemical and isotopic geothermometers

Well	TNK	TNKC	TKM	$T_{CO2-H2S}$	T_{H2-CO2}	T_{H2S}	T_{H2}	T_{H2-Ar}	$T^{18}O$	$T^{34}S$
SBY-3	293	251	217	293	284	324	284	275	273	343
SBY-5	350	2755	216	294	275	325	280	289	269	479
SBY-6	355	272	192	303	307	355	290	255	266	474
S.Vent	-	-	-	341	340	363	293	255	-	-

7.2. Recharge area

Figure 6 shows that ^{18}O and D isotope composition of recharge fluid to the reservoir is on the local meteoric line with a value of -10.1 $^{o}/_{oo}$ for ^{18}O and -64.1 $^{o}/_{oo}$ for D, respectively. If the isotope composition mentioned above is plotted into Figures 4 and 5 or calculated using equations 8 and 9, elevation of recharge to the reservoir can be obtained. Using this method, recharge of Sibayak geothermal fluid is considered to be 1100 to 1300 meters above sea level in altitude.

7.3. Chemical and isotopic geothermometers

Determination of reservoir temperature using various geothermometers of equilibrium processes of chemical or geochemical such as water, gas and mineral (host rock) in a system will inform the geochemical reaction species at different depth.

This process will inform the kinetic of prime mineral dissolution and second mineral deposition with exchange of temperature and pressure from different original fluid. The result of it, various species such as ^{18}O and ^{34}S isotopes as well as Na, K, Ca and Mg cations and gases in the fluid as a result of the process, can become a geoindicator for evaluating temperature in geothermal system at various depths.

7.3.1. Isotope geothermometers of $T^{18}O_{SO4\text{-}H2O\ and}\ T^{34}S_{SO4\text{-}H2S}$

Determination of reservoir temperature at Sibayak geothermal using 2 different geothermometer methods, i.e. $T^{18}O_{SO4\text{-}H2O\ and}\ T^{34}S_{SO4\text{-}H2S,}$ can be calculated using (3), and (4) equations of each equilibrium of SO_4-H_2O and SO_4-H_2S. The result of the calculation is shown in Table VII.

The calculation of reservoir temperature made from both geothermometer methods is very different. The average temperature calculated based on $T^{18}O_{SO4\text{-}H2O}$ $\pm 270^{o}C$ whereas based on $T^{34}S_{SO4\text{-}H2S}$ is $\pm$ $450^{o}C$. This difference does not show inconsistency of those geothermometers caused by isotopic equilibrium of geothermometers at different depth and condition.

Isotope equilibrium of ^{34}S in SO_4^{2}-H_2S species takes place deeper and very slowly. Therefore, when the fluid is moving up to the surface accompanied by exchange of temperature at the next reservoir, it does not change the formerly obtained equilibrium. The equilibrium process of SO_4-H_2S generally takes place at primer neutralized area where SO_4 and H_2S are in liquid phase. This process is in the hydrothermal system being close to association of volcanic-magmatic.

To the contrary, reservoir temperature shown by $T^{18}O_{SO4\text{-}H2O}$ takes place at reservoir dominated by water (liquid) at a shallower area where isotope equilibrium exchange of ^{18}O in SO_4 and H_2O will take place when brought into contact with water.

Figure 7 shows reaction processes of species interaction of SO_4^{2}-H_2O at geothermal reservoir having concentration of ^{18}O sulfate and being relatively enriched with isotopes concentration of ^{18}O in H_2O, because in this condition $^{18}O_{H2O}$ moves to sulfate compound. Based on the calculation of geothermometer $T^{18}O_{SO4\text{-}H2O,}$ the reservoir temperature of Sibayak is considered 260 to $270^{o}C$. The temperature obtained is relatively close to actual reservoir temperature at the present.

7.3.2. Chemical geothermometers

The main cations Ca, K and Mg as the result of dissolution and interaction between mineral, water and gas are geo-indicators for determining reservoir temperature and geochemistry equilibrium. Using the

equation presented by Fournier and Giggenbach, $T_{Na-K,}$ $T_{Na-K-Ca}$ and T_{Mg} geothermometer of production wells SBY-3, 5 and 6. Table XIII shows calculation result of chemical geothermometer.

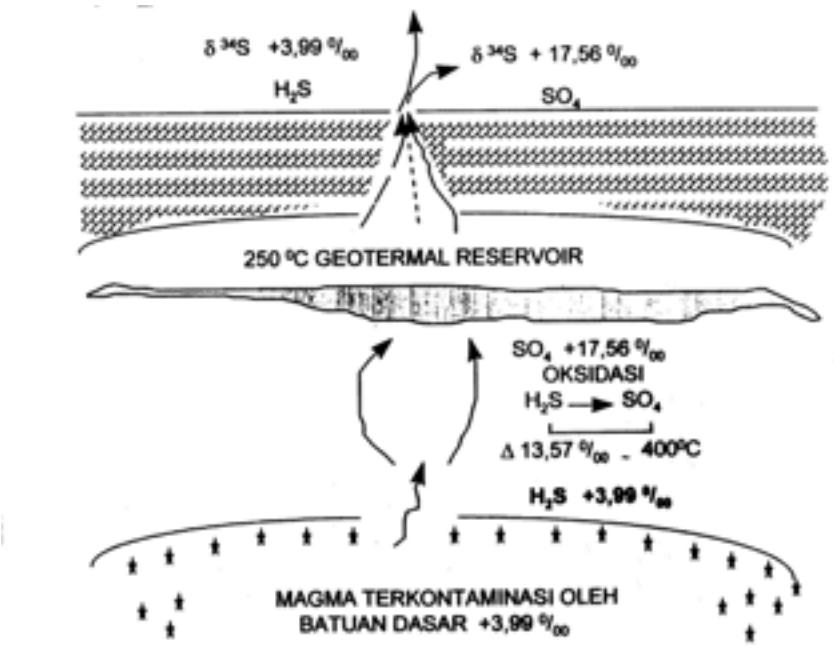

Figure 7. Evolution of δ34S in Sibayak geothermal field

The above table shows temperature based on T_{Na-K} reaching 350 ^oC (290-350^oC), whereas $T_{Na-K-Ca}$ shows temperature of 250 –270^oC and T_{Mg-K} shows the lowest temperature i.e. 190 – 217^oC.

K in T_{Na-K} is the element distributing temperature increasing where K element formed at the beginning of mineral dissolution (primer neutralization) at equilibrium of albite-feldspar. $T_{Na-K-Ca}$ especially Ca element is the element indicator decreasing temperature where Ca formed from Alumina-Silica-feldspar equilibrium. Temperature of $T_{Na-K-Ca}$ is close to measurement of custer in geothermal reservoir.

Figure 8 shows geothermometers of 4 main elements in equilibrium conditions that are different in graphic of correlation between 10 Mg (10 Mg + Ca) Vs 10 K (10K + Na) presented by Giggenbach. The graphic shows that production wells SBY-3, 5 and 6 are close to equilibrium line at the temperature 290-300 ^oC. It looks more representative showing the equilibrium of K, Na, Mg and Ca elements with secondary mineral.

7.3.3. Gas Geothermometer

The analysis data of condensable and non-condensable gas (CO_2, H_2S, He, Ar, H_2 and CH_4) show an important geo-indicator to determine reservoir temperature. In high temperature of geothermal system (>200^oC), reservoir temperature depends on the equilibrium of gases or gases-mineral controlled by concentration of the gases. There are some applicable geothermometers such as $T_{CO2-H2S}$ and T_{H2-CO2} of NEHRING and D'AMORE (1984), T_{H2S} and T_{H2} of Arnorsson and Gunlougasson (1985) and T_{h2-Ar} of Giggenbach (1989) are used to calculate the temperature of Sibayak geothermal field.

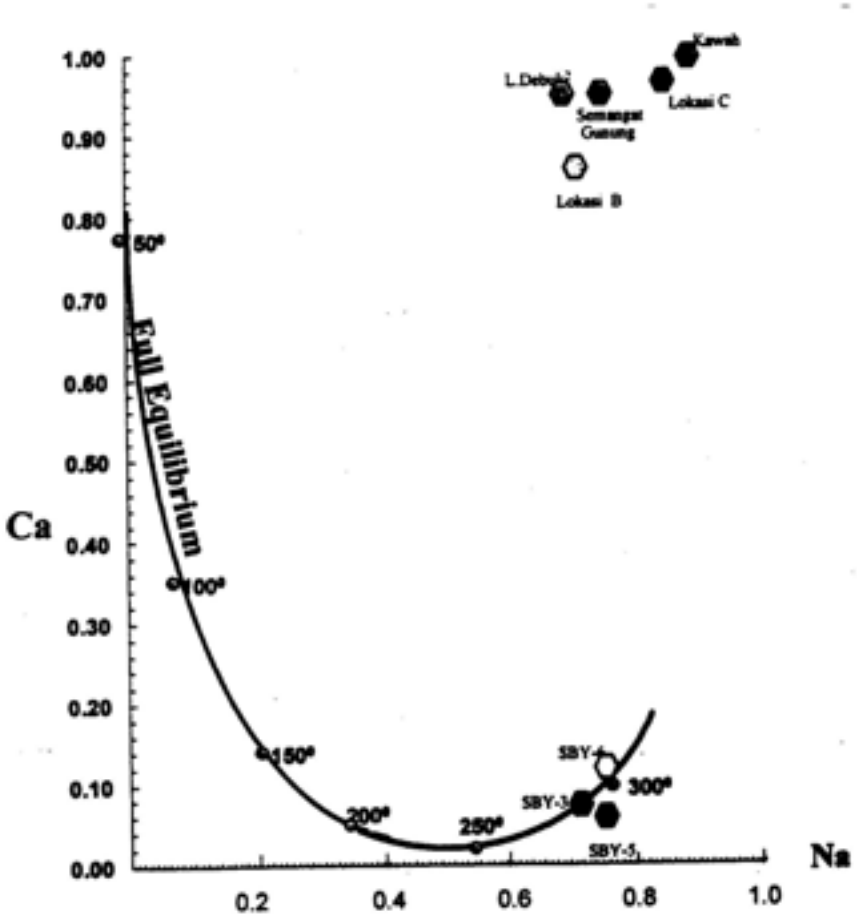

Figure 8.Chemical equilibrium based on Na, K, Ca and Mg for samples from wells, hot springs and fumaroles in Sibayak geothermal field

Table VII shows the calculation of temperature based on those geothermometers (see Appendix mathematics equation) that can be calculated from Table VIII in mmol/kg steam.

The above table shows that temperature of geothermometers $T_{CO2\text{-}H2S,}$ $T_{H2\text{-}CO2}$ and T_{H2} is relatively similar to those 3 production wells i.e. 275 – 300^{O}C, except geothermometer T_{H2S} having a temperature that is higher for those wells, i.e. 330^{o}C, whereas $T_{H2\text{-}Ar}$ shows 250 – 270^{o}C. $T_{H2\text{-}Ar}$ geothermometer has a more realistic temperature of reservoir and it is close to actual temperature.

This is caused by the Ar element originated from meteoric that can be used to indicate lower temperature. Ar gas originated from meteoric interactions with H_2 gas of deep fluid in the reservoir. Hence, gas equilibrium of H_2-Ar in fluid is similar to $T^{18}O_{SO4\text{-}H2O}$ occurring in shallower area compared to equilibrium of other gases such as CO_2-H_2S and H_2-CO_2.

Figure 9 shows equilibrium of gas multi component CO_2, H_2 and Ar in fluid phase as an equilibrium graphic of components in various temperatures presented by GIGGENBACH. The graphic shows that reservoir temperature indicated by concentration L_{CA} (log C_{CO2}/X_{Ar}) and L_{HA}(log X_{H2}/X_{Ar}) for those three wells and the steam vent is ≅ 250^{o}C.

Those multi component geothermometers show the reservoir temperature of Sibayak geothermal field. The table also shows that temperature of steam vent indicated by $T_{CO2\text{-}H2S,}$ $T_{H2\text{-}CO2}$ and T_{H2S} is 350^{o}C.

This higher temperature possibly shows equilibrium process of gas at high temperature probably affected by volcanic system.

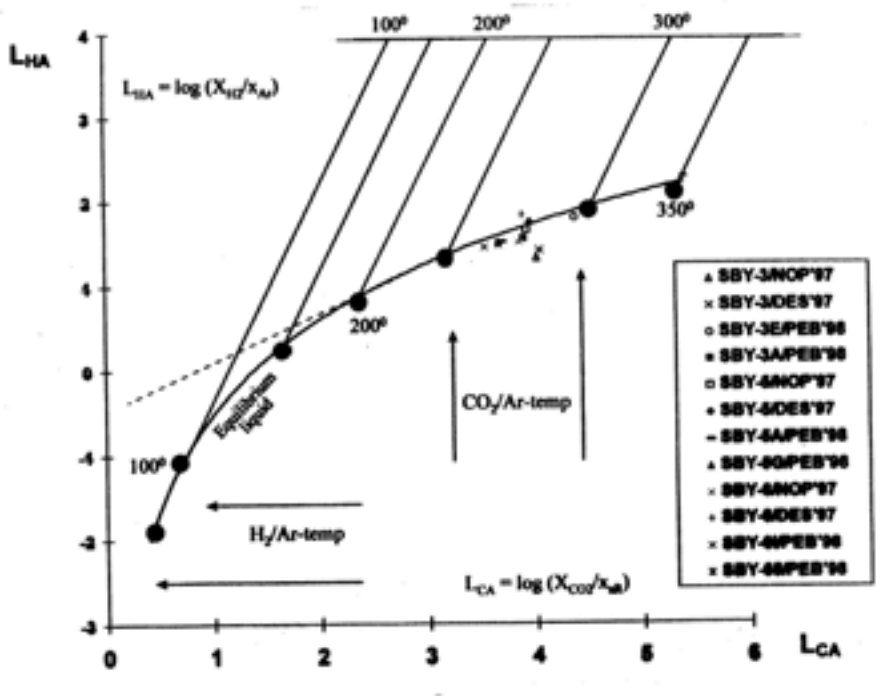

Figure 9. Ar-H_2-CO_2 gas geothermometers for well samples.

7.4. The Original Fluid

The fluid of Sibayak geothermal is "liquid dominated" having reservoir temperature ± 250°C, which is the main well producing steam. Discharge fluid in production wells SBY-3, 5 and 6 is fluid having ^{18}O and D isotope content that is identical to local meteoric. Those three wells have produced steam 80 ton/hour at SBY-3 and 100 ton/hour SBY-6 respectively, whereas SBY-5 is in bleeding condition at the present.

Figure 10 shows that ^{18}O and D isotopes from reservoir do not show great value in its ^{18}O shift (± $1^{o}/_{oo}$) and there is no mixing process with andesetic mater (magmatic). Except for the content of steam fluid from steam vent surface manifestation having more enrichment in ^{18}O and D content than fluid from surface water, the trend to mix with volcanic steam shows there. The steam vent containing ^{18}O and D isotope, respectively $-3^{o}/_{oo}$ and $-45^{o}/_{oo}$ gives the indication that steam moving up to surface comes from the process of steam extraction at high temperature. Figure 10 shows that possibility of mixing between discharge steam in steam vent and andesitic steam (magmatic) is approximately 30 %. If the composition of ^{18}O and D isotope from steam vent is compared to its composition from fumaroles, their differences will appear clearly. The composition of ^{18}O and D isotope from fumaroles more shows the process of atmospheric evaporation from the steam heated tool system and also indicates that fluid which flow out from steam vent comes from a different reservoir. The great possibility is that fluid in steam vent comes from the process of mixing between andesitic and meteoric water at high temperature.

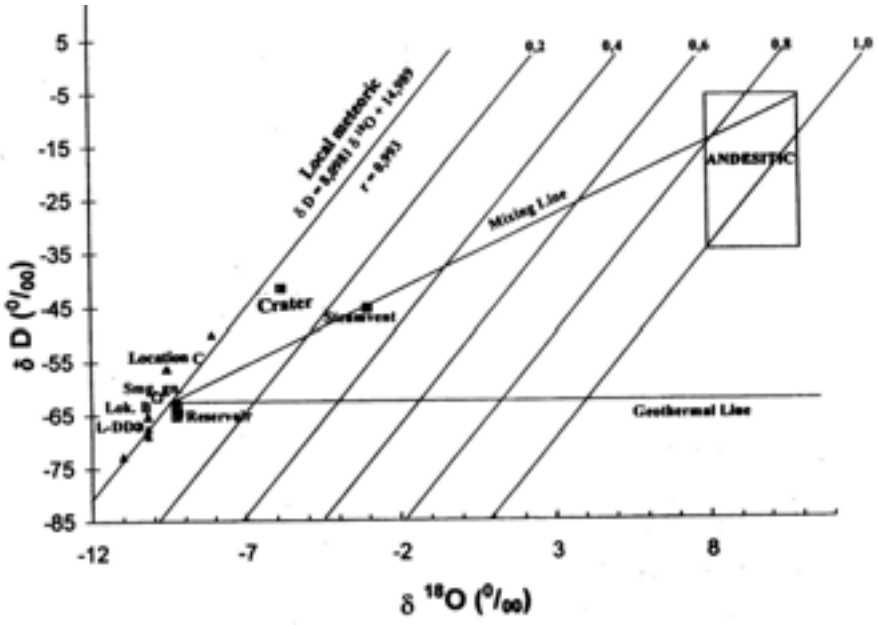

Figure 10. Isotopic composition of steam vents indicates a possible influence of magmatic fluids.

Beside the origin of water fluid explained above, it is necessary to see further about the origin of reservoir through chemical process and its gas contents. The trilinear diagram of $Cl\text{-}SO_4\text{-}HCO_3$ at Figure11 shows that reservoir fluid turns to the chloride corner at mature water area. The trilinear diagram of $CO_2\text{-}N_2\text{-}Ar$ at Figure 12 is to see clearly the origin of reservoir fluid from Sibayak field. In this diagram, the 2 sides of CO_2/N_2 and N_2/Ar gas ratio describe clearly the difference of fluid origin. CO_2/N_2 ratio shows the type of magmatic system field whereas N_2/Ar ratio shows the type of groundwater. The composition of CO_2/N_2 and N_2/Ar ratio of reservoir fluid from Sibayak does not lie on the reservoir position either magmatic or groundwater system, but it lies between them as a geothermal reservoir. Besides ^{18}O, D, chemical gases, and ^{18}O and ^{34}S in sulphate as well as ^{34}S in H_2S can play a part as a geoindicator to know the origin of fluid. Content of ^{34}S in fluid can be used as a fingerprint to know the properties of magmatic from fluid. From several analyses conducted in some places, it can be stated that the content of 34 S isotope as sulphur total magma is 0 $^{o}/_{oo}$ CDT. On the other hand, Sibayak field has ^{34}S value more variables, namely ± 1.67 up to ± 18.3 $^{o}/_{oo}$. Mostly, the production wells contain highly that ^{34} isotope from sulphate is formed from oxidation process in the deeper reservoir at primary neutralization level.

The high value of ^{34}S up to + 18 $^{o}/_{oo}$ is caused by the content of sulphate ion formed more slightly (20 – 40 ppm) so that ^{34}S from oxidized H_2S more tends to be into sulphate ion.

From ^{34}S data of Sibayak geothermal field shows that sulphur moving up to surface is dominated by host rock except sulphur content in steam vent having + 1.67 $^{o}/_{oo}$ CDT closer to the ^{34}S value from magma ($0^{o}/_{oo}$ CDT). Figure 13 shows the relationship of ^{18}O Vs ^{34}S from fumaroles and production wells. ^{34}S in sulphate for the reservoir, if compared to fumaroles, is more depleted. There is difference in the formation process to sulphate ions between them. ^{34}S isotope value that is more depleted in fumaroles shows that its sulphate ion is formed through the oxidation process from a large amount of H_2S gas in sulphate (± 7500 ppm).

Oxidation process of H_2S in surface as taken place in fumaroles, can be proved by ^{18}O value which more enriched + $2.64^{o}/_{oo}$. It is compared to ^{18}O data from reservoir $-3^{o}/_{oo}$ because ^{18}O value in O_2 is more enriched + $22^{o}/_{oo}$. In the same case, if the concentration of ^{34}S isotope in several species (SO_4 and H_2S) from Sibayak field is summed up, its value will be more than $0^{o}/_{oo}$. This reason can be seen from the field of ^{34}S analyses in SO_4 and H_2S in which all of them have enriched isotope value (positive). If it is calculated using sum of mass, the average value of ^{34}S more than $0^{o}/_{oo}$ will be obtained.

This indicates that mostly reservoir fluid of Sibayak is dominated by ^{34}S isotope from host rock and only a little part that come from magma, except ^{34}S isotope from steam vent more depleted + 1.67 $^{o}/_{oo}$.

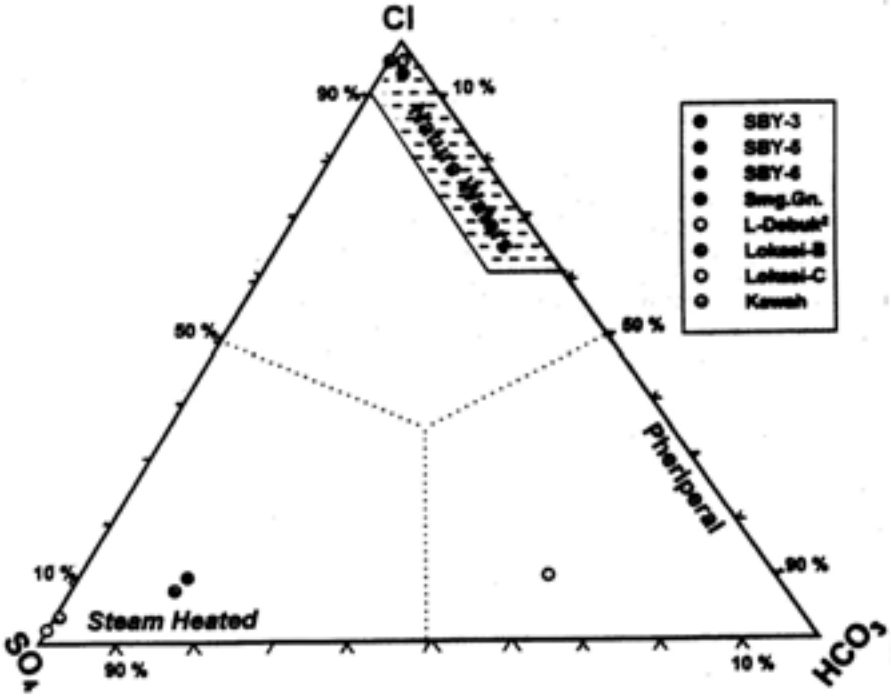

Figure 11.Piper diagram for samples from wells, hot springs and fumaroles.

7.5. Reservoir hydrology of Sibayak field

Iso-contour map of ^{18}O and chloride can be seen at Figure 14 and 15. This ^{18}O iso-contour shows that the water recharge/fluid moves from along Rim Circle of Singkut Caldera to the system. This is clearly shown by isotope contour from hot spring near to crater which has ^{18}O value ~ -10 $^{o}/_{oo}$. This value is more depleted if it is compared to the isotope concentration from Sibayak reservoir. Although the recharge water moves along Singkut fault toward north direction, ^{18}O shift reactions do not take place progressively. This might be caused by the rock properties that have undergone alteration processes (because of the mature rock). Figure-14 also shows that potential reservoir is located at point A, B and D toward north direction where there is a considerable developing border in the North. This is appointed by borderline located at 1700 m height.

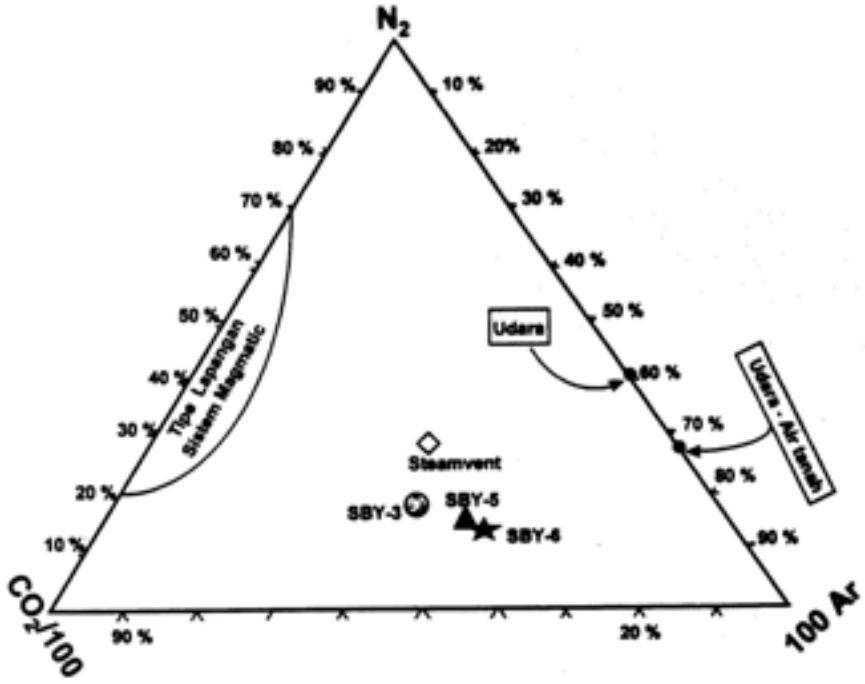

Figure 12. Trilinear diagram for gas samples from wells, hot springs and fumaroles.

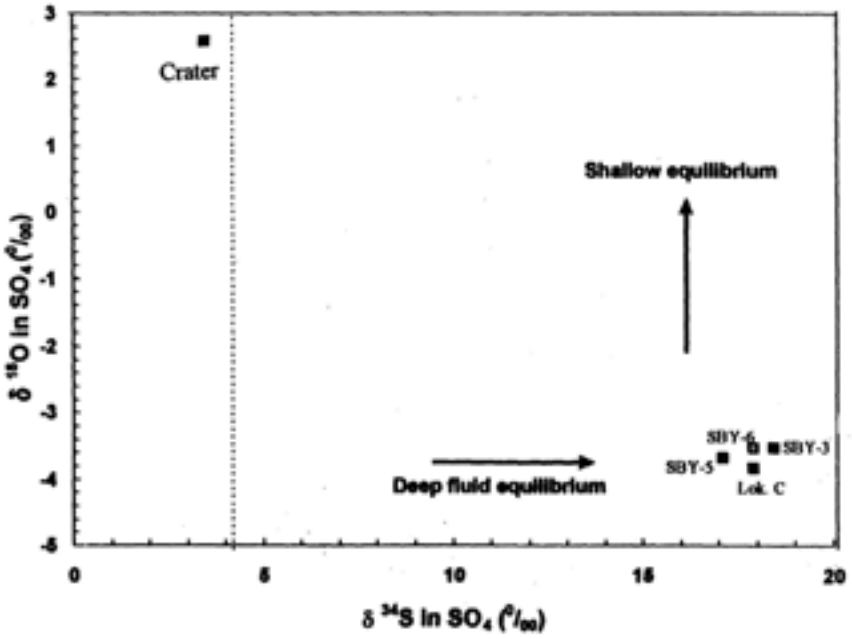

Figure 13. δ18O versus δ34S in SO4 for geothermal fluids in Sibayak.

Figure 15 shows that chloride content in the up flow zone ranges from 800–1300 ppm. The content of chloride in southern or northern Singkut fault gives the lower value because of dilution influence from recharge water. On the other hand, the chloride content gives the higher value in the direction to crater. Both sources show that reservoir in crater vicinity is potential (called as up flow zone). Hydrology of temperature iso-contour in reservoir can be seen in Figure 16. This figure gives information of

temperature iso-contour through cross-section that is completed by production wells of SBY-1, 2, 3, 5 and 6.

The iso-contour line for 250 ^{o}C and 300 ^{o}C is based on gas, chemical and isotope geothermometer, whereas the iso-contour line for 150 ^{o}C and 200 ^{o}C is based on the temperature gained from Kuster measurement of SBY-3, SBY-2 and SBY-1. Based on hydrology of temperature iso-contour, it is estimated that the up flow zone is located around the crater, and also it is known that the temperature is lower more southern of Rim caldera in Singkut. This figure shows that fluid movement is from the up flow zone to caldera Rim whereas the recharge water (originated from ground water) moves from Rim caldera. The model hydrology also shows the possibilities of fluid origin whether they come from production well or steam vent.

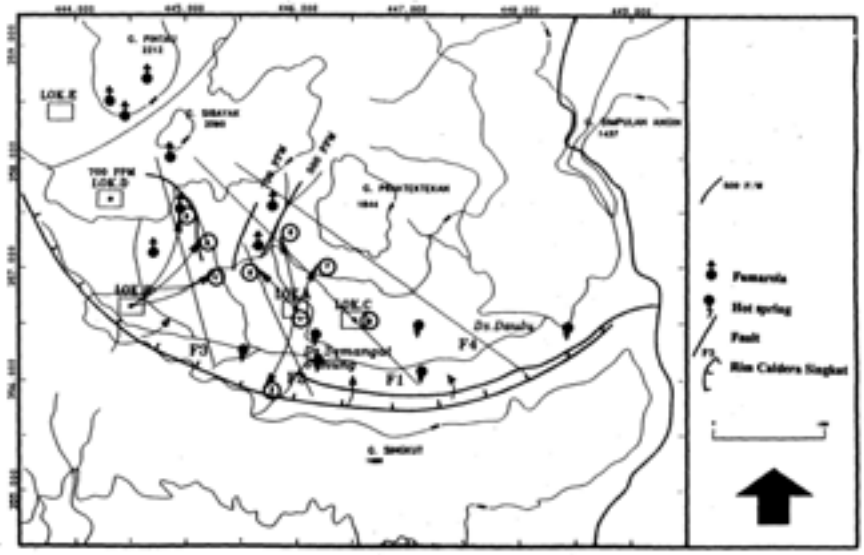

Figure 14. Iso-contour map for δ18O in geothermal fluids of Sibayak.

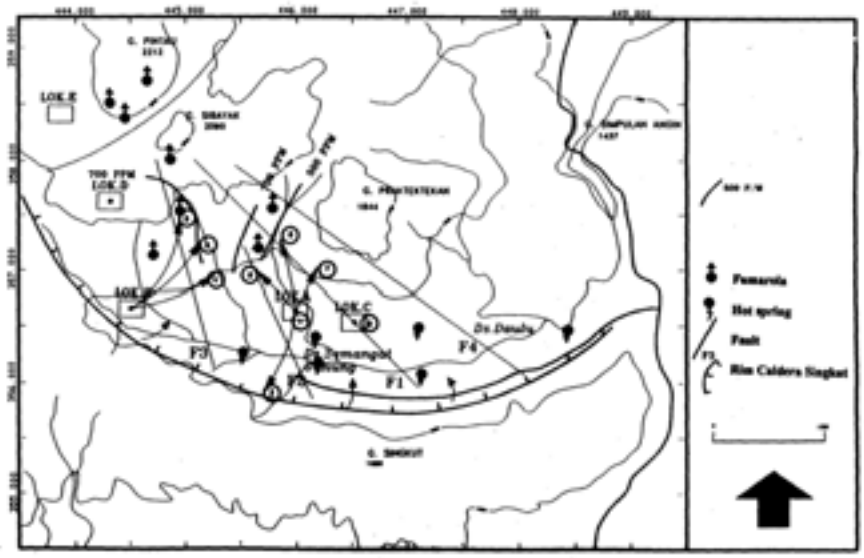

Figure 15. Iso-contour map for Cl in geothermal fluids of Sibayak.

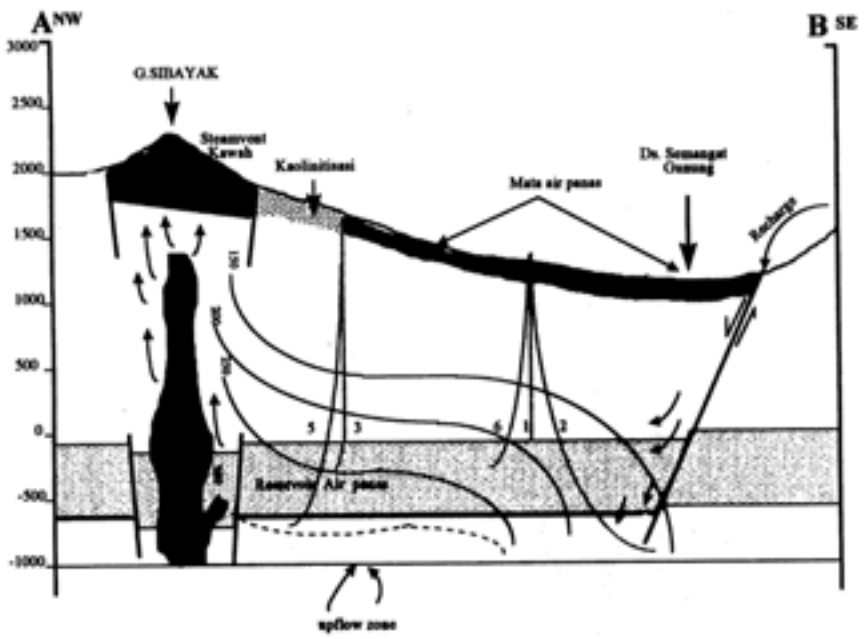

Figure 16.A schematic hydrothermal model of Sibayak geothermal field.

Fluid from steam vent is influenced by volcanic system whereas fluid from production well, mostly it comes from deep fluid has undergone some interaction/reaction with host rock.

8. Conclusions

Based on analysis of ^{18}O, D, ^{34}S isotope, chemicals, gases and also study of results as well as evaluation of water recharge, isotope, concentration in reservoir, geothermometer and reservoir hydrology problems, the reservoir condition of Sibayak can be concluded as follows:

Reservoir fluid of Sibayak geothermal field originates from meteoric water and does not indicate the volcanic system influence. This reason is supported by geochemistry observation showing that neutralization process because volcanic influence in host rock system has occurred.

Reservoir hydrology shows that a up flow zone or potential reservoir is located around the crater of Sibayak Mountain related to the developing border at points A, B and D. It seems that the reservoir can be exploited properly.

The result of some geothermometer studies shows that geothermal field of Sibayak has temperature 250^{o}C up to 270^{o}C. The reservoir fluid originates from parent fluid having the temperature ~ 350^{o}C.

Recharge of Sibayak geothermal field occurs at the elevation of 1100–1300 m above sea level. Location of this area is estimated around Rim of Singkut Crater. The recharge water flows through Singkut, enters into the reservoir and then moves to the north.

The fluid exiting the crater through steam vents at the elevation of 1900–2000 m shows that it is influenced probably by volcanic system.

Acknowledgements

This study has been carried out through cooperation between the International Atomic Energy Agency and Center for the Application of Isotopes and Radiation, National Nuclear Agency under the IAEA research contract No. 9717. A. Truesdell is thanked for his comments on an earlier version of the manuscript.

REFERENCES

[1] PERTAMINA "Indonesia Geothermal Reserves and Resources" PERTAMINA, Feb, 1995.

[2] R.H. MARINER, T.S.PRESSER and W.C. EVANS, Geothermometry and Water Rock Interaction in Selected Thermal System in The Cascade Range and Modoc Plateau, Western United States, Geothermics, 221 (1993), 1–15.

[3] F.D'AMORE, GIOVANNI GRANELLI and EGIZIO CORAZZA, The Geothermal Area of El Pilar-Casandy State of Sucre, Venezuela, Geochemical Exploration and Model, Geothermics, 233 (1994) 283–00.

[4] M.P. HOCHSTEIN and SAYOGI SUDARMAN, Geothermal Resources of Sumatera, Geothermics, 223 (1993) 181–200.

[5] M. BOEDIHARDI, SUNARYO, and DJOKO HANTONO, Tectonic Framework Characterization and Development of South Sumatra's Geothermal Prospect, Proceedings Indonesia Petroleum Association, 22nd Annual Convention, Oct. 1993.

[6] W.F. McKENZIE and A.H. TRUESDELL, Geothermal Reservoir Temperatures Estimated from The Oxygen Isotope Compositions of Dissolved Sulphate and Water From Hot Spring and Shallow Drill holes Geothermics, Vol. 5 (1976) 51–61.

[7] M.N. RAMOS-CANDELARIA, R.R. ALVIS-IISIDRO, "Introduction to Geothermal Chemistry Calculation", IAEA Regional Group Training on Isotope Geochemistry for Exploration of Geothermal energy Resources, Philippines, May 1977.

[8] WERNER F. GIGGENBACH, "Geothermal Solute Equilibria: Derivation of Na- K-Mg-Ca Geoindicator", Geochemica et Cosmochimica Acta Vol. 52, pp 2749–2768, 1998.

[9] WERNER F. GIGGENBACH and R.C. SOTTO, "Isotopic and Chemical Composition of Water and Steam Discharge from Volcanic-Magmatic Hydrothermal System of Guanacaste Geothermal Province, Costa Rica", Applied Geochemistry, Vol. 7,pp, 309–332, 1992.

[10] B.W.ROBINSON, "Sulphur and Sulphate Oxygen Isotopes in New Zealand Geothermal System and Volcanic Discharges", Proceedings of an Advisory Group Meeting, Vienna, IAEA, (1987) 31–48.

PRELIMINARY NOTES ON THE ACID FLUIDS OF THE MIRAVALLES GEOTHERMAL FIELD (GUANACASTE, COSTA RICA)

F. Gherardi[1], C. Panichi[1], A. Yock Fung[2], J. Gerardo-Abaya[3]

[1] Istituto di Geoscienze e Georisorse, Pisa, Italy
[2] Instituto Costarricense de Electricidad, Departemento de Récursos Geotérmico, San José, Costa Rica
[3] International Atomic Energy Agency, Vienna

Abstract. Four of the wells drilled for production (PGM-02, PGM-06, PGM-07, PGM-19) in Miravalles geothermal field of Costa Rica discharge acid fluids. They are located along the eastern boundary of the field close to the Miravalles volcano. Analysis of the existing chemical and isotopic data for the acidic wells in comparison with those for the pH-neutral production wells and surface natural manifestations allowed us to refine the geochemical models of geothermal field present in the literature. Two types of acidic fluids, a shallower one and a deeper one have been postulated.

1. Introduction

The Miravalles Geothermal Field is located in the northwestern part of Costa Rica (Guanacaste region), on the lower slopes of Miravalles volcano, within the Guayabo caldera. Productive wells drain from a typical liquid–dominated reservoir, filled with fluids having a neutral composition (pH~5.7 at ~240°C).

However, four of the wells intended for future production, actually discharge acid fluids. All these wells (PGM-02, PGM-06, PGM-07, PGM-19) are located along the eastern boundary of the field, where an high-density network of fractures, faults and structural alignments is recognised. Since 1994[1], studies to determine the feasibility of neutralising the acid fluids and using the wells in a safe manner were carried out. In 1996 the first practical test of neutralisation was conducted, indicating that sodium hydroxide (NaOH at 50%) injection at depth was successful in raising the surface pH from 2.5 to about 6.5[2].

In spite of the preliminary positive results of the neutralisation process, the negative aspects linked to the increasing amount of acid fluids possibly entering the Cl-type reservoir, as a consequence of the lowering of fluid pressure, cannot be excluded. Accordingly, the knowledge of the source mechanisms of the acidity production is of paramount importance for planning future field management strategies.

Unfortunately, the actual paucity of analytical data on acid fluids from wells does not permit an exhaustive understanding of the problem. For this reason, the following discussion should be mainly read as a preliminary attempt to study the acidity problem occurring in the reservoir.

Throughout this report, the available data on acid fluids were analysed in comparison with those from pH-neutral productive wells and surface natural manifestations, with the aim to refine the geochemical models of geothermal field present in the literature [3, 4].

2. The geothermal field

The Miravalles geothermal field is known to produce commercial amounts of high enthalpy fluids since 1979. In 1979–1980 the first drilling operations were made in the northeastern part of the field (see Figure 2). The positive results obtained from these early perforations encouraged further drilling and exploring [5].

Studies carried out between 1977 and 1986 provided the data for defining the resource as a liquid-dominated system filled with neutral-pH dilute fluids of a prevalently sodium-chloride nature, with reservoir temperatures of the order of 240°C [3].

The areal distribution of reservoir temperatures indicates the existence of a relative maximum in the north-eastern part of the field (255°C measured at bottom-hole of PGM-11 well). Reservoir temperatures gradually decline towards the south, along preferential flow paths controlled by a north-south trending fault system.

Accordingly, the Miravalles geothermal field could be considered as a typical example of "asymmetric mushroom-shaped" geothermal system, in which the main upflow of thermal fluids occur in a quite narrow area around the bottom-hole of few productive wells (PGM-11, PGM-01) and the discharge in a well-defined structurally-controlled direction.

Static and dynamic measurements [1] indicate that reservoir T, P conditions are sub-boiling. Geochemical monitoring of well discharges confirmed that even after 5 years of industrial exploitation no boiling is induced in the main reservoir [4].

Commercial electric generation in the Miravalles geothermal field started in 1994 with installation of a 60 MWe condensing power plant (Unit I). Steam from wells actually feed also a Well Head Unit of 5 MWe (since 1995) and Unit II, a condensing power plant of 55 MWe (producing since 1998). A new development of 27.5 MWe (Unit III) is planned for the following years, leading to a total installed capacity of about 147.5 MWe. At present the total generation is about 120 MWe.

The production system comprises mainly thirteen production wells, six steam separators and seven injection wells. Since 1994 the reinjection was conducted routinely, as a part of a program of waste disposal management and pressure regime maintenance

3. Geological setting

The Miravalles geothermal field is located in Guanacaste Province in the north-western part of Costa Rica, about 150 km north of the capital, San José (Figure 1B). At an elevation ranging between 400 and 800 m a.s.l., it extends for about 15 km^2 along the south-western slopes of the Miravalles volcano and inside a Pleistocene caldera about 15 km in diameter known as the Guayabo caldera (Figure 2). Collapse of the caldera by over 1000 m has been estimated based on stratigraphic correlations [5].

The Miravalles volcano, rising to 2028 m a.s.l., and currently inactive, is a Quaternary strato-volcano belonging to the Guanacaste Cordillera (Figure 1B). Three different stages of activity have been detected for the Miravalles Volcano, during which the activity migrated first in a northwestern direction and later towards the southeast. The latest eruptive cycle has been dated at 7000 b.p. [5].

The Guanacaste Cordillera is a volcanic arc system of Tertiary and Quaternary rocks that formed as a result of the subduction of the Cocos Plate beneath the Caribbean Plate (Figure 1A). The Tertiary rocks appear as a vast andesitic plateau with abundant intercalations of pyroclastites, ignimbrites and detritic sediments, while the Quaternary rocks are represented for the most part by lava flows that erupted from the many volcanoes in the region.
Four main fault systems have been identified in the area, revealing the existence of strong tectonic activity (Figure 2). The first of these faulting system have a north-west direction, which is the common trend of the Central-American isthmus and is parallel to the axis of the Guanacaste volcanic range. A second

system, with north-south trending, has been active in the Holocene, giving origin to the small graben structure ("Graben La Fortuna", about 3km wide, see Figure 2) which comprehends the geothermal field. The third, more recent system, trends east-west and frequently intersects the graben structure. It has been encountered in all the areas where successful wells have been drilled. Finally, the fourth system, trending north-east, is identified with the migration of the last eruptive vents of the Miravells volcano (see the relative position of Miravalles and Paleo-Miravalles summits in Figure 2).

The reservoir rocks, represented by the basal layer made up of tuff, andesitic lava and welded tuff, have a mainly secondary, fracture-derived permeability (trasmissivity values between 60 and 140 D m). The depth of main reservoir is actually located at about 700 m depth below the ground level. The estimated thickness of the reservoir is estimated in 800-1000 m.

The stratigraphic column overlying the basal productive layer comprises the following units (from the bottom to the top):

- porphiritic lavas of dacitic composition;
- volcanic sandstones and tuffaceous lutites interbedded, of possible intracalderic-lacustrine environment;
- porphiritic lavas of dacitic-latitic composition;
- upper section conformed by lahars, tuffs and andesitic lavas, all highly hydrothermally altered.

4. Thermal features

The thermal features of the Guanacaste volcanic-hydrothermal system mainly consist of spring discharges located primarily on the south-west flanks of the volcanoes Rincon de la Vieja, Miravalles and Tenorio (see Figure 3). No extensive fumarole fields occur within the investigated area, but some diffuse gas emanations is observed around the main springs of Las Pailas zone, in the Rincon de la Vieja-Santa Maria volcanic complex, and Las Hornillas zone, on the Miravalles volcano.

Based on the relative concentrations of Cl, HCO_3 and SO_4, and pH values, all the emerging thermal waters could be grouped in four different families: (A) pH-neutral Cl-rich, (B) pH-neutral HCO_3-rich, (C) pH-acid Cl-SO_4-rich and D) pH-acid SO_4-rich steam heated.

The emergence of these different water types is closely related to the morphology of the region. The sulphate-rich acid manifestations (group D, Las Pailas, Las Hornillas) are found along the slopes of the volcanoes at relatively high elevations (>600 m a.s.l.), whereas group B waters (several minor springs, not labelled here) issue from the inside of the caldera, along a N-S trending belt that corresponds to the tectonic structure of La Fortuna graben. Their emergence elevation is generally lower than 500 m a.s.l.

Finally, the Salitral Bagaces thermal spring represents the most important sample of Group A waters, while Guayabal waters belong to the type C.

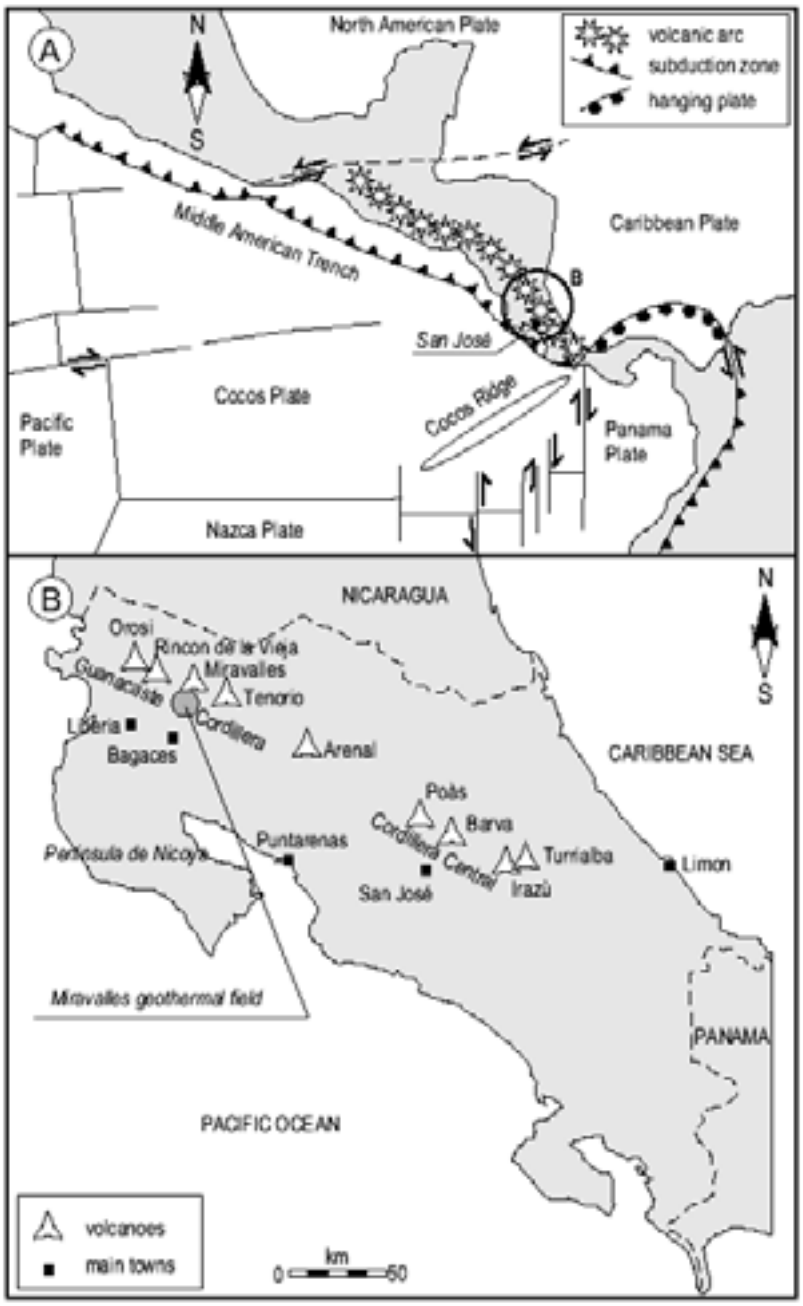

Figure 1. ***(a)*** *Tectonic sketch map of Central America. The subduction of Cocos Plate beneath the Caribbean plate is also shown, which caused the development of an interoceanic volcanic arc all along the Middle America Trench.*
(b) *Geographical map of Costa Rica with the localisation of main volcanoes and Miravalles Geothermal Field. Located in the North-East of Costa Rica, the Guanacaste arc is composed by the Orosì-Cacao, Rincòn de la Vieja-Santa Maria, Miravalles-Paleo Miravalles and Tenorio-Montezuma volcanic complexes.*

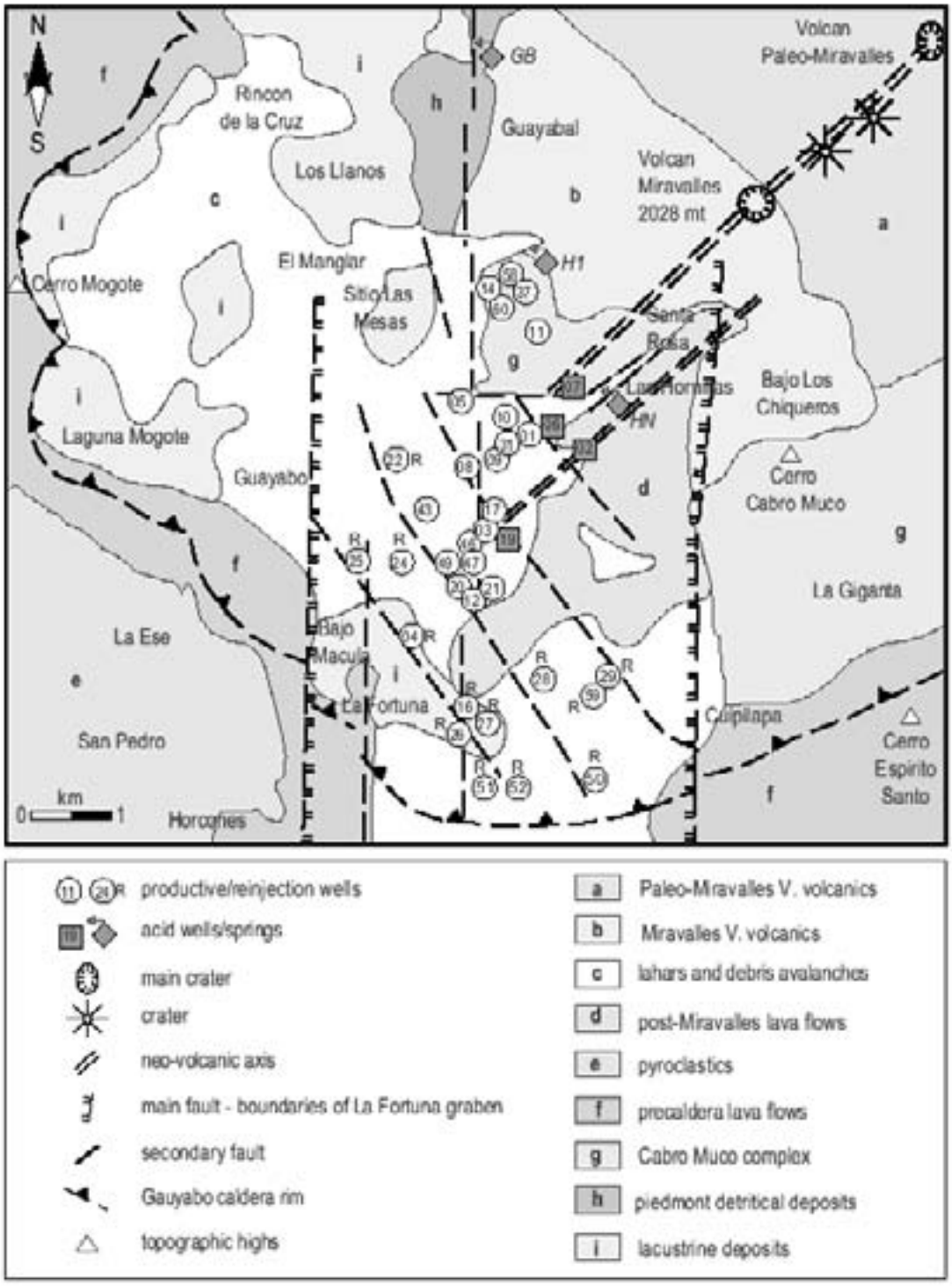

Figure 2. Schematic geological map of the Miravalles Geothermal Field, showing the location of wells and the main structural and tectonic features of the area. The occurrence of the acid wells and springs is also shown. Labels for pH-acid thermal springs are as follows: HN=Las Hornillas; H1=Herrumbre; GB=Guayabal.

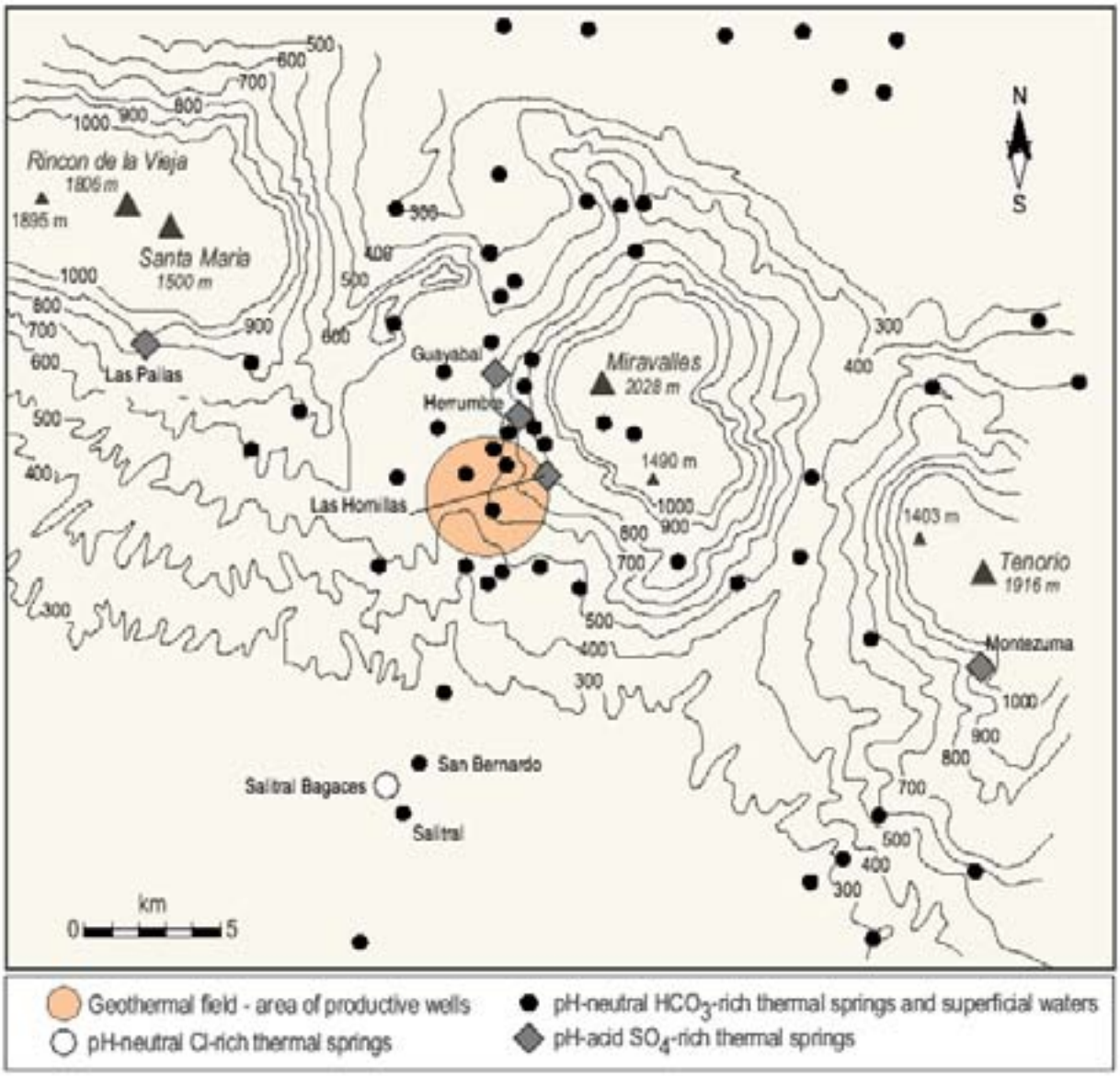

Figure 3. Sketch map of Guanacaste Geothermal Province, showing the location of main volcanoes of Guanacaste Cordillera, the geothermal field and the main thermal manifestations. Elevation contours are in meters.

5. Occurrence of acid fluids within the reservoir

Acid fluids occurred at Miravalles in PGM-02, PGM-07 and PGM-19 wells, and more recently also in PGM-06 well (see Figure 2). Unfortunately, for the latter episode no clear information is available at present.

The first evidence of such a fluid was found in 1984 during further drilling of well PGM-02. A neutral fluid typical of the producing reservoir was drained from this well to depths of 850-1100 m b.g.l. Beyond

1600 m b.g.l., however, the well crossed an acid aquifer with pH 2.48 and SO_4 concentrations of about 690 ppm at the weirbox. Temperature and salinity were similar to those of the neutral fluids.

Later the acid fluids were encountered once again during drilling of wells PGM-19 and PGM7. In the first of these, an aquifer with pH of 2.4-2.7 was crossed at a depth of 900 m b.g.l., as drilling proceeded new layers with neutral pH and a chemical composition similar to that of the productive reservoir were encountered. In the second well the pH was slightly less aggressive (3.7) and aquifer salinity was much lower than in the reservoir. Thereafter, well PGM-06 (1999) also produced acid fluids with pH of 2.3.

Well PGM-02 was designed as injector, while PGM-19, due to its greater productive capacity, was used as a laboratory to develop a neutralization system to permit its commercial utilization Sanchez-Rivera et al., 2000).

6. Data presentation and discussion

The representative chemical and isotopic composition of the different fluid types of Guanacaste region is reported in Table I. The chemical and isotope compositions of well waters were corrected for steam loss, so tabled values represent total discharge values. HCO_3 concentrations do not represent C_{TOT} at reservoir conditions, because no correction was made for $CO_{2(g)}$ separation. No δ^2H and $\delta^{18}O$ values are available for acid well waters.

A sketch map of Guanacaste Geothermal Province, showing the location of main volcanoes of Guanacaste Cordillera, the geothermal field and the main thermal features is shown in Figure 3.

Isotopic composition of waters

As previously stated, the geochemical model elaborated on the basis of the data collected during the exploration and appraisal drilling phases [3] and during the first five years of industrial exploitation of the field [4], should represent a plausible starting point for the following discussion on of acid fluids. The main evolutionary mechanisms that, as suggested by this model, control the chemical composition of the hydrothermal fluids, are satisfactorily resumed by the delta diagram of Figure 4.

Four different groups of waters are clearly distinguishable within the δ^2H vs. $\delta^{18}O$ plot: well discharges, steam-heated pools, chloride-thermal springs and bicarbonate waters, including both cold and thermal features.

The samples from producing wells cluster in an intermediate position between the andesitic magmatic component, as defined by Giggenbach[6], and the meteoric water line, showing enrichment in $\delta^{18}O$ of about 2-3‰ with respect to the latter.

The samples from the steam-heated pools, represented by points marked HN and LP, lie along straight lines with a slope of about 2.6, showing distinct isotope enrichment in both $\delta^{18}O$ and δ^2H. The surface temperatures, which are well below the local boiling point, suggest that boiling is mainly caused by the passage of gas-rich vapours rather than by flashing of steam. According to SO_4 enrichment of residual liquid phase, they are the expression of direct absorption of S-rich magmatic vapours into shallow aquifers.

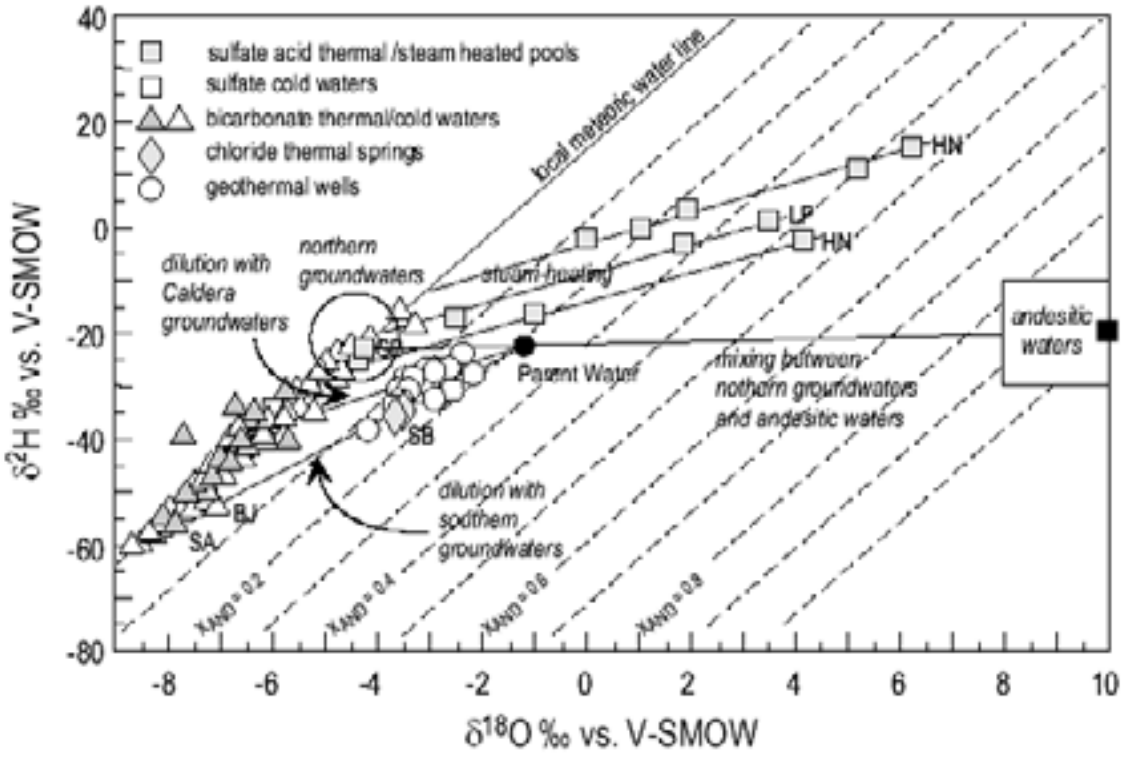

Figure 4. The isotopic composition of water samples from Guanacaste thermal region. The mixing relationships between the different groups of waters and the inferred isotopic composition of the deep Parent Water feeding the geothermal reservoir is also shown, according to the model of Gherardi et al. (2002). Labels are as follows: HN=Las Hornillas; LP=Las Pailas, GB=Guayabal; SB=Salitral Bagaces, BJ=San Bernardo, SA=Salitral.

In contrast, the Guayabal acid-water (GB) appears not to be isotopically affected by steam heating, suggesting that deep vapour has been largely intercepted before reaching the emergence point of spring. If we also take into account the relative high Cl content of GB water previously described, this may be an evidence of the renewed lateral flow to the manifestation of some Cl-rich waters similar to those of exploited reservoir.

Finally, the samples from neutral thermal springs have a composition similar to that of the local rainfall, plotting very closely to the meteoric water line. Only the Salitral Bagaces Cl-rich waters show a distinct pattern, revealing their close resemblance to reservoir fluids.

The isotope composition of Guanacaste waters has been used to define the origin of geothermal fluids and the hydrologic model of hydrothermal system, following the hypothesis that mixing relationships mainly links the different groups of waters.

Then, the isotopic composition of the geothermal parent water feeding the productive reservoir was calculated by extrapolating to higher ^{18}O and ^{2}H contents the different mixing trends shown in Figure 4. The parent water so obtained has $\delta^{18}O$ and $\delta^{2}H$ values of –1.2 and –22‰, respectively.

Table I. Selected chemical and isotopic data of the waters of Guanacaste region. Data from geothermal wells refer to concentrations corrected for steam loss. Units are as follows: concentrations: mg/kg; $\delta^{18}O$ and $\delta^{2}H$: ‰ vs. V-SMOW; enthalpy: kJ/kg.

Sample	Date	Enthalpy or t°C	pH	Cl	HCO_3	SO_4	Na	K	Ca	Mg	Fe_{TOT}	SiO_2	B	$\delta^{18}O$	$\delta^{2}H$
Salitral Bagaces	13/03/98	57	6.42	2717	1260	126	2178	86	129	6.8	0.32	105	47.2	-3.56	-33.6
Salitral	13/03/98	43	5.44	36	173	5.3	64	12	14	1.8	0	128	1.16	-7.92	-54.6
S.Bernardo	14/03/98	46	6.10	119	427	21	120	22	89	29.7	0	161	1.79	-7.48	-49.6
Guayabal	14/03/98	61	1.93	730	0	2914	57	2.0	140	7.1	57.1	258	1.62	-4.15	-26.9
Herrumbre	16/03/98	35	3.04	143	0	1726	70	10	543	116	-	107	0.84	-5.73	-33.6
las Hornillas	14/03/98	86	1.98	2.3	0	1538	18	4.3	40	4.6	78.4	288	0.36	-2.60	-17.8
Las Pailas	26/05/98	92	2.14	2.5	0	3840	7.8	2.2	0.2	0.5	-	518	1.24	3.54	0.9
PGM-01	16/06/97	1061	7.61	3012	21.7	34.2	1802	219	48.4	0.03	0.02	492	45.9	-2.93	-29.7
PGM-01	15/03/98	1076	7.60	2929	15.4	27.6	1735	221	51.0	0.06	0.03	448	46.2	-2.71	-35.9
PGM-03	17/06/97	1085	7.32	2977	28.6	31.1	1791	212	56.3	0.03	0.02	479	47.1	-2.81	-28.4
PGM-03	18/03/98	1140	7.32	2986	26.0	31.1	1793	220	56.3	0.08	0.77	448	47.9	-2.92	-30.4
PGM-05	11/06/97	1034	6.82	3136	35.8	35.8	1869	221	78.6	0.58	0.03	453	48.9	-2.99	-30.0
PGM-05	12/03/98	1046	6.50	3111	39.9	31.2	1863	226	79.8	0.10	0.03	414	47.7	-2.89	-26.5
PGM-11	20/06/97	1061	6.98	2741	60.3	25.9	1676	189	46.0	0.04	0.07	477	44.1	-2.91	-28.3
PGM-11	18/03/98	1075	7.18	2884	63.3	32.5	1741	203	48.8	0.07	0.09	463	45.4	-2.86	-36.3
PGM-12	18/06/97	1018	7.92	3119	13.3	41.9	1875	220	64.8	0.12	0.03	419	48.5	-2.60	-28.6
PGM-12	16/03/98	1008	7.69	3076	41.7	37.4	1868	225	67.2	0.10	0.82	374	48.5	-2.73	-28.8
PGM-02	1993	-	2.48	3145	0	486	1942	266	27.7	7.54	33.4	548	57.6	-	-
PGM-02	1998	-	2.4	3194	0	499	1980	272	26.0	7.44	-	553	60.7	-	-
PGM-07	1998	-	3.6	1257	0	224	771	116	18.6	1.57	-	464	32.1	-	-
PGM-19	1993	-	2.41	3006	0	381	1833	248	24.6	6.89	10.1	449	54.9	-	-
PGM-19	1998	-	2.7	2629	0	355	1579	217	21.4	6.71	-	380	52.9	-	-

Following the model proposed by Giggenbach[6] for arc-related geothermal systems, these isotopic values reflect the contribution of andesitic and local precipitations waters in relative proportions of about 20 and 80%. Of course, this 20% represents a maximum estimation of the magmatic water contribution to geothermal system, because some ^{18}O-enrichments might be also expected by exchange reactions of waters with the rocks of the reservoir (oxygen-shift).

Finally, based on the δ^2H values, the main recharge area is individuated in the north eastern slopes of the Guanacaste Cordillera, where precipitations isotopically enriched (δ^2H>-25‰) frequently occur.

By the use of Cl-$\delta^{18}O$-δ^2H relationships, and application of silica-enthalpy and chloride-enthalpy mixing models, more several independent information were obtained in close agreement with those derived by inspection of the isotope composition of water, further supporting the geochemical model proposed. All these topics were detailed in the paper of Gherardi et al. [4], and then they are not further discussed here.

Steam-heated pools

Steam-heated hot springs form when rising geothermal or volcanic steam partly or completely condense in surface waters. Accordingly, the isotope and chemical composition of these springs does not reflect the physical and chemical conditions of the deep reservoir.

However, following the approach of Giggenbach and Stewart [7] (1982), a relation may be derived allowing the degree of enrichment in ^{18}O and SO_4 to be related to the H_2S content of the vapour heating the pool.

Assuming a deep steam segregation temperature of about 230ºC, and with a surface temperature of 75ºC, then the compositional values for the parent geothermal water will be estimated in -0.2‰ and -11‰ for $\delta^{18}O$ and δ^2H, respectively.

If it is indeed true that the deep parent water is the result of mixing between a meteoric and an andesitic component having $\delta^{18}O$ and δ^2H values of about +10‰ and -20‰, respectively, we can also calculate the andesitic fraction of this supposed parent water, which corresponds to approximately 22%. This percentage is slightly higher than those previously calculated without considering data from steam-heated pools.

However, mass balance calculations indicate that measured SO_4 concentrations unlikely reflect the complete absorption and successive oxidation of H_2S from geothermal reservoir. In fact, considering the total H_2S concentration in the reservoir (up to 0.75 mmol/kg), the measured SO_4 contents in the surface pools imply that, even in the "extreme" hypothesis of complete H_2S absorption and H_2S stripping in the reservoir in adiabatic single step at 230°C, the fraction of steam in the total amount of fluid y is higher than 0.59 (up to 0.66). If, instead, we assume that the total amount of H_2S initially stored in the deep geothermal liquid quantitatively escapes in the vapour phase, the minimum y value required to explain the high SO_4 contents of Las Hornillas acid pools becomes 0.77 (up to 0.82). These high y values are inconsistent with field observations on low surface temperature and lack of vigorous boiling. Accordingly, a more likely explanation is that the hot vapour feeding the manifestations does not derive from the geothermal reservoir, but from the underlying volcanic-magmatic system, or from the root of the geothermal system where some hotter (possibly H_2S- SO_2-bearing) fluids could occur.

The rise of this "parent vapour", then, likely takes place in close proximity of the actually producing geothermal reservoir without intersecting them, due to the local anisotropic distribution of permeability.

In light of these considerations, the percentage of andesitic fraction previously calculated from isotope data of Las Hornillas should be thought as representative of these deeper levels of the system, and not of the neutral fluids of the actually producing reservoir.

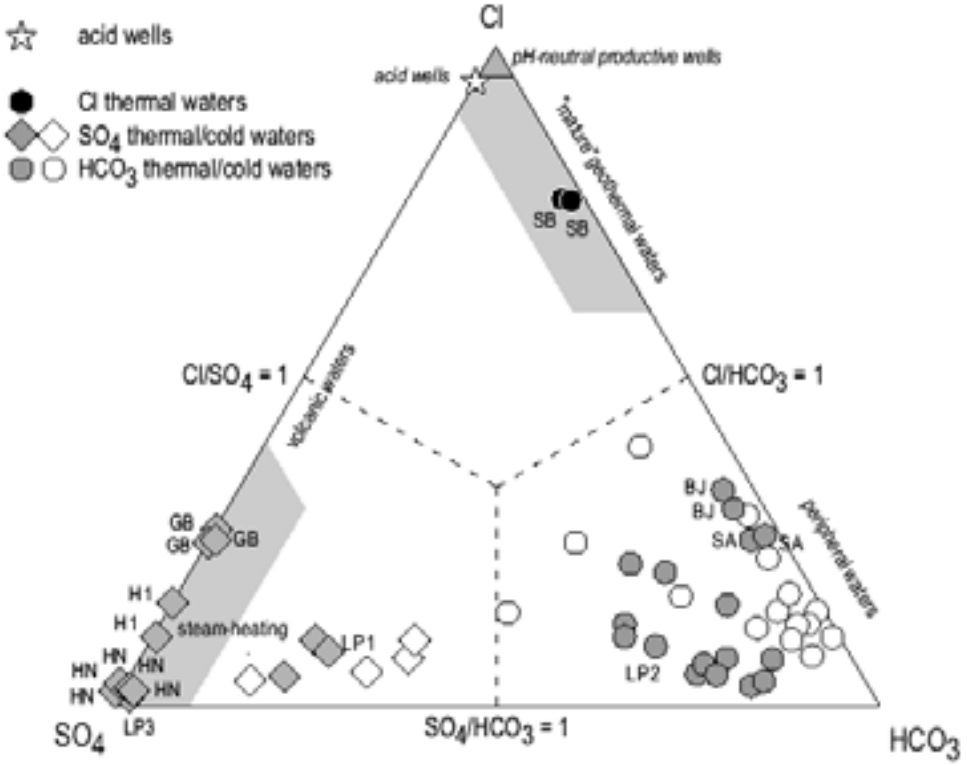

Figure 5. Cl-HCO_3-SO_4 diagram of water samples from Guanacaste geothermal area. Concentrations are in meq/kg. Labels for thermal spring samples are as follows: SB=Salitral Bagaces; SA=Salitral; BJ=San Bernardo; LP=Las Pailas; HN=Las Hornillas; GB=Guayabal; H1=Herrumbre. The measured concentrations in the liquid phase produced by the geothermal wells have been corrected for steam loss, assuming single-step adiabatic boiling between the undisturbed reservoir and wellhead. For acid wells, the assumption is made that deep temperatures are similar to those measured in the pH-neutral fluid producing wells (avg. 240°C).

Chemical composition of waters

A first evaluation of the chemical composition of sampled water is first carried-out in terms of Cl-HCO_3-SO_4 (Figure 5), (Ca+Mg)-Na-K (Figure 6a) and (Na+K)-Ca-Mg (Figure 6b) relative concentrations. All these triangular diagrams were prepared starting from concentrations in equivalent units (meq/kg), since this is the most correct way to make a classification of natural waters.

The diagram of Figure 5, by use of anions relative concentrations, discriminates between the different degrees of conversion (through neutralisation processes induced by water-rock interactions in the upper crust) of immature, acidic, originally magmatic fluids to neutral, reduced fluids typical of mature hydrothermal systems [8].

Instead, the use of both the diagrams of Figure 6, based on cations relative contents, permits a preliminary evaluation of the relative contribution of high- and low-temperature fluids in waters sampled at the surface, because Na and K tend to be the main cations in high-temperature fluids, where Ca and Mg generally are minor-to-trace constituents.

The most striking feature of these diagrams is that waters from acid wells are very similar in composition with respect to waters from pH-neutral, productive wells. The only significant difference observed for acid discharges, apart of course from pH values, is represented by higher total concentrations of SO_4 and a little relative Na+K enrichment with respect to Ca+Mg.

Acid waters from wells, instead, markedly scatter with respect to the cluster of points of the other acid waters occurring in the Guanacaste region.

As confirmed by data on total ionic salinity (not reported, but easily calculated from data in Table I), all these evidences may be related to the existence of a predominant contribution of geothermal-like waters in acid well discharges, which, in contrast, is absent in acid springs. This hypothesis is further corroborated by the very homogeneous absolute concentrations of Cl, Na and K in all the wells, independently from pH values (see Table I).

Mainly based on the total ionic salinity and hydrogen ion activity ($a_{H+}=10^{-pH}$) values, it also appear that within the group of acid well waters, the chemical composition of PGM-07 slightly differ from the others, because of significantly lower values. In fact, this sample is characterised by proportionally lower concentrations of all the major constituents, approximately 40% of Cl, Na, K and SO_4 and higher pH values (3.6). Only SiO_2 does not respect this pattern, showing very similar contents. Summing up, all these evidences indicate that waters discharged from PGM-07 likely experienced some dilution with shallower aquifers before to reach the drainage volume of the well.

In Figure 6, a triangular geothermometric Na-K-Mg diagram is used to investigate the state of equilibration and, most importantly, the homogeneity and the possible origin of geothermal fluids. Here, we propose a slightly modified version of the original graphical tool proposed by Giggenbach [9], based on the use of Na-K geothermometer of Fournier [10] instead of that of the original author.

The evaluation of analytical Na, K and Mg relative contents (Figure 7) allows a distinction to be made between waters suitable for the application of ionic solute geothermometers, such as those discharged from neutral geothermal wells and at Salitral Bagaces, and those which in contrast are unsuitable, such as those discharged from acid wells and the other thermal springs.

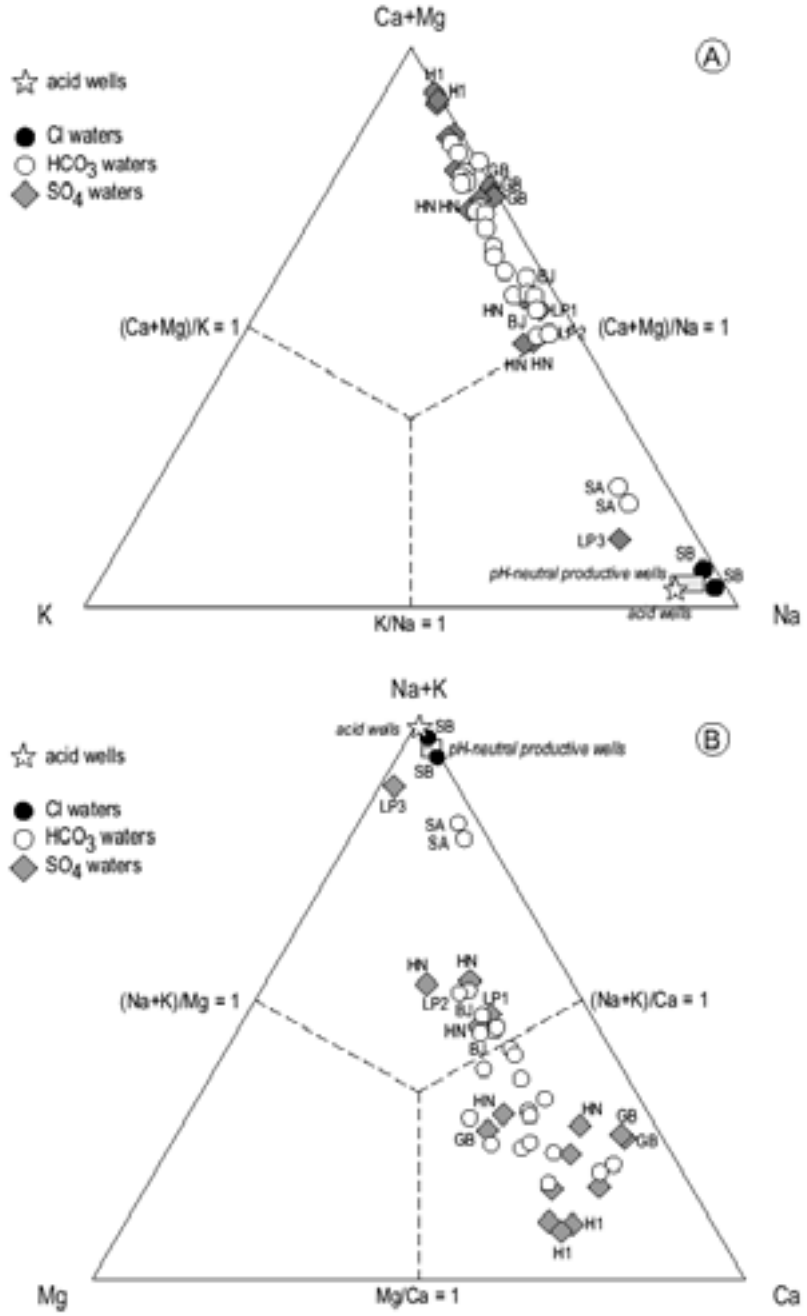

*Figure 6. Relative (Ca+Mg)-Na-K (**a**) and (Na+K)-Ca-Mg (**b**) concentrations of water samples from Guanacaste geothermal area. Chemical compositions of samples from productive and acid wells are corrected for steam loss. Data points for natural manifestations refer to thermal springs and selected cold waters. Concentrations are in meq/kg. Water samples from natural manifestations are grouped as a function of anions composition. Labels for thermal spring samples are as follows: SB=Salitral Bagaces; SA=Salitral; BJ=San Bernardo; LP=Las Pailas; HN=LAs Hornillas; GB=Guayabal; H1=Herrumbre.*

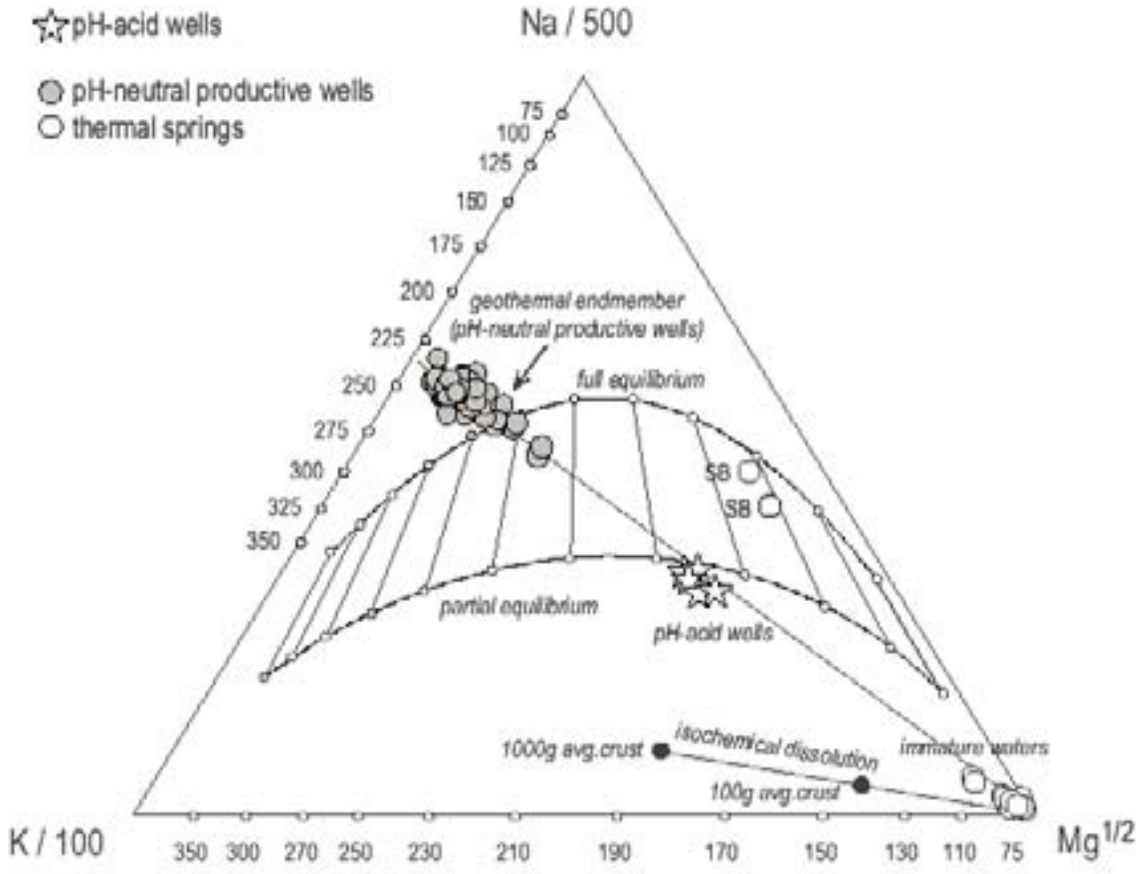

Figure 7. Geothermometric triangular plot for Na, K and Mg (modified after [9]. *Na-K and K-Mg temperatures (in °C) are calculated with the equations provided by Fournier* [10]*) and Giggenbach* [9]*, respectively. Concentrations are in mg/kg.*

Data from acid wells plot at an intermediate position between the full-equilibrated waters, representative of the local geothermal end-member, and those representative of non-equilibrium conditions, the so-called "immature, non-equilibrated waters". Both neutral and acid geothermal waters are characterised by almost constant Na/K ratios, but a significant Mg-enrichment is observed in acid discharges. The apparent Na/K equilibrium temperatures are consistent with those directly measured at bottom-hole, spanning over the range 235 to 245°C.

Data points for acid wells clearly separate also from the dissolution trend shown in the bottom of the figure (line marked "isochemical dissolution").

Because this trend is representative of the isochemical dissolution of a hypothetic rock of average crustal composition, only some magmatic-related, aggressive fluids might be expected to plot along this line [11].

Then, all considering, the position of samples for the acid fluids from Miravalles boreholes points to attainment of partial equilibrium, or most likely, indicates that these fluids probably represent an acid fluid largely mixed with pH-neutral geothermal waters.

In fact, their high Mg contents do not indicate acquisition of this element in response to decreasing temperature, but reflect the high H^+ activity of these fluids, which provokes the leaching of Mg and Fe (see Table I) from well casings and/or Mg- and Fe-bearing minerals of reservoir rocks.

Similarly, the Mg- and Fe-bearing minerals likely occurring all around the thermal features and in the soil, should represent the main source of the high Mg and Fe contents observed in the waters discharged from the acid manifestations of Las Pailas, Las Hornillas and Guayabal (see Table I).

A partial re-equilibration may be hypothesised to explain the relative Mg-enrichment of the neutral thermal waters from Salitral Bagaces, Salitral and San Bernardo springs.

The source of acidity

The definition of the chemical component that is responsible of the acidity of thermal fluids represents the main goal of the present study. Acidity-related problems developing in geothermal environments usually refer to some HCl or H_2SO_4 excesses. For example, acidity due to chloridric acid (Cl-type) has been evidenced at Larderello (Italy), The Geysers (USA), Kakkonda and Onikobe (Japan), while that from sulphuric acid (SO_4-type) has been observed at Palinpinon, Mt.Apo (Philippines) and Sumikawa (Japan).

In order to further investigate this aspect, in Figure 8 a modified Schoeller diagram for Miravalles thermal waters is shown. In the plot, some molecular ratios of major components and pH values for the three different types of acid waters occurring at Miravalles were compared with the composition of pH-neutral productive well discharges.

The most significant result of this comparison is that, in terms of Na/K and Cl/Na, the acid fluids from wells are practically indistinguishable from the neutral fluids of geothermal reservoir. Instead, the most conspicuous differences are in the SO_4/Cl ratios, which are systematically higher in the acid fluids by about one order of magnitude.

Acid fluids differ from the neutral-ones also because of lower Cl/SiO_2 ratios, in agreement with the observation that low pH values enhance the isochemical dissolution of wall rock silicates and then may increase the SiO_2 concentration in aqueous solutions.

In contrast, the highly inhomogeneous patterns shown by superficial manifestations are characterised by variable SiO_2, Na, K and Cl relative concentrations. Such anomalous values likely reflect the local availability of these species in the rocks around the features, from which they are leached quantitatively.

Even if the patterns of Las Pailas and Las Hornillas and those of Guayabal and Herrumbre clearly separate from those of acid wells, all the three groups of acid waters plotted in the diagram show a significant SO_4-enrichment with respect to pH-neutral fluids of the geothermal reservoir. Moreover, no correlation is observed between Cl and pH in all the considered acidic waters. Summing up, these patterns strongly suggest that the acid fluids at Miravalles are tied to the high concentrations of SO_4 and not Cl (acidity of SO_4-type).

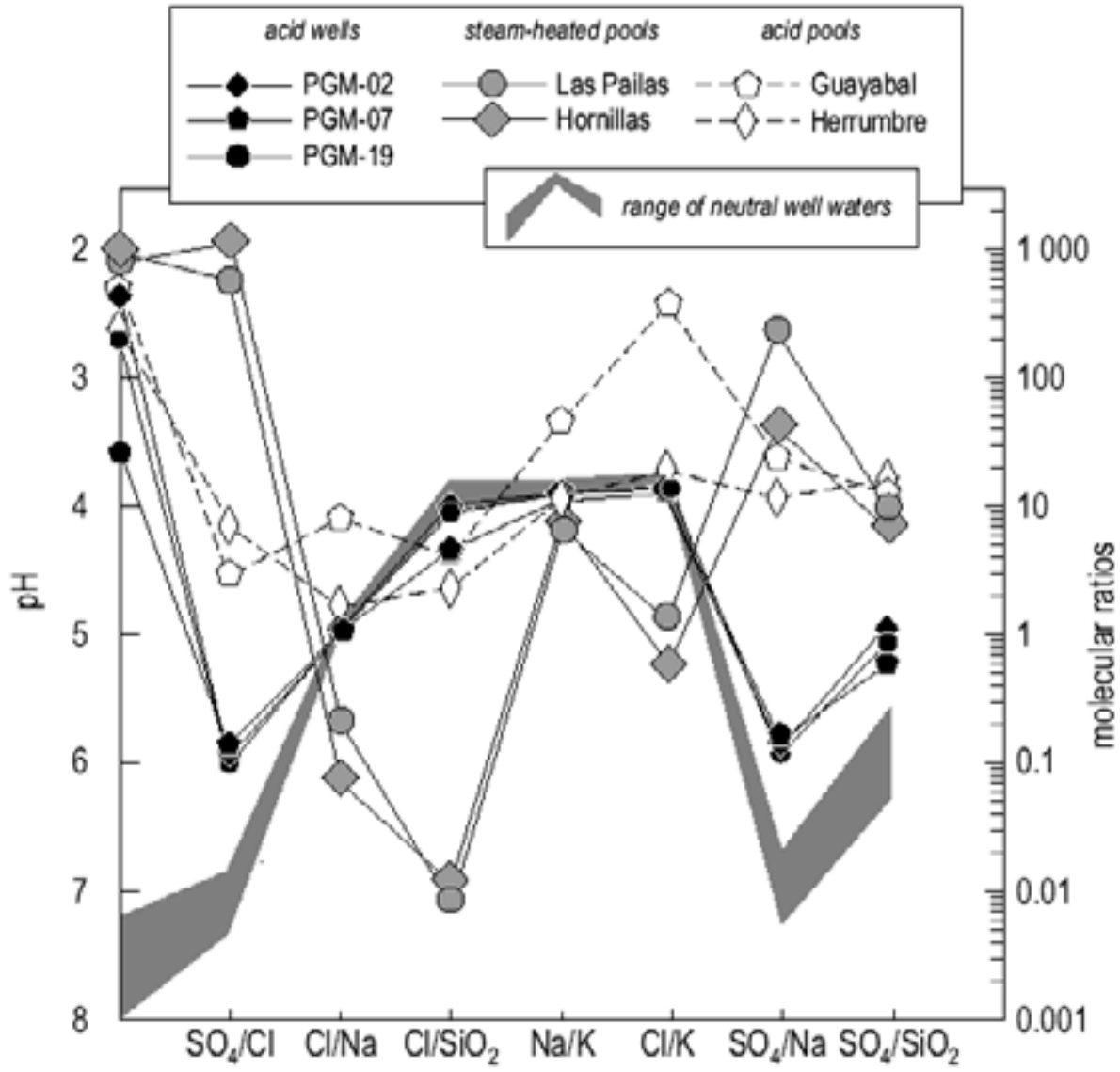

Figure 8. Modified Schoeller diagram for Miravalles thermal waters. In the plot, some molecular ratios of major components and pH values for the three different types of acid waters occurring at Miravalles were compared with the composition of pH-neutral productive well discharges. Concentrations are in meq/kg (mmol for SiO_2).

A crucial aspect in the discussion on acid fluids is then related to the investigation of the possible sources of geothermal SO_4. An accurate study on this topic requires, of course, the knowledge of S total concentrations at depth, i.e. the calculation of reservoir chemistry based on both liquid- and gas-phase analyses. Such a calculation was made for pH-neutral well discharges, but not for the acid-ones, due to the lack of gas data for these samples.

The application of the "whole system chemical geothermometry" method [12] to neutral fluids showed that anhydrite, the most likely mineral candidate to control SO_4 concentrations in geothermal waters, is systematically slightly under-saturated in the reservoir (SI= log Q/K < -0.5; calculation made with SOLVEQ code, Reed and Spycher, 1984). This evidence, coupled with the observation that anhydrite is found only episodically in some fracture mineralisations of wells PGM-02 and PGM-11[13], strongly suggest that SO_4 concentrations are not buffered by SO_4-bearing minerals within the exploited reservoir.

Then, SO_4 contents of geothermal discharges are probably controlled by the influx of S-bearing gases from depth.

According to Ellis and Giggenbach [14] and Ohmoto [15], the main mechanisms of formation of sulphuric acid in thermal solutions are satisfactorily described by the following reactions:

(a) Oxidation of H_2S (H_2S/SO_4=1)
$H_2S + 4\ H_2O \Leftrightarrow SO_4^{2-} + H^+$ [1]

(b) Hydrolysis and successive disproportioning of SO2 (H2S/SO4=1/3)
4 SO2 + 4 H2O ⇔ 3 H2SO4 + H2S [2]

(c) Hydrolysis of elemental S (H2S/SO4=3)
4 S + 4 H2O ⇔ H2SO4 + 3 H2S [3]

The stoichiometry of these reactions dictate that H_2S/SO_4 ratios of geothermal waters change depending on which process is involved in the formation of SO_4 ions in solutions. Then, in first approximation, the H_2S vs. SO_4 correlation may represent a useful tool to discriminate the sources of SO_4.

The H_2S/SO_4 ratios of pH-neutral Miravalles fluids range between 0.25 to 1.5, suggesting that both the oxidation of H_2S and the disproportioning of SO_2 may effectively control the concentration of SO_4 in the reservoir. In contrast, the hydrolysis of elemental S apparently does not play a significant role, according to the fact that no appreciable amounts of native sulphur were observed in well cuttings.

The oxidation of H_2S rarely is the cause of acidity of the deep geothermal fluids, due to the reduced conditions usually prevailing in the geothermal reservoirs. However, R_H values calculated from gas data [4] clearly indicate that the reservoir is relatively oxidised with respect to f_{O2} values predicted by the hydrothermal Fe(II)-Fe(III) buffer [16], partially supporting the occurrence of this process.

In contrast, the effectiveness of the hydrolysis of SO_2, strongly suggest the presence of relative immature waters near the productive reservoir. Their rise may be favoured by the presence in this part of the field of some important tectonic discontinuities.

In Figure 9, a triangular Cl-SO_4-B diagram is plotted with the aim to better define the source of the Miravalles acidity. In fact, in pH-neutral thermal solutions both B and Cl are known to behave as conservative elements, neither reacting with rock minerals nor separating during boiling and condensation processes [17]. In contrast, B is volatile in acid solutions, because it forms H_3BO_3 that considerably separates in vapour phase.

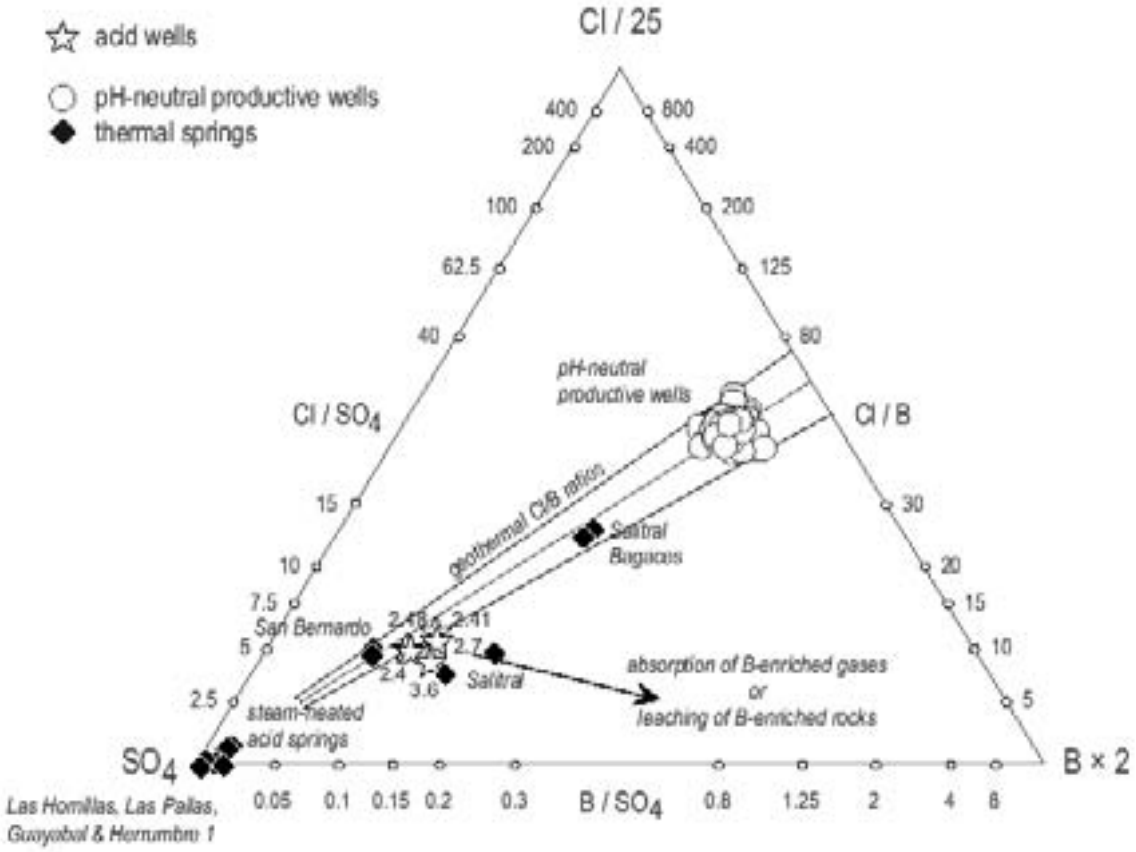

Figure 9. Relative Cl-SO_4-B concentrations of water samples from Guanacaste geothermal area. Chemical compositions of samples from productive and acid wells are corrected for steam loss. Data points for natural manifestations refer to thermal springs. Concentrations are in mg/kg. Labels for acid well samples represent the pH values measured at weir box.

Then, constant Cl/B are expected in waters having a common origin, while some relative Cl-enrichment is expected for pH-acid waters.

Data samples indicate that waters from pH-neutral reservoir belong to Cl/B values between 55 and 75 (with concentrations in mg/kg), suggesting a common origin for these fluids. Apart from PGM-07, characterised by Cl/B ratio of 39, also the acid well waters have very constant Cl/B ratios, ranging from 50 to 55. In other words, acid waters plot at the lower boundary of the Cl/B range for neutral fluids.

The comparison between the two range of values indicate that the process of selective segregation of B in vapour phase, theoretically enhanced by the occurrence of pH-acid solutions, cannot explain the observed distribution of points.

Then, a possible explanation, albeit a partial one, for this unexpected trend, is that the higher B contents of acid fluids may be acquired through further absorption of B-rich vapours, or more effective B-leaching from wall-rocks by these fluids.

7. Conclusions

The preliminary data on acid fluids discussed in this report permitted to further refine the geochemical model of the Miravalles volcanic-hydrothermal system previously proposed by Giggenbach and Corrales [3] and Gherardi et al. [4]. A cartoon depicting the main processes governing the geochemical evolution of the field is shown in Figure 10.

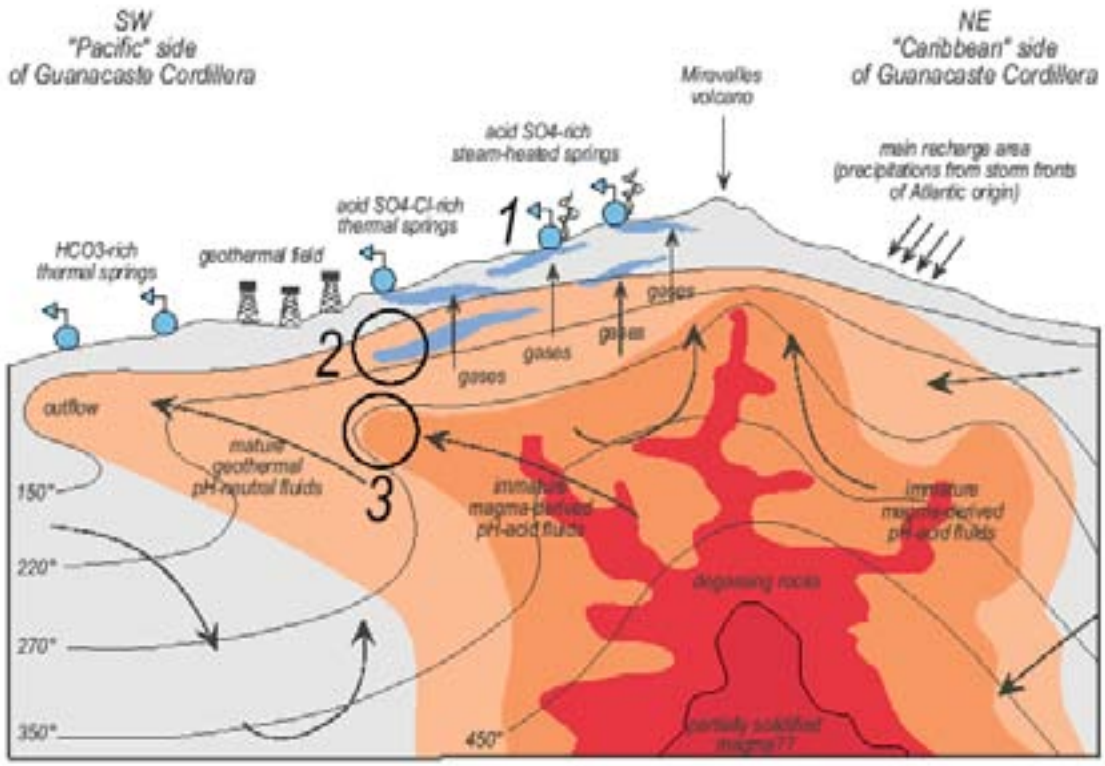

Figure 10. Cartoon of preliminary geochemical model of Miravalles Geothermal Field (modified after Giggenbach & Corrales [3]*). The possible mechanisms of acidity production within the system are also shown: 1=superficial steam-heating-related acidity - involves superficial minor aquifers - absorption of acid S-bearing gases; 2=sub-superficial acidity - involves aquifers of higher volumes - due to the high meteoric recharge of this aquifers, relatively oxidising conditions were maintained, which facilitates the oxidation of acid S-bearing gases, and ultimately H+ production - possibly, some downward percolation movements of acid waters from aquifers of type 1 may be involved, due to the high fracture density of Miravalles volcano slopes; 3=deep acidity - involves the eastern sector of the geothermal reservoir - possibly linked to the up flow of some volcanic-related brines only partially neutralised by water-rock interactions.*

The general flow of thermal waters is likely to be from north to south in the geothermal reservoir, with some deeper neutral Cl waters travelling for considerable distances from their major zone of up flow before emerging at the surface near Salitral Bagaces, some 20 km away from the Guayabo caldera.

Over in the volcano Miravalles zone, and probably elsewhere in the Guanacaste area, the absorption of volcanic-magmatic vapours into groundwaters is likely to occur.

At considerable depth and temperature, the process leads first to the formation of highly immature fluids that give rise an isochemical dissolution of reservoir rocks; further interaction converts these partially neutralised waters to the neutral Cl waters suitable for geothermal power production.

At the surface, the same mechanism produces acid steam-heated hot springs; such as they occur at Las Hornillas and Las Pailas.

All the acid waters at Miravalles are characterised by an acidity of SO_4-type. Nowhere a correlation exists between Cl contents and pH.

Incursion of acid SO_4 waters in wells located in the north eastern sector of the field may well point to the presence of a body of immature waters close to the Cl waters. These waters probably rise along some faults present in the area, in agreement with the structural, anisotropic control of permeability all over the geothermal district.

In well PGM-19, the presence of acid fluids of relatively low salinity above the reservoir could be tied to a mixing between acid SO_4-bearing waters produced at shallow levels, similar to that of the Las Hornillas manifestations.

In wells PGM-02 and PGM-07, on the other hand, the most likely mechanism is a mixing with acid fluids of deeper origin.

Any case, no definitive proofs exist to postulate the existence of a deep, acidic and hotter reservoir below that actually producing.

Moreover, if the presence of a body of immature waters should be hypothesised at the eastern boundary of the field, then, most likely that body should be also relatively small in volume. In fact, in spite of his closeness to the producing levels and the pressure lowering induced by exploitation, no change in pH with time is observed in the nearby wells, which of course, implicate that the inflow of acid waters is not enough effective to poison the neutral reservoir

All told, based on the very preliminary analyses discussed in this report, two possible sources should be hypothesised to explain the acidity encountered at Miravalles. The first-one is related to superficial H_2S oxidation, and the second-one to inflow of “immature” volcanic waters. In both the cases, independently from which process between H_2S-oxidation and SO_2-disproportioning is the most effective, relatively oxidised redox conditions are required to produce SO_4-acidity.

Gas data agree with this scenario, indicating relatively low R_H values and high relative concentrations of meteoric-derived gases, such as N_2 and Ar [4].

Acknowledgements

The authors wish to thank Zhonghe Pang and an anonymous reviewer for many helpful comments that greatly improved this paper.

REFERENCES

[1] MARINI, L., YOCK FUNG, A. (1994) Modelo teorico de neutralizacion del pozo PGM-19. (unpublished report, in Spanish)

[2] SANCHEZ-RIVERA, E., SEQUEIRA, H.G., VALLEJOS RUIZ, O. (2000). Commercial production of acid wells at the Miravalles geothermal field, Costa Rica. Proceedings of the World geothermal Congress 2000, 1629–1634.

[3] GIGGENBACH, W.F., CORRALES SOTO, R. (1992) Isotopic and chemical composition of water and steam discharges from volcanic-magmatic-hydrothermal systems of the Guanacaste Geothermal Province, Costa Rica. Applied Geochemistry 7, 309–332.

[4] GHERARDI, F., PANICHI, C., YOCK FUNG, A., GERARDO-ABAJA, J. (2002) Geochemistry of the surface and deep fluids of the Miravalles volcano geothermal system (Costa Rica). Geothermics 31, 91–128.

[5] ICE/ELC, 1986. The Miravalles geothermal project: feasibility study of first unit (in Spanish). Instituto Costarricense de Electricidad and Electroconsult, report GMV-2-ELC-R-12400 (R01), San José, Costa Rica.

[6] GIGGENBACH, W.F. (1992) Isotopic shifts in waters from geothermal and volcanic systems along convergent plate boundaries and the origin of "andesitic" water. Earth and Planetary Science Letters 113, 495-510.

[7] GIGGENBACH, W.F., STEWART, M.K. (1982) Processes controlling the isotopic composition of steam and water discharges from steam vents and steam-heated pools in geothermal areas. Geothermics 11, 71–80.

[8] GIGGENBACH, W.F., (1991). Chemical techniques in geothermal exploration. In: Application of geochemistry in geothermal reservoir development (co-ordinator F. D'Amore), pp. 119–144. UNITAR/UNDP.

[9] GIGGENBACH, W.F. (1988) Geothermal solute equilibria. Derivation of Na-K-Mg-Ca-geoindicators. Geochimica et Cosmochimica Acta 52, 2749–2765.

[10] Fournier, R.O., (1979) A revised equation for the Na/K geothermometer. Transaction Geothermal Resources Council 3, 221-224.

[11] GIGGENBACH, W.F., (1984). Mass transfer in hydrothermal alteration system — A Conceptual Approach. Geochimica et Cosmochimica Acta 48, 2693–2711.

[12] REED, M., SPYCHER, N., (1984). Calculation of pH and mineral equilibria in hydrothermal waters with application to geothermometry and studies of boiling and dilution. Geochimica et Cosmochimica Acta 48, 1479–1492.

[13] ROCHELLE, C.A., MILODOWSKI, A.E., SAVAGE, D., CORELLA, M. (1989) Secondary mineral growth in fractures in the Miravalles geothermal system, Costa Rica. Geothermics 18, 279–286.

[14] ELLIS, A.J., GIGGENBACH, W.F., (1971). Hydrogen sulfide ionisation and sulphur hydrolysis in high temperature solutions. Geochimica et Cosmochimica Acta 35, 247–260.

[15] Ohmoto, H., (1986). Stable isotope geochemistry of ore deposits. In: Stable Isotopes in High Temperature Geological Processes, Valley, J.W., Taylor, H.P. Jr., O'Neil, J.R., (eds.). Mineralogical Society of America, Reviews in Mineralogy 16, 491–555.

[16] Giggenbach, W.F., (1987). Redox processes governing the chemistry of fumarolic gas discharges from White Island, New Zealand. Applied Geochemistry 2, 143–161.

[17] Ellis, A.J. (1970) Quantitative interpretation of chemical characteristics of hydrothermal systems. Geothermics 2, 516–528.

ISOTOPE TECHNIQUES FOR CLARIFYING ORIGIN OF SO_4 TYPE ACID GEOTHERMAL-FLUID — CASE STUDIES OF GEOTHERMAL AREAS IN KYUSHU, JAPAN

K. Matsuda, K. Shimada, Y. Kiyota

Geothermal Department, West Japan Engineering Consultants, Inc.,
Fukuoka, Japan

Abstract. In a few geothermal fields in Kyushu, Japan, strongly acid waters are being produced from geothermal wells, causing terrible corrosion of casing pipes of geothermal wells and transportation pipelines of geothermal fluid. In order to develop the study methods, especially isotope techniques for evaluating acid geothermal fluid, case studies for geothermal areas in Kyushu were carried out. It was ascertained that geochemical techniques using isotope data are useful to reveal the origin and characteristics of acid fluids enriched in SO_4. In particular, the integrated interpretation using several indices based on isotope and chemical data of sulphur species, i.e. $\delta^{34}S$(S total), $\delta^{34}S$ fractionation factor and SO_4 and H_2S concentration in total fluid, are effective. A recent data set of sulphur isotope analyses including $\delta^{34}S(H_2S)$ values of the acid fluids occurring in the Hatchobaru field was used for this study with the existing data of $\delta^{34}S(SO_4)$ value of the discharge waters. Sulphur isotope ratios of the acid fluid are relatively high, suggesting that the SO_4-rich fluid is not caused by the simple oxidation of H_2S. On the basis of their isotopic and chemical characteristics, the acid fluids are thought to be the result of mixing of neutral-pH fluid with low temperature SO_4-rich fluids from shallower levels. Taking into consideration the occurrence of native sulphur in some core samples from shallow levels, a possible explanation to the origin of SO_4-rich fluids is the hydrolysis of native sulphur at a temperature lower than 224°C. However, the partial oxidation of H_2S accompanied with isotopic re-equilibration at temperatures lower than 240°C can alternatively explain the origin of SO_4-rich fluid. In either case, the distribution of acid fluid reservoirs in the Hatchobaru field is believed to be restricted to the relatively shallow level. Isotopic compositions and chemical characteristics of sulphur species in acid fluids in the Takigami field indicate that its formation mechanism is similar to that of the Hatchobaru field. Although acid fluids occurring in the Shiramizugoe are likely to be also produced by a mixing of SO_4-rich fluid, more detailed geochemical studies are necessary to reveal the formation mechanism of the acid fluids.

1. Introduction

Acid fluid discharge from geothermal wells causes corrosion of casing pipes and transportation pipelines, resulting in a serious problem in geothermal exploitation. For a successful development of geothermal resources, clarification of the origin of the acid fluid and its extent within the reservoir is very important.

Based on a main acid compound controlling its acidity, acid geothermal fluids can be classified into two groups, i.e. hydrochloric acid type (Cl-type) (e.g., Larderello, The Geysers, Kakkonda and Onikobe) and sulphuric acid type (SO_4-type) (e.g., Palinpinon, Mt.Apo and Sumikawa). In the Kyushu island, acid fluid discharge from geothermal wells is being experienced in Hatchobaru [1], Takigami (unpublished), Shiramizugoe [2] and Yamagawa [3] (Fig.1). Chemical analyses of the acid discharged water of these fields are listed in Appendix I. In former three geothermal fields, the acid fluids are of the sulphuric acid type and contain no excess chloride ion as shown in Appendix II. This study aims to evaluate the geochemical techniques using mainly sulphur isotope data to reveal the origin and behaviour of acid fluids in the geothermal fields of Kyushu.

2. Origin of acid geothermal fluids

The sulphuric acid type fluid is generally formed by any of three kinds of mechanisms, (1) oxidation of H_2S, (2) hydrolysis of SO_2, or (3) hydrolysis of S (native sulphur).

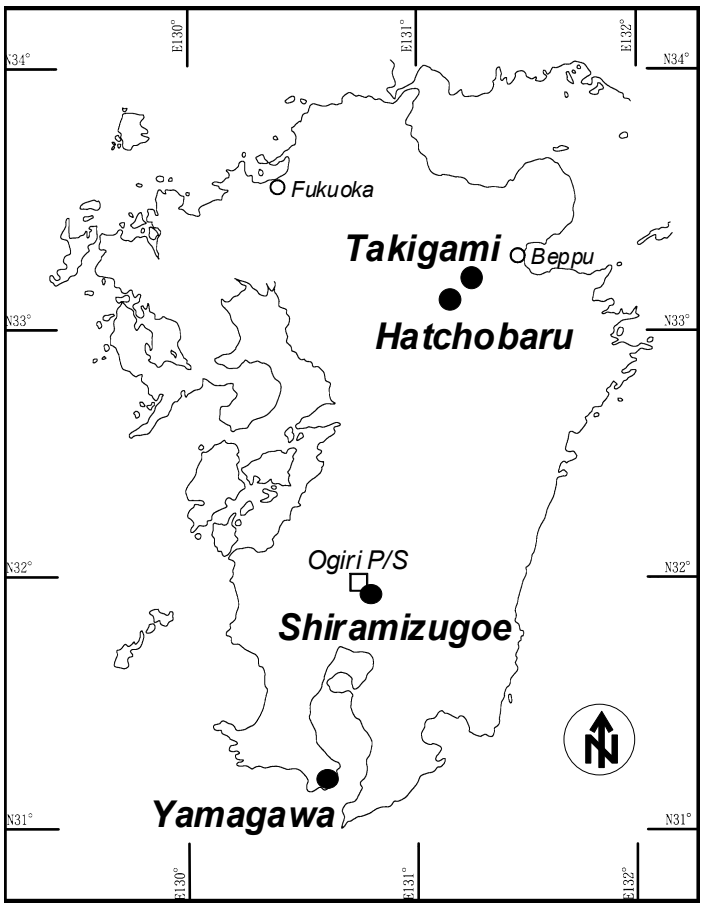

Figure 1. Map of geothermal fields where acid fluid occurs in Kushu.

The oxidation of H_2S is a typical mechanism causing acid sulphate type hot spring water. However, this mechanism rarely is the cause of acidity of the deep geothermal fluids, due to the highly reduced condition in the geothermal reservoir and the impermeable layer preventing shallower fluids from infiltration into the reservoir.

The hydrolysis of SO_2 is represented by the following equation:

$$4SO_2 + 4H_2O \rightarrow 3H_2SO_4 + H_2S \qquad (1)$$

This reaction, as well as the dissolution of HCl, is related to the source of acidity of many SO_4-Cl type hot spring waters in Japan. The formation mechanism of the sulphuric acid type of geothermal fluids in Mt.Apo [4] and Sumikawa [5] is likely to be explained by this reaction. Reflecting its formation mechanism, the acid fluids of this type tend to exist in great depth near the heat source.

The hydrolysis of native S is represented by the following equation:

$$4S + 4H_2O \rightarrow H_2SO_4 + 3H_2S \qquad (2)$$

Ellis and Giggenbach [6] mentioned that sulphur hydrolysis is believed to be common in active volcanic areas. In this paper, they described the acid sulphate-rich spring waters rising through sulphur-containing beds in Rotokaua, New Zealand, and the acid water at about 200°C from geothermal drill holes to about 500m intersected zones of rock containing several percent sulphur in Tatun, Taiwan.

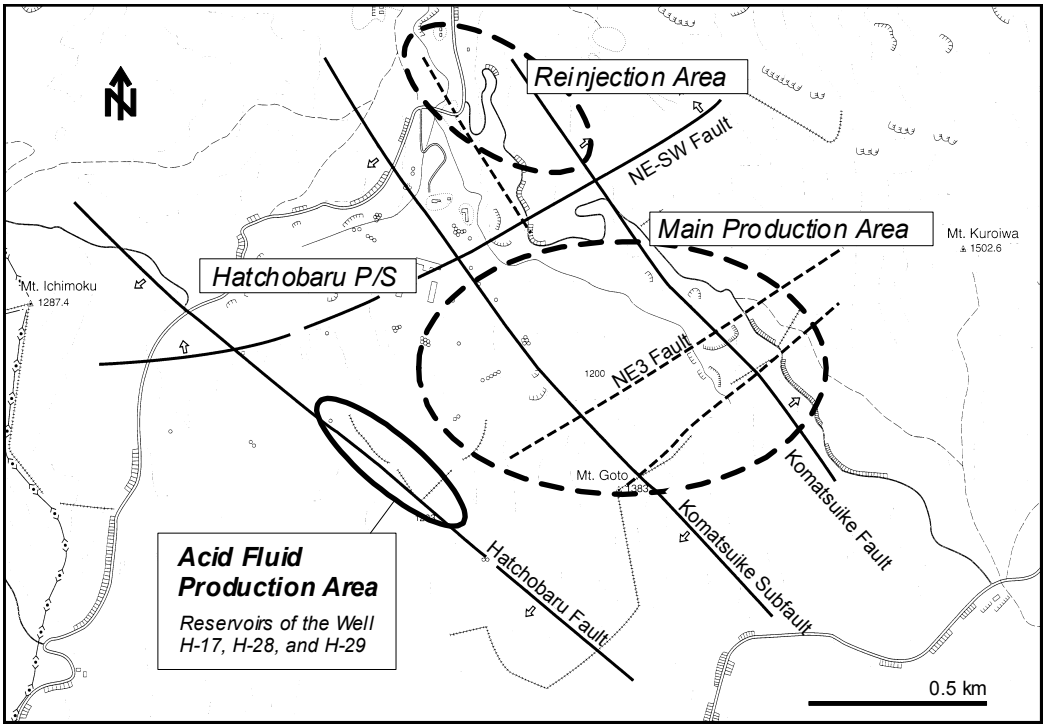

Fig. 2. Map of acid fluid production area in the Hatchobaru field.

3. Acid fluids in hatchobaru

3.1. Background

The Hatchobaru geothermal field is situated at the northeastern portion of Kyushu island. Two 55 MWe power plants are installed with the steam supplied from about 25 production wells. The geothermal reservoir is basically a water-dominated type and has been tapped within andesitic volcanics (Hohi volcanic rocks and Usa group) overlying the pre-Tertiary basement. The main production reservoir extends to a depth of 800-1,500m along the Komatsuike sub-fault and the Komatsuike fault (Fig.2).

The geochemistry of acid geothermal fluids of Hatchobaru was discussed by Shimada et al.

There are two kinds of sulphuric acid type fluid produced by geothermal wells. One, found at northern portion of the main production area, is caused by the H_2S oxidation resulting from the reaction with the air dissolved in wastewater re-injected close to this production area. The other is found along the Hatchobaru fault (Fig.2) and which has been thought to be formed by the hydrolysis of sulphur. In recent years, the discharge of this last type of acid fluids has induced corrosion in the wellhead facilities of production wells H-28, H-29 and H-17. Discussion in this study focuses on the detailed chemical and isotopic characteristics of the acid fluids produced from the reservoirs along the Hatchobaru fault.

Table I. Representative chemical and isotope data of geothermal fluids in Kyushu

Well name	Year	pH[1)]	Cl res[2)] mg/L	SO_4 res[2)] mg/L	TQz °C	$\delta^{34}S(SO_4)$ ‰oCDT	$\delta^{34}S(H_2S)$ ‰oCDT	$\delta^{34}S$(S total) ‰oCDT
Hatchobaru								
H-28	1999	3.3	1040	524	246	22.8	-2.5	12.6
H-29	1998	3.2	847	493	239	23.1	-1.3	10.4
H-17	1998	6.9	952	163	257	19.3	-0.6	0.4
2H-19	1998	7.9	2030	71.5	264	19.8	-1.2	6.4
2HD-1	1998	8.2	979	19.7	292	17.1	(-1.6)	(-1.4)
Takigami								
TT-16	1991	3.6	562	236	233	20.4	-2.8	16.5
TT-16	1989	8.8	546	142	245	14.3	(-1.8)	(8.0)
TT-13	1988	8.9	576	79	254	13.0	-	-
Shiramizugoe								
KE1-9	1984	2.8	880	271	280	16.9	-	-
KE1-11	1984	2.4	697	496	283	17.6	-	-
Yamagawa								
#7	1990	4.15	22060	28.5	273	-	-	-
#17	1990	3.99	16800	29.2	302	-	-	-
#18	1990	7.06	15740	18.4	273	-	-	-

(1) separated water pH measured at room temperature

(2) recalculated reservoir concentration

Data sources are as follows; Hatchobaru: Kyushu Electric Power Co., Inc. internal report, Takigami: [8] and Idemitsu Oita Geothermal Co., Ltd. internal report, Shiramizugoe: [9] and Nittetsu Kagoshima Geothermal Co., Ltd. internal report, Yamagawa: [10]. Values in parenthesis are mean values of available sulphur isotope data of H_2S for each field, and isotope compositions of total sulphur calculated with the mean values.

3.2. Sulfur isotope compositions

Some sulphur isotope data obtained from the discharged waters of Hatchobaru wells were described by Shimada et al. [1] and Kiyota et al. [7]. However, analysis of sulphur isotope composition of the H_2S in vapour phase had been very restricted. From 1998 to 1999, additional sulphur isotope data was obtained by Kyushu Electric Power Co. (unpublished). This data includes the isotope compositions of the H_2S from the some production wells. The $\delta^{34}S(SO_4)$ values vary from 10.9 to 23.2‰ CDT, and the values of the acid fluids are generally higher than those of neutral-pH fluids (Fig.3). On the other hand, the $\delta^{34}S(H_2S)$ values are almost constant (-2.5 – -0.6 ‰) (Table 1).

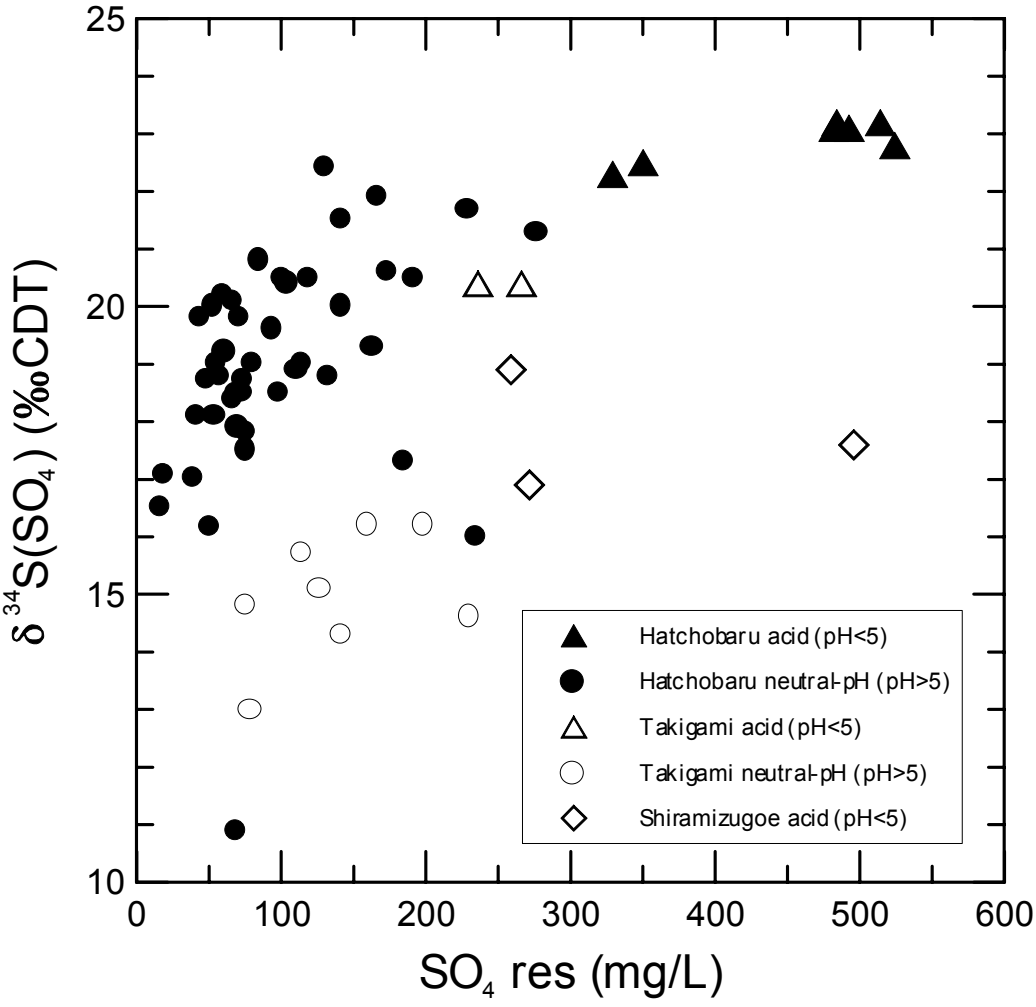

Figure 3. Plot of sulphur isotope ratios in sulphate vs. sulphate concentrations in reservoir.

The origin of sulphur in geothermal fluid is reflected by the isotope composition of total sulphur. The $\delta^{34}S$(S total) values in the total discharge were calculated using the discharge enthalpy and the concentrations of SO_4 and H_2S. In the calculations to process the data obtained before 1997 and in which only $\delta^{34}S(SO_4)$ values are available, the $\delta^{34}S(H_2S)$ values were postulated to be the mean value of the available analysed data (-1.6 ‰). The $\delta^{34}S$(S total) values of the neutral-pH fluids show a large variation from -1.6 to 18.0 ‰, whereas those of the acid fluids are relatively homogeneous (7.9 - 12.6 ‰). The $\delta^{34}S$(S total) value in the fluids of each well seems to depend mainly on its $\delta^{34}S(SO_4)$ and SO_4/H_2S ratio.

The large variation of $\delta^{34}S$(S total) in the neutral-pH fluids suggests a mixing of fluids having different $\delta^{34}S$(S total) values. The neutral-pH reservoirs existing in the main production area are affected by the re-injected water. The $\delta^{34}S$(S total) values of fluids enriched in Cl tend to be high except fluid from wells H-23 and H-25 (Fig.4); this indicates that the large variation in $\delta^{34}S$(S total) is caused by the mixing of the re-injected water. The separation of vapour phase containing H_2S gas elevates the $\delta^{34}S$(S total) value in the discharged fluid. A variation of $\delta^{34}S$(S total) among fluids enriched in Cl may reflect various degrees of H_2S recharge in the reservoirs.

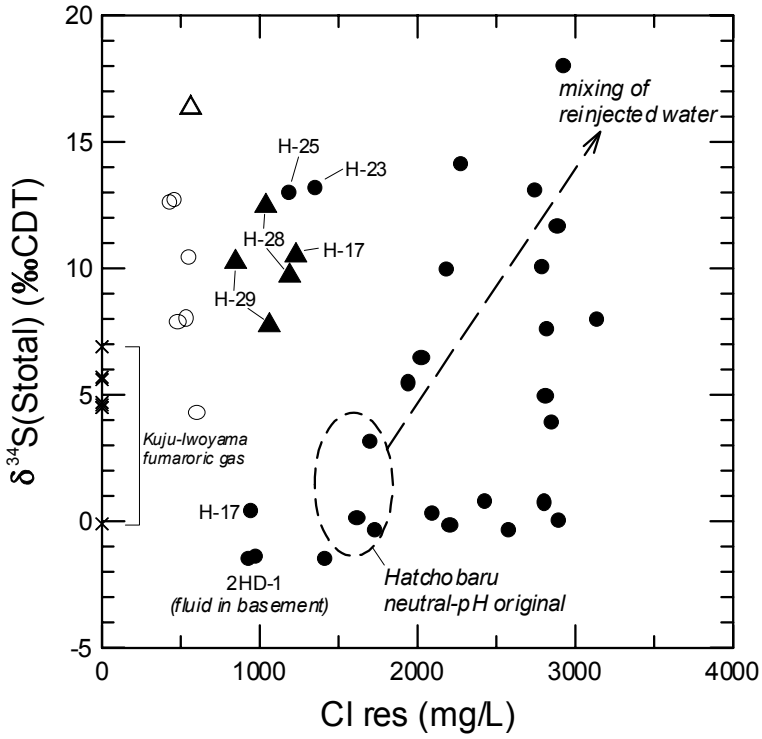

Fig. 4. Plot of sulphur isotope ratios in total sulphur vs. chloride concentrations in reservoir. Symbols are same as in Fig.3. For calculating the isotope ratios in total sulphur of several data, the ratios of H_2S were assumed to the mean value of each field. Data set of Kuju-Iwoyama fumarolic gas is from [11] and [12].

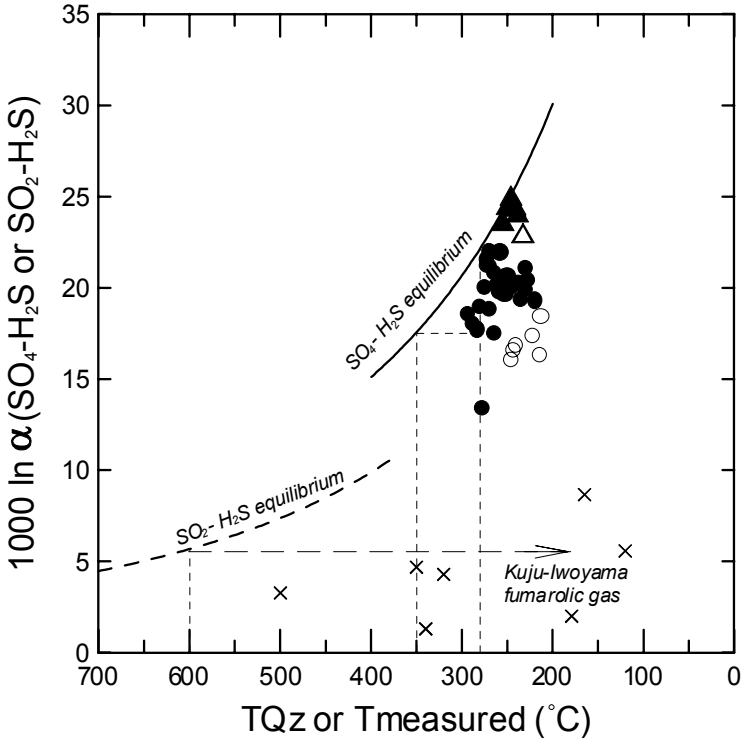

Fig. 5. Plot of sulphur isotope fractionation factors between SO_4(or SO_2) and H_2S vs. their temperatures. Symbols are same as in Fig.3. For calculating the fractionation factors of several data, the ratios of H_2S were assumed to the mean value of each field.

The original neutral-pH fluids, which are almost free from the mixing of re-injected water, exhibit ca. -1–4‰ of the $\delta^{34}S$(S total). These values are comparable to or slightly lower than those of high temperature fumarolic gases in the Kuju-Iwoyama area situated at about 5km eastward from the Hatchobaru field (Fig.4). The sulphur in the neutral-pH fluids, therefore, might be derived from a magmatic fluid. The slightly lower $\delta^{34}S$(S total) values are possibly due to sulphate mineral deposition and/or addition of H_2S in the excess steam. Moreover, the lower values are likely to be caused also by the influence of fluids stored in the basement rocks, as is the case of the fluid from the well 2HD-1 tapping the deep reservoir in the basement rocks. The isotopically lighter sulphur of the fluids in the basement rocks is thought to originate in the sedimentary sulphur of the crystalline schist constituting the basement.

Although the acid fluids are free from the mixing of re-injected water, their $\delta^{34}S$(S total) values are higher than that of the original neutral-pH fluids. This implies that the dissolved SO_4 in the acid fluids cannot be explained by the simple oxidation of H_2S. The SO_4 in the acid fluids is considered to have a different source in origin or a different mechanism of occurrence from that in the neutral-pH fluids. To reveal the origin of the SO_4 in acid fluids, it is necessary to take also the chemistry of the acid fluids into consideration.

3.3. Isotopic equilibrium condition

In equilibrium system, the SO_4-H_2S isotopic fractionation factor is controlled mainly by temperature. The fractionation factors ($1000\ln\alpha$) in the neutral-pH fluids of Hatchobaru wells deviate from the equilibration to lower values (Fig.5). This deviation may indicate that these factors are reflecting the higher temperature condition due to the slow reaction rate. According to Ohmoto and Lasaga [13], the theoretical time required for the attainment of 90% equilibrium between sulphates and sulphides at the pH of 4-7 and 250°C with total sulphur content = 0.01 mole/kg is 4.4 years. The temperature at which the fractionation factors of Hatchobaru fluids are in equilibrium is about 280 - 350°C, which is plausible at the deeper portion of the reservoir. The temperature decline caused by the mixing of re-injected water possibly magnifies the deviation of fractionation factors. The fluids with silica temperature lower than 250°C are considered to be strongly affected by the re-injected water judging from their relatively high Cl concentrations. The fumarolic gases in Kuju-Iwoyama, as well as the neutral-pH geothermal fluids, seem to have SO_2-H_2S fractionation factors equilibrated at the higher temperature (600°C or higher).

The acid fluids seem to be almost in isotopic equilibrium at about 240°C. The attainment of equilibration can be explained by the rapid reaction rate at the low pH and/or the high content of total sulphur, compared with the neutral-pH fluids. However, the calculations of reservoir pH using the computer code SOLVEQ provide estimates of 4.8–5.4 for the acid fluids, which are only 0.1–1.1 lower in pH unit than that for the neutral-pH fluids. This suggests that the isotopic reaction rate in the acid fluids is not so rapid compared to that in the neutral-pH fluids. In evaluating the fractionation factors in the acid fluids, it also should be taken into consideration that the attainment of isotopic equilibration could be only the appearance resulting from the mixing of fluids enriched in SO_4 with relatively high $\delta^{34}S$ value.

3.4. Chemical characteristics of sulfur species

The relationship between SO_4 and H_2S concentrations in the fluids may give some clue for revealing the origin of sulphur species in the acid fluids. As shown in Fig.6, the neutral-pH fluids exhibit very large variation of the SO_4 and H_2S concentrations in total discharge. The variation is believed to be caused by mixing of the re-injected water depleted in H_2S, the contribution of excess steam (the fluid with the lowest SO_4, from the well 2H-12, is almost steam only) and the contribution of fluid occurring in the basement rocks.

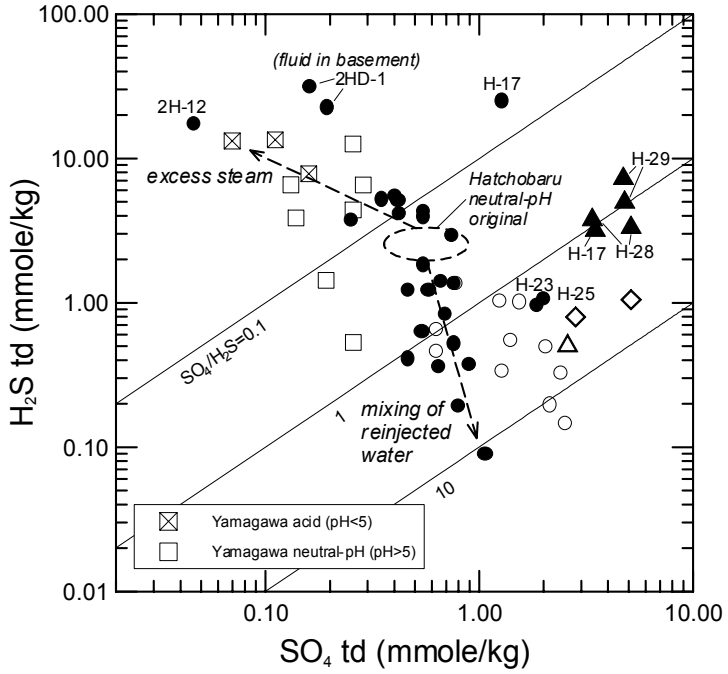

Figure 6. Plot of H_2S vs. SO_4 concentrations in total discharge. Symbols excluding for Yamagawa are same as in Fig.3. Arrows representing the effects of excess steam and mixing of reinjected water are appropriate only for Hatchobaru data.

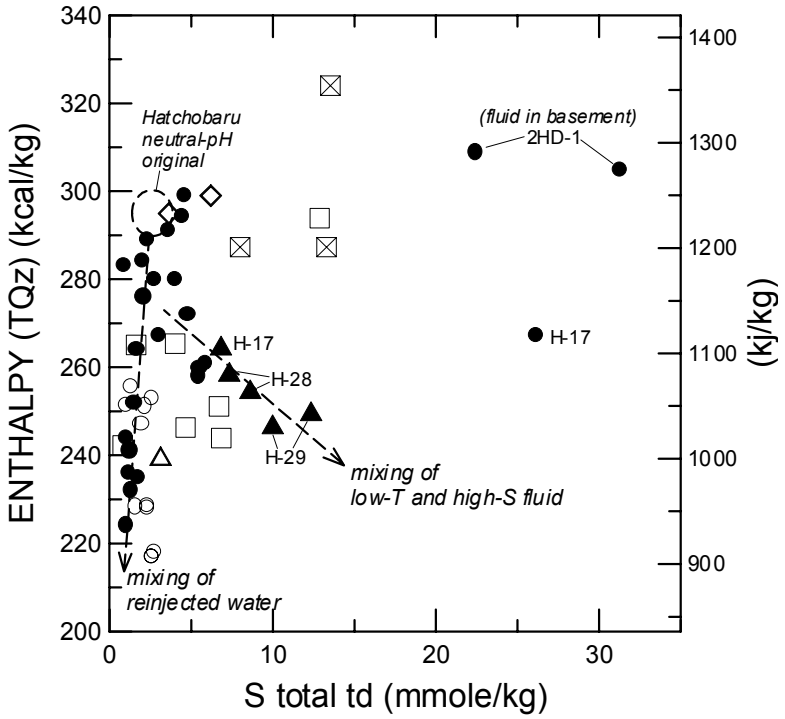

Fig. 7. Plot of fluid enthalpies based on silica temperature vs. *total sulphur concentrations in total discharge. Symbols are same as in Fig.6. Arrows representing the effect of fluid mixing are appropriate only for Hatchobaru data.*

The acid fluids show remarkably high concentrations of SO_4 with H_2S concentration corresponding to the original neutral-pH fluid, and their SO_4/H_2S ratios are approximately unity (Fig.6). If the SO_4

enrichment in the acid fluids occurs by the hydrolysis of SO_2 or the hydrolysis of native sulphur in or around the reservoir without the fractionation of sulphur species, the SO_4/H_2S ratios would be close to 3 or 1/3 in accordance with the equation (1) or (2) respectively. The relationship between SO_4 and H_2S concentrations in the acid fluids, therefore, suggests the mixing of fluid dominant in SO_4 formed at the distant portion from the reservoir, or otherwise the in situ oxidation of H_2S.

The mixing model based on the relationship between enthalpy (silica temperature) and total sulphur concentration in total discharge indicates that the acid fluids are formed by mixing of high temperature fluid depleted in sulphur, which is similar to the original neutral-pH fluids, with low temperature fluid enriched in sulphur (Fig.7). The maximum temperature of the sulphur-rich fluid would be 240°C. Thus, the hydrolysis of SO_2 cannot be regarded to be the cause of the sulphur-rich fluid, because it occurs basically at high temperature around 350-500°C [14]. Moreover, the hydrogen and oxygen isotope compositions of the acid fluids show no indication of the contribution of magmatic fluid possibly containing SO_2 gas [1].

3.5. Chemical characteristics of sulfur species

From the discussions mentioned above, the acid fluids in the Hatchobaru field are considered to be formed by the mixing of neutral-pH fluid with low temperature fluid enriched in SO_4 originating in hydrolysis of native sulphur or in partial oxidation of H_2S accompanied with isotopic re-equilibration at lower temperature.

Shimada et al. [1] also mentioned the possibility of the occurrence of hydrolysis of native sulphur in the Hatchobaru field. The occurrence of native sulphur crystals was recognized in the core samples collected at the depths shallower than 900m of the exploration well HT-4 drilled around the Hatchobaru fault. The total sulphur content in the core samples reaches 5.5wt% in maximum. The hydrolysis of native sulphur simultaneously produces three times as many sulphides than sulphates as indicated in the equation (2). Although no solfataras are known in an area along the Hatchobaru fault, the remarkable H_2S discharge from the wells H-28 and H-29 was recognized when the drilling of these wells reached depths of 160m and 90m respectively. This suggests that the H_2S gas formed by the hydrolysis of native sulphur ascends to the near surface; and the cognate SO_4 dissolved in groundwater may infiltrate the deeper level. The $\delta^{34}S$ value of the SO_4 would be lower than 24 ‰ from the observed value in the acid fluids. As no analytical data on native sulphur in the Hatchobaru field is available, assuming the $\delta^{34}S$ value of the native sulphur to be -4 ‰ which is the mean value of native sulphur in volcanic areas in Japan [15], the temperature at which the hydrolysis of the native sulphur occurs, is estimated to be lower than 224°C. In this estimate, the $\delta^{34}S$ value of the cognate H_2S in equilibrium with the native sulphur is calculated higher than -3.2 ‰.

If the oxidation of H_2S occurs at the shallow level, the oxidation would be partial and accompanied with the isotopic re-equilibration so as to explain the higher $\delta^{34}S$ value of SO_4. The SO_4 with the $\delta^{34}S$ value of higher than 24 ‰ equilibrates with H_2S with the $\delta^{34}S$ value of -1.6 ‰ at the temperature lower than 240°C. However, the full re-equilibration is not likely to be attained easily. In the Palinpinon field, in which the acid fluids are believed to be produced by partial oxidation of H_2S, only a small number of acid fluids are in equilibrium and most of the acid fluids show wide variety of $\delta^{34}S$ values of SO_4 [16].

Figure 8 shows a schematic geochemical model along the Hatchobaru fault. The low temperature fluid enriched in SO_4, which contributes the formation of the acid fluids, even if their origin is the hydrolysis of native sulphur or either of the partial oxidation of H_2S, is thought to flow downward from shallower levels. All of the main feed points of the acid wells H-28, H-29 and H-17 are located between -200 and -100 m.a.s.l. (1,350–1,250m in vertical depth). The acid fluids are thought to be stored in reservoirs located around these depths and along the permeable zone of the Hatchobaru fault. These reservoirs are probably connected to each other. This depth almost corresponds with a boundary

between the geological formations of the Hohi volcanic rocks and the Usa group, thus the reservoirs of acid fluids are likely to have also some horizontal extent.

The hot waters discharged from the well H-17, so far, have shown various pH values (3.4–8.4), however, after beginning of discharge at well H-28 in 1995 and H-29 in 1997, only neutral-pH waters have been recognized. This suggests that the acid reservoir of the well H-17 has been influenced by the discharge at wells H-28 and H-29. According to the result of the P-T production logging, well H-17 has another feed point at the level of -500m.a.s.l. (1,600m in vertical depth); so the neutral-pH fluid is likely to have been fed at this depth. Geological analysis indicates that the bottom of the well H-17 (-700m.a.s.l.) reaches very close to the top of the basement rocks. Thus, the neutral-pH fluid from the

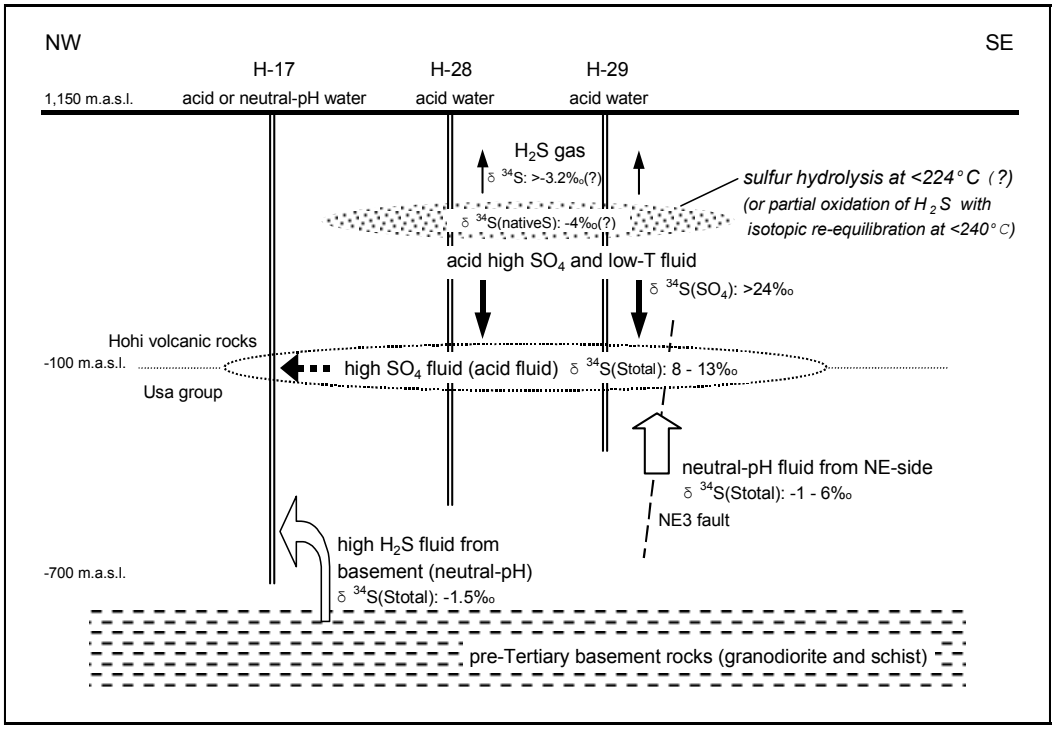

Fig. 8. Schematic geochemical model showing acid fluid formation mechanism along the Hatchobaru fault.

well H-17 is possibly contributed by the fluid stored in the basement rocks. The high contents of H_2S and total sulphur in the neutral-pH fluid as well as in the fluids from the well 2HD-1 also signify the contribution of the basement fluids (cf., Fig. 6 and Fig. 7).

The decline of the acid fluid discharge at the well H-17 after the beginning of discharge at wells H-28 and H-29 suggests that the centre of the acid reservoir along the Hatchobaru fault is located on the southeast side. The neutral-pH fluid of relatively high temperature mixing with the low temperature sulphur-rich fluid from shallower level may be supplied from the main production reservoir along NE-SW trending faults (e.g. NE3 fault).

Considering the above model, in case of production make-up drilling is done near the Hatchobaru fault, the anchor casing shoe is desirable to be set at a level deeper than -200 m.a.s.l. in order to

prevent the acid fluid from entering the borehole. The promising target would be around the same depth as the deeper feed points of well H-17.

4. Acid fluids in other areas in Kyushu

4.1. Takigami and Shiramizugoe

In Takigami field, situated 15km northeast of the Hatchobaru field (Fig.1), the discharge of acid fluid enriched in SO_4 was detected at one well (TT-16) drilled in the middle of the production area during the early stage of development. The chemical and isotopic characteristics of the acid fluid are analogous to the acid fluids in Hatchobaru field; i.e. higher $\delta^{34}S(SO_4)$ and $\delta^{34}S$(S total) values, relatively higher SO_4/H_2S and lower temperature compared to the neutral-pH fluids of the field (Table 1, Fig.3-7). This suggests that the mechanism of acid fluid formation in Takigami is similar to that in Hatchobaru. Since the acid fluid discharge at the well TT-16 occurred only in the later stage of its discharge history, the pressure draw down in the reservoir possibly induced the inflow of shallower fluids.

Shiramizugoe field is adjacent to the Ogiri production field and is one of the promising fields in the south of Kyushu (Fig.1). In this field, most of the fluids from the high temperature exploration wells are strongly acidic (Table 1). Relatively high $\delta^{34}S(SO_4)$ values and the occurrence of sulphur beds seems to be related to the hydrolysis of sulphur [2]. However, it is probable that hydrolysis of SO_2 is the cause for the acid fluids because of the high temperature (ca. 280°C). Detailed studies on well geochemistry including the $\delta^{34}S(H_2S)$ analysis are necessary to reveal the formation mechanism of the acid fluids.

4.2. Yamagawa

The acid fluids occurring in the Yamagawa field, situated at the south end of Kyushu (Fig.1), are classified as hydrochloric acid type (Table 1), and are considered to be formed mainly due to the precipitation of sphalerite [3]. Although sulphur isotope data from well fluids are not available, there seems not to be an apparent difference in isotope composition between the acid fluids and the neutral-pH. The high enthalpies and the low SO_4/H_2S ratios of the acid fluids compared to those in neutral-pH fluids indicate that the fluid with a high degree of boiling within the reservoir is readily modified towards the lower pH (Fig. 6 and Fig. 7).

5. Conclusions

The results of these case studies using geochemical techniques and isotope data (particularly sulphur isotope data) applied to geothermal areas in Kyushu are summarized as follows.

- The integrated interpretation using several indices based on isotope and chemical data of sulphur species, i.e. $\delta^{34}S$(S total), $\delta^{34}S$ fractionation factor and SO_4 and H_2S concentration in total fluid, are effective and useful to reveal the origin and characteristics of acid fluids enriched in SO_4.

- Acid fluids occurring in the Hatchobaru geothermal field are thought to be the result of mixing of neutral-pH fluid with low temperature SO_4-rich fluid from shallower levels. These shallow acid fluids originate in hydrolysis of native sulphur existing in the shallower level at a temperature lower than 224°C or in partial oxidation of H_2S accompanied with isotopic re-equilibration lower than 240°C. The distribution of acid fluid reservoirs is believed to be restricted to the relatively shallow level.

Acknowledgements

The authors are deeply grateful to Kyushu Electric Power Co., Inc., Idemitsu Oita Geothermal Co., Ltd. and Nittetsu Kagoshima Geothermal Co., Ltd. for permission to publish data.

REREFERENCES

[1] SHIMADA, K., FUJINO, T., KOGA, A., and HIROWATARI, K. (1985) Acid hot water discharging from geothermal wells in the Hatchobaru geothermal field. Journal Japan Geothermal Energy Association 22, 276–292 (in Japanese with English abstract).

[2] GOKO, K. and SHIMIZU, A. (1993) Acid geothermal fluid of the Shiramizugoe area in the Kirishima geothermal field (Abstract for the annual meeting 1992 of the Geothermal Research Society of Japan). Jour. Geothermal Research Society of Japan 15, 158–159 (in Japanese).

[3] AKAKU, K., KASAI, K., NAKATSUKA, K., and UCHIDA, T. (1997) The source of acidity in water discharged from high temperature geothermal reservoirs in Japan. Proc. 22nd Workshop on Geothermal Reservoir Engineering, 427–434.

[4] SALONGA, N.D. (1996) Fluid and mineral equilibria in acid NaCl(+SO_4) reservoir: The case of Sandawa Collapse, Mt. Apo hydrothermal system. Proc. 17th Annual PNOC-EDC Geothermal Conference, 119–129.

[5] UEDA, A., KUBOTA, Y., KATO, H., HATAKEYAMA, K., and MATSUBAYA, O. (1991) Geochemical characteristics of the Sumikawa geothermal system, northern Japan. Geochem. J. 25, 223–244.

[6] ELLIS, A.J. and GIGGENBACH, W.F. (1971) Hydrogen sulphide ionization and sulphur hydrolysis in high temperature solution. Geochim. Cosmochim. Acta 35, 247–260.

[7] KIYOTA, Y., MATSUDA, K., and SHIMADA, K. (1996) Characteristics of acid water in the Otake-Hatchobaru geothermal field. Proc. 17th Annual PNOC-EDC Geothermal Conference, 131–135.

[8] TAKENAKA, T. and FURUYA, S. (1991) Geochemical model of the Takigami geothermal system, northeast Kyushu, Japan. Geochem. J. 25, 267–281.

[9] KODAMA, M. and NAKAJIMA, T. (1988) Exploration and exploitation of the Kirishima geothermal field. Journal Japan Geothermal Energy Association 25, 201–230 (in Japanese with English abstract).

[10] YASUDA, Y. (1998) Studies on the fluid chemistry in the Fushime geothermal system, Japan. Proc. 23rd Workshop on Geothermal Reservoir Engineering, 196–203.

[11] SAKAI, H. and MATSUBAYA, O. (1977) Stable isotopic studies of Japanese geothermal systems. Geothermics 5, 97–124.

[12] MIZUTANI, Y., HAYASHI, S., and SUGIURA, T. (1986) Chemical and isotopic compositions of fumarolic gases from Kuju-Iwoyama, Kyushu, Japan. Geochem. J. 20, 273–285.

[13] OHMOTO, H. and LASAGA, A.C. (1982) Kinetic reactions between aqueous sulfates and sulfides in hydrothermal systems. Geochim. Cosmochim. Acta 46, 1727–1745.

[14] OHMOTO, H. (1986) Stable isotope geochemistry of ore deposits. In: STABLE ISOTOPES in high temperature geological processes, Valley, J.W., Taylor, H.P.Jr., and O'Neil, J.R. (Ed) Reviews in Mineralogy 16, Chap.14, 491–559.

[15] UEDA, A., SAKAI, H., and SASAKI, A. (1979) Isotopic composition of volcanic native sulphur from Japan. Geochem. J. 13, 269–275.

[16] HERMOSO, D.Z., MEJORADA, A.V., and RAE, A.J. (1998) Determination of the nature of acidic fluids in the Palinpinon geothermal field, Philippines through the use of $\delta^{34}S$ in sulfates and sulfides. Proc. 19th Annual PNOC-EDC Geothermal Conference, 65–75.

Appendix I.
Chemical analyses of acid discharged water of the geothermal fields in Kyushu

		Hatchobaru	Takigami		Shiramizugoe		Yamagawa
WELL	H-28	H-29	TT-16	KE1-9	KE1-11	#7	#17
pH	3.3	3.2	3.4	2.8	2.4	4.15	3.99
Na	1030	890	423*	818	765	19100	15100
K	200	178	45.3*	190	167	5340	4850
Li	-	-	1.67*	5.8	5.7	-	-
Ca	13.4	12.5	9.2*	8.1	17.4	2310	1490
Mg	11.2	9.85	0.42*	2.0	4.8	9.8	14.0
Fe	-	-	0.53*	26.0	39.7	31.8	69.6
Al	-	-	31.3*	0.47	0.09	-	-
Cl	1470	1210	556*	1180	980	38600	31100
SO_4	742	704	266*	364	697	49.8	54.1
F	-	-	2.8*	ND	Tr	-	-
B	21.2	18.3	6.8*	84.3	83.7	90.0	133
SiO_2	658	620	394*	1000	1036	922	1274

* re-calculated to reservoir concentration (mg/L)

Appendix II.
Na-K-Cl ternary plot of acid water

(HCl dissolved rock water compositions are after Giggenbach (1988).)

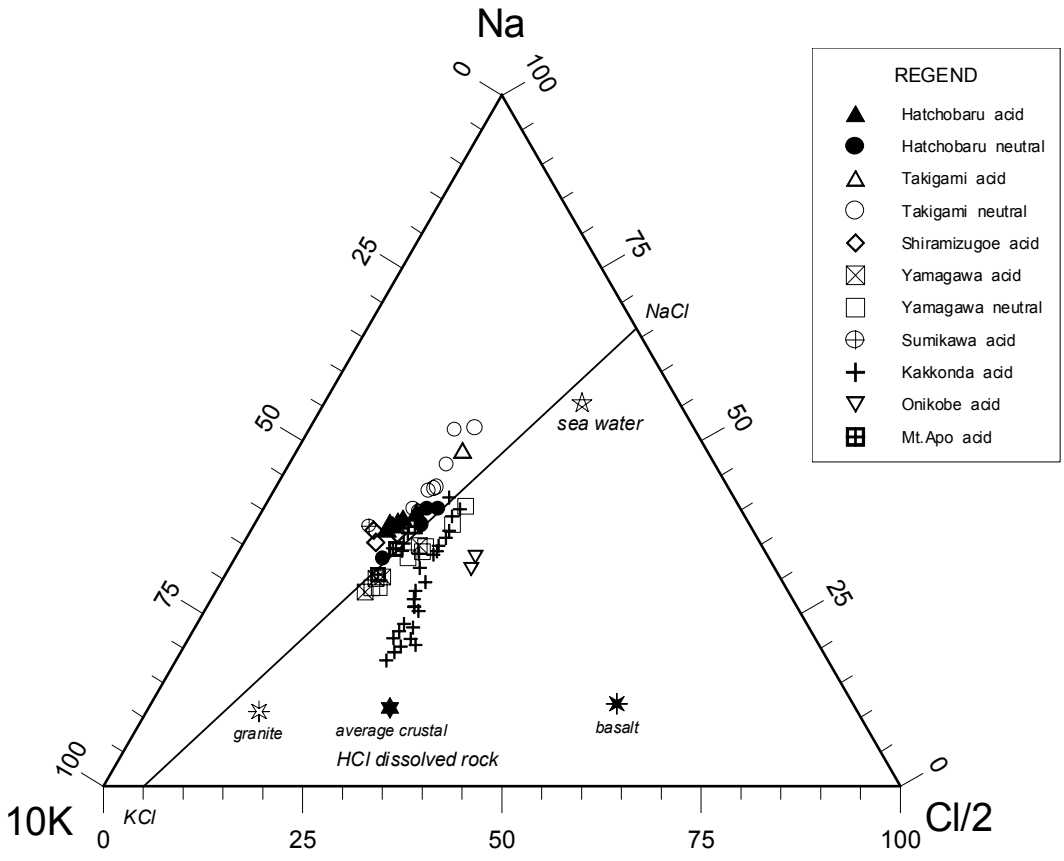

CHEMICAL AND ISOTOPIC STUDY TO DEFINE THE ORIGIN OF ACIDITY IN THE LOS HUMEROS GEOTHERMAL RESERVOIR

E.H. Tello[1], R.A. Tovar[1], M.P. Verma[2]

[1]CFE, Gerencia de Proyectos Geotermoeléctricos,
Morelia, Michoacan, Mexico
[2]Geotermia, Instituto de Investigaciones Electricas,
Morelos, Mexico

Abstract. Chemical and isotopic analyses of geothermal fluids were carried out at the Los Humeros, México, geothermal field in order to establish the water-rock equilibrium state and to determine the origin of the acidity in the reservoir. From the perspective of water-rock equilibrium, the Los Humeros geothermal reservoir is out of equilibrium. This is probably the case since it is associated with recent volcanism, with magmatic components in the geothermal fluids that are not neutralized by reaction with feldspar and mica. Superheated magmatic steam contains HCl gas, which condenses or mixes with liquid at moderate temperature (< 374°C) to form acid waters. This appears to have occurred at Los Humeros because high concentrations of HCl were detected in the steam phase. In addition, high concentrations of boron and arsenic also favor the definition of the Los Humeros as a recent volcanic system. Most wells of this field have high fluid enthalpy and almost all produce high steam fractions at the wellhead. Chemical characteristics of the fluids show that the produced brine is low-salinity water, whose geochemical character varies according to both well type and production. Shallower wells produce sodium bicarbonate (H-1) type water, whereas deeper wells produce sodium chloride (H-6) type. It was also found, according to enthalpy data, that well H-1 is located in a zone where the liquid phase is dominant, while the remaining wells are producing in a two-phase zone. As a result, the chemical composition of the total discharge from well H-1 is the same as that of the reservoir fluid. Measured temperatures at bottom hole vary between 260 and 340°C and are in agreement with geothermometer calculations from Na/K of 295± 10°C and from H_2/Ar of 270 to 340°C. The isotopic composition of the Los Humeros wells shows an $\delta^{18}O$ shift which is characteristic of fluids of geothermal origin that have reached equilibrium with the rock at high temperatures. The isotopic compositions of cold spring waters in the area are mostly located on the meteoric line. The sample from Alchichica lagoon has an isotopic composition typical of evaporated water.

1. Introduction

The Los Humeros field is the second geothermal reservoir after Los Azufres to produce electricity in the area of the Mexican Volcanic Belt (MVB). The Los Humeros geothermal field is situated in the eastern part of the MVB, at an average altitude of 2800 masl about 200 km east of México city (Figure 1). Geothermal exploration in the area including detailed geological, geophysical and geochemical studies was begun at the end of the 1960s. The exploration activities covered an area of about 80 km^2. The first production well was drilled in 1980 and in 1990 the first wellhead power plant was constructed. At present there are 7 wellhead power plants of 5 MWe each. The Los Humeros geothermal system has presently an installed capacity of 35 MWe and approximately 40 wells have been drilled. CFE is planning in the near future to expand the field, with the installation of two more units of 25 MWe each. Two reservoirs have been identified in this field. Although the deeper one has a very high temperature (>350°C), its exploitation may not be feasible due to the high content of HCl in its fluids. The occurrence of acidic fluid has been found in many geothermal reservoirs, and its corrosiveness in geothermal plants has led to constant efforts to understand the origin of acidic fluids in the reservoir and devise methods for their mitigation (Verma et al., 1997).

The objective of this paper is to integrate all available isotopic and chemical data on the Los Humeros geothermal field, in order to understand the state of water-rock interaction and define the origin of the acidity of the fluids produced by the wells.

2. Geologic setting

The Los Humeros geothermal system is located on a complex volcanic Caldera system (less than 500,000 years old), which is at the eastern end of the Plio-Pleistocene Trans-Mexican Volcanic Belt (Yañez, 1980; Ferriz, 1982; Ferriz and Mahood, 1984; Martínez, 1983; Negedank et al., 1985). Thermal manifestations as well as most of the exploration boreholes are located in a small area of 35 km^2 called the Central Collapse Zone (Figure 1). Geologic studies of both cuttings and surface samples show that the basement of the region is formed by Late Cretaceous limestone sequences (Viniega, 1965; Yañes, 1980). Most boreholes penetrate a hydrothermally-altered rock sequence more than 2200 m thick consisting of andesites, dacites, rhyodacites, rhyolitic tuffs, rhyolites and some basaltic rocks overlying a complex basement more than 500,000 years old (Ferriz and Mahood, 1984; Martinez, 1993). The most recent event was an eruption of an olivine basalt lava flow that occurred less than 20,000 years ago.

The subsurface structure at the Los Humeros system has been inferred from geophysical studies to consist of a sequence of graben and horst blocks surrounded by fractures and faults associated with caldera collapse (Campos and Arredondo, 1992; Martinez, 1996).

Petrographic and geochemical studies were carried out at the Los Humeros system by Viggiano and Robles (1988); Prol (1990); Martinez (1993); and Martinez and Alibert (1994). These studies showed that volcanic rock sequences were affected by the circulation of hot water (>290°C), with less than 2500 mg/l of total dissolved salts, transforming the primary rock forming minerals into phases stable at new physico-chemical conditions. Geochemical analyses of the present-day fluids discharged from the boreholes suggest that these fluids result from mixing of geothermal fluids with meteoric water, along with the addition of a high percentage of steam (between 30 and 80%) at shallow depth (Tello, 1992; Barragán et al., 1991; Martínez, 1993). Presently the geothermal system behaves as a mixed two fluid phase system with high enthalpy.

Hydrothermal alteration found in cores and cuttings consists of a shallow argillic zone (0–600m) with mostly zeolites, calcite and oxides, intermediate zones (600–1700 m), of propylitic alteration (epidote, Chlorite, calcite, quartz and sulfides) and deep (>1700 m) zones of calc-silicate alteration containing amphibole, garnet, clinopyroxene and biotite where temperatures are over 320°C. Pyrite is the most ubiquitous sulfide mineral throughout the altered volcanic sequences.

3. Geochemistry of geothermal brine and springs

CFE systematically performs chemical analysis of fluid coming from production wells (López, 1982; López and Munguía, 1989; Barragán et al., 1991; Truesdell, 1991; Tello, 1992, 1994; Tovar, 1999). The chemical analysis of water and gases of samples from 1981 to 1999 display significant variations in the concentrations of the main constituents. Chloride concentrations range from 1.4 to 982 ppm. The most important contribution to the total dissolved solids comes from boron (from 67 to 3169 mg/l), Table I.

In order to indicate the types of fluid produced by the wells and springs, figure 2 was prepared showing the contents of Cl, HCO_3 and SO_4 (Giggenbach, 1989). As shown, only deep wells discharge a mixture of chloride and bicarbonate waters from a zone where deep geothermal fluid, steam heated waters and cold meteoric waters are mixed (Tello, 1992). Enthalpy data show that the deep production zone (deeper than 1500 m) in most wells of this geothermal field seems to be located in a two-phase reservoir (Tello, 1992).

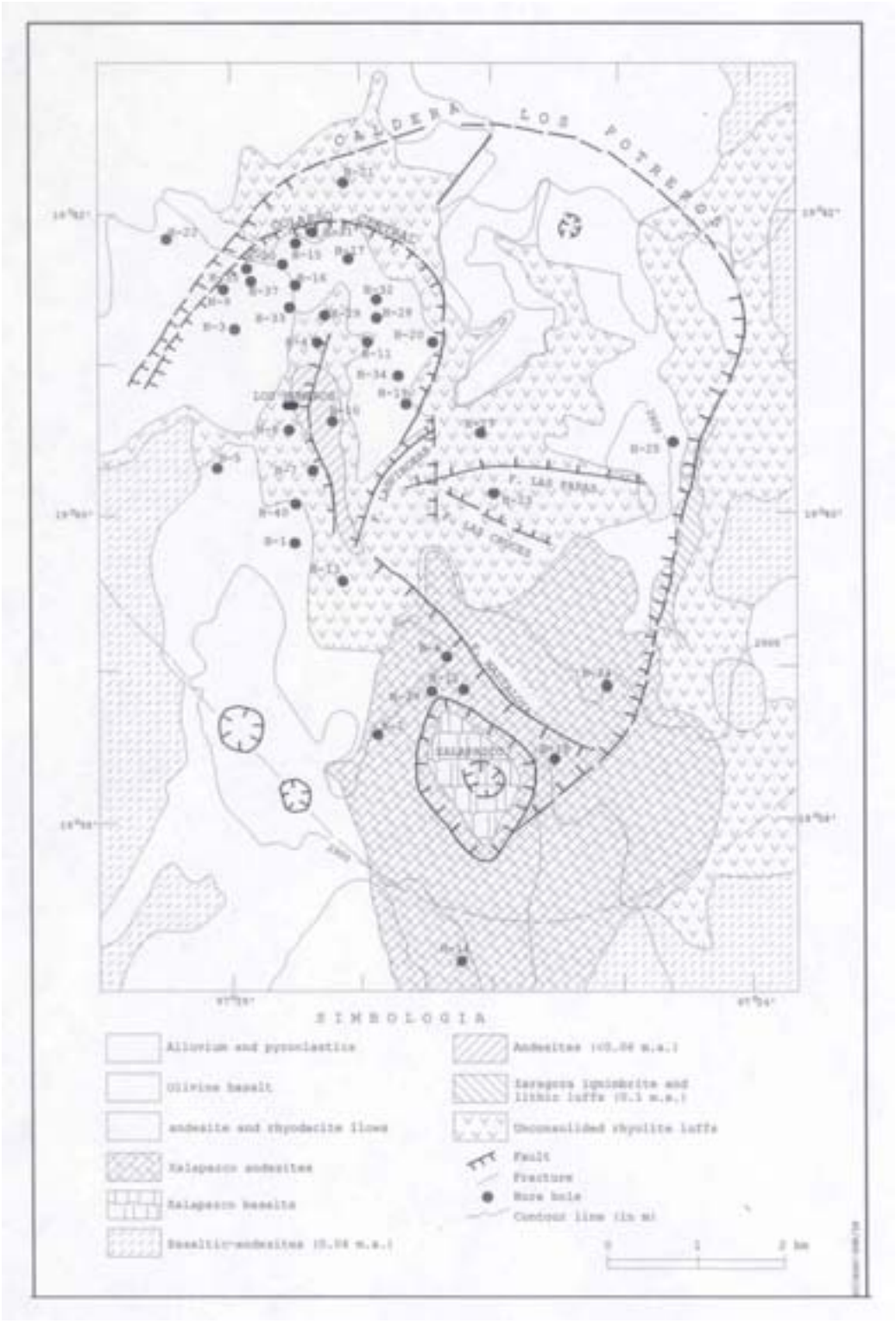

Fig. 1. Geologic map of the Los Humeros Caldera System (taken from Martinez, G., 1994).

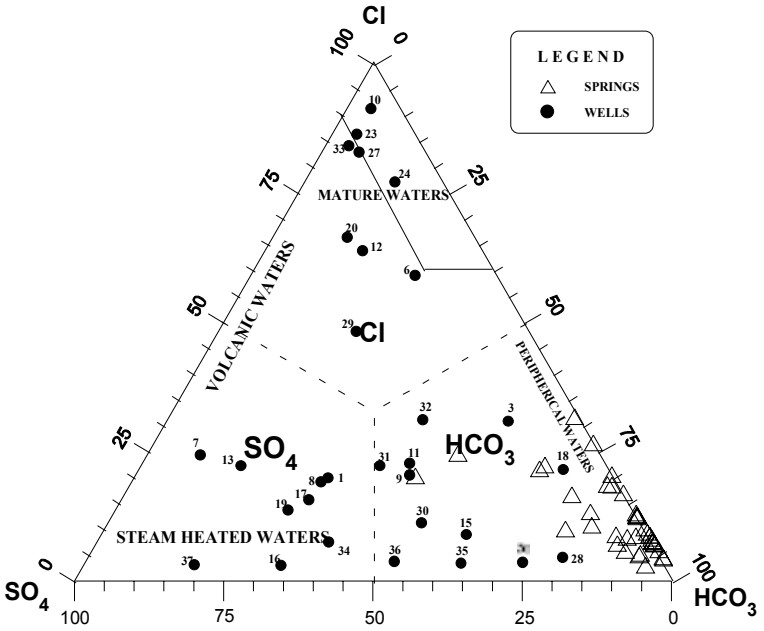

Fig. 2. Relative Cl:SO_4:HCO_3 contents of geothermal brine and springs from the Los Humerosgeothermal field.

CFE has also monitored the water composition of 41 springs on the boundaries of the Los Humeros (Table II). This study assists environmental study of the shallow aquifer, and may indicate if the shallow aquifer has been modified by either exploitation or by injection into the reservoir. The springs are generally sodium bicarbonate waters with low chloride (<12 mg/l) and boron (<1 mg/l), and high concentrations of calcium suggesting that these waters originate as meteoric fluids circulating through shallow volcanic rocks and that water-rock interaction occurred at low temperatures.

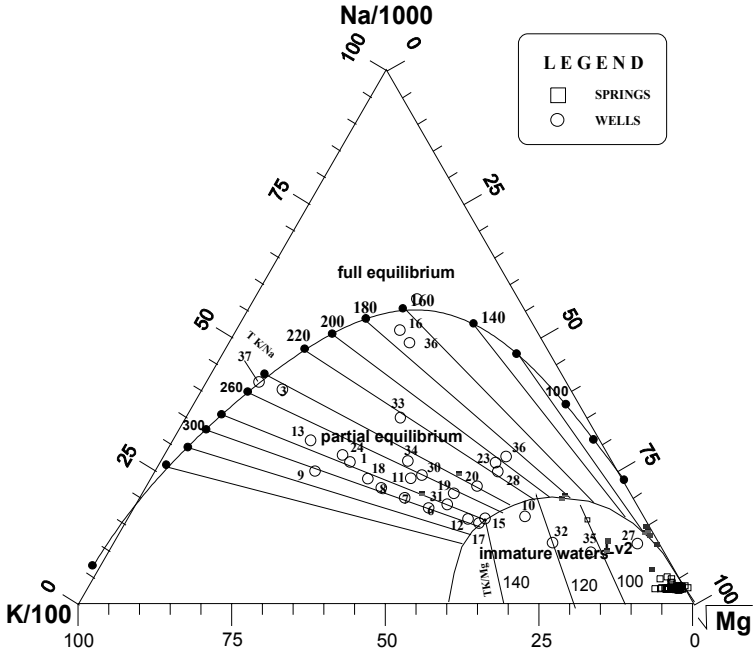

Fig. 3. Evaluation of Na:K:Mg temperatures from the Los Humeros geothermal field.

Table I. Chemical composition of separated water from the Los Humeros geothermal field

Wells	Date	Enthalpy	Elect. Cond.	Orifice	pH	Concentrations in mg/l										
No	dd/mm/yy	KJ/kg	µmhos/cm	mm		Na	K	Ca	Mg	Cl	SO_4	HCO_3	B	SiO_2	Li	As
H-1	04-Jan-96	1179	1270	50.8	8.3	267	45	2.04	0.119	90.2	233	162	218	1005	0.47	2.79
H-3	05-oct-94	-	1420	50.8	8.2	420	49	1.60	0.019	174.8	71	334	477	556	1.60	4.00
H-6	04-Jan-96	2441	780	63.5	8.1	142	31	1.60	0.180	104.1	23	48	345	946	0.42	27.41
H-7	04-Jan-96	-	950	127.0	7.6	177	36	2.24	0.180	83.3	239	34	946	915	0.41	8.50
H-8	04-Jan-96	1981	1150	76.2	8.1	243	48	2.04	0.219	76.3	213	139	453	1120	0.30	3.10
H-9	03-Jan-96	2726	1160	127.0	7.5	250	52	2.08	0.080	50.3	89	122	1823	838	0.49	73.62
H-10	19-jul-89	2662			6.0	142	19	1.80	0.400	982.7	33	28	1716	909	0.83	N.A.
H-11	05-Jan-96	-	1030	50.8	7.9	207	32	2.56	0.160	74.5	113	156	443	844	0.45	7.60
H-12	04-Jan-96	-	530	50.8	7.6	87	19	0.22	0.119	41.6	12	11	695	688	0.30	16.35
H-13	05-oct-95	1332	2300		8.4	341	54	3.61	0.070	140.1	409	117	219	1006	1.37	N.A.
H-15	03-Jan-96	2551	540	76.2	8.3	113	21	1.20	0.219	6.9	30	61	200	797	0.39	0.50
H-16	06-Jan-96	-	2400	76.2	9.0	549	24	1.20	0.080	4.1	408	216	402	580	0.45	7.90
H-17	03-Jan-96	-	500	50.8	7.8	91	19	1.40	0.160	24.3	91	55	333	893	0.37	24.41
H-18	13-oct-89	1747	1645	50.8	8.0	123	23	0.92	0.04	112.3	43	397	118	229	0.37	N.A.
H-19	05-Jan-96	2141	700	63.5	6.9	140	21	2.18	0.141	23.8	112	57	1873	486	0.41	21.71
H-20	09-Jan-96	-	760	50.8	7.9	160	20	1.80	0.180	114.5	35	20	447	838	0.40	5.53
H-23	13-nov-87	2064	2700	50.8	6.3	290	22	37.00	0.401	622.0	57	21	194	114	0.40	
H-24	18-may-89	2491	1500	38.1	7.6	285	46	1.50	0.109	324.6	27	58	423	406	0.90	
H-27	14-feb-89	2314	1025	76.2	7.4	68	3	1.80	0.4	232.8	26	14	136	100	0.17	
H-28	05-Jan-96	-	1000	50.8	8.7	228	19	0.60	0.299	7.6	56	267	67	424	0.46	1.90
H-29	10-Jan-92	-	220		6.6	220	6	0.20	0.001	36.0	21	17	513	80	0.03	
H-30	03-Jan-96	-	820	50.8	7.8	205	29	1.74	0.160	9.7	39	55	1203	747	0.44	37.31
H-31	08-Jan-96	2689	530	76.2	8.3	115	21	2.00	0.119	8.3	16	16	421	869	0.38	7.60
H-32	05-Jan-96	-	380	50.8	7.6	64	12	0.22	0.241	26.8	23	38	592	710	0.24	18.71
H-33	03-Jan-96	-	2300	76.2	7.7	363	33	2.24	0.141	399.6	49	13	978	458	0.47	29.51
H-34	05-Jan-96	2436	830	38.1	8.5	177	24	1.00	0.080	9.0	91	67	202	1130	0.30	0.50
H-35	09-Jan-96	-	340	63.5	5.8	30	5	1.60	0.100	1.4	43	80	2930	231	0.19	10.60
H-36	08-Jan-96	2663	5500	44.4	6.8	1201	52	3.16	0.520	60.4	1133	3498	3169	16	0.50	0.50
H-36	08-mar-96	2663	1330	44.5	7.6	266	17	2.40	0.321	10.6	300	347	1864	304	0.48	6.44
H-37	11-mar-96	2547	2500	50.8	8.2	466	56	4.60	0.010	4.3	407	102	1660	594	0.47	0.96

Table II. Chemical and isotopic composition of springs from the Los Humeros geothermal field, where C.E. is the electrical conductivity and Tm is sampling temperature

No	Name	Date	Tm	pH	C.E.	Concentrations in mg/l										Isotopic Composition ‰VSMOW		
		dd/mm/yy	°C		µmhos/cm	Cl	B	HCO_3	CO_3	SiO_2	SO_4	Na	K	Ca	Mg	δD	$\delta^{18}O$	TU
1	HUICHOTITA	24-Jan-96	0	7.2	88	2.1	0.0	25.4	0.0	63.5	0.05	5.60	4.60	5.90	0.80	-68.5	-10.6	9.7
2	ATOLUCA	24-Jan-96	13	6.9	65	2.1	0.0	28.0	0.0	12.3	0.05	4.20	2.80	4.50	0.90	-64.8	-9.8	8.3
3	MIXQUIAPAN	24-Jan-96	17	8.4	100	0.8	0.0	33.7	0.0	21.9	0.05	7.20	2.10	6.00	2.10	-67.1	-10.2	0.7
4	CHAGCHAR	24-Jan-96	0	7.7	137	1.4	0.0	53.3	0.0	31.5	0.05	9.50	0.50	12.20	1.60	-72.2	-11.0	8.4
5	ZOTOLA	25-Jan-96	12	6.7	110	3.5	0.0	8.7	0.0	21.9	6.10	6.50	4.70	5.20	1.50	-82.6	-12.0	11.7
6	HUITZILPOPO	25-Jan-96	8	7.2	107	3.5	0.0	28.1	0.0	50.3	0.05	7.80	4.00	4.40	1.40	-80.4	-12.4	
7	XICALAHUA	25-Jan-96	18	8.3	530	24.1	0.0	218.0	0.0	21.9	23.30	20.00	14.50	33.00	21.00			
8	SAN MIGUEL	25-Jan-96	16	7.7	430	14.2	0.0	173.3	0.0	21.9	11.40	26.00	15.70	23.30	13.00			
9	SAN ROQUE	26-Jan-96	11	8.2	420	17.7	0.0	121.7	0.0	12.3	11.50	45.00	5.60	20.00	19.00	-72.2	-10.8	
10	CUYOACO	26-Jan-96	18	8.1	300	5.6	0.0	82.4	0.0	50.3	0.05	15.00	4.00	28.30	4.80			
11	EL TREBOL	26-Jan-96	17	8.0	370	5.6	0.0	131.8	0.0	23.9	8.40	41.00	6.50	22.00	2.30			
12	SAN IGNACIO	27-Jan-96	16	7.9	380	6.3	0.0	179.1	0.0	37.1	6.83	48.90	4.20	23.90	3.40			
13	POCHINTOC	27-Jan-96	11	8.3	330	12.0	0.0	26.5	0.0	21.9	12.09	24.00	5.10	20.00	5.80			
14	TEMOXIXA	27-Jan-96	0	7.6	98	1.4	0.0	22.7	0.0	21.9	0.05	7.00	2.50	7.80	1.10	-68.3	-10.6	
15	MAZAPA	29-Jan-96	16	7.3	145	7.1	0.0	53.4	0.0	90.0	0.05	13.00	4.30	7.10	2.90	-68.5	-10.6	3.5
16	EL TESORO	29-Jan-96	23	8.0	900	75.1	0.0	352.7	0.0	90.0	5.70	94.00	13.60	27.00	25.00	-77.3	-11.2	0.8
17	CHIGNAUTLA	29-Jan-96	17	7.4	135	1.4	0.0	25.6	0.0	63.5	0.05	12.10	2.30	9.00	2.00	-68.2	-10.6	4.0
18	XIUTETELCO	30-Jan-96	16	7.8	106	2.1	0.0	36.6	0.0	10.7	0.05	12.00	3.70	6.20	1.70	-71.4	-10.1	2.6
19	ZOATZINGO	30-Jan-96	17	7.5	116	3.5	0.0	14.5	0.0	21.9	0.05	6.80	5.00	6.50	1.50	-53.3	-8.6	
20	TRES OCOTES	30-Jan-96	12	7.4	45	2.1	0.0	16.8	0.0	116.4	0.05	3.40	3.40	5.00	0.30	-67.9	-10.2	
21	CUATLAMING	31-Jan-96	0	7.3	88	1.4	0.0	22.6	0.0	63.5	0.05	7.30	3.60	3.50	0.90	-67.5	-10.5	
22	EL RANCHO	31-Jan-96	13	6.7	118	2.8	0.0	44.9	0.0	21.9	0.05	5.00	3.80	8.20	3.20	-52.7	-7.9	
23	LA BARRANCA	31-Jan-96	16	7.6	93	2.8	0.0	6.1	0.0	103.2	0.05	5.90	2.80	5.80	1.80	-66.8	-10.3	
24	AHUACATLAN	01-feb-96	0	7.8	75	1.4	0.0	11.6	0.0	31.5	0.05	6.00	4.40	4.80	1.90	-45.9	-8.1	
25	LA PASADA	01-feb-96	13	6.6	81	2.1	0.0	22.7	0.0	21.9	0.05	4.30	3.80	4.60	0.80	-53.7	-8.6	
26	LA CUEVA	01-feb-96	0	6.9	128	3.5	0.0	11.5	0.0	21.9	2.01	6.90	5.10	6.00	1.50	-65.5	-9.8	
27	ACUACO	02-feb-96	0	7.3	200	2.8	0.0	67.3	0.0	37.1	0.05	10.00	3.00	18.70	3.10	-73.2	-10.9	2.5
28	HUITZILAPA	02-feb-96	0	7.4	185	8.5	0.0	42.1	0.0	76.7	5.02	10.30	5.00	12.70	3.10	-75.0	-10.6	2.5
29	XALTIPANAPA	02-feb-96	21	7.8	310	11.3	0.0	153.9	0.0	76.7	7.13	27.00	1.60	23.00	5.60	-66.3	-10.1	
30	CALZACATENO	03-feb-96	0	7.3	73	2.1	0.0	16.9	0.0	10.7	0.05	6.00	3.80	3.70	0.60	-66.3	-10.3	
31	PGH-5	03-feb-96	15	7.5	163	4.2	0.0	69.9	0.0	12.3	5.08	11.00	3.10	14.10	1.00			
32	EL CISNE	03-feb-96	15	7.6	2400	60.2	0.4	790.0	0.0	142.8	21.90	32.10	23.00	30.00	78.00			
33	VPH 1	06-feb-96	0	8.2	730	61.7	0.0	332.8	0.0	31.5	0.80	61.00	8.20	28.00	25.00			
34	SANTA ROSA	06-feb-96	17	7.8	380	11.3	0.0	104.3	0.0	63.5	18.17	31.00	3.80	25.00	9.00			
35	LA CALERA	06-feb-96	16	7.7	380	22.0	0.0	70.1	0.0	76.7	10.83	20.00	5.20	27.00	13.00			
36	TETEPONGO	07-feb-96	17	7.6	330	5.1	0.0	162.2	0.0	12.3	6.83	41.00	3.80	22.00	1.80			
37	LOMA LARGA	07-feb-96	0	8.4	930	75.1	0.2	347.8	8.3	31.5	8.70	93.00	13.70	22.00	28.00			
38	PEPSI COLA	07-feb-96	18	7.7	190	7.0	0.0	92.3	0.0	21.9	0.05	13.00	4.20	12.80	5.90			
39	PGH – 4	08-feb-96	0	7.7	380	2.1	0.0	229.0	0.0	31.5	9.30	30.00	5.10	27.00	10.40			
40	EL ATRIO	08-feb-96	16	7.0	169	9.9	0.0	28.3	0.0	10.7	0.05	6.90	4.70	13.70	4.30	-62.0	-9.6	4.2
41	COLELO	08-feb-96	15	7.0	71	1.4	0.0	6.1	0.0	50.3	0.05	5.70	3.00	2.70	0.70			
	Alchichica	01-Dec-87														-12.3	0.7	
	Pizarro	25-Jan-88														-48.4	-5.3	

4. Geothermometry and solute-rock chemical equilibrium

Figure 3 shows the state of equilibrium and the water-rock interaction temperatures. This diagram was proposed by Giggenbach to evaluate the Na-K-Mg-geothermometers and the state of chemical equilibrium (Giggenbach, 1988). Only well H-37 is close to the full equilibrium line. Its deep temperature lies a little bit beyond the theoretical line due to steam loss. However, most of the well waters fall in the partial equilibrium area, and waters from wells H-10, H-15, H-17, H-32 and H-35 fall in the area of shallow waters. This is probably because these wells produce little water and sampling is very difficult. The indicated equilibrium temperature of these wells ranges between 200°C and 300°C. Figure 3 is also used to determine the equilibrium state. Only two samples are located in the region of partial equilibrium; the remaining sodium bicarbonate springs are displaced towards the magnesium field and display a K/Mg geothermometer temperature less than 100°C. This indicates that they are shallow waters that have equilibrated with the rock at low temperatures.

5. Gas chemical equilibrium and thermometry

The chemical composition of the gases can be also used both to estimate deep temperatures and to establish their origins. The composition of well gases at the Los Humeros is typical of a geothermal environment: CO_2 is the predominant gas (about 95% in dry volume), and H_2S varies from 1.0% to 12.3% molar concentrations (Table III). In Figure 4, H_2/Ar gas geothermometer temperatures (Giggenbach, 1989) vary from 270°C (H-3) to 338°C (H-12). These temperatures are in some cases consistent with both measured and calculated K/Na temperatures using Giggenbach (1989) geothermometers.

In Figure 5, values of log H_2/Ar versus log CO_2/Ar are plotted. A full equilibrium line, defined as equilibration of all dissolved gases in a single liquid phase, is observed. In the same figure the horizontal line corresponds to compositions expected for equilibration in the vapor phase. The lines describe intermediate conditions: either addition of equilibrium vapor, or loss of Ar prior to re-equilibrium (Giggenbach, 1989). Most well discharges fall near the theoretical liquid phase, full equilibrium line. The position of well H-12 and the U-3 samples indicate either the admixture of equilibrium vapor or of the loss Ar.

N_2, Ar and He form the most readily accessible conservative gas group in thermal discharges. Ar and He are noble gases and chemically inert. N_2 may take part in chemical reactions to form NH_3 (Giggenbach, 1989). Generally, N_2 is the predominant nitrogen species in thermal gases. Giggenbach (1988) provided a triangular diagram based on a large number of analysis of gases discharged from a wide variety of terrestrial sources. Figure 6 shows data for relative N_2, He and Ar contents. This triangular diagram shows three major source components: A meteoric component, represented by air saturated groundwater and contributing, N_2 and Ar with a molar ratio of 38, a crustal component made up largely of radiogenic He, and a magmatic component characterized by N_2/Ar ratios around 800. In this last component N_2/Ar ratios of up to 2000 have been observed. Helium-4 contents are expected to increase with increasing gas residence time in the crust (Giggenbach, 1989).

Relative N_2-He-Ar contents are shown in figure 6. Gases from wells H-3, H-6, H-9, H-12, H-20 and H-30 are located between air and air-saturated water. H-15 gas is located in the zone of waters recently saturated with air. The high content of He detected in the rest of the wells suggests very slow, deep circulation of magmatic fluids in the crust (Figure 6). A well-defined linear distribution exists between gases of deep circulation and gases of atmospheric origin (air). Analysis of gases from well H-1 indicates a long residence time of fluid in the crust.

Table III. Chemical composition of gases from Los Humeros geothermal field. On water-free basis, in mmol/mol. Where Pc is the wellhead pressure. Ts is the separation temperature and Cg is the gases total content on water-free basis.

Well No	Date dd/mm/yy	Enthalpy kJ/kg	Pc Kg/cm^2	Ts °C	Cg	CO_2	H_2S	NH_3	He	H_2	Ar	N_2	CH_4	HCl ppm	HF ppm
H-1	140494	1179	9.2	176	17.7	982.1	10.9	2.00	0.0128	1.16	0.02	2.33	1.56	416.3	57.1
H-3	130494	2241	3.2	91	34.3	935.0	27.5	5.02	N.D.	7.50	0.30	21.90	2.72	239.3	219.6
H-6	140494	2441	29.2	186	21.5	910.1	58.6	5.02	N.D.	5.59	0.09	3.69	16.89	112.8	58.0
H-7	140494	2671	13.2	177	11.2	928.2	50.5	4.15	0.01017	4.54	0.12	9.34	3.14	32.7	24.1
H-8	140494	2072	12.2	179	17.4	946.5	36.9	2.12	0.00718	3.66	0.11	6.27	4.43	209.8	54.1
H-9	140494	2713	18.0	206	11.0	857.4	70.3	9.80	N.D.	14.00	0.30	14.54	33.69	18.0	33.6
H-11	140494	2663	14.4	196	21.0	962.4	25.6	2.31	0.00945	2.12	0.05	3.31	4.26	195.0	36.2
H-12	140494	2634	11.3	182	40.5	921.1	40.0	2.54	0.0000852	6.55	0.03	2.82	27.04	313.0	72.5
H-15	130494	2551	16.2	201	18.5	863.5	73.2	5.29	N.D.	12.30	0.26	6.39	39.14	121.0	34.0
H-16	130494	2667	14.8	178	8.1	868.3	90.4	3.11	N.D.	8.20	0.16	7.60	22.21	136.0	43.8
H-17	140494	2663	22.2	198	11.6	913.8	59.0	5.67	0.00442	4.50	0.08	4.37	12.51	195.0	73.6
H-19	120494	2141	20.1	205	15.4	958.8	33.0	2.30	0.00778	1.58	0.03	3.65	0.58	62.2	54.3
H-20	120494	2658	42.3	203	24.7	897.0	70.0	4.02	N.D.	5.85	0.08	4.18	18.89	32.7	47.2
H-28	140494	2663	13.4	192	18.1	958.3	24.7	3.98	0.00405	2.72	0.05	3.41	6.79	224.5	32.1
H-30	130494	2580	13.4	192	8.7	820.3	123.0	7.06	N.D.	11.48	0.29	12.56	25.23	224.5	61.3
H-31	130494	2689	21.9	192	14.9	870.5	73.2	3.72	N.D.	10.73	0.20	7.97	33.68	62.2	20.3
H-32	140494	2663	19.8	203	10.6	914.2	61.0	3.61	0.00268	4.13	0.08	3.84	13.12	298.3	36.9
H-33	130494	2663	11.1	179	8.1	864.4	90.5	8.06	N.D.	9.11	0.24	10.28	17.46	313.0	70.3
H-34	120494	2436	-	166	22.6	969.4	18.5	2.66	0.00751	1.98	0.03	2.60	4.81	3.0	58.7
U-2	140494	-	-	179	11.7	936.3	45.6	4.73	0.00664	3.54	0.10	7.36	2.38	77.0	34.9
U-3	150494	-	-	181	18.4	901.5	56.6	2.70	N.D.	7.26	0.05	3.27	28.69	372.0	63.8
U-4	130494	-	-	176	5.7	851.7	104.2	6.70	N.D.	8.14	0.23	8.29	20.75	209.0	51.7
U-5	130494	-	-	180	16.0	872.4	73.2	3.80	N.D.	10.37	0.19	6.90	33.15	3.3	56.5
U-7	140494	-	-	175	7.9	919.7	57.9	5.10	0.00531	3.56	0.06	3.66	9.98	165.5	25.7

Note: U-2 to U-7 are generation units.

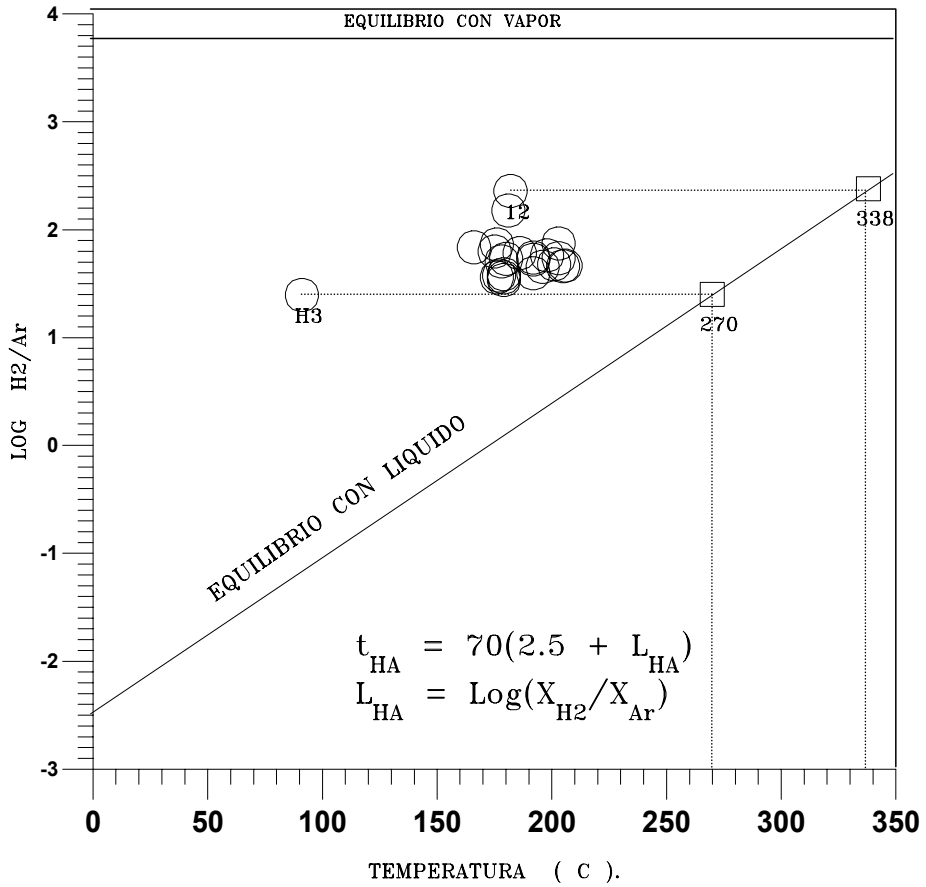

Fig. 4. Estimation of H_2-Ar temperatures for gas discharges of wells from the Los Humeros geothermal field (on per mil molar basis).

6. Isotopic geochemistry

Verma et al., (1997) conducted monitored the chemical and isotopic composition of rainwater at Los Humeros and its surroundings, in order to determine the rain water quality in the region. A side product of that study was determination of the local meteoric line. There was a wide spread in the isotopic data. The effects of altitude and precipitation volume are very prominence. However the data show good linear correlation between δD and $\delta^{18}O$ values and equation of this line (the local meteoric water line) is $\delta D=7.75\delta^{18}O + 12.14$. The precipitation volume weighted average isotopic composition of rainwater is -11.0 and –78 for $\delta^{18}O$ and δD, respectively.

The isotopic compositions ($\delta^{18}O$ and δD) of surface manifestations (springs and shallow wells) are taken from Tello (1992). Figure 7 shows the isotopic composition of all types of water in the region including local and worldwide meteoric water lines. The average isotopic composition of geothermal wells (production and re-injection) are also plotted in figure 7. The deep reservoir compositions are assumed to be equal to total discharge values.

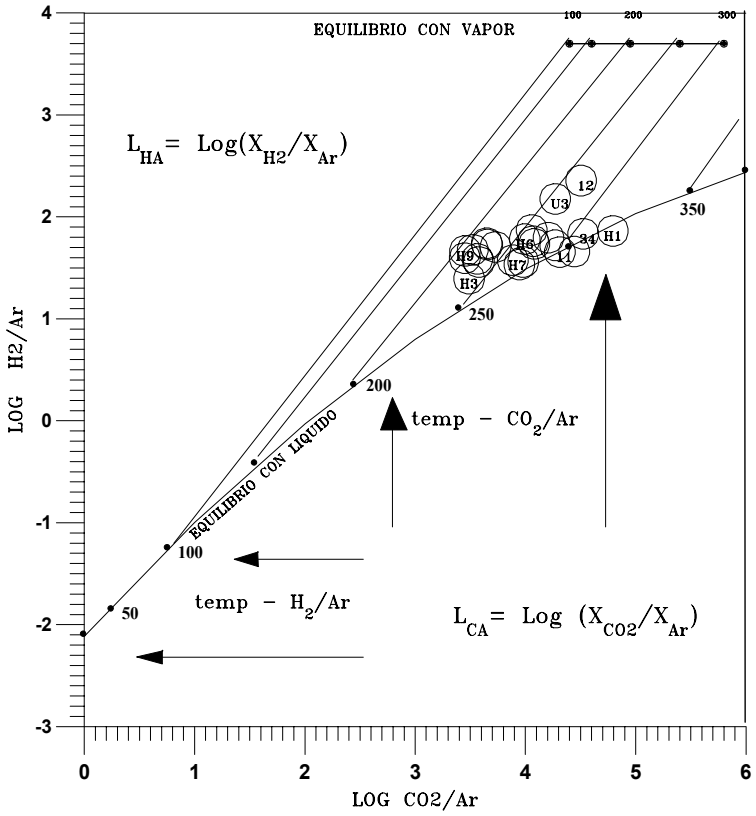

Fig. 5. Evaluation of H_2-Ar, CO_2-Ar equilibration conditions for wells gas discharges from the Los Humeros geothermal field (on per mil molar basis).

There is a wide spread in the total discharge composition of production wells, which could be due to deep mixture of geothermal reservoir fluids. Although the rainwater data are only for one year, the variation with altitude, precipitation volume, and annual temperature are quite consistent as observed in the isotopic data of WMO-IAEA data for the worldwide sampling stations. The geothermal well waters show a $\delta^{18}O$ shift characteristic of geothermal fluids. This enrichment of $\delta^{18}O$ is due to water rock interaction at high temperatures. On the contrary, most of the springs are located along the meteoric water line. The isotopic composition of samples of the lagoons and wells such as Alchichica and Pizarro are characteristic of waters modified by evaporation at atmospheric temperature.

The average isotopic composition of shallow well waters within the caldera are -11.89 and -85.0 for $\delta^{18}O$ and δD, respectively. These isotopic compositions are slightly lighter than the average rainwater data. The isotopic data of geothermal wells are heavier in both oxygen-18 and deuterium. This could be due to evaporation during collection.

7. Steam excess

There exists an excess of steam in the reservoir if the discharge enthalpy of a well exceeds that of saturated liquid at the reservoir temperature (Arnorsson, 1982). The discharge enthalpy of wells at Los Humeros varies from 1179 to 2726 kj/kg. High enthalpy discharge reflects the existence of two phases (steam and water) in the reservoir or the vaporization of water during production. Only well H-1 produces from a clearly liquid-dominated zone. The rest of wells are located in a two-phase zone (Tello, 1992).

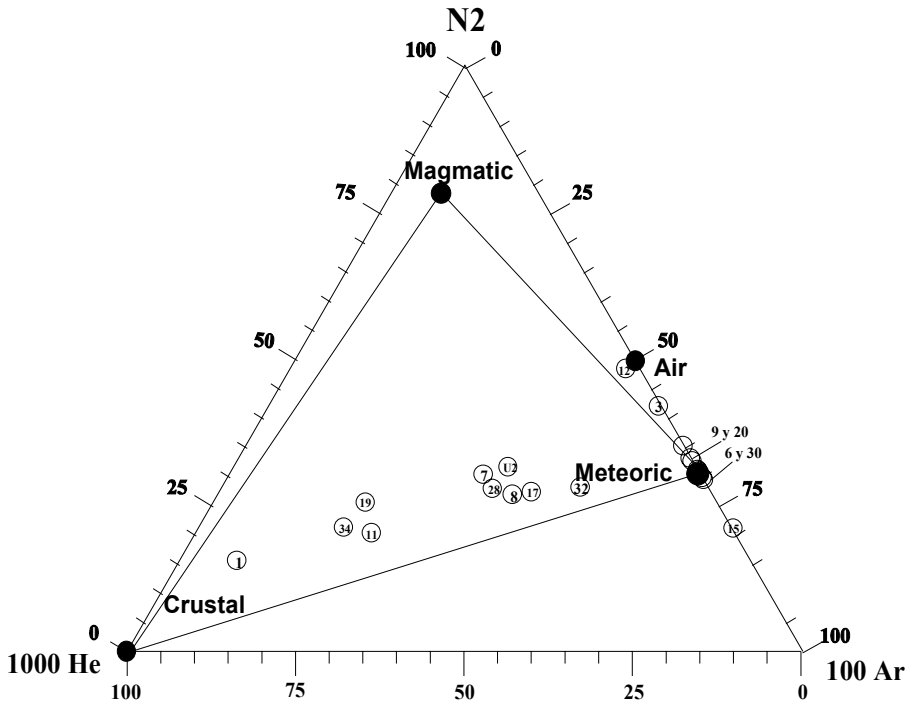

Fig. 6. Relative N_2:He and Ar contents for gas discharges of wells from the Los Humeros geothermal field (on per mil molar basis).

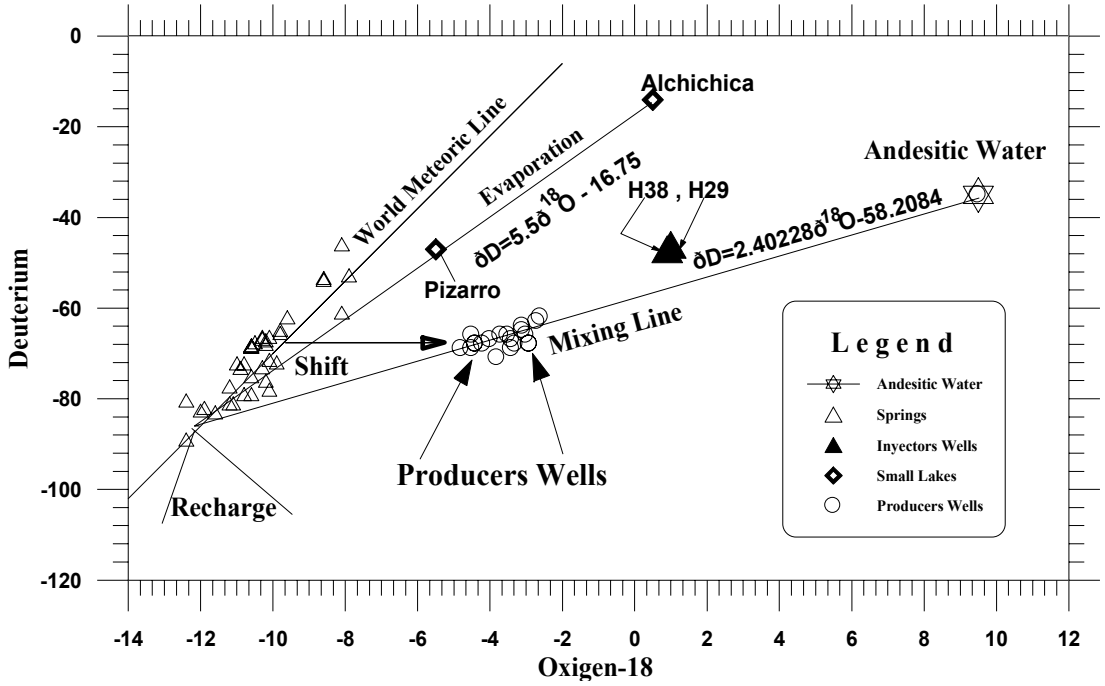

Fig. 7. Deuterium versus oxygen-18 contents for waters from the Los Humeros, Mexico, geothermal field.

8. Origin of acidity

Truesdell (1991) explained the occurrence of acid fluid in geothermal reservoirs. It could be produced by either the introduction of volcanic fluids (SO_2 or HCl) or from volatilization and transport of HCl. HCl transport is expected to appear in boiling high temperature reservoirs as they lose liquid and start producing superheated steam. At Los Humeros superheated, high HCl steam is produced by the flow of fluids from a deep, hot, dry reservoir to a shallow water-saturated reservoir with strong corrosion and scaling resulting from fluid mixing and reaction with casing and rock (Verma, 1997).

Several hypotheses have been presented about the origin of acidity in Los Humeros. The Volcanic Fluid theory states that, based on water-rock chemical equilibrium, the Los Humeros geothermal reservoir is in a non-equilibrium state (Tello, 1992), and acid indicates that the geothermal reservoir fluids were derived from volcanic fluids incompletely neutralized by a reaction with feldspars and micas; Superheated steam containing HCl generated at high temperature from vaporization of chloride brine, or reaction of halite with silicates forms acid where it condenses or mixes with liquid at moderate temperature (<300°C). This theory is in agreement with the Los Humeros case, because high concentrations of HCl and HF were detected in the steam phase. However, high fluid concentrations of boron and arsenic indicate that the Los Humeros is a recent volcanic system (Tello, 1995).

The Los Humeros geothermal system has been considered as being formed by two reservoirs, although there is no lithological unit separating them. The shallow reservoir contains vapor and liquid whereas the deeper one has only superheated steam at high temperature (>300°C). The production of HCl vapor in the deeper reservoir is a result of water-rock interaction at high temperature and low amount of water (Verma et al., 1997). The high corrosiveness and scaling in the wells due to these deeper fluids has limited the exploitation of the reservoir to its upper part.

According to Truesdell (1997), the most important question regarding the Los Humeros field is the presence and characteristics of a possible deeper reservoir. The presence of acid fluids in a number of Los Humeros well discharges and evidence of subsurface acid attack of casing and country rock along with the high down hole temperatures (300–400°C) and varied fluid compositions have been taken as evidence that a deeper reservoir exists however there is little "hard evidence" of the existence of this reservoir. The constituents that have been assumed to be from the deep reservoir including Cl, B, HCl and H_2S are all are soluble in superheated steam or could result from vaporization of chloride brine, or reaction of halite with silicates combined with acid attack of casing and wall rock. The "primary" constituents HCl, B and H_2S are also present in the shallow reservoir (with HCl represented as NaCl). It is very important to note that in the natural state before drilling there is no evidence of acid fluids. The andesite contains calcite, feldspars, and mica; the hornfels and skarn are composed in part of carbonate rocks and normally contain calcite. If in the natural state of the reservoir, reservoir fluid contained significant HCl and B, then it would be expected that minerals such as calcite and feldspars would not occur and that boron minerals such as tourmaline would be found. The lack of mineralogical evidence for deep acid or high boron suggests that the deep fluids observed in H-16 and H-4 may be a part artifacts of drilling formed by flows of shallow water down the well bore (Truesdell, 1997).

A shut-in drill hole penetrating both the shallow, liquid-filled reservoir and the deep reservoir containing only high-temperature steam would be a conduit for downward flow of liquid between the two zones. Liquid flowing down the well would quickly vaporize as it reached the high-temperature zone and it would form highly saline brine, precipitate salts and evolve gases. Some constituents such as B (as H_3BO_3) would partition between solid and vapor. The continued down flow of upper-zone water could cause accumulation of significant quantities of alkali chlorides (mainly halite) and sulfates, boric acid, and amorphous silica and release CO_2 (from HCO_3) and NH_3 (from NH_4) into the steam. The steam in contact with this deposit of salts would have high H_3BO_3 and significant HCl formed by halite-silicate reaction. With production, gases and volatile salts would be drawn upward to mix with the shallow reservoir water and produce the observed

inhomogeneous fluid compositions and, in some wells, acid corrosion. If this idea is correct, then shallower drilling at Los Humeros could have avoided the formation of acid steam as well as its introduction into drill holes (Truesdell, 1997).

9. Conclusions

The chemical characteristics of fluids showed that the brine produced by the wells is a low-saline water, whose geochemical character varies according to well type and production. Shallower wells produced sodium bicarbonate (H-1) type water, whereas the deeper wells exhibited a sodium chloride type (H-6). Water-rock equilibrium calculations indicate that the Los Humeros geothermal reservoir fluid is in a non-equilibrium state. Enthalpy data shows that well H-1 is in a zone where the liquid phase is dominant, while the remaining wells are producing from a two-phase zone. Measured temperature at bottom hole varies between 260ºC and 340ºC. These variations are in agreement with geothermometer calculations.

About the origin of acidity in the geothermal reservoir there are several hypotheses. High concentrations of HCl and HF were detected in the steam phase. Based on water-rock chemical equilibrium Los Humeros geothermal reservoir is in non-equilibrium state and magmatic components in the geothermal fluids are not neutralized by the reaction with feldspars and micas. Alternatively, the high temperatures at the bottom of the Los Humeros drill holes have caused the release of CO_2, HCl, and B into steam formed from boiling of upper reservoir flowing down the boreholes.

Acknowledgements

This paper was supported by an IAEA-Coordinated Research Programme (Research Contract MEX9827-849F) on the use of isotope techniques for the investigation of acidic fluids in geothermal reservoirs in exploitation (1997–2000). The authors would like to thank Dr. J.L. Quijano for encouragement and discussions and to the authorities of the CFE for permitting its publication. The authors are indebted to Mario Cesar Suarez A. and to Julio C. Viggiano for their critical comments of the manuscript. Alfred Truesdell did final editing.

REFERENCES

[1] ARNORSSON, S., and GUNNLAUGSSON, E., 1982. The chemistry of geothermal waters in Iceland. III. Chemical geothermometry in geothermal investigations. Science Institute, University of Iceland.

[2] BARRAGÁN, R.M., NIEVA, D., SANTOYO, E., GONZALEZ, P.E., VERMA, M.P., LÓPEZ, M.J.M., 1991. Geoquímica de fluidos del campo geotérmico de Los Humeros, México. Geotermia 7, 23–47.

[3] CAMPOS, E.J.O., and ARREDONDO, F.J.J., 1992. Gravity study of Los Humeros Caldera complex México: Structure and associated geothermal system. J. Volcanol. Geotherm. Res., 47, 149–159.

[4] FERRIZ, H., MAHOOD, G.A., 1984. Eruption rates and composition trends at Los Humeros volcanic center, Puebla, México. J. Geophys. Res. 89, 8511–8524.

[5] FOURNIER, R.O., 1977. Chemical geothermometer and mixing models for geothermal systems. Geothermics. Vol. 5, pp. 47–49.

[6] GIGGENBACH, W., 1988. Geothermal solute equilibria. Derivation Na-K-Mg-Ca-geoindicators. Geochim. Cosmochim. Acta, 52, pp. 2749–2765.

[7] GIGGENBACH, W., 1989. Techniques for the interpretation of water and analysis in geothermal exploration. Chemistry Division. Department of Scientific and Industrial Research. Petone, New Zealand.

[8] LÓPEZ, J.M., 1982. Geoquímica del agua y gases separados del pozo Humeros No 1 en producción, en el campo geotérmico de Los Humeros, Puebla, México. Internal Report CFE, 15 pp.

[9] LÓPEZ, M. J.M. and MUNGUÍA, F. Evidencias geoquímicas del fenómeno de ebullición en el campo de Los Humeros, Puebla. México. Geotermia 5, 89–106 pp.
[10] MARTÍNEZ, S.R., 1993. Caracterisation mineralogique, géochimique et isotopique du champ géothermique du Los Humeros, Mexique. Interactions fluide-roche dans un systeme a fluide mixte (eau-vapeur). These de I`INPL., Nancy, France 232 pp.
[11] MARTÍNEZ, S.R., and ALIBERT, Ch., 1994. Características geoquímicas de las rocas volcánicas del sistema geotérmico Los Humeros, Puebla y su relación con la mineralogía de alteración. International Geophysish, Vol. 33, No. 4, pp. 585–605.
[12] MARTÍNEZ, S.R., JACQUIER, B., ARNOLD, M., 1996. The $\delta^{34}S$ composition of sulfates and sulfides at the Los Humeros geothermal system, México and their applications to physico-chemical fluid evolution. J. Volcanol. Geotherm. Res. 73, pp 99–118.
[13] NEGEDANK, J.F.W., R. EMMERMAN, R., KRACZYK, F., MOOSER, H., and WEHRLE, D., 1985. Geological and geochemical invetigations on the eastern Transmexican Volcanic Belt. Geophys. Int. 24, 4, 447–575.
[14] PROL, L.R.M., 1990. Recent cooling in Los Humeros geothermal field (México), inferred from clay minerals distribution. Geotherm. Resource Council Trans. 14, 959–964.
[15] TELLO, H.E., 1992. Características geoquímicas e isotópicas de los fluidos producidos por los pozos de Los Humeros, Puebla. Geotermia 8, 3–48.
[16] TELLO, H.E., 1994. Caracterización geoquímica de agua y gases de Los Humeros, Puebla. I. Implicaciones de equilibrio. C.F.E. GPG. Internal Report. GQ-010-94.
[17] TELLO, H.E., 1995. Corrosión de aceros en ambiente geotérmico de los Humeros, Puebla, Tesis de Maestría. ITM. Morelia, Michoacán. México.
[18] TRUESDELL, A., 1991. Origin of acid fluids in geothermal reservoirs. G.R.C. Trans. Vol. 15, 289–296.
[19] TRUESDELL, A., 1997. In prep. Report for project Mex/8/20. About Los Humeros, Puebla, Mexico.IAEA- CFE.
[20] TOVAR, A.R., 1999. Resultados analíticos de agua, gases, y vapor condensado de Los Humeros, Puebla. CFE.GPG. Residencia de Los Humeros.
[21] VERMA, P.M., TELLO, H.E., NIEVA, D. 1997. Acid fluid in Los Humeros geothermal reservoir. IAEA-CRP on the use of Isotope Techniques. Vienna, Austria.
[22] VIGGIANO, J.C., and ROBLES, J., 1988. Mineralogía hidrotermal en el campo geotérmico de Los Humeros, Puebla. I. Sus usos como indicadores de temperatutra y el régimen hidrológico. Geotermia 4, 15–28.
[23] VINIEGRA, O.F., 1965. Geología del Macizo de Teziutlán y la cuenca Cenozoica de Veracrúz. Bol. Asoc. Mex. Geólogos Petroleros. 17, No 7–12, 100–135.
[24] YAÑEZ, G.C., 1980. Informe geológico del proyecto geotérmico Los Humeros-Derrumbadas. Estados de Puebla y Veracrúz. CFE. GPG. Internal Report, 59 pp.

SULPHUR ISOTOPE RATIOS IN PHILIPPINE GEOTHERMAL SYSTEMS

F.E.B. Bayon, H. Ferrer

Geothermal Division, Energy Development Corporation,
Philippine National Oil Company,
Manila, Philippines

Abstract. This paper presents data on sulfur isotope ratios in dissolved sulfate, H_2S gas, anhydrite and pyrite minerals in four Philippine geothermal fields - Palinpinon, Mahanagdong, Mt. Apo and Bacon-Manito. Isotope ratios are used to determine the source of sulfur species in each geothermal system. Fluid temperature estimates using sulfur pairs are also included in the discussion. Finally, oxygen isotope distribution in dissolved sulfate, anhydrite and water is introduced. Dissolved sulfate sulfur isotope ratios can be divided into three groups: heavy ($\delta^{34}S$>15‰ CDT), light (~0‰) and transitional or mixed ratios (1-15‰). The heavy samples represent waters that have attained some degree of isotopic equilibrium with co-existing sulfides, either in the present geothermal environments or at deeper, hotter levels of the hydrothermal systems. Most of the well fluids in Palinpinon, Mahanagdong and Bacon-Manito belong to this group. Light fluids, on the other hand, are typical of surface and shallow thermal features, where H_2S gas is oxidized and converted to SO_4. The $\delta^{34}S_{SO4}$ ratios here mirror that of the source H_2S. Slightly heavy ratios, characteristic of Mt. Apo well waters, are apparently produced by dilution of "heavy" fluids with "light" waters, in this specific case the light end-member being steam condensate. $\delta^{34}S_{H2S}$ of well samples in Palinpinon, Mahanagdong and Bacon-Manito are in the vicinity of 0‰, similar to that of magmatic H_2S and H_2S produced from SO_2 disproportionation. This implies that geothermal H_2S in these fields are derived either directly or indirectly from a magmatic source. In Mt. Apo, $\delta^{34}S_{H2S}$ are depleted at -3 to -4‰. Although the ultimate source is still magmatic in origin, the depleted ratios are thought to be effects of extensive degassing of an originally $\delta^{34}S$-enriched reservoir fluid. Sulfur ratios in anhydrite are similar to those of dissolved SO_4, suggesting that dissolved sulfate is the sulfur source of anhydrite alteration. Pyrite, likewise, give ratios very similar to H_2S, again indicating that H_2S gas supplies sulfur for secondary pyrite. In Mt. Apo, however, pyrite ratios here are higher at 0 to +3‰ (as against -3‰ in H_2S), which could be reflective of the ratio of the original, unboiled H_2S. When used on acidic, high temperature fluids, sulfur isotope geothermometry reflects measured fluid temperatures. This is because the elevated temperature and low pH enhance isotope exchange reactions and speed up reaction rates, allowing attainment of isotopic equilibrium in this fluid type. In neutral waters, however, chemical conditions are not favorable for isotopic exchange so that re-equilibration is not achieved, and calculated temperatures do not agree with measured temperatures. The temperatures estimated in neutral fluids probably reflect deeper, hotter equilibrium conditions.

1. Introduction

For the past few years, the Philippine National Oil Co. – Energy Development Corp. (PNOC-EDC) and the International Atomic Energy Agency (IAEA) have been implementing a series of studies on sulfur isotope ratios of common sulfur-bearing species in Philippine geothermal systems. The areas included in the research programs were Palinpinon in Negros, Mahanagdong in Leyte and Mt. Apo in southcentral Mindanao. The primary aim of these studies was to characterize the acidic and neutral fluids in each steamfield in terms of $\delta^{34}S$ in dissolved SO_4, H_2S, anhydrite and pyrite, and $\delta^{18}O$ in sulfate and anhydrite. The applicability of sulfur and oxygen isotope geothermometers were also evaluated in each study area.

This paper presents a compilation of isotope data for the three mentioned fields, plus Bacon-Manito in southern Luzon (Fig. 1) where a much earlier study was jointly conducted by PNOC-EDC and the New Zealand government. Discussions will focus on sulfur isotopes, although $\delta^{18}O$ data in SO_4 are also given. This paper aims at giving an overall picture of the characteristics and state of equilibrium of sulfur isotopes in Philippine geothermal fluids. In-depth discussions on each geothermal field are given in individual reports, and will therefore not be repeated here.

2. Data presentation

Pertinent chemical and isotopic data for the 4 geothermal fields in the Philippines are summarized in Tables I to IV. Although this section will present data according to sulfur species, data for each field are separately plotted to minimize clutter in the graphs.

2.1. Dissolved and mineral SO_4

Sulfur isotope ratios for dissolved SO_4 can be grouped in three main clusters - a "light" group at ≤0‰, a "heavy" group at >15‰, and a "transition" group with ratios between 1-15‰. The "light" cluster is made up mostly of surface thermal waters, while the "heavy" group is dominated by well samples. In Mahanagdong, Palinpinon and Bacon-Manito (Bacman), $\delta^{34}S$ in dissolved SO_4 are dominated by ratios ≥15‰ (Fig. 2a). The "transition" group is most prominent in Mt. Apo, where prevailing ratios are 11-15‰, and Bacman, where the number of samples belonging to this group is significant. The transition group is also dominated by well samples, although it also includes some thermal waters.

The distribution of $\delta^{34}S$ ratios in mineral sulfate (anhydrite) is mostly confined to the "heavy" cluster (Fig. 2b); the "light" samples are conspicuously missing in mineral sulfate samples. It is worth noting that even in Mt. Apo, the dominant ratios are in the heavy group. In Bacman, however, most isotope ratios are lighter (11–15‰) compared to those of dissolved SO_4. Here, the "transition" group is even more pronounced. The transitional ratios here include scraper samples, though these may not be characteristic of scraper anhydrites as some scraper samples are even more enriched than alteration anhydrite.

2.2. H_2S gas and sulfide mineral

In comparison to ratios in dissolved sulfate, those in well and solfatara H_2S gas fall within a narrower range of about –5 to +5‰ (Fig. 2c). In all areas except Bacman, ratios are dominantly ≤0‰. This is most pronounced in Mt. Apo, where 13 of the 15 ratios fall under 0‰. In Bacman, there are an equal number of samples with ratios <0‰ and 1-5‰.

Pyrite samples yield the same general results (Fig. 2d) – ratios fall within –5 to +5‰. Palinpinon and Bacman mineral sulfides have ratios that are mostly <0‰, while in Mahanagdong and Mt. Apo, there are more samples with ratios between +1 and +5‰.

2.3. ^{18}O in SO_4

The most significant $\delta^{18}O$ in dissolved SO_4 ratios are between 0 and +5‰ (Fig. 2e), and these are a mix of surface and well waters. Samples with slightly lighter and heavier ratios have also been noted, but these are not as significant. Curiously, in Mt. Apo, the more $\delta^{18}O_{SO4}$-enriched waters are surface features, while well waters have the lightest $\delta^{18}O_{SO4}$. In Bacman, though, more samples have ratios between 6 and 10‰. As far as $\delta^{18}O_{Ah}$ is concerned, the dominant ratio group is similar to that of dissolved sulfate above (Fig. 2f). There are, nonetheless, more slightly $\delta^{18}O_{Ah}$-enriched samples compared to the fluid counterparts.

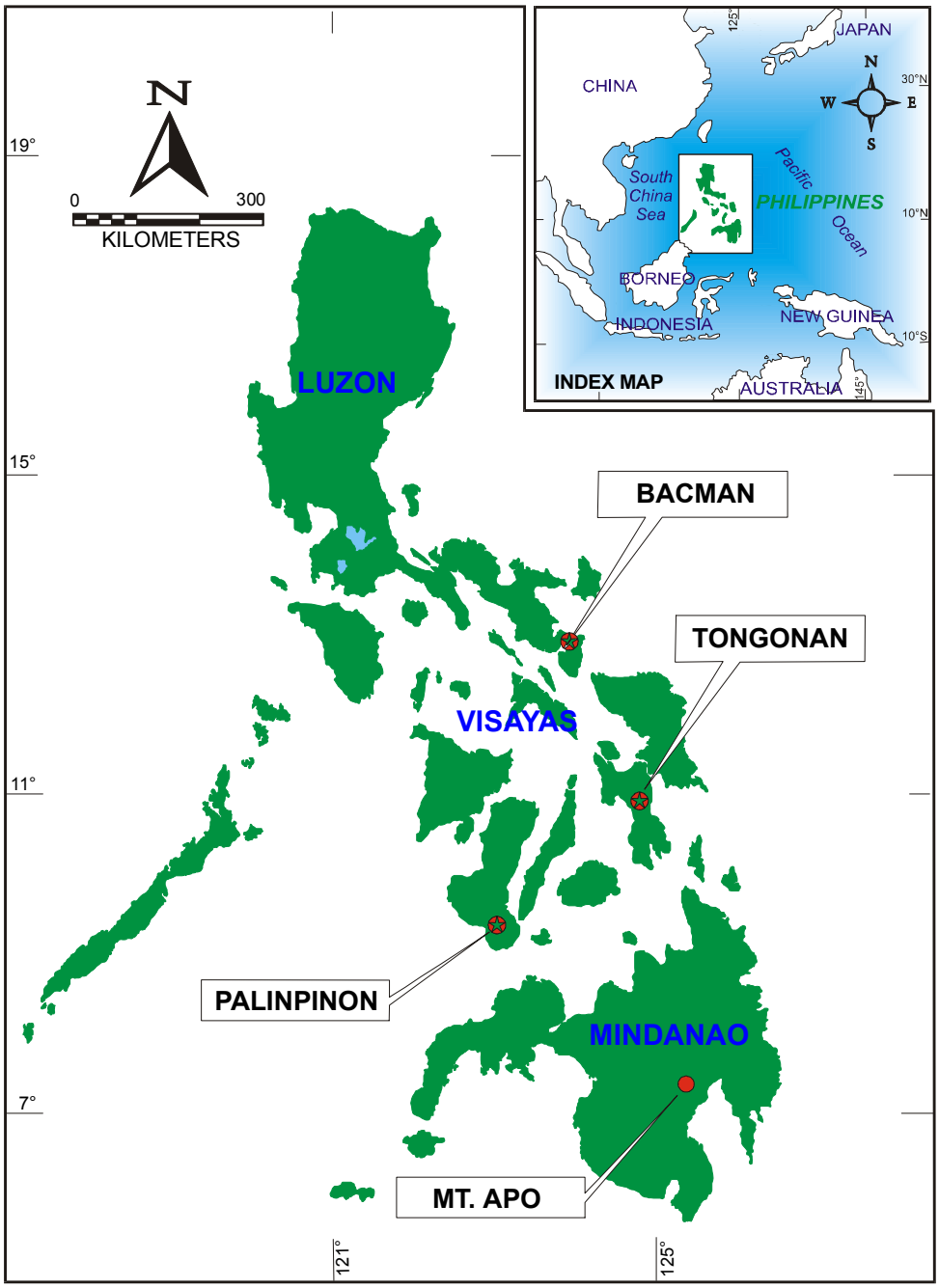

Figure 1. A location map of geothermal systems included in this study.

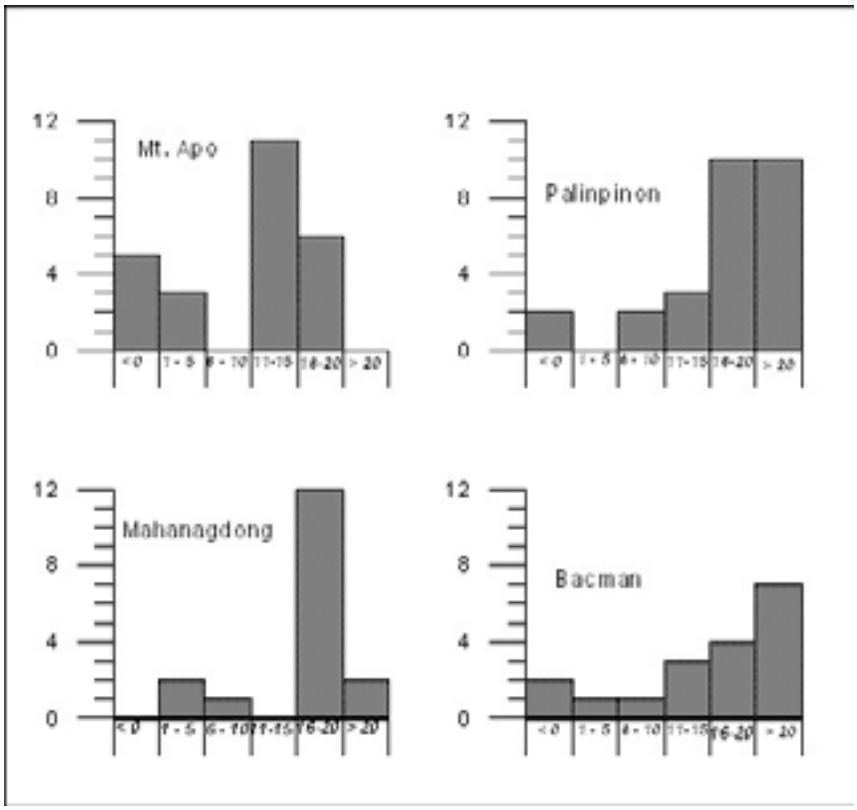

Figure 2a. $\delta^{34}S$ in dissolved SO_4 distribution plot.

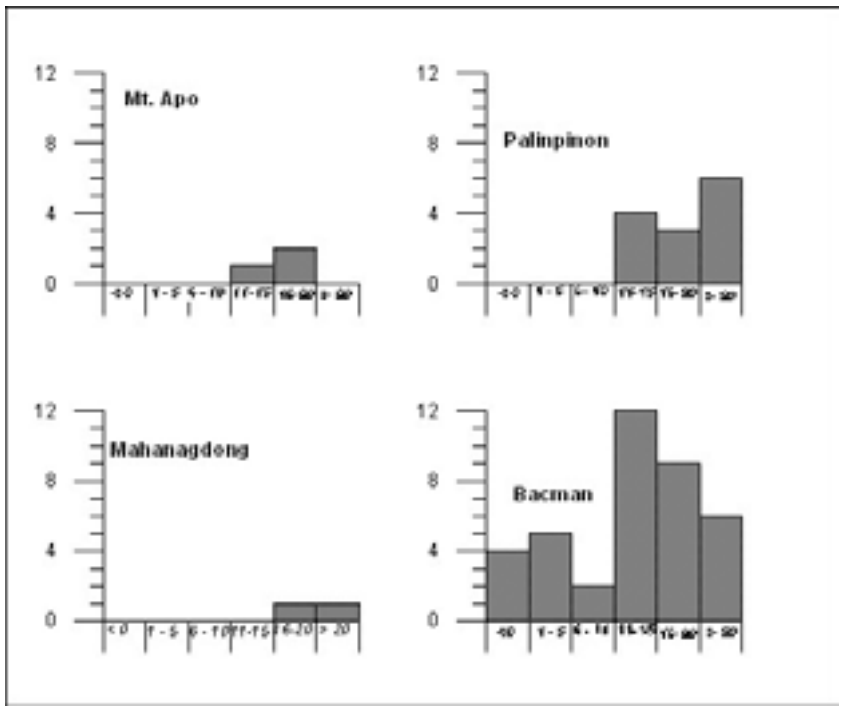

Figure 2b. $\delta^{34}S$ in Anhydrite distribution plot.

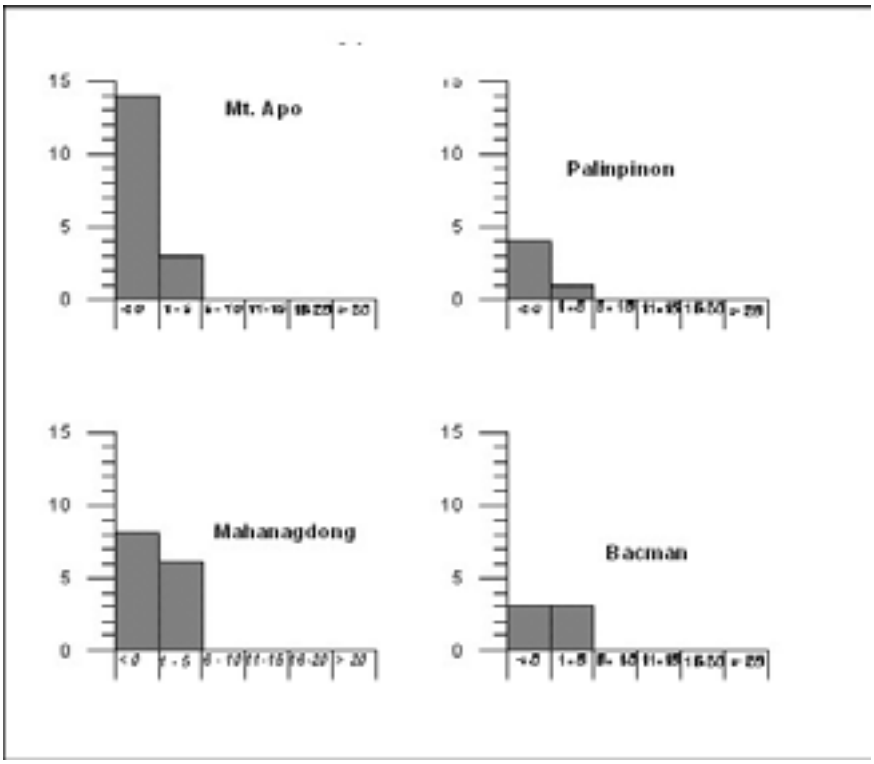

Figure 2c. $\delta^{34}S$ in H_2S distribution plot

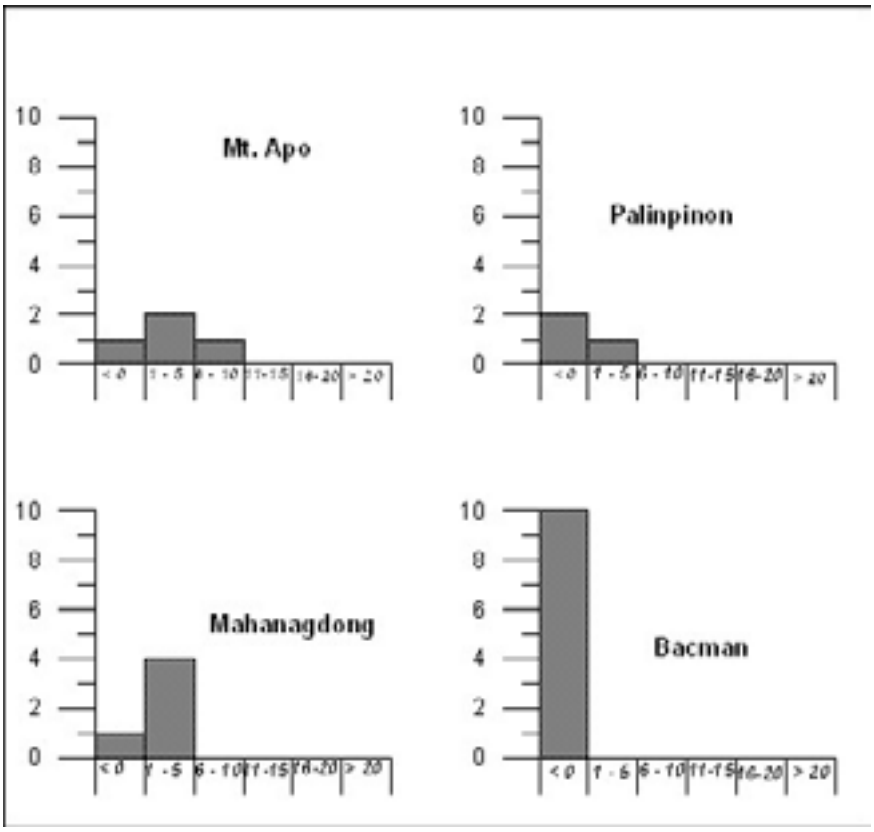

Figure 2d. $\delta^{34}S$ in Pyrite distribution plot

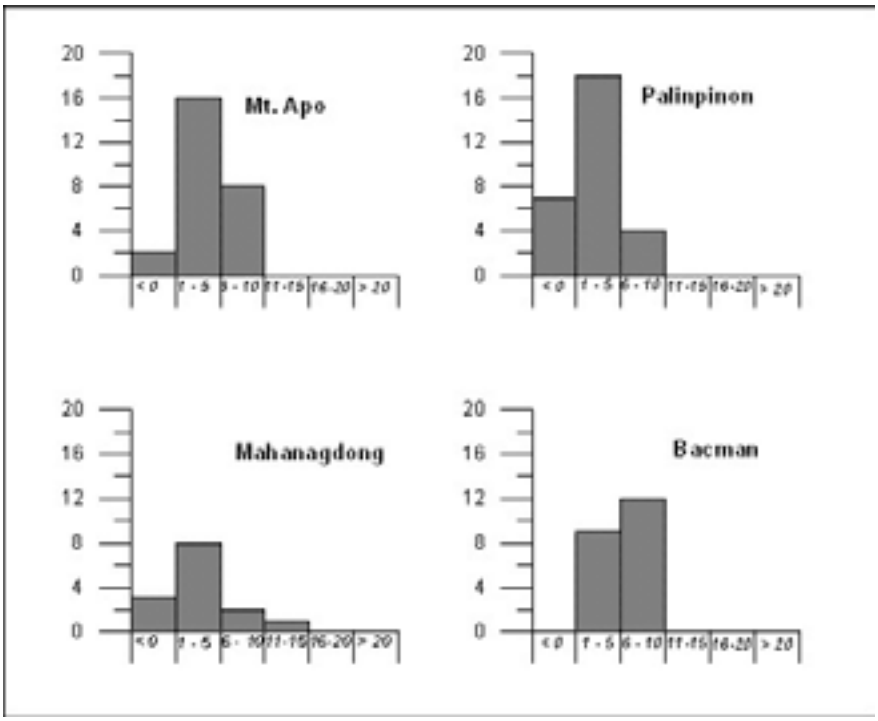

Figure 2e. $\delta^{18}O$ *in dissolved* SO_4 *distribution plot*

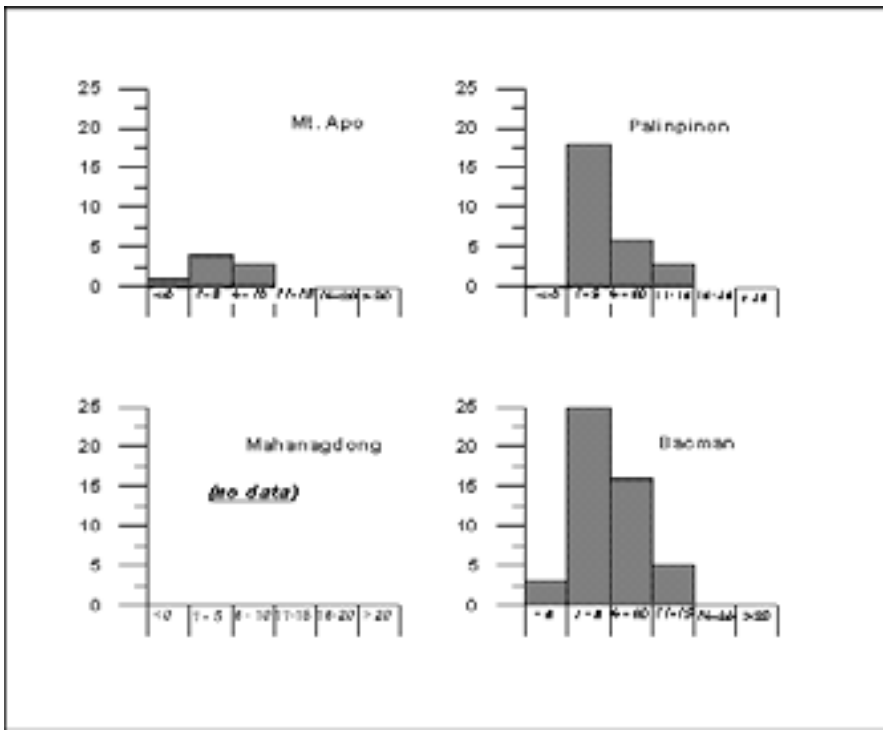

Figure 2f. $\delta^{18}O$ *in Anhydrite distribution plot*

3. Evaluating the state of isotopic equilibrium

In order to assess the state of isotopic equilibrium of sulfur isotopes between sulfate and sulfide, correlations between the two isotopes are presented in this section. In addition, relationship between chemistry (specifically pH, SO_4 content and temperature) and isotope ratios are shown, plus the comparison of estimated temperatures from known sulfur isotope geothermometers to both fluid and mineral pairs against measured well temperatures.

3.1. SO_4 vs. sulfide isotope ratios

Although there is no clear and consistent correlation between sulfate and sulfide isotope ratios (Fig. 3), most of the data points seem to be aligned one way or another. In Mahanagdong (fluid), Palinpinon and Bacman (mineral), for example, enriched $\delta^{34}S_{SO4}$ correspond to higher $\delta^{34}S_{sulfide}$, though there are data points that depart from this general alignment (i.e., N6 in Palinpinon and P8 in Bacman). In Mt. Apo (fluid and mineral) and Palinpinon (fluid), on the other hand, the reverse trend is observable. The more enriched $\delta^{34}S_{SO4}$ is, the lighter the corresponding $\delta^{34}S_{sulfide}$. Again there are departures from this trend, for instance K3 and TM1 in Mt. Apo. The fluid samples in Bacman do not show any trend, while the Mahanagdong mineral samples are too few to establish any apparent relationship.

Assuming that the process of isotopic equilibration is either ongoing (as retrograde exchange) or complete, enrichment in $\delta^{34}S_{SO4}$ should be accompanied by a decrease in the corresponding $\delta^{34}S_{sulfide}$ pair. In short, the ratio difference between sulfate and sulfide pairs should increase with decreasing equilibration temperatures, although the absolute change in isotope ratio may not be the same for sulfate and sulfide. Existing data from volcanic areas all over the world, for instance, indicate that $\delta^{34}S_{H2S}$ do not depart significantly from 0‰; it is the $\delta^{34}S_{SO4}$ which is more "unstable" and tends to cover wider bands of ratios. Following the above reasoning, it appears that only the Mt. Apo (fluid & mineral) and Palinpinon (fluid) samples behave "normally" as these trends conform to thermodynamic expectations. This may indicate that it is only these select sulfur pairs from these fields that are undergoing or have undergone isotope equilibration in the present-day geothermal setting. This deduction remains to be confirmed, however, through the comparison of sulfur isotope ratios with other parameters.

3.2. Chemistry vs. sulfur isotope ratio

Although fluid pH is supposed to play a major role in the sulfur isotope equilibration process, data from Philippine geothermal systems show otherwise (Fig. 4). In Mahanagdong, for example, dissolved SO_4 and H_2S display consistent bands of $\delta^{34}S$ irrespective of pH. The same can be generally said for Palinpinon, as well as all H_2S data points in the other fields. The Mt. Apo plot for dissolved SO_4 faintly shows two groups, one covering the low pH/high $\delta^{34}S$ and another the opposite of the first. The former group is composed of well waters, while the latter comprise surface thermal features. But as will be discussed later, this is not a manifestation of pH control on $\delta^{34}S$, but rather the effect of the sulfur source on the isotope ratios. The Bacman dissolved SO_4 data has too much scatter to show any observable trend.

Plots of sulfur concentration vs. isotope ratio are shown for fluid and mineral sulfur species reveal no evident correlation (Fig. 5a & 5b; in order to include minerals in the plot, it is assumed that the sulfur content in fluid is constant). There is too much dispersion in the data points for all study areas to recognize any relationship that might be present in the plots. Or, there was no real relationship between sulfate concentration and sulfur isotope ratio to start with. Figure 6, which plots fluid temperature (represented here by quartz geothermometer temperature) vs. sulfur isotope ratio, also shows no clear correlation between the two parameters.

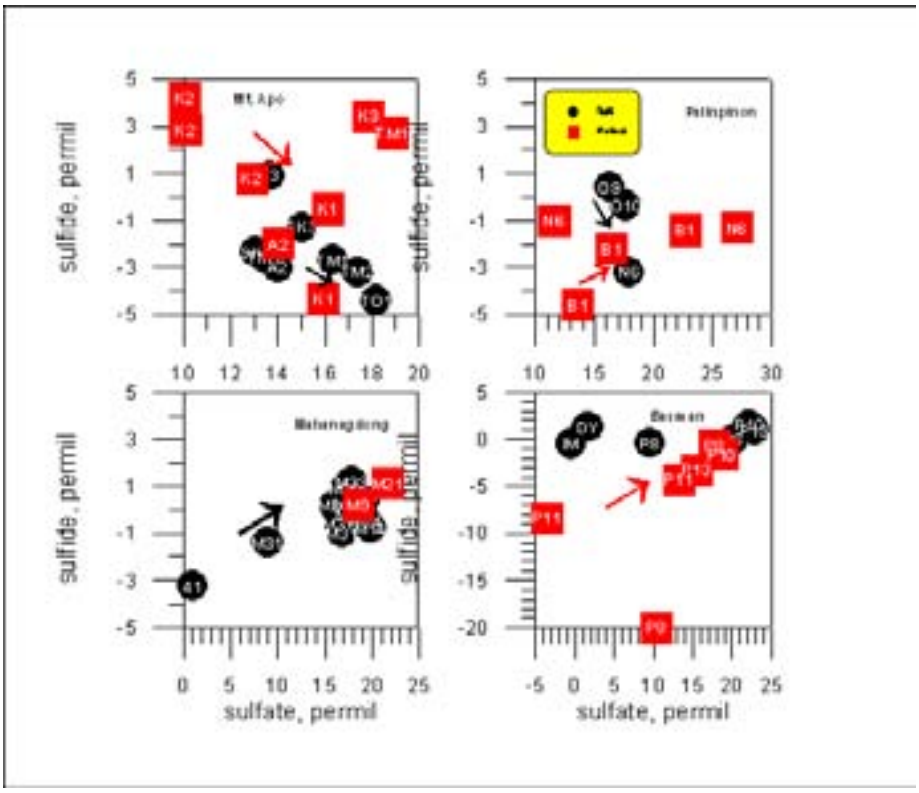

Figure 3. S isotope cross plots.

3.3. Sulfur isotope geothermometry

Perhaps the fastest and simplest way to determine the state of sulfur isotope equilibrium is to apply established sulfur isotope geothermometers to sulfur pairs and compare these with actual bore and fluid temperatures. Currently, there are two known sulfur isotope geothermometers – one for SO_4-H_2S fluid pairs and one for Ah-Py minerals. Since quartz geothermometer temperatures are almost the same as measured temperatures in all study areas, T_{qtz} will be used here to compare temperatures estimated from sulfur pairs. Plots are shown in Figure 7; the "equilibrium line" (solid blue line) shown indicates equal temperature for all geothermometers.

Except for a few data points which plot along the equilibrium line indicating almost equal estimated and measured temperatures (i.e., TO1, TM1 and TM2 in Mt. Apo, N6 in Palinpinon, P13 and P10 in Bacman and M14, M9 and M21 in Mahanagdong), most of the points plot off and to the right of the equilibrium line. Sulfur isotope geothermometers, therefore, give higher estimates than present-day fluid temperatures. This is a clear indication that sulfur isotopes in majority of the samples in the four study areas have not equilibrated in the present geothermal environment.

Almost all of the points which plot along the equilibrium line are, curiously, high temperature acid wells (e.g., M9, M21 in Mahanagdong, TO1, TM2 in Mt. Apo, and N6 in Palinpinon). The good agreement in the high temperature, acid wells is not perceived to be incidental because of its consistent occurrence in the areas of interest. Isotopic equilibrium of these well fluids in the present environment is believed to be a real phenomenon. Elevated temperatures and low pH probably combine to enhance isotope exchange rates in the wells for the waters to attain isotopic equilibrium.

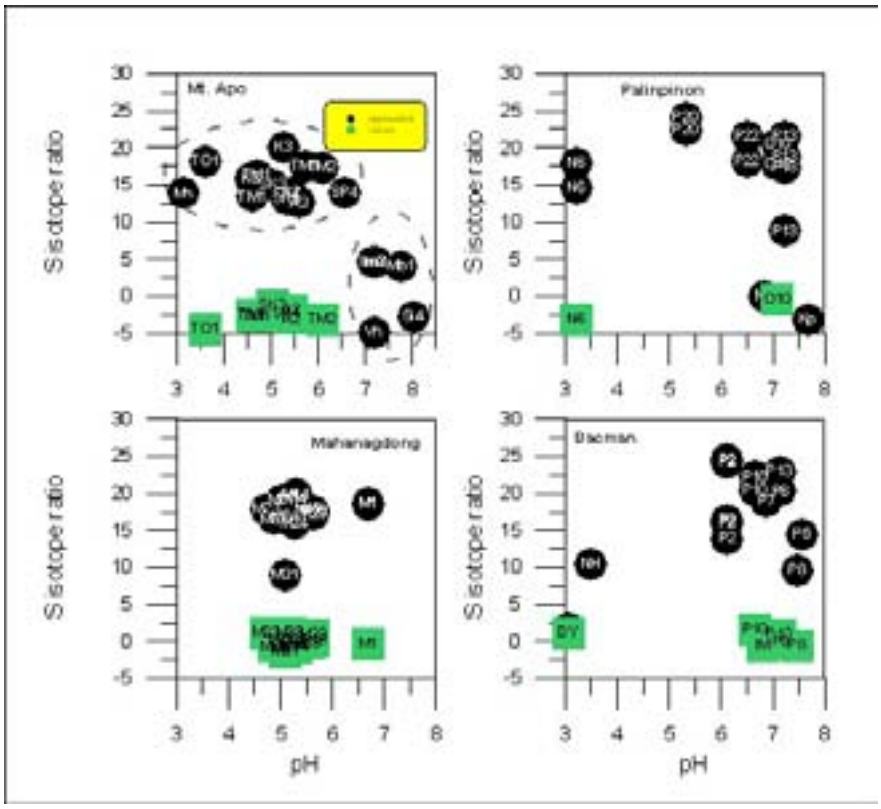

Figure 4. pH vs. S isotope cross plots.

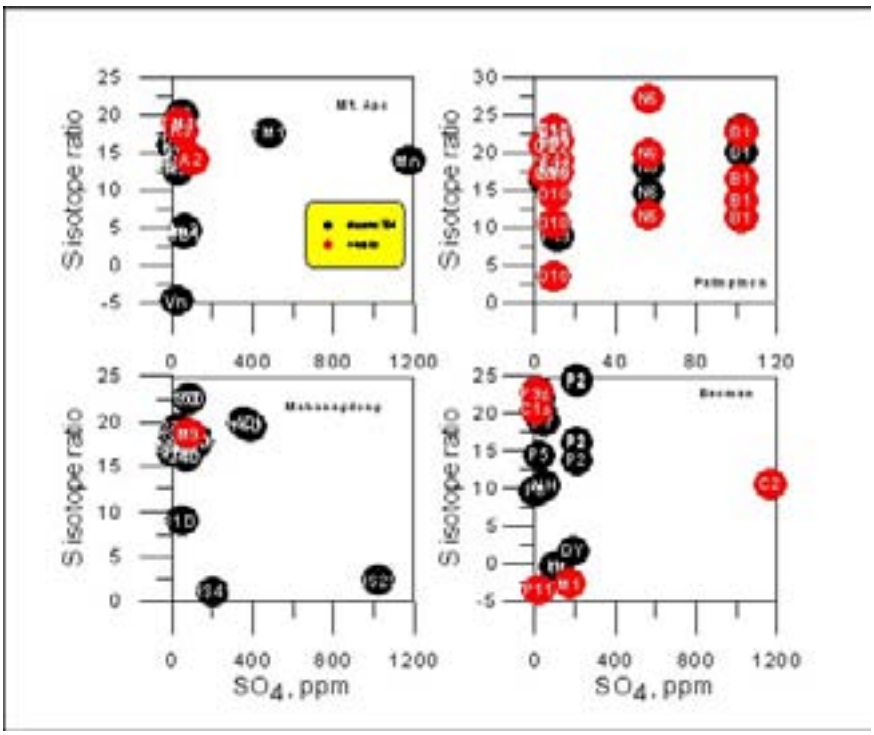

Figure 5a. SO_4 vs. S isotope cross plots.

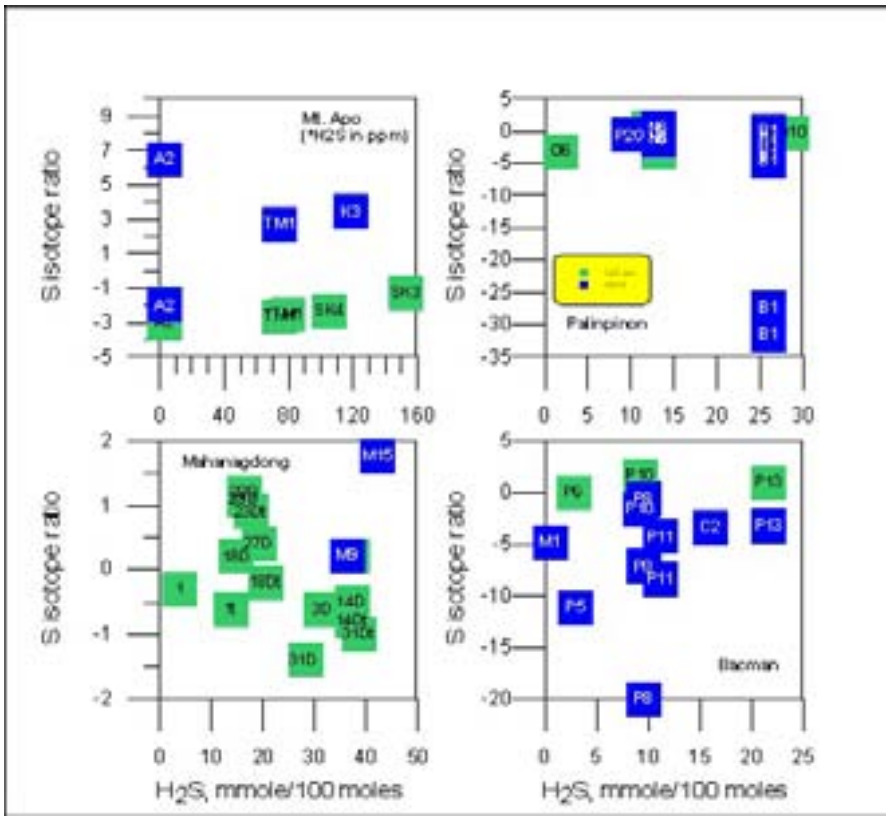

Figure 5b. H_2S vs. S isotope cross plots.

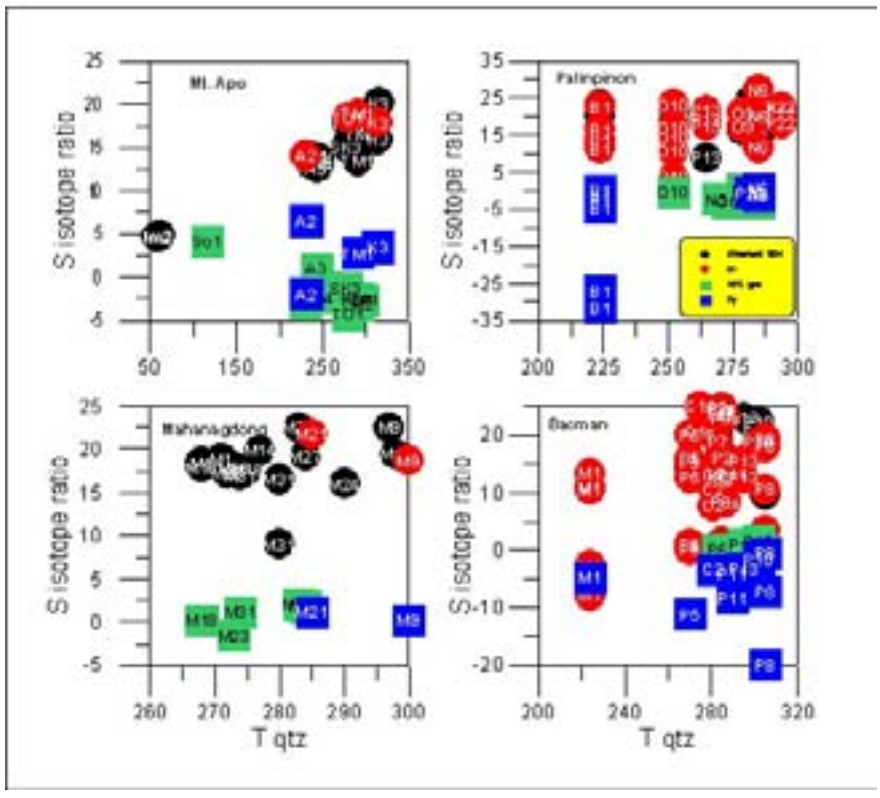

Figure 6. Fluid T vs. S isotope cross plots.

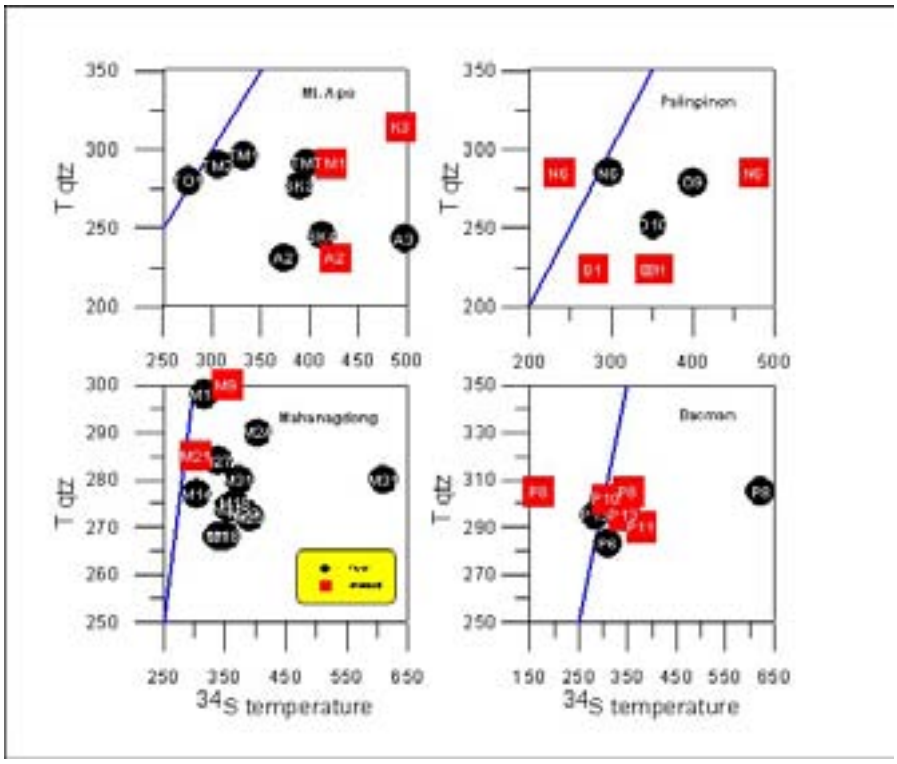

Figure 7. Tqtz vs. Tisotope cross plots.

These observations clearly illustrate that chemistry (pH and sulfur content in fluid) and temperature exercise no major influence on the state of sulfur isotope equilibrium in Philippine geothermal systems, save for high temperature acid well fluids. There is almost nothing to indicate that sulfur isotope ratios correlate even slightly with fluid chemistry and/or temperature, further suggesting that sulfur isotopes are not reflective of equilibrium conditions in the geothermal environment.

4. Discussion

4.1. Sulfur isotope geothermometer

The sulfur isotope geothermometers often give higher temperature estimates than actual well temperatures. The higher isotope-estimated temperatures are commonly taken to reflect isotope equilibrium at deeper and hotter portions of the hydrothermal systems below drilled depths; And in some fields, i.e., Mahanagdong, Palinpinon and perhaps Bacman, the consistency of the estimated S-temperatures for both fluid and mineral pairs (about 300–400^{o}C) may be a true indication of deeper, hotter isotopic equilibrium. Nevertheless, these are all inferences without actual data to confirm temperatures at greater depth. There is currently no direct evidence to state with full confidence that the sulfur pairs are indeed equilibrated at deeper levels of these systems.

In Mt. Apo, although the sulfur-estimated temperature range is also quite consistent (≈350–450^{o}C excluding those in equilibrium), these are merely coincidental and not a function of deeper isotope equilibration because of the interpreted source of sulfur of the system.

4.2. Origin of Sulfur compounds

Almost all dissolved sulfate in deep geothermal fluids are believed to be derived from the disproportionation of magmatic SO_2 at sub-critical temperatures, according to the reaction:

$$4SO_2(aq) + 4H_2O(gas) \Leftrightarrow 3HSO_4^- + 3H^+ + H_2S(aq).$$

This reaction, aside from producing a low pH fluid, also gives a $\delta^{34}S$-enriched sulfate product. The range in recorded $\delta^{34}S_{SO4}$ observed in different areas and different samples is perhaps a function of the starting $\delta^{34}S$ in SO_2 and kinetic effects during isotope exchange.

The "heavy" (>15‰) dissolved sulfates in the four Philippine study areas are thought to be directly derived from SO_2 disproportionation at greater depth. The isotopes cease to equilibrate within the geothermal environment (except in hot acid waters) because of unfavorable conditions for isotope exchange, and thus retain the signature of the last equilibrium temperature. This temperature is most probably the temperature of SO_2 disproportionation. The above conclusion is based on the consistent, albeit high, sulfur isotope estimated temperatures. The close to 0‰, "light" sulfates, on the other hand, which are typically found in thermal areas, draw sulfate from H_2S oxidation at or near the surface. There is no isotope exchange at all in this shallow environment, thus the sulfate adopts the ratio of the source sulfide. Those sulfates with ratios in between (i.e., 0‰ > X > 15‰), are most likely produced by mixing of the deep, $\delta^{34}S_{SO4}$-enriched fluid and the shallow, $\delta^{34}S_{SO4}$-depleted water (such as in thermal features and steam condensates).

The disproportionation of SO_2 produces H_2S gas, which cannot be differentiated from magmatic H_2S because both sulfides have similar isotope ratios of close to 0‰. Since most of the samples are within this $\delta^{34}S$ value, H_2S gas in geothermal fluid is believed to be a) derived directly from a magmatic source and b) produced from SO_2 disproportionation. In most cases, the source may be both. Variations in $\delta^{34}S_{H2S}$ may be due merely to kinetic effects.

Sulfate $\delta^{34}S$ ratios in secondary anhydrite are consistently >15‰, very similar to the "heavy" dissolved sulfates. Sulfide sulfur in pyrite, likewise shows ratios akin to H_2S gas. It is logical to assume that these alteration minerals derive their sulfur from species dissolved in fluid. There is probably no isotope exchange between the two minerals, and the ratios are direct products of mineral precipitation and controlled purely by the respective sulfur sources.

The case of Mt. Apo deserves more discussion, because this field is different from the three others in terms of sulfur isotope systematics. In the three areas, there are primarily two sulfur fluid types - one directly derived from SO_2 and the other shallow sulfate derived from H_2S oxidation. The mixed fluid type is minor in these systems. But in Mt. Apo, the dominant fluid type is a mixture of a deep, acid fluid with a heavy isotope ratio (>15‰) originating from the upflow region, and a shallow, $\delta^{34}S$-depleted fluid; thus the preponderance of ratios between +10 and +15‰. The light end-member is thought to be steam condensate, derived from the natural steam cap of the system present even during the pre-exploitation stage. Because the $\delta^{34}S$ values of sulfate result from mixing, and considering that sulfur isotopes do not tend to equilibrate in the geothermal environment, the high isotope temperatures in this field are purely coincidental and not actually reflective of deeper equilibration. Furthermore, $\delta^{34}S$ values in pyrite are heavier than $\delta^{34}S_{H2S}$, which can be interpreted as an effect of boiling. Secondary pyrite reflects the $\delta^{34}S$ ratio of the original, unboiled Mt. Apo hydrothermal fluid. Continuous boiling has led to the progressive depletion of $\delta^{34}S$ in H_2S that remains in solution. The H_2S currently being discharged by wells represents the boiled remainent of the original H_2S gas, resulting in the depleted ratios noted in the gas samples. If it is assumed that the $\delta^{34}S$ in pyrite (-3‰) is reflective of the magmatic H_2S source, then $\delta^{34}S$ of magmatic sulfur species in Mt. Apo are probably depleted compared to those in other areas in the Philippines ($\delta^{34}S_{H2S} \sim 0$‰).

5. Conclusions

Sulfur isotope ratios of fluid and mineral samples from the four Philippine areas of interest reveal that isotopic equilibrium is not attained in the present-day geothermal systems, save for acidic, high-temperature fluids in each field. Most of the $\delta^{34}S$ ratios reflect equilibrium environments that are much hotter and deeper than that reached by drilled wells. In one geothermal field, sulfur isotopes represent the product of mixing of the deep reservoir fluid and shallow steam condensate derived from the existing natural steam cap. In hot, acidic waters, conditions are such that isotope exchange reactions are enhanced to allow almost full attainment of sulfur isotopic equilibrium.

Dissolved sulfate in wells is derived from the disproportionation of SO_2 gas and is therefore indirectly of magmatic origin. Dissolved sulfate in thermal manifestations, on the other hand, draw sulfur from the oxidation of H_2S at shallow levels of the geothermal systems. Sulfur in pyrite and anhydrite originate from sulfate and sulfide dissolved in fluid, respectively.

Acknowledgements

This paper would not have been made possible without the support of the International Atomic Energy Agency, who funded the isotope analyses for the individual research contracts. The PNOC-EDC management is also thanked for giving permission to publish this paper. Lastly, the author wishes to thank those who painstakingly read and reviewed an early draft of the paper.

REFERENCES

[1] BAYON, F.E.B., 1996. Sulphur isotope applications in two Philippine geothermal systems. GRC Transactions Vol. 20. pp. 651–660.

[2] BAYON, F.E.B. and B.M.G. SAMBRANO, 1999. Differences in sulfur stable isotope ratios between neutral and acid waters in the Mt. Apo geothermal fluid, Southern Philippines. PNOC-EDC Internal report.

[3] GIGGENBACH, W.F., 1992. Isotopic and chemical composition of water and gas discharges from the Zunil geothermal system, Guatemala. In: Geothermal investigation with isotope and geochemical techniques in Latin America. IAEA TECDOC. pp. 245–278. Vienna, Austria.

[4] MCKIBBEN, M.A., C.S. ELDRIDGE and A.G. REYES, 1997. Sulfur isotope systematics of the June 1991 Mount Pinatubo eruptions: A SHRIMP ion microprobe. In: C.G. Newhall and R.S. Punongbayan (eds): Fire and Mud Eruptions and Lahars of Mt. Pinatubo, Philippines. University of Washington Press. pp 825–844.

[5] OHMOTO, H., 1986. Stable isotope geochemistry of ore deposits. In J.W. Valley, H.P. Taylor and J.R. O'Neil (eds): Stable isotopes in high temperature geological processes. Reviews in Mineralogy. Vol. 16, pp 491–556.

[6] OHMOTO, H. and R.O. RYE, 1979. Isotopes of sulfur and carbon. In: H.L. Barnes (ed): Geochemistry of hydrothermal ore deposits, Second Edition. John Wiley and Sons, Ney York. pp 509–567.

[7] ROBINSON, B.W., 1987. Sulphur and sulphate-oxygen isotopes in New Zealand geothermal systems and volcanic discharges. Studies in sulphur isotope variations in nature. pp. 31–48.

[8] ROBINSON, B.W., L.B. VILLASENOR and V.C. CLEMENTE, 1987. Preliminary stable isotope investigations of acid fluids in geothermal systems of the Philippines. Proceedings, 9th New Zealand Geothermal Workshop. pp. 73–78.

[9] SALONGA, N.D., F.E.B. BAYON, M.M. MARTINEZ and E.V. PARILLA Jr., 1999. The implications of ^{34}S and ^{18}O isotope systematics on the origin and equilibration of fluids in Mahanagdong hydrothermal system. Leyte, Philippines. PNOC-EDC technical report.

[10] THODE, H.G., 1963. Sulphur isotope geochemistry. In "studies of analytical geochemistry." D.M. Shaw (ed). The Royal Society of Canada Special Publication no. 6

Table Ia. Mt. Apo sulfur & oxygen isotope data and calculated fluid temperatures

LABEL	SOURCE	$\delta^{34}S$ SO_4	$\delta^{18}O$ SO_4	$\delta^{18}O$ H_2O	$\delta^{18}O$ H_2O TD*	$\delta^{34}S$ H_2S	$\delta^{34}S$ fluid	Sulfur T fluid**
TM1	TM-1D	13.46	3.97	-3.79	-6.36	-2.56	16.02	398
TM1	TM-1D	16.37	6.83	-2.66	-5.34	-2.66	19.03	333
SK3	SK-3D	15.03	4.94			-1.29	16.32	391
SK4	SK-4B	13.08	3.73			-2.34	15.42	413
SK4	SK-4B	13.69	2.35					
SP4	SP-4D	13.98	10.93			N/A		
SP4	SP-4D	12.96	6.57					
A3	APO-3D	13.66	5.58			0.9	12.76	498
A3	APO-3D	12.59	5.28			N/A		
A2	APO-2D	14.02		-5.5	-6.66	-2.99	17.01	374
A2	APO-2D					-1.83		
K3	KN-3D	15.9	4.69					
SK1	SK-1D			-4.26	-9.78	-3.31		
Im2	IMBA 2	4.63	4.14					
Im3	IMBA 3	4.76	4.57					
Si3	SISI 3			-7.47	-7.47			
Vn	Venado	-4.81	9.11					
Mb1	Marbel 1	4.1	4.26					
Mn	Mainit	13.86	7.09					
Si4	Sisi 4	-2.76	3.81	-7.39	-7.39			
Mc	Macadac			-4.65	-4.65			
AgS	Agco S	-3.96	1.56					
AgM	Agco M	-4.23	0.94					
AgB	Agco B	-3.67	7.13					
TM2	TM-2D	17.4	-0.68			-3.2	20.6	306
TO1	TO-1D	18.2	-2.14			-4.4	22.6	277
K3	KN-3	20.1	0.3	-2.87	-4.43			
Mn	Mainit	13	4.63	-9.84				
Mn	Mainit		4.63	-7.59				
ApoS	APO sol					1.6		
KU	Kuong					-6.3		
Ad	Adtapan					-3.2		
Ag	Agco					-2.2		
Mn	Manda					-3.3		

*TD = Total Discharge

**SO_4-H_2S fluid pair geothermometer

***Ah-Py mineral pair geothermometer

Table Ia. Continued

SOURCE	DEPTH	LABEL	$\delta^{34}S$ Ah	$\delta^{34}S$ Py	$\delta^{34}S$ mineral	Sulfur T mineral***	$\delta^{18}O$ Ah
TM-1D	1200-1300	TM1	18.88	2.71	16.17	422	6.19
APO-2D	1150-1450	A2	14.03	-2	16.03	427	4.96
APO-2D	1150-1450	A2	N/A	6.45			
KN-3D	1300-1500	K3	17.87	3.43	14.44	494	4.54
TO-1D		TO1	18.4				
Apo Sol		ApoS		-3			
Kuong		KU		1.3			
KN-2D	1400-1500	K2	10.09	2.87	7.22		-1.48
KN-2D	1900-1950	K2	12.9	0.76	12.14	637	4.97
KN-2D	2050-2200	K2	10.05	4.22	5.83		5.61
KN-1D	1107-1295	K1	16.14	-0.51	16.65	405	5.66
KN-1D	1372	K1	15.95	-4.33	20.28	309	4.82
KN-1D	1613	K1	N/A	8.48			
KN-1D	1653	K1	N/A	0.67			
SK-2D	1700-1768	SK2	N/A	-1.13			
TO-2D		TO2		1.3			

*TD = Total Discharge

**SO_4-H_2S fluid pair geothermometer

***Ah-Py mineral pair geothermometer

Table IB. Mt. Apo fluid chemistry data (reduced to reservoir condition)

LABEL	SOURCE	WHP (MPaa)	SP (MPaa)	SO_4 (ppm)	H_2S (ppm)	H (J/g)	pH	Na*	K	Ca	Mg	Fe	Cl	HCO_3	SiO_2	CO_2**	NH_3	H_2	N_2	CH_4	Tqtz
TM1	TM-1D	0.593	0.504	40	79.59	1351	4.61	2572	682	84	1.30	1.11	4752		638	1310	15.78	0.520	76.990	0.380	291
TM1	TM-1D	0.593	0.495	35	74.76	1260	4.70	2775	701	87	1.43	1.00	5199		653	1195	10.31	0.530	50.610	0.390	296
SK3	SK-3D	1.104	1.016	46	152.82	1384	5.02	2952	697	94	0.09	0.12	5250		580	2610	1.47	0.350	15.670	0.330	277
SK4	SK-4B	1.065	1.026	31	105.69	1093	5.34	2412	363	89	0.05	0.11	4110		447	887	1.56	0.090	10.330	0.090	245
SK4	SK-4B	1.065	1.026	31	105.69	1093	5.34	2412	363	89	0.05	0.11	4110		447	887	1.56	0.090	10.330	0.090	245
SP4	SP-4D	1.055	0.698	43	32.64	1004	6.56	2402	379	110	1.30	0.18	4306		422	17	1.10	0.030	22.240	0.140	238
A3	APO-3D	0.849	0.795	32	28.06	1052	5.60	2600	398	110	0.14	0.11	4655		436	534	0.83	0.020	10.860	0.330	243
A2	APO-2D	0.586	0.61	105	3.31	913	5.43	1438	179	28	0.73	0.25	2214		382	4236	8.05	0.020	132.880	0.530	231
A2	APO-2D	0.586	0.61	105	3.31	913	5.43	1438	179	28	0.73	0.25	2214		382	4236	8.05	0.020	132.880	0.530	231
K3	KN-3D	5.813	0.09	10.07		1916	4.57	3502	899	118	0.22	2.68	6542		816		0.71				314
Im2	IMBA 2			69.46	1.63		7.21	771	71	47	5.55	0.35	1294	71.56	169	57	0.65				59
Im3	IMBA 3			66.42	1.5		7.17	824	82	57	6.19	0.33	1424	80.54	180	61	0.60				61
Si3	SISI 3			41.75	0.2		9.00	73	4	1	0.06	0.30	12	133.50	65	130	0.03				65
Vn	Venado			26.93	2.06		7.18	4	1	7	1.13	0.35	1	4.64	21	3	0.03				
Vn	Venado			26.93	2.06		7.18	4	1	7	1.13	0.35	1	4.64	21	3	0.03				
Mb1	Marbel 1			60.63	2.09		7.76	958	78.5	58.9	2.44	0.35	1543	88.59	136	58.97	0.17				
Mn	Mainit			1177	1.66		3.15	52	8	379	42.20	1.06	6		79		0.66				
Si4	Sisi 4				1.17		8.01	376	29.6	6.87	0.25	0.48	457	166.94	120	122.35	0.14				
Jr	Jordan			16.72	2.24		5.39	4.17	4.06	2.77	0.81	0.45	2.25	9.76		7.04	0.02				
Mc	Macadac			8.41	0.15		5.51	3.12	2.97	1.16	0.34	0.58	1.68	6.05		5.81	0.04				
TM2	TM-2D	1.96	0.303	37		1172	6.10			23.2	0.07		5141		629						290
TO1	TO-1D	0.583	0.634			2063	3.61			31	13.20		164		466						280
K3	KN-3	1.583	0.833	54	118.71	1542	5.28	3560	960	100	0.52	0.62	6357		720	1905.69	1.10				315
TM1	TM-4D	0.366	0.367	486.11	211.25	2675	5.73	527	61.51	38.52	1.71	3.89	643.72		521	3824.63	2.99	0.420	15.780	0.520	280
So1	SOLF 1																				116
So2	SOLF 2																				

*concentrations in ppm

**concentrations (of all gases except H_2S) in mmoles/100 moles steam

Table II. Palinpinon isotopic and chemical data

SOURCE	LABEL	$\delta^{18}O$ SO_4	$\delta^{34}S$ SO_4	$\delta^{34}S$ H_2S	$\delta^{18}O$ Ah	$\delta^{34}S$ Ah	$\delta^{34}S$ Py	$\delta^{18}O$ TD*	Sulfur T fluid**	Sulfur T mineral***	T (O-18) fluid****	pH	H (J/g)	SO_4 res	Cl res	T SiO_2	H_2S TD
PN-13D	P13	2	8.8					-2.56			304	7.23	1541	11.5	8714	265	1.21
PN-13D	P13	1.13	21.5					-2.56			335	7.23	1541	11.5	8714	265	1.21
PN-13D	P13	1.67	17.4					-2.56			315	7.23	1541	11.5	8714	265	1.21
PN-13D	P13	1.74	18.9					-2.56			313	7.23	1541	11.5	8714	265	1.21
PN-22D	P22	0.5						-5.36			265	6.5	2545	10	1466	294	20.35
PN-22D	P22	0.11	21.6					-5.36			276	6.5	2545	10	1466	294	20.35
PN-22D	P22	0.25	21.6					-5.36			272	6.5	2545	10	1466	294	20.35
PN-22D	P22	0.86	21.5					-5.36			255	6.5	2545	10	1466	294	20.35
PN-22D	P22	4.72	18.2					-5.36			178	6.5	2545	10	1466	294	20.35
PN-22D	P22	0.11	21.6					-5.36			276	6.5	2545	10	1466	294	20.35
NJ-3D	N3	-0.3		-2.5				-5.2			293			15.7	3298	269	
NJ-5D	N5	-2	10.8					-5.56			340						
NJ-5D	N5		14.3					-5.56									
NJ-5D	N5	1.67	17.8					-5.56			231						
NJ-6D	N6	5.2						-4.64			182	3.22	1727	56.8	1181	285	13.16
NJ-6D	N6	0	14.6					-4.64			301	3.22	1727	56.8	1181	285	13.16
NJ-6D	N6	-0.89	18	-3.2				-4.64	297		333	3.22	1727	56.8	1181	285	13.16
OK-6	O6	-0.9						-6.11			283			16.9	3295	273	1.8
OK-6	O6	-0.5		-3.2				-6.11			272			16.9	3295	273	1.8
OK-9D	O9	2.93	16.3	0.4				-4.15	401		235			5.8	5238	279	12.1
OK-9D	O9	8.91	20.9					-4.15			137			5.8	5238	279	12.1
OK-9D	O9	9.51	17.1					-4.15			130			5.8	5238	279	12.1
BL-1D	B1	0	20					-6.31			253		2570	102.9	2849	224	26.1
BL-1D	B1	1.83	23					-6.31			212			102.9	2849	224	26.1
OK-10D	O10	6.2	20.6					-5.28			157	7.09	2232	10	3066	252	28.71
OK-10D	O10	-0.24	17.7	-0.37				-5.28	352		288	7.09	2232	10	3066	252	28.71
PN-20D	P20	0.3	22.4					-4.12			308	5.32	1512		2130	282	9.85
PN-20D	P20	1.36	24.1					-4.12			275	5.32	1512		2130	282	9.85
Kaipohan	Kp	-1.82	-3.1									7.68					
Mag-aso	Ma	0.08	0									6.84					

Table II. Continued

SOURCE	LABEL	$\delta^{18}O$ SO_4	$\delta^{34}S$ SO_4	$\delta^{34}S$ H_2S	$\delta^{18}O$ Ah	$\delta^{34}S$ Ah	$\delta^{34}S$ Py	$\delta^{18}O$ TD*	Sulfur T fluid**	Sulfur T mineral***	T (O-18) fluid****	pH	H (J/g)	SO_4 res	Cl res	T SiO_2	H_2S TD
PN-13D	P13				1.13	21.5						7.23		11.5		265	
PN-13D	P13				1.67	17.4						7.23		11.5		265	
PN-13D	P13				1.74	18.9						7.23		11.5		265	
PN-18	P18				9.62	8.13											
PN-18	P18				9.34	17.8											
NJ-5D	N5				1.67	17.8											
OK-9D	O9				8.91	20.9								5.8		279	
OK-9D	O9				9.51	17.1								5.8		279	
PN-22D	P22				4.72	18.2						6.5		10		294	
OK-10D	O10				4.1	14.35						7.09		10		252	
OK-10D	O10				11.62	10.5						7.09		10		252	
OK-10D	O10				15.93							7.09		10		252	
OK-10D	O10				12.85	3.5						7.09		10		252	
BL-1D	B1				4.11	16.5	-2.2			349				102.9		224	26.1
BL-1D	B1				6.37	22.7	-1.4			278				102.9		224	26.1
BL-1D	B1				2.51	11.3								102.9		224	
BL-1D	B1						-3.6							102.9		224	26.1
BL-1D	B1				6.37	13.6	-4.6			357				102.9		224	26.1
BL-1D	B1						-31.5							102.9		224	26.1
BL-1D	B1						-27.3							102.9		224	26.1
BL-1D	B1						-0.1							102.9		224	26.1
NJ-6D	N6				4.35	11.6	-1			475		3.22		56.8		285	13.16
NJ-6D	N6						0.4					3.22		56.8		285	13.16
NJ-6D	N6				2.9	19.9						3.22		56.8		285	
NJ-6D	N6				1.11	27.1	-1.3			236		3.22		56.8		285	13.16
PN-20D	P20						-0.7					5.32				282	9.85
PN-22D	P22				1	20.8						6.5		10		294	
PN-22D	P22				1.1	22.4						6.5		10		294	
PN-22D	P22				0.8							6.5		10		294	
OK-10D	O10				1.4	22.97						7.09		10		252	
OK-10D	O10				1.7	23.13						7.09		10		252	
OK-10D	O10				4.1	16.95						7.09		10		252	
OK-10D	O10				0.3							7.09		10		252	

*TD = Total Discharge

**SO_4-H_2S fluid pair geothermometer

***Ah-Py mineral pair geothermometer

****SO_4-H_2O oxygen geothermometer

Table IIIa. Mahanagdong Sulfur and oxygen isotope data and calculated temperatures

LABEL	SOURCE	WHP (MPaa)	SP (MPaa)	SO4 (ppm)	H2S (ppm)	$\delta^{34}S$ SO_4	$\delta^{18}O$ SO_4	$\delta^{18}O$ liquid	$\delta^{18}O$ steam	y	$\delta^{18}O$ H_2O TD	$\delta^{34}S$ H_2S	$\delta^{34}S$ fluid	Sulfur T fluid	$\Delta^{18}O$	Oxygen T fluid
M18	MG-18D/throttled	2.395	2.325	114	56.08	17.91		-2.68	-4.5	0.183091	-3.01	-0.2	18.11	351		
M23	MG-23D/FO	1.843	1.773	15.83	48.17	17.89		-2.03	-4.07	0.221234	-2.48	1.2	16.69	382		
M27	MG-27D/FO	1.442	1.372	28.83	81.91	19.17	2.77	-1.76	-3.94	0.244648	-2.29	0.4	18.77	338	5.063	288
M29	MG-29D/FO	1.292	1.252	24.02	74.08			-1.26	-3.48	0.338555	-2.01	1.1			2.012	413
M31	MG-31D/throttled	1.742	1.662	39.51	133.46	16.88	3.2	0.17	-1.98	0.640747	-1.21	-1	17.88	356	4.408	309
M24	MG-24D/FO	1.342	1.272	56.53	169.91	15.97	4	0.79	-1.53	0.301467	0.09	0.2	15.77	404	3.909	327
M14	MG-14D/throttled	2.295	2.255	304.96	110.59	19.86	3.78	0.95	-1.05	0.378016	0.19	-0.8	20.66	305	3.586	339
M23	MG-23D/throttled	2.593	2.553	13.22	37.63	17.25						0.9	16.35	390		
M1	MG-1/FO	2.092	0.562	25.94	22.89	18.46	2.85					-0.3	18.76	338		
M18	MG-18D/FO	1.295	1.225	17.47	59.57	17.56	11.69					0.2	17.36	367		
M31	MG-31D/FO	1.192	1.122	43.33	119.44	8.94	6.02					-1.4	10.34	610		
M14	MG-14D/FO	1.295	1.255	305.37	93.92	19.44	3.41					-0.5	19.94	317		
M31	MG-3D/FO	1.275	1.275	7.09	131.49	16.48	5.31					-0.6	17.08	373		
M1	MG-1/throttled	2.092	0.562	25.94	22.89	18.77	4.79	-2.42	-3.25	0.267081	-2.64				7.432	227
41	HS-41			205		1.02	-1.39	-4.15				-3.25	4.27			
29	HS-29			1025		2.26	-0.77	-5.19								
M9	MG-9D (1994)					22.5	4.28									
M21	MG-21D (1994)					22.5	-2.06									

Table IIIa. Continued

SOURCE	DEPTH	LABEL	$\delta^{34}S$ Ah	$\delta^{34}S$ Py	$\delta^{34}S$ mineral	Sulfur T mineral
MG-9	1517-1686	M9	18.59	0.21	18.4	353.68
MG-13	1420-1440	M13		-1.57		
MG-15	1600-2005	M15		1.76		
MG-20	1560-1600	M20		2.09		
MG-21	1515-1580	M21	21.72	1.12	20.6	302.234

Table IIIB. Mahanagdong reservoir fluid chemistry

LABEL	SOURCE	WHP (MPaa)	SP (MPaa)	SO_4 (ppm)	H_2S*	H (J/g)	pH	Na	K	Ca	Mg	Fe	Cl	HCO_3	SiO_2	CO_2	NH_3	He	H_2	Ar	N_2	CH_4	T qtz
18Dt	MG-18D/throttled	2.395	2.325	130	20.52	1284	6.15	1619	225	12	0.82	0.12	2695	139.90	619	3480	4.68	0.010	0.743	0.079	7.522	7.194	268
23D	MG-23D/FO	1.843	1.773	19	16.5	1307	6.52	1246	352	28	0.65	0.12	3352	60.30	695	1015	1.67	0.000	0.166	0.051	3.317	2.094	273
27D	MG-27D/FO	1.442	1.372	37	19.22	1307	6.56	2421	470	45	0.76	0.14	4329	40.90	786	860	4.32	0.000	0.393	0.021	1.492	0.312	284
29D	MG-29D/FO	1.292	1.252	31	16.38	1477	6.60	3167	736	84	0.51	0.14	5845	29.60	784	769	3.38	0.001	1.503	0.077	5.482	1.922	283
31Dt	MG-31D/throttled	1.742	1.662	48	38.62	2102	6.10	2538	454	35	0.64	0.13	4477	40.50	695	1026	7.37	0.014	2.236	0.029	1.575	1.588	274
24D	MG-24D/FO	1.342	1.272	74	37.4	1405	6.48	2187	512	46	0.43	0.10	3976	83.30	819	2546	7.21	0.037	2.678	0.065	4.533	11.088	290
14Dt	MG-14D/throttled	2.295	2.255	360	37.41	1641	6.40	2617	463	14	0.89	0.52	4268	24.80	689	1371	7.37	0.008	1.943	0.015	1.886	2.984	277
23Dt	MG-23D/throttled	2.593	2.553	15	17.65	1307	6.18	1770	335	35	0.54	0.07	3131	59.90	642	1239	2.05	0.027	0.257	0.078	4.882	2.853	272
1	MG-1/FO	2.092	0.562	35	3.89	1218	6.32	2166	398	27	0.51	0.10	3652	53.20	770	65	1.16	0.007	0.067	0.024	0.630	0.030	268
18D	MG-18D/FO	1.295	1.225	122	14.92	1284	6.63	1841	327	16	0.53	0.22	2943	175.70	728	2485	4.08	0.014	0.652	0.075	6.888	6.470	275
31D	MG-31D/FO	1.192	1.122	56	28.2	2102	6.20	2745	499	40	0.89	0.04	4746	35.20	774	818	7.69	0.018	2.157	0.038	2.156	1.522	280
14D	MG-14D/FO	1.295	1.255	390	37.5	2632	6.18	3431	663	22	1.17	0.84	5605	27.70	852	1358	7.47	0.014	2.755	0.014	3.085	4.903	298
3D	MG-3D/FO	1.275	1.275	9	31.43	2548	6.65	3393	897	222	2.60	0.57	6340	32.00	749	757	7.42	0.009	1.808	0.010	0.632	0.475	280
1t	MG-1/throttled	2.092	0.562	24	13.8	1218	6.15	1741	313	33	0.70	0.80	2974	48.70	627	14	1.30	0.021	0.692	0.077	5.117	2.776	271
3Dt	MG-3D/throttled	1.365	2.69	5	35.05	2548	6.22	2600	740	187	2.00	0.32	5179	40.20	627	694	6.89	0.015	2.992	0.019	0.995	0.779	270
HS41	HS-41			205																			
HS29	HS-29			1025																			
9D	MG-9D (1995)		0.46	87	36.4	1531	3.45	3267	950	100	15.50	51.00	6106	0.00	987	653	0.10		0.758		3.952	0.960	297
15D	MG-21D (1994)		1.56	88	42.4	1269	3.63	2307	560	40	9.60	22.10	4256	0.00	769	1358	7.47	0.014	2.755	0.014	3.085	4.903	283

*: unit is mmol/100mol

Table IV. Bacon-Manito chemical and isotope data.

WELL	CODE	$\delta^{18}O\ SO_4$	$\delta^{34}S\ SO_4$	$\delta^{34}S\ H_2S$	$\delta^{18}O$ Ah	$\delta^{34}S$ Ah	$\delta^{34}S$ Py	$\delta^{18}O\ H_2O$	pH	H_2S	Cl	SO4	T Oxygen (fluid)	T Sulfur (fluid)	T Sulfur (mineral)	measured temp.
IM-1	I1	1.57	-0.3							2.3	8152	102				281
PAL-2D	P2	6.2							4.73	5.5	3781	213				285
PAL-2D	P2	4.9	24.4						6.12	5.5	3781	213				285
PAL-2D	P2	6.7	24.2						6.12	5.5	3781	213				285
PAL-2D	P2	6.3	13.8						6.12	5.5	3781	213				285
PAL-2D	P2	6.2							6.12	5.5	3781	213				285
PAL-2D	P2	6.2	16						6.12	5.5	3781	213				285
PAL-2D	P2	5.7	16.3						6.12	5.5	3781	213				285
PAL-2D	P2	5	24.5						6.12	5.5	3781	213				285
PAL-5D	P5	1.4	14.4					-3.26	7.56	3	5442	25	300			270
PAL-5D	P5	2.9						-3.26	7.56	3	5442	25	257			270
PAL-6D	P6	6.4	20.3	-0.04					7.15	2.8	5879	31		311		283
PAL-7D	P7	2.6	18.9					-3.01	6.88	2.3	5754	48	272			283
PAL-7D	P7	3.2	18.9					-3.01	6.88	2.3	5754	48	256			283
PAL-8D	P8	6.1	9.65	-0.46					7.47	9.5	6655	8		624		305
PAL-10D	P10	6	20.43					-0.45	6.66	9.2	5815	24	249			302
PAL-10D	P10	6	22.19	1.55				-0.45	6.66	9.2	5815	24	249	306		302
PAL-13D	P13	6.5	22.93	0.9				-2.01	7.13	21.7	6287	18	205	285		295
Inang Maha	IM	1.6	-0.5	-0.5				-0.65	6.8		14	120	400			
Naghaso	NH	7.3	10.4					-0.6	3.5		2207	53	217			
Damoy	DY	1.2	1.7	1.25				-5.7	3.06		4	195	239			
PAL-2D	P2				-1.74	1.37			6.12							285
PAL-2D	P2				-1.03	1.12			6.12							285
PAL-2D	P2				-1.2	15.8			6.12							285
PAL-2D	P2				0.5				6.12							285
PAL-2D	P2				6.8	12.24			6.12							285
PAL-5D	P5				12	1		-3.26	7.56							270
PAL-5D	P5				1.9	19.9		-3.26	7.56							270
PAL-5D	P5				12			-3.26	7.56							270
PAL-5D	P5				1.1	0		-3.26	7.56							270
PAL-5D	P5				1.1			-3.26	7.56							270
PAL-5D	P5				1.2			-3.26	7.56							270
PAL-5D	P5						-11.2	-3.26	7.56	3						270
PAL-5D	P5				8	12.5		-3.26	7.56							270
PAL-5D	P5				8			-3.26	7.56							270
PAL-5D	P5				11.42	15.86		-3.26	7.56							270
PAL-5D	P5				12	15		-3.26	7.56							270
PAL-5D	P5				1.1			-3.26	7.56							270
PAL-5D	P5				2			-3.26	7.56							270
PAL-5D	P5				2			-3.26	7.56							270
PAL-6D	P6				7.1	12.9			7.15							283

Table IV. Continued

WELL	CODE	$\delta^{18}O\ SO_4$	$\delta^{34}S\ SO_4$	$\delta^{34}S\ H_2S$	$\delta^{18}O$ Ah	$\delta^{34}S$ Ah	$\delta^{34}S$ Py	$\delta^{18}O\ H_2O$	pH	H_2S*	Cl**	SO4**	T Oxygen (fluid)	T Sulfur (fluid)	T Sulfur (mineral)	measured temp.
PAL-7D	P7				7.4	0.34		-3.01	6.88							283
PAL-7D	P7				4.4	18.8		-3.01	6.88							283
PAL-8D	P8						-7.2		7.47	9.5						305
PAL-8D	P8				7.16	10.48	-20		7.47	9.5					168	305
PAL-8D	P8				0.9	17.84	-0.63		7.47	9.5					351	305
PAL-8D	P8				1.68	17.84	-0.63		7.47	9.5					351	305
PAL-8D	P8				6.3	19.3			7.47							305
PAL-8D	P8				15.5	3.27			7.47							305
PAL-10D	P10						-1.66	-0.45	6.66	9.2						302
PAL-10D	P10				7.2	18.7	-1.66	-0.45	6.66	9.2					307	302
PAL-11D	P11				5.1	-3.5	-8.4		7.08	11.25	6402	24				290
PAL-11D	P11				5				7.08							290
PAL-11D	P11				6.8	13.2	-4.3		7.08	11.25					378	290
PAL-13D	P13				7.5	12.4		-2.01	7.13							295
PAL-13D	P13				6.1	15.5	-3.3	-2.01	7.13	21.7					343	295
CN-2D	C2				5	10.6			3.79	16.07	3068	1174				281
CN-2D	C2				7.3	13.2			3.79							281
CN-2D	C2				3.1	7.6			3.79							281
CN-2D	C2						-3.4		3.79	16.07						281
MO-1	M1				3	-2.7			3.09	0.47	6486	180				224
MO-1	M1				5.4	-8			3.09							224
MO-1	M1				3.7	13.3			3.09							224
MO-1	M1				0.3	10.9			3.09							224
MO-1	M1				4.6	10.3			3.09							224
MO-1	M1						-4.9		3.09	0.47						224
PAL-2D	P2s				6.4	24.5			6.12							285
PAL-2D	P2s				5.6	23.5			6.12							285
PAL-2D	P2s				4.7	24.65			6.12							285
PAL-7D	P7s				2.6			-3.01	6.88							283
PAL-7D	P7s				3.5			-3.01	6.88							283
PAL-9D	P9s				4.8	22.75		-1.78	7.13	3.97	6071	14				287
PAL-9D	P9s				4.1	8.25		-1.78	7.13							287
CN-1	C1s				2.7	20.52			7.71	14	5766	14				275
CN-1	C1s				2.5	24.93			7.71							275

ISOTOPE GEOCHEMISTRY OF THERMAL SPRINGS IN THE KARYMSKY GEOTHERMAL AREAS, KAMCHATKA, RUSSIAN FEDERATION

G.A. Karpov[1], A.D. Esikov[2]

[1]Institute of Volcano logy, Far East Division, Russian Academy of Sciences, Russian Federation
[2]Institute of Water Problems, Russian Academy of Sciences, Moscow, Russian Federation

Abstract. The main goal of our research was to study the conditions and characteristic features of the formation of saline composition of water in acid caldera lakes as basins conjugate with hearths of discharge of powerful hydrothermal systems in areas of andesitic volcanism. These hydrothermal systems are used for production of geothermal energy, and problems with acid hydrothermal fluids found during drilling have become rather important recently. We estimated the dynamics of the process of saline composition change within the large fresh-water basin of the Karymskoe Lake. The preceding data and arguments show that saline compositions of thermal springs and acid lakes in caldera hydrothermal systems genetically connected with "andesite" volcanism form in different ways. Two main types of hydrothermal water co-exist in calderas of the "Karymsky" type having magmatic chambers with continuing intense intrusive-explosive activity. The first is represented by alkaline waters of the "geyser" type; the second one by acidic "Karymsky"-type complex composition waters. The so-called "geyser" type of Cl-Na composition is connected with abyssal fractures and delimits the area of generation of thermal-mass-flow from abyssal zones of volcanic-tectonic structures. These flows are manifest in zones of joint linear and circular fractures tending to ancient magmatic structures. In this case, acid solutions and acid lakes appear in zones of resurgent magmatic activity and are connected directly with a flow of acid fluids from apical zones of a peripheral magmatic chamber. In thermal waters of Cl-Na content, the saline compositions are formed from abyssal fluids that contain high NaCl at temperatures of 800–900˚C and pressures 1–8 kbar and react with deep country rocks – neutralizing their predominantly acid compositions. Finally these rocks undergo propylitization. Infiltrating surface waters contribute greatly to the formation of "geyser" type thermal waters. The main source of mineral components in acid waters is recently erupted fresh magmatic rocks that are mainly of basic composition (basalts). An acidic contribution to these solutions is supplied by oxidation of sulphur-containing compounds and by halide (HCl, HF) gases in fluids separated from shallow magmatic chambers. In addition, a large part of water acidification results from extraction of acid components from fresh ashes entering lacustrine basins. The water component of such sources and basins is mainly meteoric.

1. Introduction

The main goal of our research was to study the conditions and characteristic features of formation of water in recent acid caldera lakes as basins conjugate with hearths of discharge of powerful hydrothermal systems in areas of andesitic volcanism. These hydrothermal systems are used for production of geothermal energy and problems with acid hydrothermal fluids found during drilling have become rather important recently.

From one point of view, crater and caldera lakes work as reservoirs from which water is supplied to a descending flow of infiltrating waters, which takes part in the recharge of hydrothermal systems. Thus, it can be supposed that complex research on such lakes will further the understanding of formative processes of different hydrochemical types and will provide material for practical methods for mitigation and recommendations on use of complex hydrothermal systems with reservoirs of acid waters.

Acid lakes are met in many areas of recent volcanism — in Japan, Indonesia, New Zealand, North America and other countries [9, 10, 17, 21–24, 32]. In Kamchatka the most vivid representatives of objects interesting for us are the well-known hydrothermal systems of the Uzon caldera and Karymsky volcanic centre [3–7, 12–14, 16, 20, 29, 30, 33].

The largest hydrothermal system with natural discharge of 62000 kcal/s is located in the Uzon caldera. Here, most high-temperature waters have sodium-chloride composition and pH between 6,5 and 7,5. But other hydrochemical water types are also widely represented and there are several lakes with pH values of 2,5–5,0 and chloride-sulphate solution compositions, as for example Lakes Fumarolnoe, Chloridnoe and Bannoe [3, 4].

The Karymsky volcanic centre became well known after the sub aqueous eruption in the caldera lake Karymskoe in 1996, which resulted in formerly fresh lake water becoming acid [8, 15, 19, 29].

2. Characteristics of water of atmospheric origin

Information on chemical and hydroisotope compositions of atmospheric precipitation in the areas under study was obtained from analysis of water and snow samples taken monthly at the hydrometric station Puschino and also using analyses from seasonal sampling of cool creeks and snow water in the Uzon caldera and in the area of the Karymsky lake.

Generally, as can be seen from Table I and Figures 1-5, temperature, precipitation quantity, total mineralization and content of main components vary concordantly in annual cycles of atmospheric precipitation for all months except in the periods from October to December 1998 and 1999 when the quantities of K, Na, Cl, HCO_3, H_4SiO_4 and total mineralization of precipitation varied inversely. Apparently, this is connected with the fact that in Kamchatka this period of the year has the most unstable weather and wind directions. In our study fluctuations of hydroisotopic compositions are very significant and at the same time descriptive. The lowest concentrations of ^{18}O were noted in March and April of 1998. The highest concentrations of ^{18}O were marked in September of 1998. The last fact is possibly explained by the correlation of the usual decrease of ^{18}O concentration after downpours [5] that just occurred in August of 1998. There was a notable direct correlation of ^{18}O with temperature (Figure 6A), although some deviations from the straight line are observed for precipitation in September and December of 1998 and in January of 1999. The relationship between ^{18}O and precipitation quantity is of more complicated character (Figure 6B). Here it also foreshadowed deviation for the same months including October 1998 and February 1999. Water from snow samples taken in 1999 directly on the shore of Lake Karymskoe ($\delta^{18}O$ = -14,47; δD = -73,76‰) and from 20 km towards the ocean ($\delta^{18}O$ = -11,28; δD = -80,24‰) and also water of the cool Gremuchiy creek flowing into Lake Karymskoe ($\delta^{18}O$ = -12,68; δD = -91,44‰) and water of the cool Vesyoly creek in the Uzon caldera ($\delta^{18}O$ = -13,45; δD = -97,6‰) proved to have very different isotopic compositions. Nevertheless, practically all these data fall on the Craig's meteoric water line and this is evidence of unity of formation laws of atmospheric precipitation isotope composition. Generally, our data also correspond with the results of studies of oxygen isotope composition in atmospheric precipitation and in Kamchatka rivers [1].

Table I. Results Of Regime Observations And Hydrochemical Analyses Of Atmospheric Precipitation According at Puschino Hydrometeostation

№ of sample	Date of sampling	Q-ty of precipi-tation	t°C	pH	Chemical Concentration, mg/l										∑ mg/l	$\delta^{18}O$, ‰ SMOW	δD, ‰ SMOW
					Na	K	Ca	Mg	Cl	SO_4	HCO_3	F	H_4SiO_4	H_3BO_3			
1	2	3	4	5	6	7	8	9	10	11	12	13	14	15	16	17	18
P-3/98	Mar. 1998	18.7	– 11.4	6.8	0.46	0.34	0.1	1.20	0.70	1.00	4.9	–	–	1.4	10.1	– 20.4	– 153
P-4/98	Apr. 1998	21.6	– 4.2	7.1	2.80	1.53	2.8	2.19	5.00	1.44	19.5	0.09	4.6	0.6	40.55	– 19.7	– 148
P-5/98	May 1998	23.2	– 4.7	7.1	2.89	1.53	2.8	2.76	5.3	–	21.9	0.07	4.6	0.6	42.36	– 15.2	– 103
P-6/98	June 1998	2.1	15.2	7.1	–	–	–	–	–	–	–	–	–	–	–	–	–
P-7/98	July 1998	46.5	16.2	7.2	1.30	1.70	1.2	5.0.	2.10.	2.80.	31.7	0.15	5.5	6.8	58.25	–	–
P-8/98	Aug. 1998	164.2	13.1	7.0	0.50	0.40	0.4	3.20.	0.70.	2.90.	14.6	0.08	6.0	10.9	39.68	–	–
P-9/98	Sep. 1998	7.0	9.0.	7.0	–	–	–	–	–	–	–	–	–	–	–	– 8.31	–
P-10/98	Oct. 1998	63.0.	0.9	7.1	2.80	0.70	1.6	2.40	1.40	2.90	20.7	0.07	15.3	11.1	58.97	– 14.61	–
P-11/98	Nov. 1998	41.2	– 11.7	7.5	3.60	2.00	1.6	2.40	1.40	1.40	26.8	0.01	15.4	2.6	57.11	– 17.94	–
P-12/98	Dec. 1998	117.0	– 15.5	7.3	2.82	1.56	1.2	1.21	0.35	1.44	18.3	0.07	6.0	0.6	33.55	– 17.96	– 131.3
P-1/99	Jan. 1999	214.4	– 14.2	7.4	1.89	1.19	1.2	0.97	0.35	1.44	12.2	0.06	6.7	0.6	26.6	– 11.66	–
P-2/99	Feb. 1999	83.8	– 15.7	7.4	1.95	0.98	1.2	0.97	0.35	1.44	12.2	0.06	6.4	0.6	26.15	– 13.93	–
P-3/99	Mar. 1999	75.4	– 12.9	7.6	3.60	2.20	1.2	2.07	0.70	1.44	25.0	0.06	4.7	0.6	41.57	– 13.46	–
P-4/99	Apr. 1999	51.3	– 4.3	7.13	4.1	1.5	2.4	2.2	3.6	4.8	24.4	0.05	10.5	0.5	54.04		
P-5/99	May 1999	21.5	4.9	7.37	4.3	1.7	4.0.	1.2	1.4	2.9	34.2	0.05	11.5	0.5	61.54		
P-6/99	June 1999	38.4	11.4	7.31	1.2	1.0.	9.6	3.4	2.1	4.8	45.2	0.07	2.0	0.5	68.86		
P-7/99	July 1999	85.9	14.3	7.35	1.2	0.6	2.8	2.9	2.1	1.9	23.2	0.05	3.2	0.5	28.44		
P-8/99	Aug. 1999	78.2	12.8	7.32	1.2	0.6	2.8	3.2	1.4	3.8	23.2	0.05	3.2	0.5	39.94		
P-9/99	Sep. 1999	62.5	8.4	7.18	1.33	0.92	4.4	2.7	0.7	2.88	31.1	0.03	3.0	0.5	47.66		
P-10/99	Oct. 1999	58.0	1.9	7.35	2.14	1.40	5.2	1.7	0.7	2.88	31.1	0.01	2.6	0.5	48.43		
P-11/99	Nov. 1999	63.7	– 6.4	7.5	1.50	1.00	4.8	0.97	1.05	2.88	24.4	0.01	4.1	0.5	41.41		
P-12/99	Dec. 1999	147.3	– 15.9	6.70	3.93	1.17	3.6	0.97	1.75	2.88	28.1	0.03	6.5	0.5	49.63		

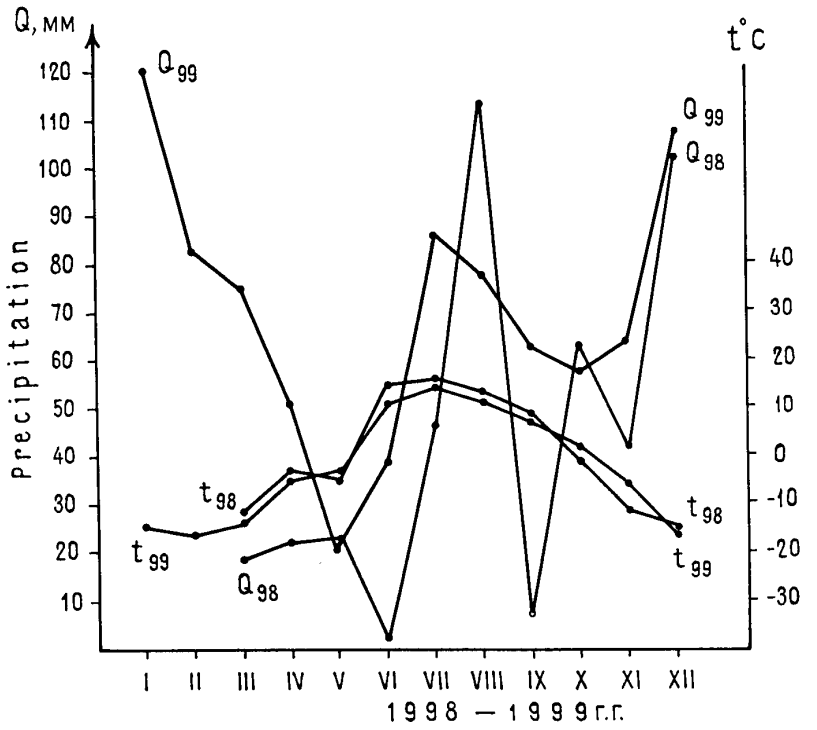

Figure 1. Temperature variations and atmospheric precipitation quantity according to the Puschino meteorological station data in 1998–1999.

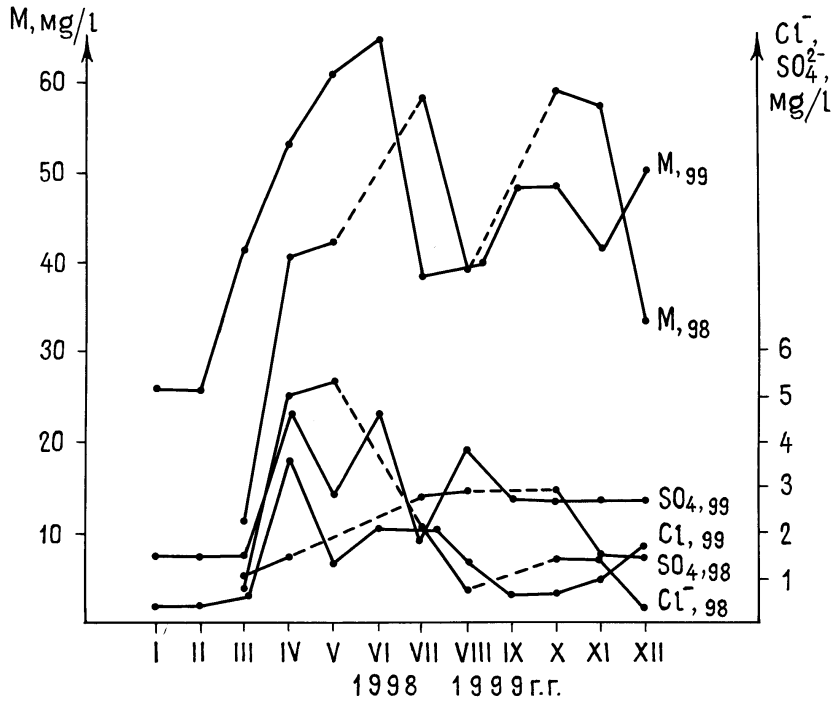

Figure 2. Variations of Cl and SO_4 quantity and total mineralization of atmospheric precipitation according to the Puschino meteorological station data in 1998–1999.

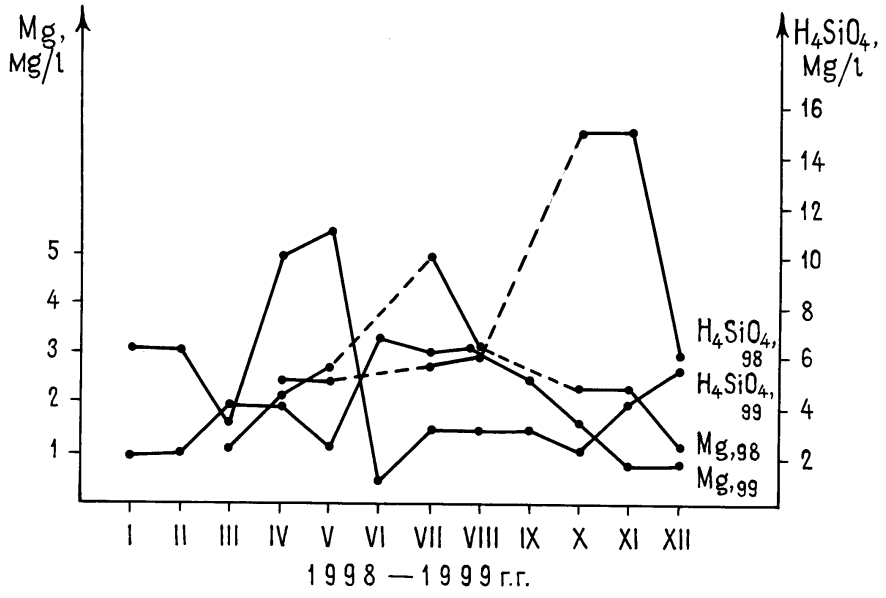

Figure 3. Variations of Mg and H_4SiO_4 quantity in atmospheric precipitation according to the Puschino meteorological station data in 1998–1999.

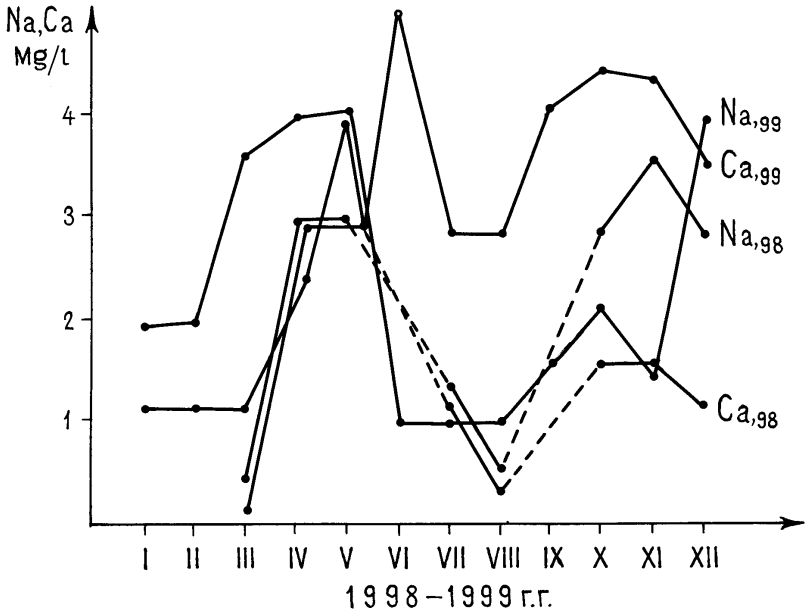

Figure 4. Variations of Na and Ca quantity in atmospheric precipitation according to the Puschino meteorological station data in 1998–1999.

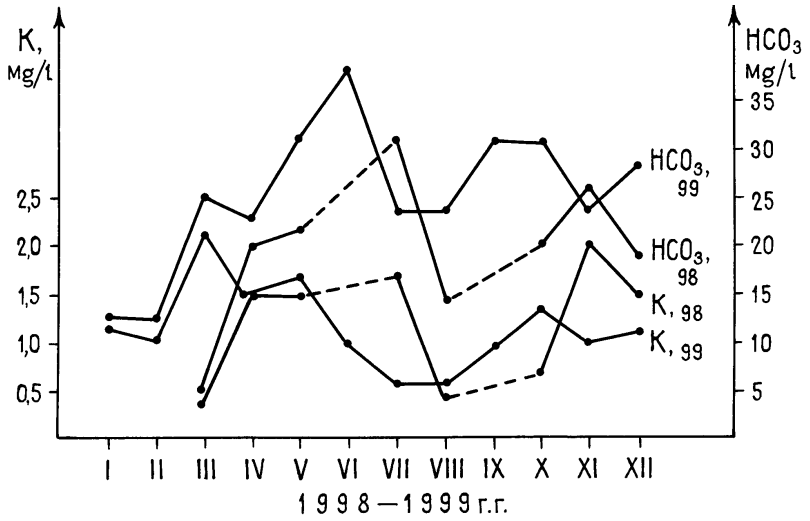

Figure 5. Variations of K and HCO_3 quantity in atmospheric precipitation according to the Puschino meteorological station data in 1998–1999.

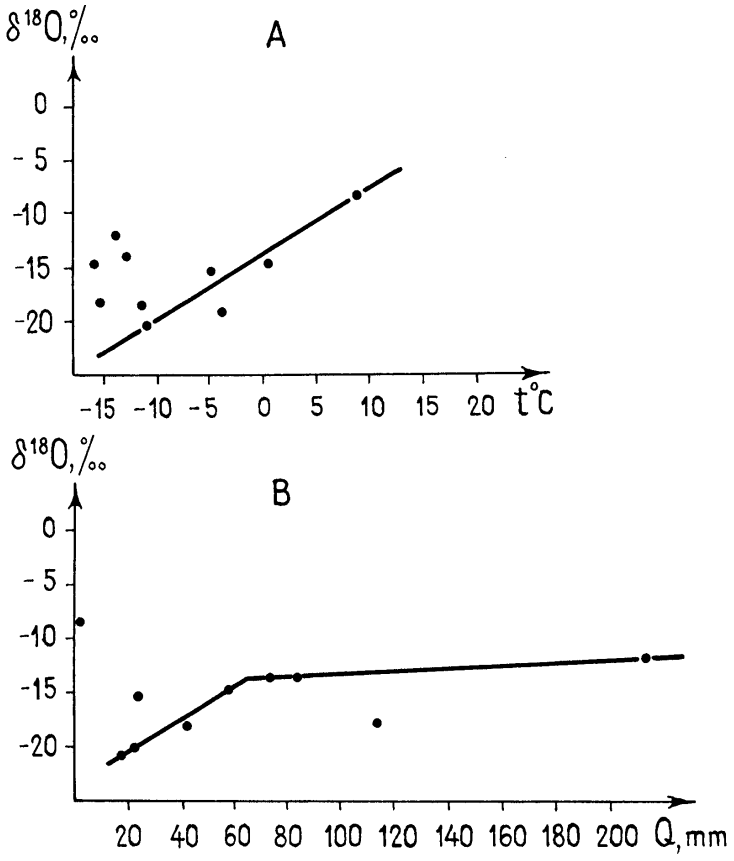

Figure 6. Correlation of $\delta^{18}O$ - t° C (A) and $\delta^{18}O - Q_m$ (B) according to the data of atmospheric precipitation sampling at Puschino meteorological station.

3. Thermal waters of Lake Karymskoe area

Lake Karymskoe is the third largest lake in quantity of its water mass (after Lakes Kronotskoe and Kurilskoe) located in the Eastern volcanic belt of Kamchatka. Before the sub aqueous eruption in 1996, it was a fresh water basin although the andesite-dacite volcano Kronotsky, situated at a distance of 6 km north of the lake, erupted at intervals of 7–12 years and great quantity of its ash usually fell into the lake. The lake cone is of volcano-tectonic genesis and is the caldera of the Akademii Nauk volcano [31]. (Figure 7).

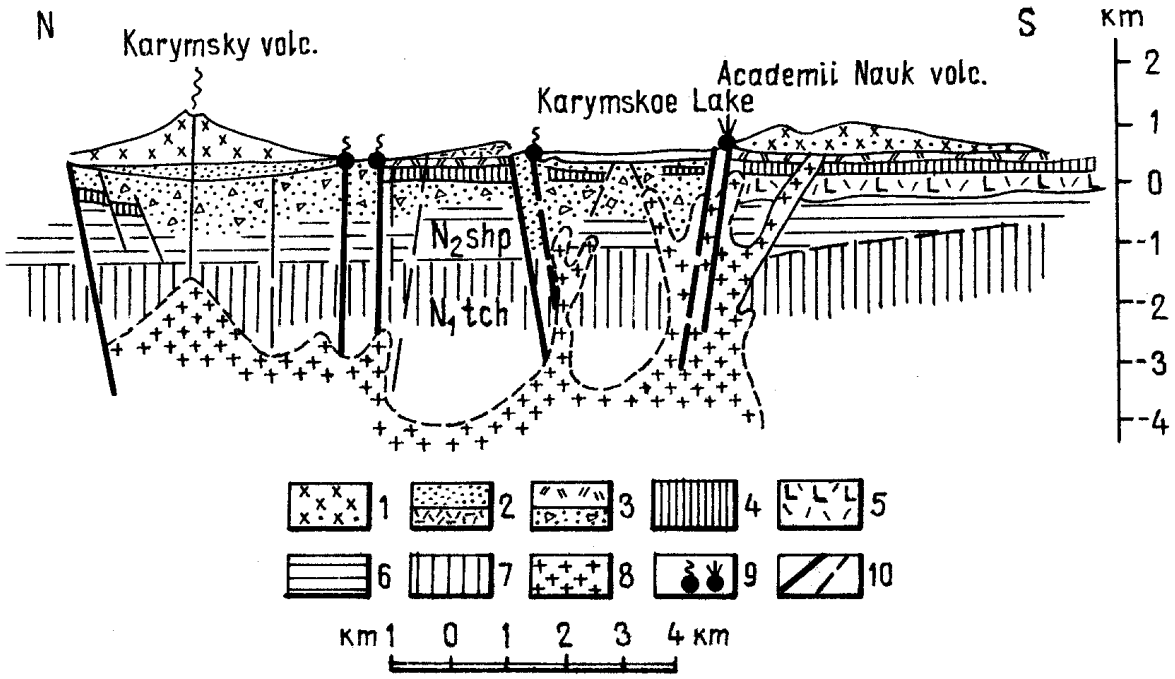

Figure 7. A schematic N-S geological cross-section of the Karymsky volcanic centre.
***Legend**: 1 – Andesite-dacites of the Karymsky volcano and dacites of the Akademii Nauk volcano (Q_3^3); 2 – Caldera-lacustrine deposits (early Holocene) and pumice pyroclastics (Q_3^3); 3 – Pyroclastics' flows of intercaldera filling (Q_2) and collapse-explosion deposits of intercaldera volcanogenic formations ($Q_3 – Q_4$); 4 – Andesite-basalts, basalts, their tuffs (remnants of the ancient volcanoes $Q_1 – N_2$); 5 – Deposits of Toumrok and Storozhevaya suites (N_2); 6 – Deposits of Schapinskaya suite (N_2, shp); 7 – Deposits of Tyushevskaya series (N_1, tch); 8 – Intrusions of granitoid's composition; 9 – Thermal springs and geysers; 10 – Tectonic faults.*

3.1. Thermal-hydrochemical regime of Lake Karymskoe

The natural cataclysm of the sub aqueous eruption in 1996 can be considered as a giant experiment as a result of which the Lake Karymskoe hydrochemical system was greatly changed within a very brief period. Quite extensive long-term observations of the thermal-hydrochemical regime of Lake Karymskoe and a series of thermal manifestations in this area have led to conclusions about the degree of degradation and the commencement of self-recovery of the basic parameters of the lacustrine basin.

The attempt to evaluate the dynamics of alteration of the saline composition of objects under study was made on the basis of Table II in which the results of observations of hydrochemical parameters of streams in the area of Lake Karymskoe and this lake itself are given. Thus, concordant alteration of the contents of chloride, sodium, sulphate, calcium, magnesium, silicic acid, metaboric acid, pH and total mineralization was observed in the surface waters of Lake Karymskoe as well as in the crater cone of

the eruption in 1996 within the period of research from 1996 till 1999 (Figure 8, 9). At the same time, a different picture was observed in the vertical profile of the lacustrine water mass. As in the abyssal sampling at intervals 10m carried out by S.V.Ushakov in May of 1996 and 1998 (analyses were performed by S.M.Fazlullin presented orally) great amounts of Na^+, Mg^{2+}, Ca^{2+} and Cl^- was contained in 1996 to the depth of 30m in the center of the lake water area as well as in the crater cone of the 1996 eruption and these quantities were undergoing weak and generally synchronous fluctuations. Maximum concentrations of Na^+, Mg^{2+} and Cl^- were noted in the crater cone. On the contrary, increased quantity of sulphate was found in the lake water, which was well mixed at depths 50–60m and practically the same chemically all over the lake. It should be pointed out that there is a sudden increase (by more than 200 mg/l) of sulphate ion content with some increase of sodium ion content at the depth of 30 m in the lake water which occurred simultaneously with the decrease of sulphate and the rise of sodium ion content in the crater funnel.

This draws attention to the fact that in 1996 the concentrations of magnesium, calcium and sulphate ions were high everywhere in the lake (over the whole area as well as at all depths). Apparently, this was due to the great mass of ash from the erupting Karymsky volcano, which fell into the lake water, as well as to dissolution of parts of the fluid components of the sub aqueous eruption itself in the lake water. SO_2 was found in the composition of occluded gases of volcanic bombs of this eruption. Native sulfur, sulfates (gypsum, coquimbite, voltaite, halotrichite-pickeringite, alunogen, and epsomite), and free sulphuric acid were found in the mineral products of the post-magmatic stage of activity in one of the explosive funnels in the northern sector of the lake [30].

Water extracted from the sample of andesite-dacite ash of the Karymsky volcano taken on the 3rd January, 1996 contained (in mg/l): H^+-0,24; Na^+-133,4; K^+-23,5; Ca^{2+}-872,0; Mg^{2+}-54,4; Fe^{2+}+Fe^{3+}-24,0; Cl^--163,5; F^--12,6; and SO_4^{2-}-2643,0; at pH=3,07. As can be seen sulfate, calcium, sodium and magnesium prevail in the water-soluble fraction of the ash. Naturally the solution has acid reaction, very similar to that observed in the lake after the sub aqueous eruption in 1996.

Our experiments with underwater traps showed that daily about 100 tons of ash from the erupting Karymsky volcano entered the water of Lake Karymskoe in 1999. In 1996 the intensity of the Karymsky volcano explosive activity was ten times greater and, additionally, materials washed from basaltic material of the structure of the sub aqueous eruption in 1996 was supplied into the lake with lateral run-off.

Thus, the persistance of the saline composition and low pH of the lake water is quite explicable by influence of the long-term eruption of the Karymsky volcano, although processes of extraction of the water-soluble component from products of the underwater and above-water structure of the eruption in 1996 (total weight of which is evaluated to be 70 million tons), apparently play the main part [19].

However, it is difficult to explain the sudden 1996 increase of sulfate-ion in the crater cone at the depth of 30 m, of sodium at depths of 30 and 50 m in the crater cone and lake water, and also the sudden decrease of chloride at the depth of 50 m in the crater cone (considering its stability in the lake water). It can be supposed that lateral run-off from the underwater crater structure at various depths plays its part.

The comparative analysis of curves (Figure 8, 9) shows that over time there is distinctive trend consisting of decrease of calcium and sulphate; the decrease of sodium, H_3BO_3, H_4SiO_4 and total mineralization is less clear. Water pH rises very slowly. It can also be distinctly seen in the Karymskaya river effluent (Table II).

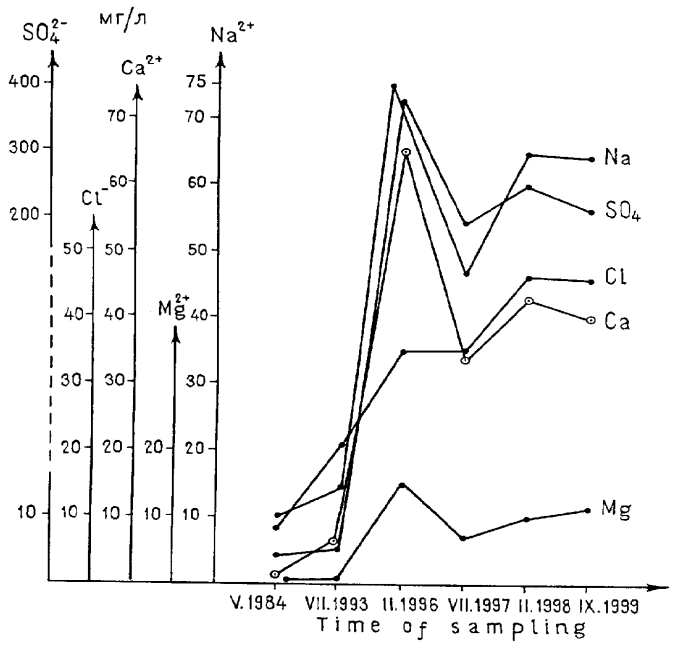

Figure 8. Variations of Na, Ca, Mg, Cl^- and SO_4^{2-} in waters of Lake Karymskoe within the period of observations in 1984–1999.

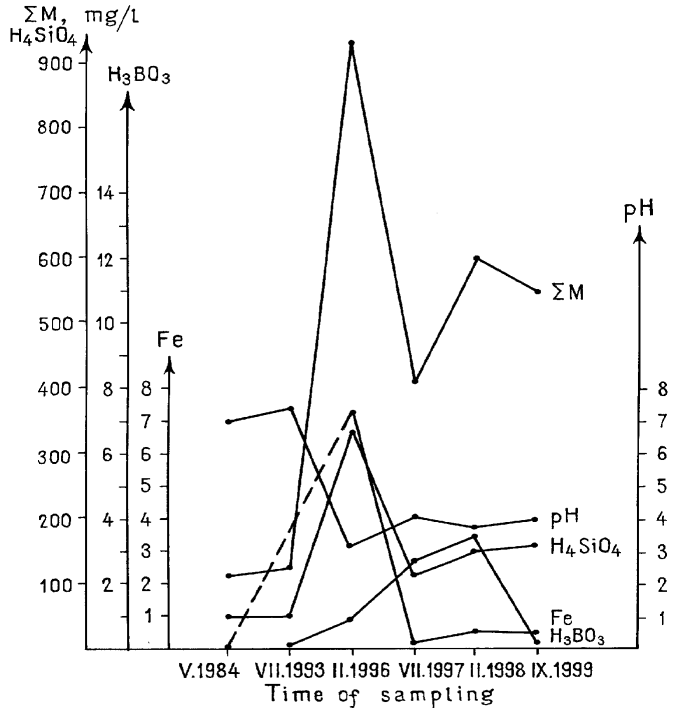

Figure 9. Variations of H_3BO_3 and H_4SiO_4 quantity, total mineralization and pH in waters if the Karymskoe Lake for the period of observations in 1984–1999.

By 1999, total mineralization in the explosive funnel of the small lake (Table II) dropped by more than half. Concentrations of magnesium, calcium, sodium and sulphate considerably decreased. Hydrogen sulphide disappeared. The quantities of boric acid, carbonate and bicarbonate fluctuate constantly and pH rises. By 1999, concentrations of calcium, metaboric acid and total mineralization distinctly decreased in all thermal springs. The other components undergo quite irregular variations, though in comparison with 1998 a noticeable increase of sulphate is observed in all springs. Note that the Novy geyser water has the most stable chemical composition.

On the basis of isotopic data (analyst A. D. Esikov — Institute of Water problems, RAS), it is concluded that atmospheric precipitation contributes most of the water to all water-manifestations in the area under study except for the lake in the explosive funnel № 4 (maar). The peculiar chemical composition of water in explosive funnel № 4 with high total mineralization, high quantities of boron and potassium and $\delta^{18}O$= -8,85‰ suggests that an endogenic fluid component takes a great part in its forming.

3.2. Hydrological regime of Lake Karymskoe water and surrounding thermal springs

Inflow to Lake Karymskoe includes 8 constant creeks and 27 temporary cool water streams. The temporary streams usually function as long as ice remains in hollows in the inner slopes of the Akademii Nauk caldera. Lake Karymskoe is also recharged by three hot-water creeks constantly supplied from the Eastern and Western thermal fields of the group of Akademii Nauk springs and also by numerous independent discharges of hot (and boiling) springs concentrated along the southern, south-eastern, south-western, north-north-eastern and, mainly, northern sectors of the lakeshore (Map, Figure 10). The large river Karymskaya flows out of this lake. In addition, after the sub aqueous eruption in 1996 the lakeshore morphology was altered at the outflow of the Karymskaya river. An accumulative terrace more than 2m high was formed here. Numerous thermal springs feeding the Goryachaya Rechka creek flowing into the Karymskaya river come from beneath it. The bed of the Goryachaya Rechka creek is sub-parallels to that of the Karymskaya river for 100m between the first and second bends, where regime measurements of the Karymskaya river discharge are carried out. The saline composition of the Goryachaya Rechka creek water is intermediate between Lake Karymskoe composition and composition of high-temperature springs discharged near the edge of the creek. Thus, taking into account the low hypsometric level of the Goryachaya Rechka creek bed its discharge is to be referred to Lake Karymskoe subsurface drainage.

From the results of three-year hydrological observations carried out in July–August of 1997–1999, the hydrologic regime of all of these streams is very unsteady (Table III). For example, in 1997 the total discharge of all hot waters flowing into Lake Karymskoe was 243 l/s and in 1998 it was 202 l/s. In 1999, hot water discharge somewhat decreased visually.

The Lake Karymskoe basin water balance has the following factors: Q_1 – inflow of all hot water discharges into the lake; Q_2 – inflow of all cool water creeks into the lake; Q_3 – quantity of atmospheric precipitation getting into the lake; Q_4 – the Karymskaya river discharge; Q_5 – evaporation from the lake surface; and Q_6 – the lake subsurface drainage (as manifested by the discharge of the Goryachaya Rechka creek having mixed chemical composition). Therefore, the complete equation of balance is:

$$Q_1 + Q_2 + Q_3 = Q_4 + Q_5 + Q_6$$

Table II. Results of regime measurements of hydrochemical parameters of Lake Karymskoe basin (unit: mg/l)

Site	Date	T°C	PH	Na	K	Ca	Mg	Fe	Cl	SO_4	$HCO_3 + CO_3$	H_4SiO_4	H_3BO_3	H_2S	TDS mg/l	$\delta^{18}O$‰ SMOW	$\delta^{2}H$‰ SMOW
1. Lake Karymskoe water area, center																	
20	20.05.84	1,0	7,0	10,4	1,6	1,6	0,5	0,0	8,5	3,8	35,1	48,0	0,0	0,0	109,6	-	-
20	15.07.93	4,0	7,4	14,0	0,8	6,0	0,6	0,0	21,3	4,8	22,0	48,0	0,1	0,0	125,7	-	-
20	11.02.96	19,0	3,2	75,0	7,3	66,0	14,4	7,3	35,5	379,0	-	330,0	0,9	-	921,7	-12,8	-96,0
20	19.07.97	14,0	4,1	46,0	5,2	34,0	6,7	0,1	35,5	168,0	-	114,0	2,7	-	412,9	-11,3	-92,0
20	17.09.99	10,8	4,0	64,8	7,1	40,1	9,7	0,1	44,0	220,9	-	165,0	<0,5	-	552,1	-	-
2. The crater of the sub aqueous eruption in 1996, center																	
19	11.02.96	20,0	3,2	78,0	7,3	67,0	13,2	7,3	39,0	379,0	0,0	333,0	1,0	-	920,1	-12,8	-96,0
19	02.07.98	15,5	3,7	65,0	8,5	42,0	9,7	0,6	46,7	249,6	0,0	147,9	0,35	-	595,2	-11,53	-82,24
19	19.09.99	11,2	4,0	64,0	7,7	40,1	10,9	0,5	46,2	220,9	-	161,6	<0,5	-	552,3	-	-
3. The Karymskaya river effluent																	
24	09.10.96	10,0	3,7	69,2	7,1	62,0	10,9	2,8	49,3	317,0	-	157,0	<1,0	-	676,3	-10,8	-76,4
24	03,01.97	3,0	3,4	62,0	7,0	58,0	14,5	3,2	42,6	307,0	-	192,0	<1,0	-	688,7	-11,7	-
24	28.05.98	4,5	3,7	74,9	9,1	46,1	14,6	1,2	41,9	249,8	-	152,8	<1,0	-	591,3	-12,01	-86,08
24	28.08.99	12,0	4,0	60,0	7,8	40,1	8,5	0,1	44,0	220,0	-	145,4	10,5	-	529,0	-12,03	-86,24
4. The lake in eruptive funnel №4 (maar)																	
25	06.02.96	32,0	6,3	276,0	36,7	132,0	18,2	6,4	185,7	1066,0	84,1	340,5	6,8	23,8	2276,0	-	-
25	02.07.98	27,0	8,5	172,0	16,3	20,4	1,9	0,0	140,6	172,9	52,5	430,0	27,0	-	1034,0	-8,85	-
25	28.08.99	17,3	9,0	190,0	19,3	24,0	2,4	0,0	134,9	240,2	79,6	180,0	3,9	-	874,3	-	-
5. Hot water seepage in the shore area of the lake northern sector																	
17	03.01.97	81,0	7,3	255,0	24,0	48,0	9,7	-	282,0	240,0	152,0	390,0	16,3	-	1417,0	-11,74	-83,92
17	02.07.98	71,0	7,6	225,0	20,0	50,0	4,9	-	175,7	336,0	98,9	276,3	10,9	-	1199,0	-11,83	-84,64
17	28.08.99	72,0	7,6	280,0	30,2	38,1	3,6	-	176,1	393,8	92,8	293,1	5,2	-	1313,0	-11,82	-84,56
6. The thermal spring on the left bank of the Goryachaya Rechka																	
1	28.05.98	78,0	6,8	532,0	32,2	60,1	17,0	-	688,7	288,2	154,0	426,3	36,0	-	2235,0	-11,8	-84,0
1	29.08.99	82,0	7,4	440,0	56,6	50,1	10,9	-	507,7	345,8	98,9	333,0	13,1	-	1856,0	-	-
7. The hot river in the effluent of the Karymskaya river, the middle part																	
2	03.01.97	50,0	6,9	314,0.	36,0	110,0	31,5	-	451,0	355,0	190,0	217,0	24,5	-	1729,0	-	-
2	28.05.98	64,0	7,0	308,0	49,9	44,1	12,2	-	316,0	278,6	160,0	308,0	20,4	-	1509,0	-12,2	-87,8
2	20.09.99	73,0	7,8	378,9	44,6	44,1	7,3	-	408,3	355,4	87,9	298,4	9,2	-	1634,0	-11,88	-85,04
8. The Novy geyser in the group of the Akademii Nauk springs																	
12	02.07.98	97,0	8,5	354,0	18,7	2,8	0,1	-	436,7	115,3	96,0	427,0	50,3	-	1503,0	-11,5	-81,9

Notes: a dash means that a component is not determined in the sample. Analyses are performed in the central chemical laboratory of Institute of Volcanology FED RAS. Analysts: Sergeeva, S.V. and Maryniva, V.K.

The quantity of atmospheric precipitation entering the lake is calculated using data from the Puschino hydrometeorlogical station. Precipitation during 1998 was 840mm and during 1999, 973mm. The area of Lake Karymskoe area is 9,8km^2, so on the average during 1998 Q_3 = 260 l/s and during 1999 Q_3 = 300 l/sec were supplied from atmospheric precipitation. According to the data from the same hydrometeorlogical station in 1998 about 400mm/year was lost by evaporation, so from the lake area Q_5 = 124 l/s.

Substituting the data from Table III into the above equation and along with calculated values of atmospheric precipitation and evaporation, we find a deficiency for 1998 of about 850 l/s. Thus, apparently, hydrothermal discharge comparable with the above figure takes place on the bottom of Lake Karymskoe.

Table III. The results of hydrological regime measurements in the area of Lake Karymskoe in 1997-1999 (l/s)

№	Discharge centers	1997	1998	1999
1	Hot creeks from geysers and the Akademii Nauk pulsating springs in the south of Lake Karymskoe	27	30	33
2	Hot springs in the lake shore zone in the area of the Akademii Nauk springs	20	15	10
3	Hot springs on the south-eastern shore of Lake Karymskoe	10	8	5
4	Hot springs on the south-western shore of Lake Karymskoe	10	7	5
5	Seepage of hot water in the shore zone of Lake Karymskoe northern sector	105	90	Not measured
6	Seepage of hot water in the mouth of the Medvezhy creek	3	2	Not measured
	Total hot water	175	152	-
7	The Goryachaya Rechka creek (subsurface drainage of Lake Karymskoe)	68	50	60
8	The Karymskaya river (upper fold)	1900	1400	1530
9	Summary discharge of all cool creeks inflowing into Lake Karymskoe	1000	600	500

3.3. Geochemical characteristics of waters of the Akademii Nauk caldera hydrothermal system

Before the eruption in 1996, only manifestations of boiling sub-alkaline hydrothermal waters (geysers and springs) of sodium chloride composition were known in the Akademii Nauk caldera most of which is occupied by Lake Karymskoe. These manifestations were located in the southern sector of the lake, near the waters edge. After the phreatic-magmatic eruption in 1996, numerous discharges of sub-neutral springs of complex Cl-SO_4-Ca-Na composition at temperatures of 60–90ºC appeared in northern sector of the lake related to the sub aqueous explosive cone with the diameter of 600m [29]. In addition Lake Karymskoe itself, once fresh water became acid with a complex, mainly SO_4-Ca-Na composition. Combinations of thermal manifestations of various compositions are quite common for hydrothermal systems connected with active andesite and dacitic volcanoes [18, 25–28]. It is

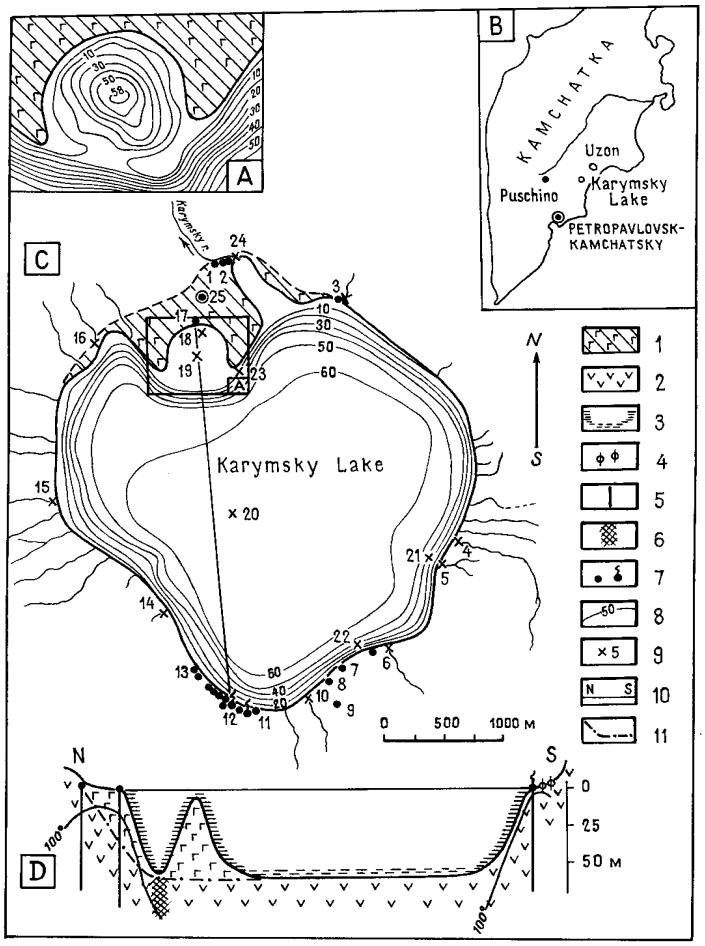

Figure 10. Lake Karymskoe map
Legend: 1 – Basalts of the eruption in 1996; 2 – andesites; 3 – Non-consolidated friable recent bottom deposits; 4 – Geyserite structures; 5 – Fractures; 6 – The zone of fracturing (the canal of supply of magmatic product and gases of the eruption in 1996); 7 – Thermal springs and geysers; 8 – Isobaths; 9 – Water sampling points; 10 – The section "north-south"; 11 – Lake Karymskoe bottom before the eruption in 1996. A – the lake fragment and subaqueous crater of the eruption in 1996; B – Total view of Kamchatka peninsula and location of objects under study; C – Total plan of Lake Karymskoe; D - section "north-south" through Lake Karymskoe.

It is considered that these waters are connected genetically, the primary factors being abyssal ultra-acid waters becoming neutralized during infiltration through rocks. But these ultra-acid waters are not everywhere confirmed by drilling, though their manifestations are present on the surface. In such cases, it is supposed that separate hydrothermal systems co-exist in the volcanic structure [26]. There are grounds for thinking that this is the case in the Akademii Nauk caldera.

As it can be seen from the schematic geological section of the Karymsky volcanic center (Figure 7), the Akademii Nauk volcano is composed by a series of rocks of Upper Pleistocene-Holocene age of dacitic composition underlain by andesite-basalts, and basalts and their tuffs of a more ancient volcanic structure. Based on geophysical studies there is intensive extension of the earth's crust (up to 0,5–1,2 cm/year) in Lake Karymskoe area and northward from it. Calculations [8] showed that a shallow magmatic chamber with a diameter on the order of 4 km (comparable with Lake Karymskoe diameter) can occur in this area. An apical part of the magmatic chamber represented by a peculiar dike may approach the earth surface along a zone of fracturing.

According to the above, sub-alkaline springs tend to occur on the southern shore Lake Karymskoe and sub-neutral springs, on the northern one. Lake Karymskoe became acid after the 1996 sub aqueous eruption located between them. It is observed that sub-alkaline thermal waters are practically free of magnesium, whereas magnesium is found in considerable amounts in sub-neutral springs as well as in acid lake water. The conclusion is that both sub-neutral springs and Lake Karymskoe acid waters have the same origin and source of supply. Thus the Akademii Nauk thermal springs relate to the other separate hydrothermal system.

What data support this supposition? Firstly, in the triangular diagrams SO_4^{2-}-Cl^--HCO_3^- and (Na + K)-Ca-Mg (Figure 11) these water types occupy separate fields. Secondly, as shown in Figure 12A, direct correlation of Cl and B is observed for practically all newly-formed springs and Lake Karymskoe water, i.e. their formation is connected with mixing solutions. In this figure, the Akademii Nauk geyser field waters are located well away from this mixing trend. Less distinctly, the same picture is reflected in correlation of Cl and SO_4 (Figure 12B). Apparently, surface effects of oxidation of sulphur-containing compounds and mixing with cool waters contribute considerably to the formation of hydrothermal waters.

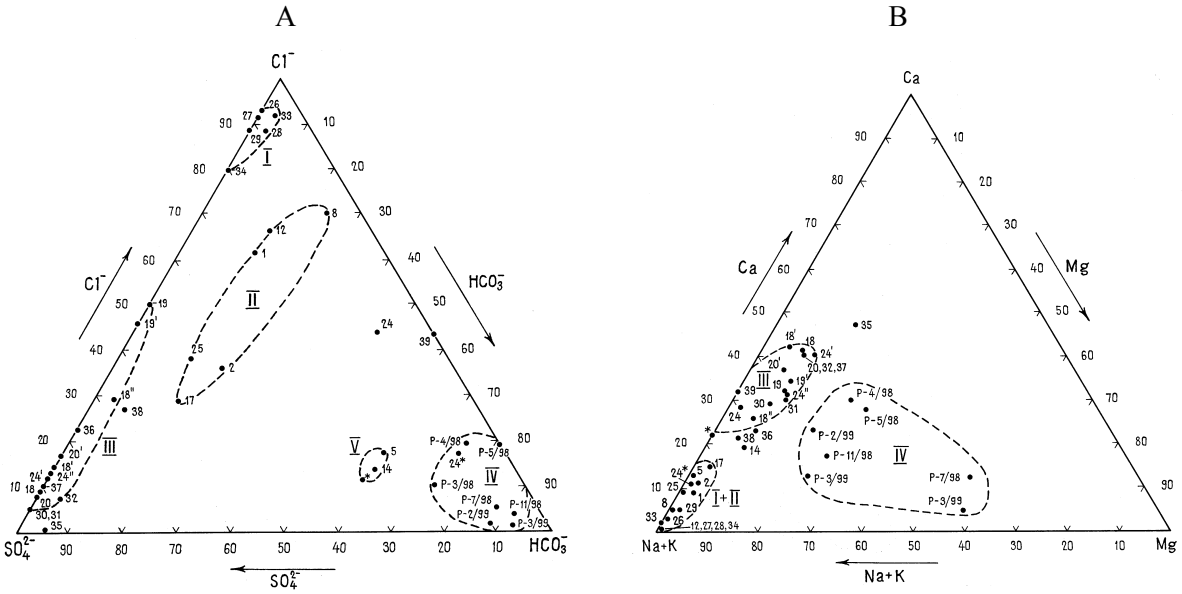

Figure 11. Triangular diagrams of SO_4^{2-} - Cl -HCO_3 (A) and (Na^+K) – Ca – Mg (B) of composition of thermal springs and water manifestations of the calderas of Akademii Nauk and Uzon.

I-V – variation fields: I – of chemical composition of thermal sources' waters (including drilling holes) and water of the Fumarolnoe and Chloridnoe Lake in the Uzon caldera.II – of chemical composition of thermal sources in the Akademii Nauk caldera.III – of water composition in the Karymskoe Lake, river Karymskaya and Bannoe Lake (in the Uzon caldera). IV – of precipitation composition (on data of hydrometeostation Puschino). V - of composition of cold freshwater springs and snow water in the region of the Karymskoe Lake.

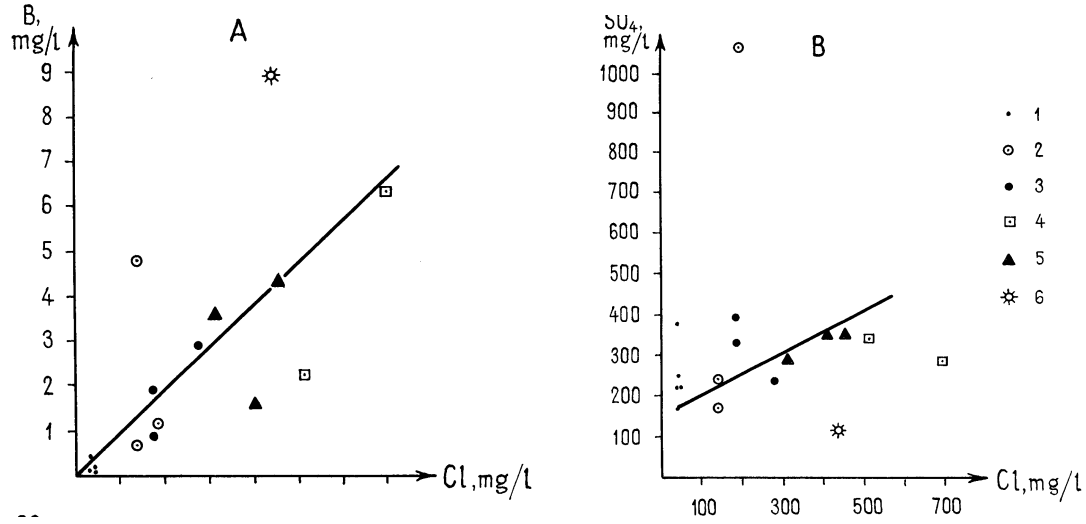

Figure 12. Correlation of Cl with B (A) and SO_4 with Cl (B) concentrations in thermal springs and other water manifestations of the Akademii Nauk caldera.

Legend: 1 – water of Lake Karymskoe; 2 – water of the lake in the maar; 3 – thermal springs on the northern shore of Lake Karymskoe; 4 – spring № 1 in the effluent of the Karymskaya river; 5 – Goryachaya Rechka creek; 6 – geysers in the group of the Akademii Nauk springs.

3.4. Solution-rock interaction effects and hydrothermal equilibrium

In order to evaluate the degree of equilibrium between a solution and enclosing rocks, W.F. Giggenbach introduced the diagram Na-K-Mg that indicates the so-called hydrological maturity of thermal waters [11]. In this diagram, fields of "mature waters" being in chemical equilibrium with rock components are located near the line of complete equilibrium.

For this purpose, we used the triangular diagram Na-Si-Mg (Figure 13) because these components were characteristic of the Karymsky area hydrothermal waters and basic temperatures were calculated using Na-K and Si geothermometers.

In Figure 13 showing data for the Karymsky and Uzon geothermal areas, points for sub-alkaline Cl-Na waters of geysers and the Akademii Nauk springs occupy a quite separate field in the upper corner of the diagram left of the 200°C isotherm. Points for Lake Karymskoe acid waters and sub-neutral hot springs of SO_4^2-Cl-Ca-Na composition trend towards the magnesium corner of the diagram with temperatures lower than 170°C. It is obvious that these waters are still far from equilibrium with rock minerals and are "immature". The Uzon caldera thermal waters occupy an intermediate position in the diagram.

3.5. Isotope compositions of waters

Isotope characteristics of all water types studied in the two geothermal areas are shown in the diagram $\delta^{18}O$- δD (Figure 14). In this figure, the Akademii Nauk caldera waters as well as the Uzon caldera waters of hot springs and thermal lakes gravitate towards Craig's meteoric water line, i.e. atmospheric precipitation, have been active in their formation. Considerable deviation is observed only for the Uzon caldera mud pots undergoing strong evaporation.

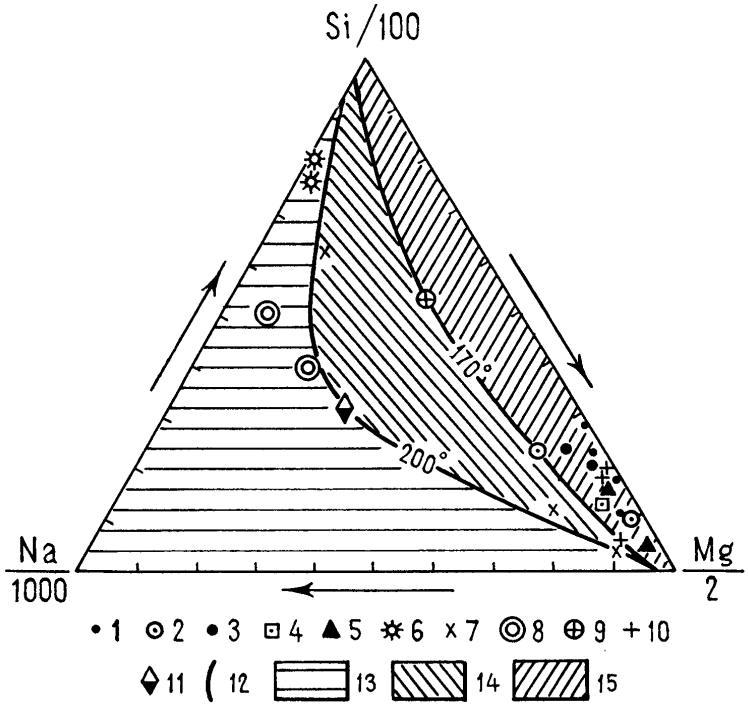

Figure 13. Triangular diagram of the relative concentration of Na, Si and Mg and fields showing the degree of "hydrological maturity" (according to Giggenbach, 1988) for thermal waters of the calderas Uzon and Akademii Nauk (Lake Karymskoe area) in Kamchatka.

***Legend**: 1 – water of Lake Karymskoe; 2 – water of the small lake in the maar (the funnel of the explosion in 1996, dia = 20 m); 3 – springs on the northern shore of Lake Karymskoe (subaqueous crater of 1996); 4 – spring № 1 in the outflow of the Karymskaya river; 5 – Goryachaya Rechka creek in the Karymskaya river outflow; 6 – geysers in the group of the Akademii Nauk springs; 7 – water of the Fumarolnoe Lake in the Uzon caldera; 8 – water from wells in the Uzon caldera; 9 - water of the Chloridnoe Lake in the Uzon caldera; 10 – water of mud pots in the Uzon caldera; 11 – water of the Tsentralny spring in the Uzon caldera; 12 – isothermal lines (according to the calculated Na-K and Si- geothermometers); 13 – field of equal weight relations in the system "water-rock"; 14 – field of relatively balanced "water-rock" relations; 15 – field of unbalanced relations "water-rock" (immature waters).*

Existence of endogenic component in the composition of thermal solutions can be judged by the degree of correlation of O^{18} and D with Cl contents in them as chlorine is one of the basic components in volcanic gases. As it can be seen in Figure 15, a, points of water composition of geysers and Akademii Nauk springs as well as solutions of the Goryachaya river from Lake Karymskoe area and Lake Fumarolnoe water in Uzon caldera gravitate towards the trend of direct correlation δ^{18}O-Cl pointed at the primary – magnetic water. The analogous relation is manifested in the diagram δD-Cl (Figure 15, b). In both diagrams, Lake Karymskoe water composition points turn to be far aside from this trend but they also group together with springs having similar ion-saline composition in Lake Karymskoe shore area.

Summarizing all the above, it can be concluded that in fact two greatly different types of thermal waters: Cl-Na and Cl-SO_4-Na-Ca occur in the Akademii Nauk caldera.

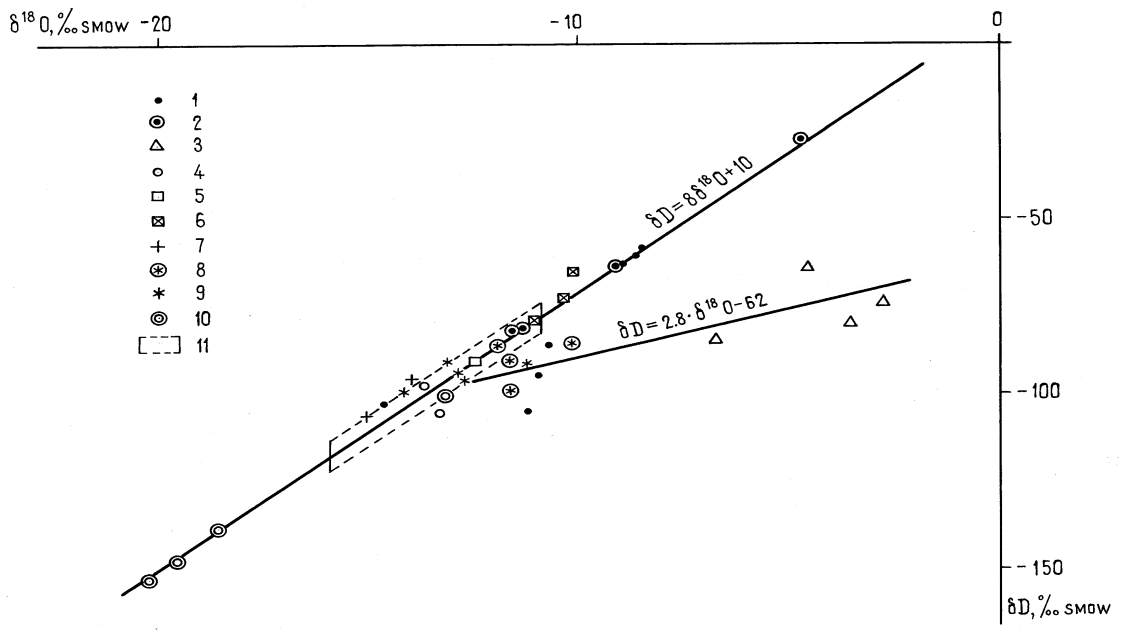

Figure 14. Isotope compositions of thermal and cold waters of the Uzon caldera and Karymsky geothermal region.

Legend: *1 – Thermal sources and waters of the Fumarolnoe Lake in the Uzon caldera; 2 – Thermal sources in the Akademii Nauk caldera (Lake Karymskoe area); 3- Waters of mud cauldrons in the Uzon caldera; 4 – Waters of the thermal Bannoe Lake in the Uzon caldera; 5 – Fresh cold waters in the Akademii Nauk caldera springs flowing in Lake Karymskoe; 6 – Snow water from Lake Karymskoe area; 7 – Fresh cold waters of the Uzon caldera; 8 – Waters of the Karymskaya river; 9 – Waters of Lake Karymskoe; 10 – Precipitation of the Puschino hydrometeorlogical station; 11 – Field of variations of isotope compositions of Kamchatka precipitation from reference data.*

The first water type is characteristic of long-established springs and geysers of Akademii Nauk. They definitely bear some endogenic component and have developed their "profile" of equilibrium with surrounding rocks.

The second water type appeared on the surface recently and apparently has a heterogeneous origin. Their high magnesium content is evidence of obvious connection with high-magnesia basalts of the sub aqueous eruption in 1996 and unsettled saline composition is evidence of their immaturity. They are yet far from being in equilibrium with surrounding rocks.

3.6. Geological-geochemical model of the Akademii Nauk caldera hydrothermal system

Thus according to the geochemical data, after the sub aqueous eruption in 1996, two independent hydrothermal waters (near-alkaline Cl-Na waters of the Akademii Nauk and acidic waters of complex $Cl\text{-}SO_4$-Ca-Na composition in Lake Karymskoe northern sector) co-exist simultaneously in the Akademii Nauk caldera. The latter are genetically similar to Lake Karymskoe acid waters. What explanation can be found for such condition from a geological viewpoint? We have included all presently available geological and geochemical information about the area under study and our genetic constructions in Figure 16. It is distinctly seen that the source of discharge of boiling Cl-Na thermal waters obviously originating from the deep magmatic chamber thermal-mass-flow is confined to the Akademii Nauk volcano slope. Apparently, it can be logically supposed that the Akademii Nauk water-dominated hydrothermal system is localized in the strata of basaltic tuffs and subjacent

volcanogenic-sedimentary rocks underlying dacites of the volcano structure (Figure 7). Evidently, propylitized rocks serve as the host of this hydrothermal system because occasional fragments of these rocks were found in products of phreatic-magmatic eruption in 1996. The fact that there are few such fragments, is the evidence of propylite pinching out northward from the caldera. Judging from the location of the funnel of the explosion occurred in 1996, the peripheral magmatic chamber (or its apical part), which initiated the eruption in 1996, is located under the northern sector of Lake Karymskoe. This chamber is the source of fluids dominated by the gases: H_2O, HCl, HF, SO_2, H_2S, CH_4 and CO. Magmatic gases are partially neutralised as a result of solution-rock reaction taking place while passing through the zone of fracturing caused by magmatic-tectonic action. Later when deep fluids are mixed with infiltrating cool waters of surface origin, reduced gases are oxidized, dissolve and form hydrothermal solutions.

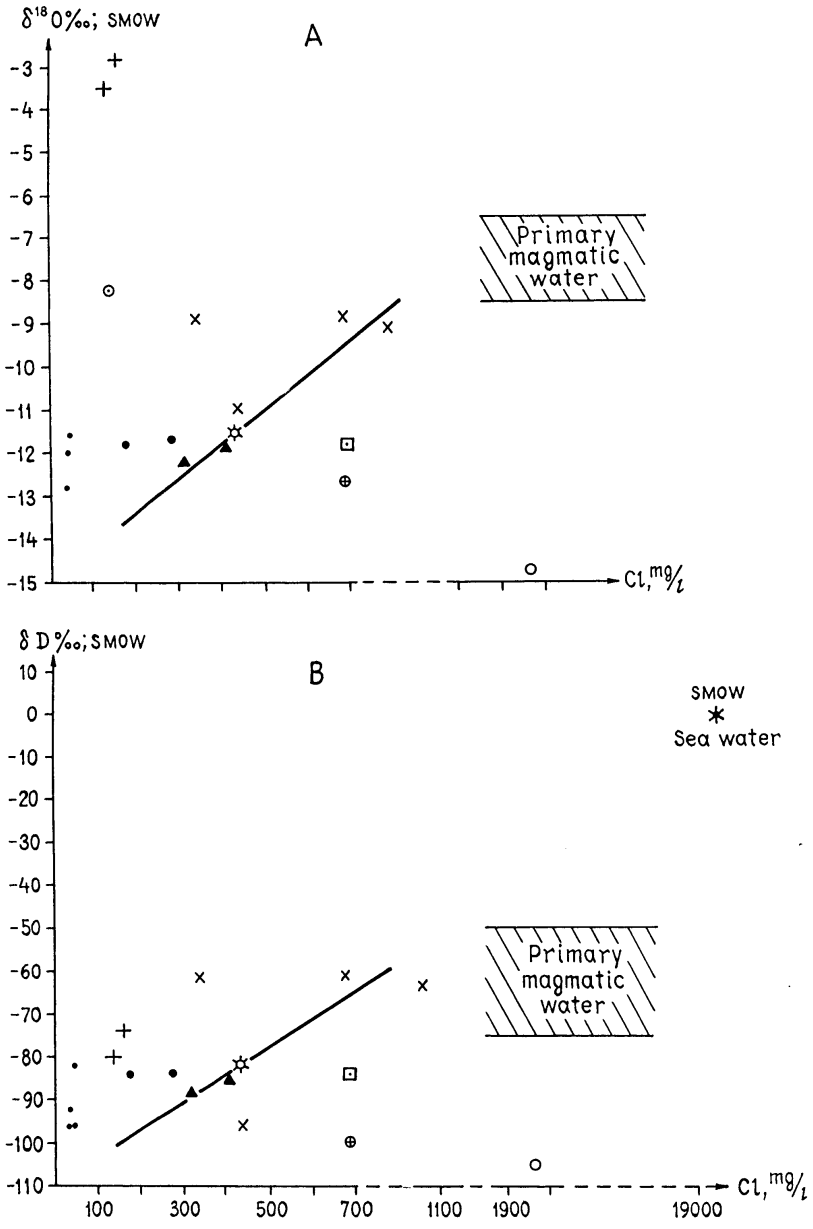

Figure 15 - Correlation diagram of δ O – Cl and δ D – Cl in thermal water of the Uzon caldera and Lake Karymskoe area in Kamchatka. The legend is the same as in Figure 12.

Thus, both gas and solute compositions of newly formed hot springs in the northern sector of the Akademii Nauk caldera and Lake Karymskoe water mineralization are affected by the flow of magmatic fluids from a recent peripheral chamber. It can be supposed that the pH differences of thermal spring waters and cool waters of the Karymsky Lake are caused by discharge of less neutralised acid fluids carrying sulphur (from our calculations - more than 70 t/day) as sulphate on the bottom of Lake Karymskoe and by the fact that surface discharges are in their way "processed" by flow through zones of argillization and silicification.

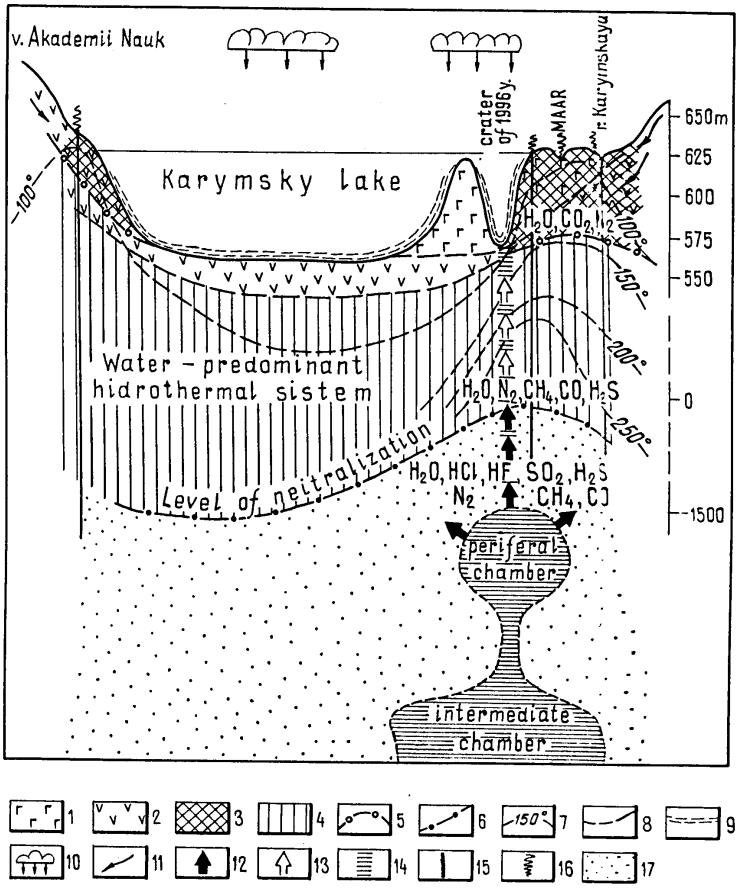

Figure 16. A schematic geologic-geochemical model of the hydrothermal system in the Akademii Nauk caldera (Kamchatka)
***Legend**: 1 – basalts of the 1996 eruption; 2 – andesites; 3 – the area of oxidation of gases, argillization and silicification of rocks; 4 – the area of propylitization; 5 – limits of mixing of surface and deep waters; 6 – the level of neutralisation of acid magmatic fluids; 7 – isothermal lines; 8 – limits of separation of lithologically different rocks; 9 – non-consolidated bottom deposits; 10 – atmospheric precipitation (and volcanic ash); 11 – paths of migration of infiltration waters; 12 – flows of magmatic fluids; 13 – flow of neutralized (hydrothermal) fluids; 14 – the zone of relatively permeable rocks; 15 – tectonic fractures; 16 – thermal springs; 17 – rocks enclosing magmatic chambers.*

These conclusions are totally logical, however, it is quite possible that there is another mechanism of forming sub-neutral and moderate-acid solutions if we accept that the former are steam condensates of high-temperature (more than 300°C) ultra-acid magmatic fluids and the latter are the result of mixing ultra-acid solutions and infiltrating surface waters. Then it follows that the level of steam separation (boiling zone) is located not very deep because, on the one hand, such depth is enough for enrichment

of solutions with main components – Na, K, Ca and Mg (owing to reaction with rocks during their movement) and, on the other hand, this path is not very long (based on the low total mineralization of these solutions shown in Table II). The great quantities of boron and chlorine indicate an endogenic component. Sulfate is provided by oxidation reactions of sulphur-containing compounds.

4. Conclusions

The preceding data and arguments show that saline compositions of thermal springs and acid lakes in caldera hydrothermal systems genetically connected with "andesite" volcanism form in different ways. Two main types of hydrothermal water types co-exist in calderas of the "Karymsky" type having magmatic chambers with continuing intense intrusive-explosive activity. Some hydrothermal waters, the so-called "geyser" type of Cl-Na composition, are connected with abyssal fractures and delimit the area of generation of thermal-mass-flow from abyssal zones of volcanic-tectonic structures. These flows are manifest in zones of joint linear and circular fractures within ancient magmatic structures.

In this case, acid solutions and acid lakes appear in zones of resurgent magmatic activity and are connected directly with a flow of acid fluids from apical zones of a peripheral magmatic chamber. In thermal waters of Cl-Na content, the saline compositions are formed from abyssal fluids that contain high NaCl at temperatures of 800–900˚C and pressures 1-8 kbar and react with deep country rocks – neutralizing their predominantly acid compositions. Finally, these rocks undergo propylitization. Infiltrating surface waters contribute greatly to waters feeding "geyser" type thermal waters.

The main source of mineral components in acid waters has recently erupted fresh magmatic rocks that are mainly of basic composition (basalts). An acidic contribution to these solutions is supplied by oxidation of sulphur-containing compounds and by halide (HCl, HF) gases in fluids separated from shallow magmatic chambers. In addition, a large part of water acidification results from extraction of acid components from fresh ashes entering lacustrine basins. The water component of such sources and basins is mainly meteoric.

REFERENCES

[1] BREZGUNOV, V.S., ESIKOV, A.D., FERRONSKY, V.I. and Salkova L.V. (1998). Spatial-Timely Variations of Oxygen Isotope Composition of Atmospheric Precipitation and River Waters on the Territory of the Northern Part of Eurasia and their Connection with Temperature Alteration: Water Recourses. Vol. 25, № 1. Pp. 99–104

[2] CREIG, H. The Isotopic Geochemistry of Water and Carbon in Geothermal Areas: Nuclear Geology of Geothermal Areas: Pisa. CNR. 1963. pp. 17–53.

[3] EROSCHEV-SHAK V.A., KARPOV G.A., SCHERBAKOV A.V. and ILYIN V.A. Formation of Precipitation in the Hydrothermal Lakes of Kamchatka: DAN USSR. 1985. T.280. №1, pp.165–169. In Russian

[4] EROSCHEV-SHAK, V.A., KARPOV, G.A., LAVRYSHIK , V.YU. and ILJIN, V.A. 1996. Formation Conditions and Composition of Bottom Sediments of Recent Caldera Thermal Lakes in Kamchatka: Lithology and Useful Minerals. № 2. Pp. 196–207.

[5] ESIKOV, A.D. 1989. Isotope Hydrology of Geothermal Systems. M.Nauka. pp.208.

[6] ESIKOV A.D., KARPOV, G.A. and CHESHKO, A.D.1990. Isotope-Hydrochemical Study of Recent Hydrothermal Activity in the Uzon Caldera (Kamchatka). I. Differentiation of Water Manifestations in Hydrothermal System of Uzon Caldera and Evaluation of its Thermal Parameters: Volcanology and Seismology. Vol. 11. №2, pp.161–179 (Gordon and Breach Science Publishers).

[7] ESIKOV A.D., KARPOV G.A.and CHESHKO A.D. 1991. Isotope Hydrochemical Study of Recent Hydrothermal Activity in Uzon Caldera (Kamchatka). II. Hydroisotope Model of Uzon

Caldera Hydrothermal System: Volcanology and Seismology.Vol.11.№ 4, pp.499–522 (Gordon and Breach Science Publishers).

[8] FEDOTOV, S.A. 1997. On Eruptions in the Akademii Nauk Caldera and Karymsky Volcano in Kamchatka in 1996, Their Study and Mechanism. Volcanology and Sesmology. № 5. pp. 3-37.

[9] GAVRILENKO, G.M., DVIGALO, V.N., FAZLULLIN, S.M. and IVANOV V.V. Modern condition of the volcano Maly Semyachik (Kamchatka): Volcanology and seismology. №2. Pp.3-7. In Russian.

[10] GIGGENBACH, W.F. 1974. The Chemistry of Crater Lake, MtRuapehu (New Zealand) During and After the 1971 Active Period. №7. J.Sci., 17. pp.33–45.

[11] GIGGENBACH, W.F. 1988. Geothermal Solute Equilibria: Derivation of Na-K-Mg-Ca Geoindicators: Geochim. Acta. V. 52. pp. 1749–1765.

[12] KARPOV, G.A. 1988. Recent Hydrothermae and Mercury-antimony-arsenic Mineralization. M. Nauka. 1988. pp. 183.

[13] KARPOV, G.A., FAZLULLIN, S.M. and NADEZHNAYA T.B.1966. Liquid Sulphur at theBottom of a thermal Lake in the Uzon Caldera, Kamchatka: Volcanology and Seismology. Vol.18. pp.171–186 (Gordon and Breach Science Publishers).

[14] KARPOV G.A., KAZMIN, L.A. and OSIPOV, V.P. 1998 A Physical-chemical Model for Nature Sulphur Melt Formation in the Hot Lake Bottom, 1998/Volcanology and Seismology. Vol.19. pp. 797–804 (Gordon and Breach Science Publishers).

[15] KARPOV, G.A., MURAVJEV, YA.D. et al.1996. Subaqueous Eruption from the Caldera of Akademii Nauk Volcano on January 2–3,1996: Current Researches on Volcanic Lakes. Newsletter of the IAVCEI Commission on Volcanic Lakes. N9. March. pp. 15–21.

[16] KARPOV, G.A. 1998; 1999. Isotope Geochemistry of Thermal Springs in the Uzon-Geyserny and Karymsky Geothermal Areas (Kamchatka): Informational reports on the Research Contract № 9828/R, 9828/R1.

[17] MARKHININ, E.K. 1960. Eruption of the Zavaritsky Volcano on the Seampushir Island in Autumn of 1957. Bulletin of Volcanological Station. Academy of Sciences of the USSR. № 29. In Russian.

[18] MARKHININ, E.K. AND STRATULA, D.S. 1977. Hydrothermae of the Kuril Islands. M. Nauka. pp. 212.

[19] MURAVIEV,YA.D., FEDOTOV, S.A. et al. Volcanic Activity in the Karymsky Centre in 1996: Summit Eruption at Karymsky and Phreatomagmatic Eruption in the Akademii Nauk Caldera: Volcanology and Seismology. Vol. 11. № 6. pp. 873–897 (Gordon and Breach Science Publishers S.A.)

[20] PILIPENKO, G.F. 1991. Hydrothermae of the Karymsky Volcanic Center in Kamchatka: Volcanology and Seismology. Vol. 11. № 6. pp. 873–897. (Gordon and Breach Science Publishers S.A.)

[21] SIDOROV, S.S. 1966. Hydrothermal Activity of the Golovnin Caldera (Kunashir island): Bulletin of Volcanological Stations. № 42. pp. 22–29.

[22] SKRIPKO, K.A., FILKOVA, E.M. and KHRAMOVA G.G. 1966. Condition of the Ebeko Volcano in Summer of 1966: Bulletin of Volcanological Stations. 1966. № 42. pp. 42–55. In Russian.

[23] Stetter, K.O. 1982 Ultrathin Mycelia-forming Organisms from Submarine Volcanic Areas Having an Optimum Growth Temperature of 105ºC: Ilbid. Vol. 300. pp. 258–260.

[24] TAKANO, B., OHSAWA, S. and GLOVER R.B. 1994. Surveillance of Ruapehn Crater Lake, New Zealand, by Aqueous Polythionates: Journal of Volc. and Geoth. Research 60. Pp.29-57.

[25] TARAN, YU.A., ESIKOV, A.D. and CHESHKO, A.L. 1986. Deuterium and Oxygen-18 in Waters of the Mutnovsky Geothermal Area (Kamchatka): Geochemistry, 1986. № 4. pp. 458-462.

[26] TARAN, YU.M., ZNAMENSKY, V.S. and YUROVA, L.M. 1995. A Geochemical Model of the Baranskogo Volcano Hydrothermal System (Iturup Island, the Kuril Islands): Volcanology and Seismology. № 4–5. pp. 19–115.

[27] TRUESDELL, A.H. and HULSTON, J.R. 1980. Isotope Evidence on Environments of Geothermal Systems: Handbook on Environmental Isotope Geochemistry. Vol. 1. pp. 179-226.
[28] UEDA, A., KUBOTA, Y. et al.1991. Geochemical Characteristics of the Sumikava Geothermal System, Northeast Japan. Geochem. J. Vol.25. pp. 223–244.
[29] VAKIN, E.A. and PILIPENKO, G.F. 1998. Hydrothermal Activity in Lake Karymskoe after the 1996 Underwater Eruption. Volcanology and Seismology. Vol. 19. № 5. pp. 737–767. (Gordon and Breach Science Publishers S.A.).
[30] VERGASOVA L.P., KARPOV G.A. et al. 1998. Post-eruptive Activity in the Akademii Nauk Caldera, Kamchatka: New Mineral Deposition, Radon Concentration in Gaseous Emissions, and Changes in the Biota: Volcanology and Seismology. Vol.19. № 5. pp.693–712 (Gordon and Breach Science Publishers).
[31] Volcanic Centre: Structure Dynamics Substance (Karymsky Structure). 1980. Moscow. Nauka. pp. 300 (in Russian).
[32] WHITE, D.E., HUTCHINSON, R.A. and KEITH, T.E.C. 1988. In: The Geology and Remarkable Thermal Activity of Norris Geyser Basin, Yellowstone National Park, Wyoming (Washington: U.S. Government Printing Office). pp. 42–44.

RESEARCH ON ISOTOPE TECHNIQUES FOR EXPLOITATION OF GEOTHERMAL RESERVOIRS IN WESTERN TURKEY

S. Simsek

International Research and Application Center for Karst Water Resources (UKAM), Hacettepe University, Beytepe, Ankara, Turkey

Abstract. The regional grabens of Western Anatolia of Turkey were formed by neotectonic activities since Miocene. East-west aligned Buyuk Menderes and Afyon Grabens were formed as a result of the doming uplift and mainly north-south tensional forces. The main high enthalpy geothermal fields of Western Anatolia investigated (and their reservoir temperatures) are Denizli-Kizildere (242ºC), Aydin-Germencik (232ºC). low enthalpy areas are found in Afyon (66–107ºC) and Soke (20–42ºC) regions. The Kizildere field is situated in the eastern part of the Buyuk Menderes Graben. The power plant with 20 MWe capacity was installed in 1984 by TEAS. Also, a factory started to produce CO_2 in 1986 with a capacity of 120.000 ton/year. Besides 20 exploration and production wells, a reinjection well (R1), at a depth of 2261 m. was drilled in 1998 by MTA. The highest reservoir temperature determined for this area is 242ºC. The chemical analyses show the water type to be $NaHCO_3$. Germencik geothermal field is located 100 km to the west of Kizildere. The temperatures of the first and second reservoirs are between 203–217ºC. The water types are NaCl in well waters but NaCl-$NaHCO_3$ for springs. The geothermal waters are of meteoric origin without significant magmatic inputs. Kizildere and Germencik waters are partially equilibrated and deep reservoir temperatures estimated using different geothermometers are between 240–260ºC. Geothermal fluids from deep reservoirs in Kizildere and Germencik fields are slightly acidic with pH values of 5.5–5.9 and 4.9–5.5, respectively. There are clear $\delta^{18}O$ shifts from Mediterranean Meteoric Water Line (MMWL) in Kizildere and Germencik fields that are more significant for higher temperature fields. In Soke region low temperature, small isotope shift, shallow circulation and mixing with shallow cold water and seawater are suggested. In Afyon region medium temperature (66–107ºC), slight isotope shift, deep and shallow circulation are postulated.

1. Introduction

Geothermal activity is thought to be a consequence of tensional forces that resulted from the rigid behavior of Western Anatolia during the Neogene which has caused the formation of extended coastal grabens. The geothermal areas that were identified and explored naturally lie along these grabens mainly the Buyuk Menderes, Gediz, Simav, Bakircay, Izmir and Edremit grabens. A total of 123 hot springs were identified and 36 geothermal areas were located [1, 2 and 3]. The reservoir and cap rock characteristics which affect the water circulation system and the source and mechanism of heating are still under investigation. Up to now a total of about 600 shallow and deep wells have been drilled in the fields (including about 200 shallow gradient wells in the high temperature fields of Kizildere, Seferihisar and Tuzla). As a result of the studies that have been done, a pilot electrical power plant (20 MWe) was installed in Denizli-Kizildere field in 1984 and then, important developments in applications of greenhouse and dwelling heating systems have been obtained in Turkey. Approximately 52 000 residences and greenhouses of 300 000m^2 are heated by geothermal energy (493 MWt). Balneolocigal utilization in 194 spa area reached up 327 MWt, and total installed capacity is 820 MWt. Since the geothermal sources are clean, cheap and renewable, there is an expectation for widespread applications all around the country in the near future.

The main purpose of geothermal area investigations in Turkey is the development of hydrogeological and geothermal models, determination of the energy capacity, utilization possibilities, and disposal areas for reservoirs wastewater (reinjection). However, operation-management and maintenance strategies for an optimum utilization require the knowledge of some important hydrochemical interactions and behavior of the reservoir. Considering this fact, this project is designed to determine the relations between chemical properties such as acidity, and origin of fluid and the reservoir parameters, such as recharge, production and reinjection at Western Anatolia mainly Buyuk Menderes Graben Geothermal Province which includes Kizildere, Tekkehamam, Germencik, Salavatli geothermal fields as well as the adjacent fields such as Pamukkale and Golemezli (Figure 1, 2). The

water of reservoir fluid in Kizildere, Tekkehamam and Germencik is acidic character. To establish the relations between recharge, production and reinjection, similar studies have been performed in several such fields as Larderallo, Italy and Palinpinon, Philippines geothermal fields in the world.

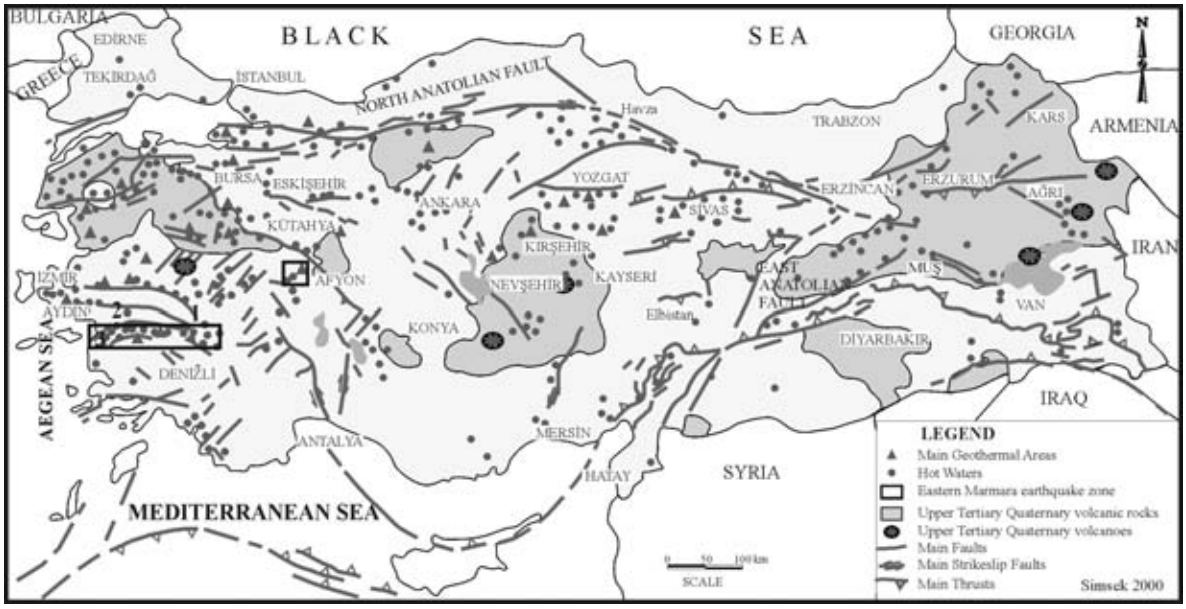

Figure 1. Main tectonic lines and hot spring distribution of Turkey. Study areas: 1- Afyon 2- Kizildere 3- Germencik 4- Soke.

Recharge mechanism, geochemistry and hydrodynamic structure of the system and effects on hydrothermal system have to be investigated and explained very carefully in order to use the geothermal field at optimum capacity [4, 5, 6, 7, 8, 9, 10 and 11]. Without doubt, this will be accomplished by isotope techniques on samples which will be taken from geothermal fluid, a very useful tool in the above mentioned investigations and studies [12]. For that reason, sampling points, sampling time and periods chosen accordingly and studies performed according to the study program.

This study realized under the project of "Research on Isotope Techniques for Exploitation of Geothermal Reservoirs in Western Anatolia" (HU-IAEA Research Contract 9829/RO) carried out in the body of the Coordinated Research Programme "The Use of Isotope Techniques in Problems Related To Geothermal Exploitation" was performed between 1997–1999 and gave a successful result for geothermal exploration.

The aims of the research project are as follows:

- Survey of the reservoir chemistry for exploration and exploitation of the fields for hydrogeologic model,
- Estimation of origin, temperature and acidity of reservoir fluids,
- Research on extention capacity of the field under exploitation.

Detailed hydrogeological and hydrogeochemical studies have been carried out and periodic geochemical analyses made in Hacettepe University UKAM Laboratories. A total of 50 analyses of the samples (^{2}H, ^{18}O, ^{3}H) which were periodically collected from thermal and cold water points in the study area have been made in IAEA [13].

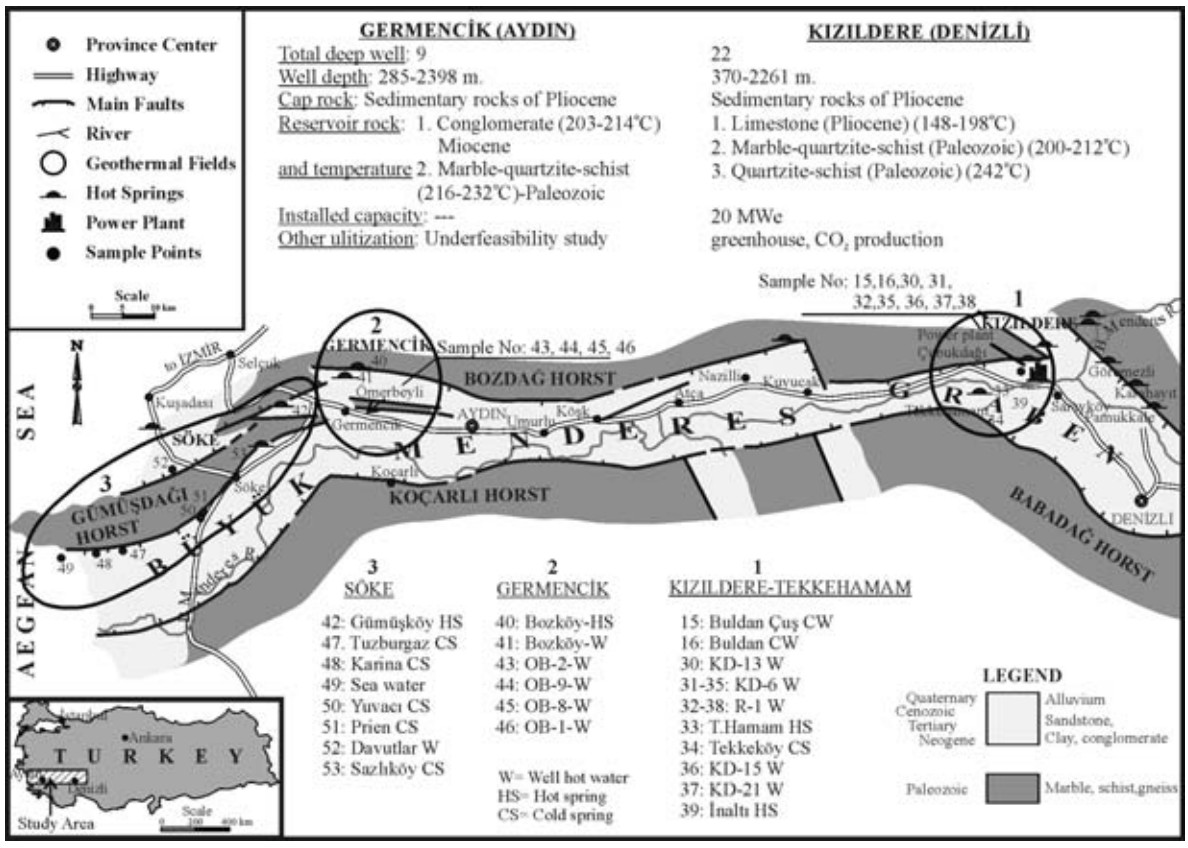

Figure 2. Main geothermal fields and sampling points of the study area.

2. General characteristics of the project area

The regional grabens of Western Anatolia of Turkey have formed due to neotectonic activity from Miocene until now. East-west aligned Buyuk Menderes, Kucuk Menderes, Gediz, Bakircay, Edremit, Afyon and Simav Grabens have been formed as a result of the doming uplift and mainly north-south tensional forces. The grabens are generally asymmetric while symmetric in some places. A typical step faulting system was determined at the graben flanks. The thickness of the Neogene and Quaternary deposits in the grabens reaches 2 500 m. Geological findings and interpretations have been supported by geophysical, geochemical survey, and drilling data in the grabens.

The basement rocks in the region are Paleozoic metamorphic rocks of the Menderes Massif. These rocks are composed of mainly gneisses, schists, marble, and quartzite units. The Neogene and Quaternary deposits overlie the basement with an angular unconformity [2].

The Buyuk Menderes Graben that includes the Aydin and Denizli provinces is located south of the Menderes Massif. The length of the graben is 200 km, the width is 5–40 km and it has continuity in the Aegean Sea.

In the region, crust thinning and magma approach has developed in places together with graben formations. Belts suitable for the geothermal systems have developed especially along dislocation or intersection zones of faults. The slip along the northern flank of the faults where the graben is effective is more than the southern flank (approximately a total of 3 000 m). Many hot springs and fumaroles are located along these lines. However, there is thermal activity also along the graben faults on the southern flank near Buharkent (Cubukdagi) where the graben is partially symmetric.

The geothermal areas in the region are located especially along the main graben fault where the basement units crossed to young sediments and syntetic and antitetic faults that occurred simultaneously with the main fault.

The hard and brittle lithologies have gained secondary permeability due to active graben tectonism in the region. The first geothermal reservoir in Denizli is limestone (Pliocene) and conglomerates (Miocene) in Aydin. On the other hand, the second reservoir, composed of marble-quartzite unit of the basement, can be used economically [14].

The geothermal fluid rising along the main faults of the grabens in the fields is collected in the permeable zones and moved to the middle parts of the grabens.

Some important geothermal fields have been discovered as a result geothermal exploration carried out by MTA along the Buyuk Menderes Graben. These fields and their reservoir temperatures are as follows: Denizli-Kizildere (242°C), Aydin-Germencik (232°C) and Afyon (107°C).

The pilot project areas are located in Western Anatolia. Aydin, Denizli and Afyon areas are located at Buyuk Menderes Massif representing one of the regional grabens which are situated in this region (Figure. 2).

The selection criteria of project area are:
- Location of thermal springs and reservoirs (determined by wells) with the highest temperatures in the region (20–242 °C).
- Presence of thermal springs and discharge water of the wells in temperature (low-high) at the same field.
- Presence of varying metamorphic and sedimentary reservoir and cap rock in the region.
- Presence of SO_4, Cl and HCO_3 waters in the same area.
- Presence of acidic reservoir fluids.
- Geothermal exploitation has been realized at Kizildere (Denizli) field. A pilot Power Plant (20 MWe) is generating electricity, CO_2 production (120 000 ton/year) is realized at the same field. Also district heating, greenhouse heating (in Afyon), industrial and balneological uses are important applications in the region.
- Initiation of reinjection drilling in exploitation fields.
- Presence of geothermal fields where investment plans for geothermal energy use is considered by government and/or private enterprises.

3. Results of the hydrogeologic – chemical and isotope survey of the project area

Buyuk Menderes Geothermal Province located in the Western Anatolia. Total 4 groups of fields are situated in the project area. These fields are Kizildere (Denizli), Germencik, Soke (Aydin) and Afyon fields (Figure 1, 2). Climate of the area is a typical Mediterranean climate. Winter and spring times are the mainly rainy season. Average precipitations are 431, 670 and 893 mm/year respectively in 1960-1990 period.

3.1. Afyon-Omer, Gecek Fields

Omer-Gecek field is located 15 km NW from the city of Afyon this field has important potential for geothermal energy. The oldest unit in the area is the Paleozoic metamorphic rocks (marble, calcschist, micaschist, etc). Neogene sediments as conglomerate, sandstone, marl, clay, tuff and agglomerate overlie the basement rocks. Travertine and alluvium are the youngest formations of the area [15]. The first reservoir rocks are basalts (Neogene) and second reservoir rocks are marbles, quartzite, calcshist, phyllites and micaschist of Paleozoic (Figure 3). The temperatures of the first and second reservoirs are found to be 48–54°C and 66–107°C respectively. The main cap rocks are clay, tuff, siltstone and marl of Neogene. The temperature of hot water springs are changing between 25–92ºC and discharges

are between 0.1-3 l/s in Omer-Gecek field. There are 20 hot water wells which were drilled by MTA. The temperature of these wells changes between 48–98ºC and discharges 0.4–100 l/s. The deepest well in the area is AF-1 which has depth of 905 m. [12]. The geothermal waters are used for heating 4000 residences of Afyon city.

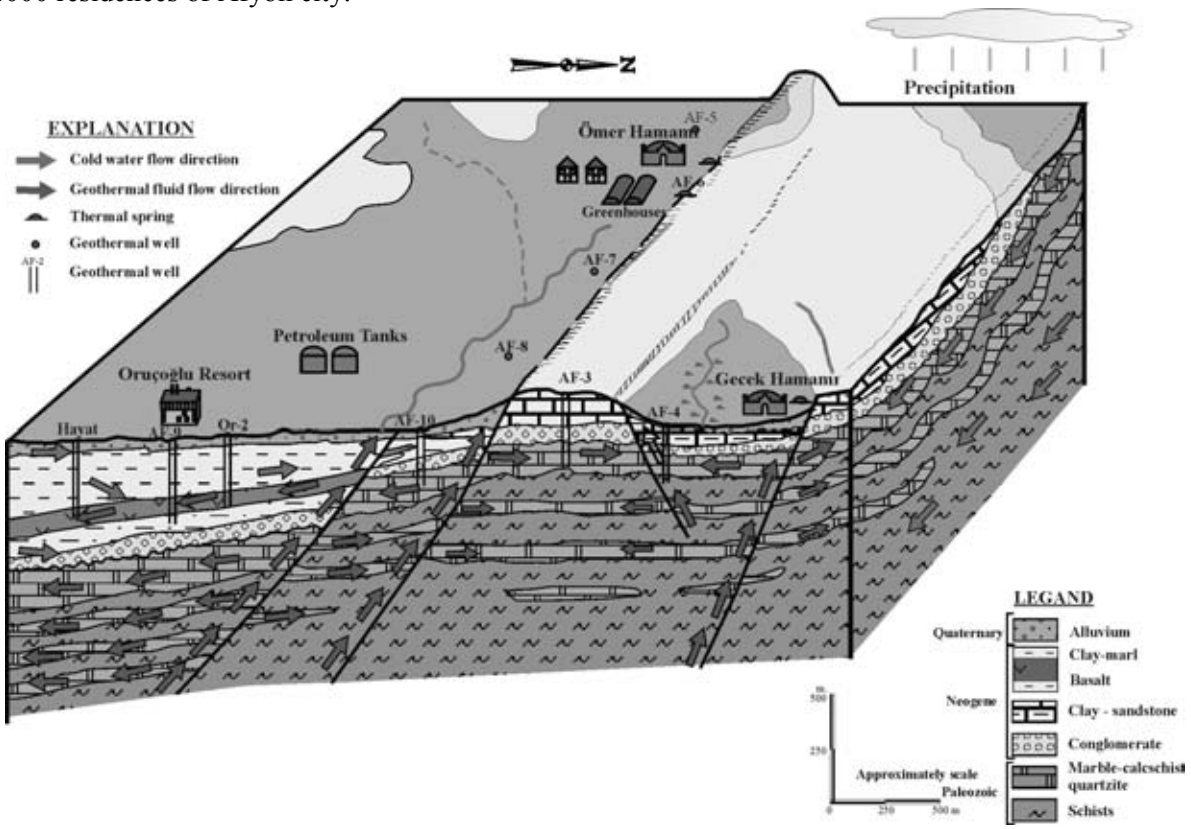

Figure 3. Schematic block diagram of Afyon-Ömer, Gecek geothermal fields.

The chemical and isotopic compositions of 4 water samples in 1998 which were taken from hot spring and wells (AF-7, AF-9 and cold water) have been analysed (Tables I and II). This chemical analyses result shows the chemical composition of Na+K>Ca>Mg and Cl>HCO_3+CO_3>SO_4 for geothermal well and hot spring waters (Figure 4). As illustrated in the Na-K-Mg diagram the well discharge waters are pointed as partially equilibrated fluids (Figure 5). A close relation was obtained between the data from geothermal wells (107^{o}C in AF-1) and the chemical geothermometers (102^{o}C–147^{o}C). The results of stable isotope are given in Table II. As a result of the water samples in the Afyon fields, the geothermal waters are originated from meteoric origin. Cold water partially scattered along local meteoric line. Evaporation and mixing effects on cold waters cause the slightly deviation from line. The water rock interaction and mixing of meteoric water cause the deviation from local meteoric line direction to the $\delta^{18}O$ shift (Figure 6). This suggests that, water rock interaction there is small process for geothermal fluid according to deep circulation and temperature effect. Hot waters and deep well samples almost no tritium was found so the ages of the thermal fluids in the field are older than 50 years (Figure 7).

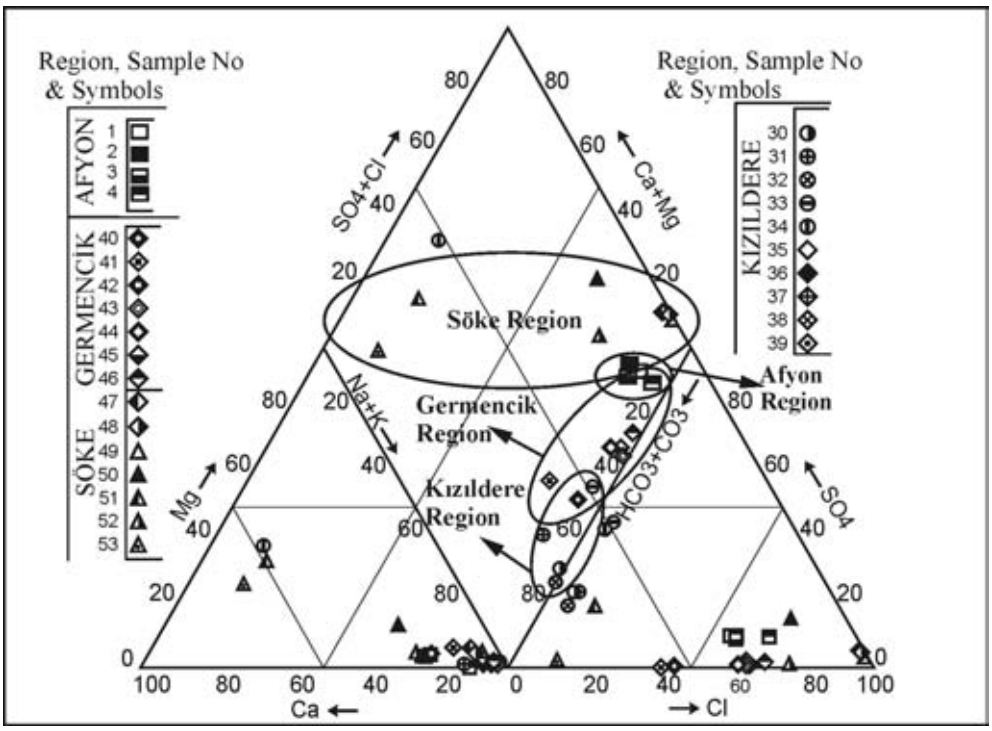

Figure 4. Triangular diagram of the thermal waters in the study areas.

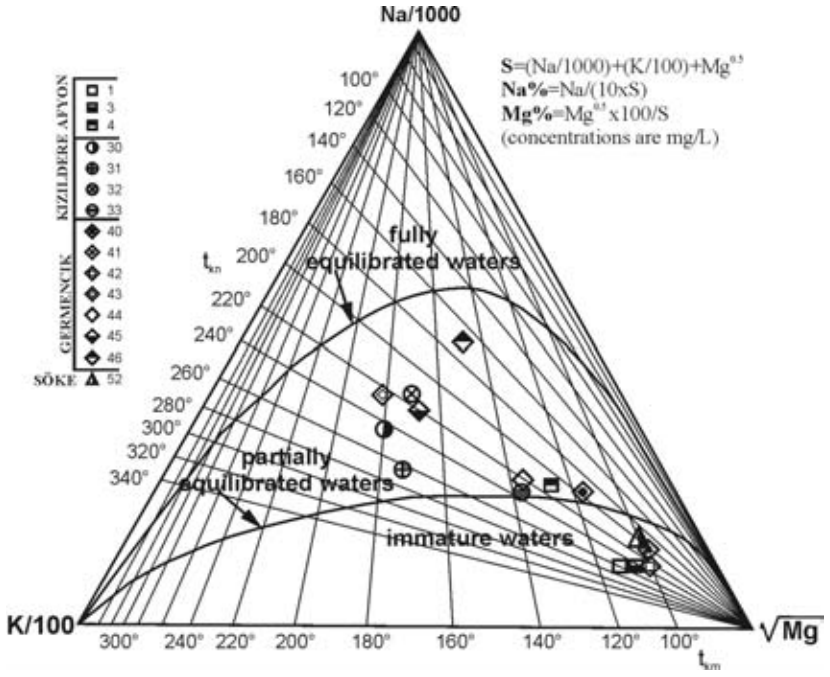

Figure 5. Na-K-Mg diagram showing Kizildere and Germencik fluids located partially equilibrated water zone. Soke waters (low enthalpy field) are immature waters.

Table I. The chemical results of cold and hot waters of Afyon, Kizildere, Germencik and Soke regions (July 1998)

Region	Sample No	Sampling Location	T (°C)	pH	EC (µS/cm)	Na (ppm)	K (ppm)	Ca (ppm)	Mg (ppm)	CO_3 (ppm)	HCO_3 (ppm)	Cl (ppm)	SO_4 (ppm)	B (ppm)
AFYON	1	Orucoglu HW (MTA)	50.00	5.92	6000	805.00	90.00	182.50	32.50	179.40	644.22	957.15	277.52	4.58
	2	Orucoglu CW	19.10	6.16	3600	640.00	70.00	165.00	27.50	140.19	513.07	779.90	233.54	4.39
	3	Orucoglu HW(Private)	50.00	5.92	6000	820.00	70.00	187.50	32.50	190.65	575.78	992.60	279.44	4.88
	4	AF7 HW	93.00	7.80	15500	1655.00	122.50	165.00	17.50	13.05	1166.87	1967.47	463.02	8.09
KIZILDERE	30	KD13 HW	79.50		11000	1125.00	132.50	20.00	1.00	19.56	2214.48	102.80	637.03	11.75
	31	KD6A HW	83.80		10000	955.00	132.50	122.50	1.50	32.61	2055.33	102.80	617.91	8.30
	32	R1 HW	76.70		12500	1595.00	127.50	25.00	1.50	45.66	3222.20	147.12	747.95	19.10
	33	Tekkehamam HS	67.80		9000	905.00	92.50	45.00	4.50	218.70	820.94	88.62	988.84	9.72
	34	Tekkekoy CS	28.90		1300	32.50	17.50	125.00	65.00	56.07	302.13	21.27	290.91	1.70
	MRBK	Menderes RW	14.10		900	51.70	11.00	91.00	46.00	72.90	199.53	63.81	141.15	1.40
	MRAK	Menderes RW	19.10		1200	72.40	35.00	135.00	70.00	56.07	239.42	67.35	415.21	1.59
GERMENCIK	40	Bozkoy HS	59.50		10000	1505.00	90.00	90.00	17.50	285.99	1818.59	1152.12	46.30	20.49
	41	Bozkoy-Confined HS	55.00		10000	1320.00	100.00	167.50	67.50	489.12	1611.13	1063.50	3.66	10.85
	42	Gumuskoy HW	38.70		5000	705.00	62.50	152.50	30.00	56.07	729.74	957.15	37.50	2.99
	43	OB2 HW	47.50		9000	1445.00	135.00	30.00	1.00	0.00	1419.53	1559.80	33.30	31.32
	44	OB9 HW	88.60		14200	1440.00	140.00	85.00	10.00	336.45	860.83	1542.07	43.62	27.83
	45	OB8 HW	48.50		8800	1410.00	122.50	62.50	1.50	0.00	1396.72	1488.90	96.02	29.00
	46	OB1 HW	30.00		6500	1440.00	60.00	50.00	1.00	0.00	1140.21	1595.25	125.85	31.06
SOKE	47	Tuzburgazi HS	20.60		39500	9230.00	360.00	640.00	437.50	39.24	267.97	15598.00	1577.87	3.83
	48	Karina HS	26.60		45000	11725.00	480.00	715.00	462.50	22.44	119.74	19852.00	1858.98	5.12
	49	Sea Water	27.50		46000	12110.00	485.00	505.00	477.50	56.07	62.71	20029.20	1786.32	5.89
	50	Yuvaci CS	19.50		2200	360.00	20.00	120.00	47.50	44.85	153.90	638.10	212.51	1.67
	51	Prien CS	21.40		750	29.00	15.00	93.00	40.00	50.46	267.97	42.54	92.19	1.62
	52	Davutlar HW	41.70		12000	1650.00	110.00	462.50	80.00	112.14	1185.78	2747.37	58.73	2.22
	53	Sazlikoy HS	26.80		1130	37.30	7.00	152.00	44.00	112.14	437.86	49.63	22.59	1.74

Abbreviations; HW (hot water well), HS (hot water spring), CS (cold water spring), RW (river water)

Table II. Environmental isotope (^{18}O, ^{2}H and ^{3}H) data of the cold-hot waters Afyon, Kızıldere, Germencik and Soke regions

Region	Sample No	*Sampling Location	Oxygen-18 $\delta^{18}O$ (‰)	Deutrium $\delta^{2}H$ (‰)	Tritium ^{3}H (TU)	Tritium Error (TU)
AFYON	1	Orucoglu HW (MTA)	-10.38	-76.70	0.20	0.34
	2	Orucoglu CW	-10.08	-73.20	0.14	0.34
	3	HW Orucoglu (Private)	-10.37	-76.30	0.06	0.34
	4	AF7 HW	-10.43	-77.50	0.01	0.33
	20	Gecek CS	-11.77	-79.70		
KIZILDERE	30	KD13 HW	-6.13	-56.20	0.39	0.34
	31	KD6A HW	-6.67	-57.00	0.16	0.33
	32	R1 HW	-4.10	-51.30	0.09	0.33
	33	Tekkehamam-DS HS	-6.18	-54.70	0.21	0.35
	34	Tekkekoy CS	-7.35	-46.70	1.15	0.35
	35	KD6 HW	-6.28	-55.25	0.05	0.34
	36	KD15 HW	-5.23	-55.50	0.10	0.34
	37	KD21HW	-5.45	-59.30	0.24	0.33
	38	R1 HW	-4.64	-52.90	0.26	0.33
	39	Inalti HS	-6.13	-53.50	0.52	0.33
GERMENCİK	40	Bozkoy HS	-2.78	-40.45	0.89	0.34
	41	Bozkoy-Confined HS	-3.18	-47.60	0.70	0.34
	42	Gumuskoy HW	-5.43	-32.40	5.44	0.41
	43	OB2 HW	-2.64	-41.20	0.23	0.33
	44	OB9 HW	-1.74	-37.90	0.64	0.33
	45	OB8 HW	-2.27	-41.90	0.50	0.33
	46	OB1 HW	-3.53	-40.20	0.69	0.33
SÖKE	47	Tuzburgazi CS	-0.02	2.70	1.02	0.35
	48	Karina CS	1.37	-73.10	0.20	0.33
	49	Whaf of Gendame SW	1.58	9.50	3.03	0.36
	50	Yuvaci SW	-5.71	-27.90	5.45	0.40
	51	Prien-Pinar CS	-6.02	-32.70	6.50	0.42
	52	Davut -Radon T. HW	-5.34	-29.10	0.84	0.33
	53	Sazlikoy CS	-5.97	-32.50	3.03	0.36

* Abbreviations: HW (hot water well), HS (Hot water spring), CS (Cold water spring)

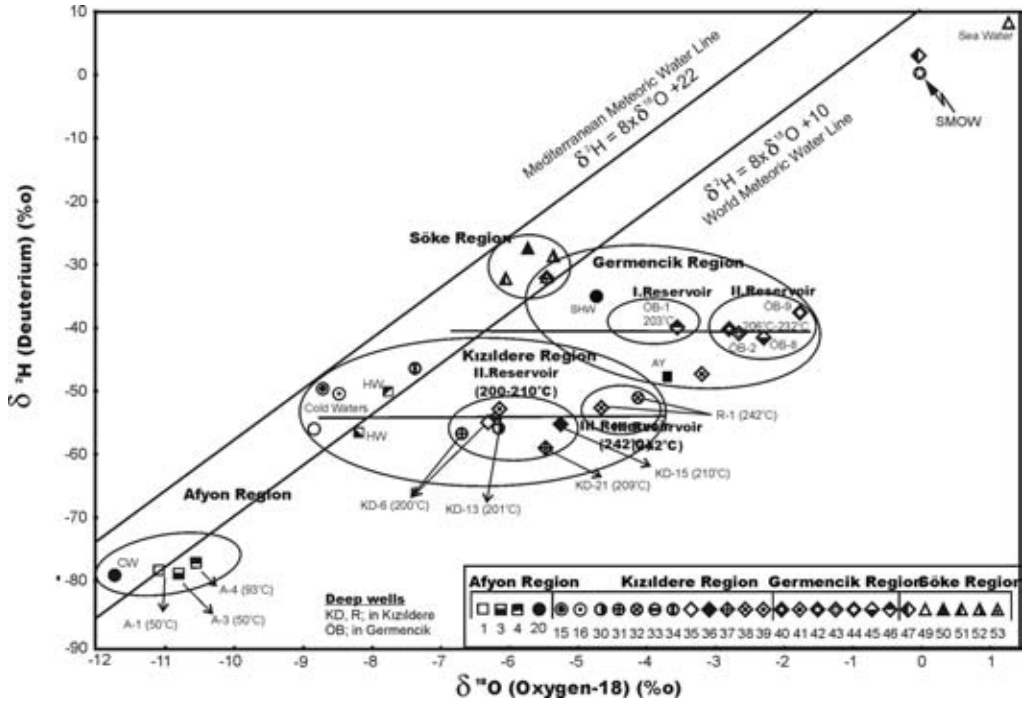

Figure 6. Stable isotope compositions of the geothermal reservoir fluids in the study areas.

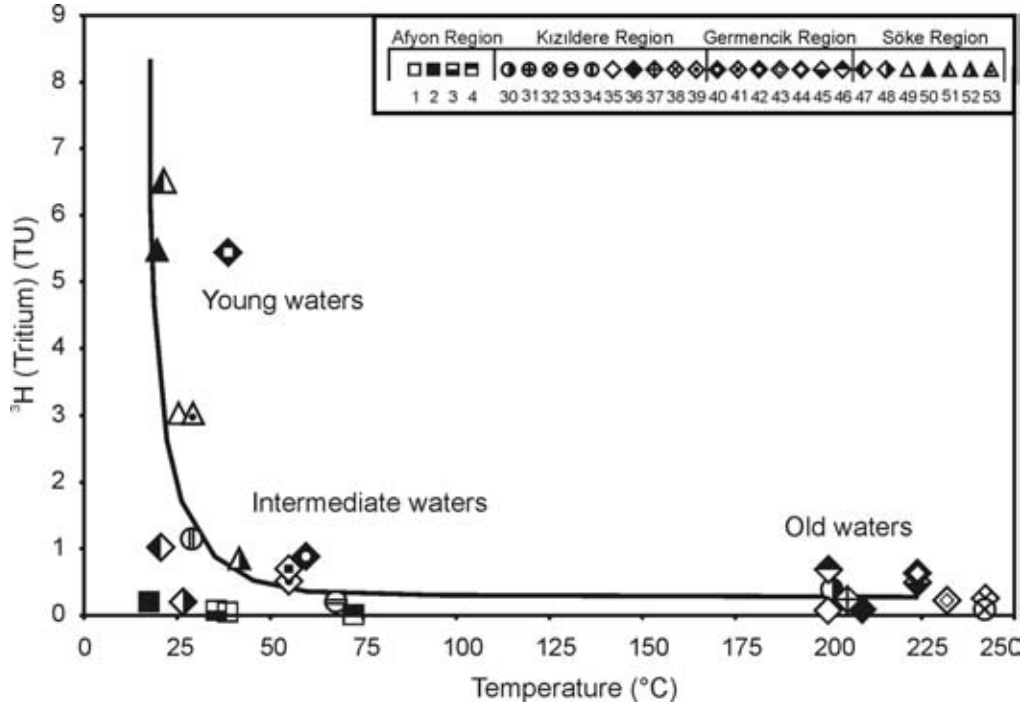

Figure 7. ^{3}H (tritium) and temperature diagram of thermal and cold waters in the study area.

3.2. Denizli-kizildere geothermal field

Kizildere Geothermal Fields is located 40 km west of Denizli city. This field was discovered by the cooperation project between MTA-UNDP in 1968. The Kizildere field is situated in the eastern part of the Buyuk Menderes Graben (Figure 2). After the geological, geophysical and geochemical studies, 20 deep wells with a depth changing from 370m to 1241m were drilled in the years between 1968–1973.

The field has 2 reservoirs; first reservoir (130–198°C) and the second reservoir (200–212°C) is in production. The power plant with 20 MWe capacity has been installed in the area by TEAS (Turkish Electricity Authority) in 1984. Also the factory started production of CO_2 in 1986 with a capacity of 120000 ton/year. In addition, there is application of greenhouse heating (6000 m^2).

Besides of 20 exploration and production wells, the reinjection explanatory well (R-1), which is the depth of 2261m. was drilled by MTA on behalf of TEAS in 1998 and the highest reservoir temperature (242°C) in the metamorphic basement (quartzite-schist) has been determined in this field, also in Turkey. This third reservoir was assumed to exist to exist in the area by hydrogeological and chemical indications [2 and 11].

The chemical and isotopic compositions of some 12 water samples which were taken from R-1 and other wells (KD-6, KD-13, KD-15, KD-21) from second reservoir and different temperatures in the field (200–210°C) have been analyzed (Figure 8). These chemical analyses show the water type is $NaHCO_3$ for well R-1 same as other wells in the field (Table I). (Figure 4). The geothermal water samples have the chemical composition of Na+K>Ca>Mg and HCO_3+ CO_3>SO_4>Cl and due to Na-K-Mg diagram are pointed partially equilibrated fluids (Figure 5). The main geochemical difference between second and third reservoir fluids is HCO_3^- and CO_2 contents. The noncondensible gas content of the R-1 (third reservoir) is about %3 by weight while in other wells approximately are %1-1.8. As a result of ^{13}C analyses, the origin of CO_2 gas derived mainly from decomposition of carbonate rocks [16]. Also contribution of magmatic CO_2 is important. Helium isotope compositions of the Western Anatolian fluids reveal mixing between mantle and crustal helium components [17]. It is calculated that geothermal fluid in deep reservoirs has low acidic character (pH: 5.5–5.9). A close relation between the data from geothermal wells (maximum 242° C) and the cation geothermometers (240-260° C) have been observed.

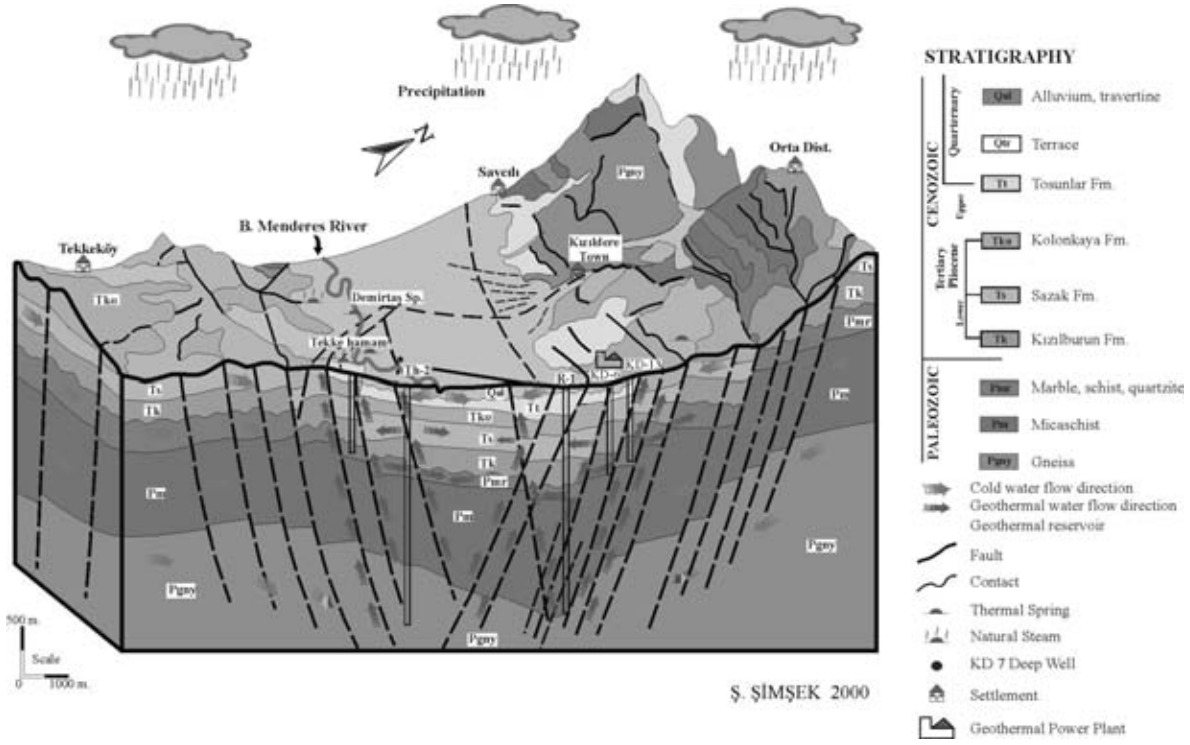

Figure 8. Block diagram of Denizli-Kizildere geothermal field.

The results of stable isotope results are given in Table II. As a result of the water samples in the Kizildere field, the geothermal waters are originated from meteoric origin. There is a clear $\delta^{18}O$ shift

from the MMWL and cold water values (Figure 6). This suggests that, water-rock interaction is an important process for geothermal fluid according to deep circulation and high temperature effect.

Hot spring waters and deep geothermal well sampled waters almost no Tritium so the age of the thermal fluids in the field are older than 50 years (Figure 7).

According to the results of ^{14}C contents, thermal waters have a relatively age of 10000 to 30 000 years [18].

3.3. Aydin-germencik geothermal field

This area is placed on 100 km west of Kizildere in Western Anatolia. The geological, geophysical and geochemical studies have been performed in Germencik, Omerbeyli field [19]. After these studies a total of 9 exploration wells with a depth of 285-2398 m have been drilled between 1982-1987. The temperatures of the first (Miocene conglomerate) and second reservoirs (Paleozoic marble and schist) are found to be 203-217 °C and 216-232 °C (Figure 9). The average flow rate is 300 ton/hour and steam ratio changes from 13% to 20%.

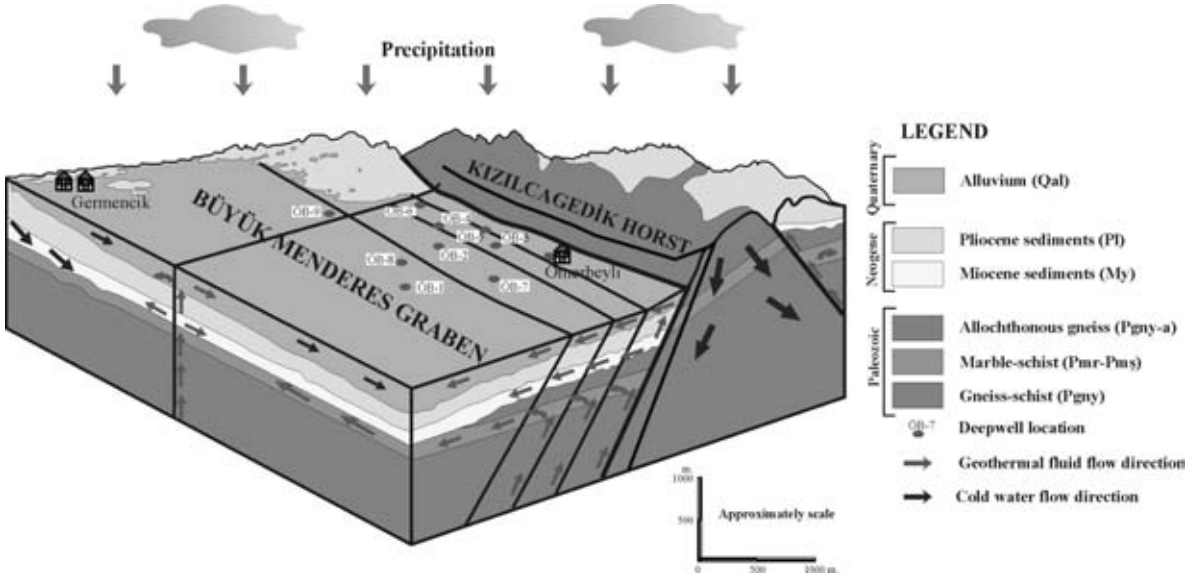

Figure 9. Block diagram of Germencik-Omerbeyli geothermal field.

The collected data indicate that, the field has an important geothermal potential. This potential can be used for generation of electricity, district and greenhouse heating, cooling, industry, touristic and balneological centers.

The chemical and isotopic compositions of some 7 water samples which were taken from hot springs and deep wells (OB-1, OB-2, OB-8, OB-9) have been analyzed (Tables I and II). This chemical analyses result shows the water type in NaCl for deep wells, shallow wells and hot springs in the field. The geothermal water samples have the chemical composition of Na+K>Ca>Mg and $Cl>HCO_3+CO_3>SO_4$ or $HCO_3+CO_3>Cl>SO_4$ for shallow well and hot spring waters (Figure 4).

As illustrated in the Na-K-Mg diagram most of the well discharge waters are pointed as partially equilibrated fluids (Figure 5). It is calculated that geothermal fluid in deep reservoirs has low acidic character (pH: 4.9–5.5).

A close relation was obtained between the measured temperatures from geothermal wells (202 – 232°C) and the chemical geothermometers (230–260°C).

The results of stable isotope results are given in Table II. The geothermal waters are originated from meteoric waters.

There is a clear $\delta^{18}O$ shift from the MMWL and cold-low temperature Soke region waters (Figure 6). This suggests that, water-rock interaction is an important process for most of chloride hot spring and deep geothermal well waters, at Germencik reservoirs.

3.4. Aydin-soke geothermal area

This area is situated between Germencik geothermal area and Aegean Sea. Hot water springs located northern flank on the main faults of the B. Menderes Graben and north side of the Gumusdag horst. The temperature range is 20.6–27.5ºC for springs and 41.7ºC for well (Davutlar well). The chemical and isotopic compositions of some 7 water samples have been collected and analyzed from 3 hot water springs, 2 cold water springs, 1 shallow well and 1 sea water.

Main lithologic formations are karstic marble and schists of Paleozoic age. According to hydrogeological studies water samples collected from karstic springs are Ca>Mg>Na+K and $HCO_3+CO_3>Cl>SO_4$ (Sazlikoy and Priene springs). There is mixing with karstic water and sea water from inland to Aegean Sea and the water composition change to Na+K>Mg>Ca and $Cl>SO_4>HCO_3+CO_3$ character.

Evaluation of Na-K-Mg diagram is shown in Figure 5. The position of all the data points indicates that the thermal systems of the Soke region are immature waters.

The stable isotope results are given in Table II. Isotopic values of cold waters are very close to MMWL equation $\delta^2H=8x\delta^{18}O+22$. Slight deviations from the line shows that, there is an effect of evaporation on cold waters and they originate from shallow circulation and low temperature system (Figure 6 and 7).

The isotopic composition of the thermal waters in the Soke areas shows that they are of meteoric origin. Seawater mixing with this water occurs in the west part of the Soke, particularly near coast. Seawater flow into the West Soke area is along the main E-W graben fault lines.

4. Results

Hydrogeological and hydrochemical survey have been completed in the project area. Periodical samples have been collected from thermal and cold water points for isotopic and chemical analyses.
The geothermal waters are of meteoric origin and have accumulated their heat during circulation in the fault systems. Only west Soke region shows mixing with seawater.

Evaluation of Na-K-Mg diagram indicates that the geothermal systems of the Kizildere, Germencik and Afyon fields are partially equilibrated fluids.

Deep reservoir temperatures estimated by different chemical geothermometers for two major fields, Kizildere and Germencik are 240–260°C and 230–260°C, respectively.

Geothermometer applications have been encouraged for deep reservoir explorations in Kizildere and Germencik geothermal fields. The results of new exploratory wells show that the geothermometer estimates are reliable for Kizildere (242°C) and Germencik (232°C) fields.

The geothermal fluids of deep reservoirs in Kizildere and Germencik fields are low acidic character as pH: 5.5–5.9 and pH: 4.9–5.5 respectively.

The absence of tritium in Kizildere, Germencik and Afyon geothermal waters indicates that residence time of recharging water in the geothermal system is more than 50 years while at the Soke region thermal waters appear to be young in age. According to the result of ^{14}C contents, thermal waters have a relatively age of 10000 to 30000 a.

There are clear $\delta^{18}O$ shift from MMWL in Kizildere and Germencik high temperature fields. Also good relation with high temperature and $\delta^{18}O$ shift are determined. It shows deep circulation and water-rock interactions. There are slight $\delta^{18}O$ shift in Afyon fields. But, in Soke region low temperature, low shift, shallow circulation and mixing with shallow cold water and seawater are observed.

According to results, the fields are important for geothermal development and utilization in Denizli-Kizildere and Germencik for generation of electricity, central heating CO_2 production balneological and Afyon-Omer, Gecek geothermal fields for central heating and balneological point of view.

Using isotope technology methods in the geothermal fields of Western Anatolia provided a very useful tool in developing the hydrogeological model of the area. Improvement of the laboratories of the agency as to be able to analyze other isotope contents of both water and gas would contribute to much to the research project that will be implemented in the future.

Acknowledgements

This study has been carried out within the framework of the IAEA Coordinated Research Program. "The Use of Isotope Techniques in Problems Related to Geothermal Exploitation "(Research Contract No 9829/RO-R1). Sincere thanks to staff members of Isotope Hydrology Section of the IAEA. The authors are deeply thank Prof. Dr. GUNAY (Director of UKAM) for his support made this work successful. The authors are grateful M. S. DOGDU and B. AKAN from UKAM and to Mr. N. YILDIRIM from MTA for his assistance and scientific advance during the sampling and evaluation of data. The authors express their appreciation to N. TURKMEN from TEAS (Turkish Electricity Authority Manager of Kizildere Geothermal Power Plant). I also thank E. ONCEL and F. MUSLU for chemical analyses and B. TOPUZ for office works.

REFERENCES

[1] MTA, Inventory of Hot and Mineral Waters in Turkey, MTA report. Ankara (1980) 1–78.
[2] SIMSEK, S., Geothermal Model of Denizli, Saraykoy-Buldan Area, Geothermics, Vol. 14, No 2–3, Pergamon Press. Great Britain (1985) 393–417.
[3] SIMSEK, S. and OKANDAN, E., The Geothermal Development in Turkey, Geothermal Resources Council Transaction, Vol. 14, Part 1, USA (1990) 257–266.
[4] ARNORSSON, S., Chemical Equilibria in Icelandic Geothermal Systems. Implications for Chemical Geothermometry Investigations: Geothermics, vol. 12, (1983) 119–128.
[5] ELLIS, A.J. and MOHAN, W.A.J., Geochemistry and Geothermal Systems, Academic Press, New York, USA. (1977).
[6] GERARDO, J.Y., Isotope Applications in Geothermal Energy Development, Report on Advisory Meeting, Vienna (1995).
[7] GIGGENBACH, W. F., Geothermal Solute Equilibria. Derivation of the Na-K-Mg-Ca Geoindicators. Geochim. Acta, 52 (1988) 2749–2765.
[8] PANICHI, C. and GONFIANTINI, L., Isotope Geochemistry, Turkish-Italian Geothermal Energy Seminar Notes, Ankara, Turkey (1982).

[9] TRUESDELL, A., H., Origins of Acid Fluids in Geothermal Reservoirs, Geothermal Investigations with Isotope and Geochemical techniques in Latin America, Proceedings of Final Research Co-ordination Meeting held in San Jose, Costa Rica, 12–16 November 1990, IAEA-TECDOC-641, Vienna-Austria. (1990).
[10] YILDIRIM, N., Scaling Problem in The Geothermal Fields of Turkey and Its Alternative Solution, UN Seminar on New Developments in Geothermal Energy EP/SEM. 14/R. 23, Ankara (1989) 1–13.
[11] YILDIRIM, N. and OLMEZ, E., Kizildere (Denizli-Saraykoy) Sahasinda Yeni Acilan Kuyular (R1-TH2) ile Uretim Kuyulari Arasindaki Hidrojeokimyasal Iliski. Proceedings of BAKSEM'99 Symposium, Izmir, (1999) 336–345 (in Turkish).
[12] SIMSEK, S., DOGDU, M. S. and CELIK, H. Final Report of Isotope Survey of Geothermal Systems of Central Anatolia, HU-IAEA Research Contract 6716/RB. Ankara (1993) 1–77.
[13] SIMSEK, S., DOGDU, M. S., AKAN, B. and YILDIRIM, N. Chemical and Isotopic Survey of Geothermal Reservoirs in Western Anatolia, Turkey. Proceedings World Geothermal Congress 2000, Japan, (2000) 1765–1770.
[14] SIMSEK, S., Evolution of Buyuk Menderes Graben and Its Geothermal Energy Possibilities, 28th International Geological Congress, Abstract, Vol. 3, Washington, USA (1989) 121.
[15] ERISEN, B., Utilization of Geothermal Energy of Afyon Area in Domestic Heating and Agriculture, Seminar on Utilization of Geothermal Energy for Electric Power Production and Space Heating, UN Economic Commission for Europe, EP/SEM-9/R46, Florence, Italy (1984).
[16] FILIZ, S., Investigation of the Important Geothermal Areas by Using C, H, O Isotopes, Seminar on Utilization of Geothermal Energy for Electric Power Production and Space Heating, UN Economic Commission for Europe, EP/SEM-14/R3, Ankara, Turkey. (1984). 1–13.
[17] GULEC, N., Helium-3 distribution in Western Turkey. MTA Bulletin 108, (1988) 35–42
[18] OZGUR, N. Hydrogeochemical and isotope geochemical features of the thermal waters of Kizildere, Salavatli and Germencik in the rift zone of the Buyuk Menderes, Western Anatolia, Turkey: Preliminary studies. Water-Rock Interaction. Balkema- Rotterdam (1998) 645–648.
[19] SIMSEK, S., Aydin-Germencik-Omerbeyli Geothermal Field. Seminar on Utilization of Geothermal Energy for Electric Production and Space Heating. United National Economic Commission for Europe EP/SEM. 9/R. 37. Florence-Italy (1984) 1–30.

CHEMISTRY OF NEUTRAL AND ACID PRODUCTION FLUIDS FROM THE ONIKOBE GEOTHERMAL FIELD, MIYAGI PREFECTURE, HONSHU, JAPAN

A.H. Truesdell[1], S. Nakanishi[2]

[1]Centre for Isotope Geochemistry, Lawrence Berkeley National Laboratory, Berkeley, California, United States of America
[2]Japan Electric Power Development Company, Honshu, Japan

Abstract. This investigation has shown that production fluids at Onikobe vary widely in chemical composition and concentration but have certain characteristics in common. These characteristics include a rather narrow range of reservoir temperatures from 230 to 255ºC measured temperatures; 225 to 280ºC calculated from enthalpy assuming no excess steam; 241 to 270ºC calculated from the quartz saturation geothermometer and 253 to 280ºC calculated from the most reasonable Na/K geothermometer. The agreement between enthalpy derived and other temperatures suggests that there is little excess steam as does inlet vapour fraction (IVF) values, which are less than 0.1 for almost all samples. The largest variations in concentration are in pH and acid sensitive constituents including Fe, Mg, Ca which are dissolved from reservoir rocks and casings by low pH waters and other constituents with volatility depending on pH (NH_4, HBO_3). The pH varies from 2.8 to 8 and Fe varies from 0.01 to 371 ppm. The variation of other acid sensitive constituents, although not as large, is also significant. The source of the acid is not yet understood. The large "chloride excess" and the strong correlation of low pH with high chloride indicate that the acid enters the water as HCl, but some SO_4 acidity could have been removed by reaction with plagioclase to form anhydrite. There is a consistent increase in salinity with time along with indications that the waters are gas depleted. These observations are interpreted as showing that injected waters enriched in salts and depleted in gases are contributing to production waters. The acid reservoir seems to be limited to moderate depths in the middle of the drilled area. Drilling either to the NW where wells 134, 135 and 128 (before its casing leak) produced neutral waters or to the S where well 129 produces neutral waters would seem to be the best strategy. The relative homogeneity of the neutral waters suggests that there is a large reservoir of these fluids.

1. Introduction

The Onikobe geothermal field is located in northern Honshu, Japan, within the nearly circular, 2 million year old Onikobe caldera. Within the Onikobe caldera, most surface activity consists of acid-sulfate springs in the Katayama area, a highly-faulted, central collapse zone just to the SE of the center of the caldera, and neutral-chloride springs in the Miyazawa, Fukiage and Mitaki areas, along two NE (and one SE) trending faults in the caldera SW of the Katayama area. This field has been developed by the Electric Power Development Company (EPDC), which has graciously allowed the use of their data in this report. The deep production wells are all drilled 20 to 40 degrees from vertical in the center of the Katayama area where the temperature gradients are highest (Figure 1). There are a number of papers published on the Onikobe field. Of these the most useful is by M. Abe (1993) and discusses the engineering necessary to use acid fluids for energy production.

2. Onikobe deep production fluids

The chemical compositions of typical separated waters from Onikobe deep production wells are shown in Table I and represented on a Schoeller plot in Figure 2. In this type of plot, the logarithm of the concentration (in mg/kg) of each constituent of an analysis is connected so that each analysis is represented by a line. Where data are missing, the line is broken. With this many data, only general

[1] Present address: 700 Hermosa Way, Menlo Park, CA 94025, USA.

patterns can be seen but the patterns for individual wells can be compared in separate Schoeller plots shown later. In comparing these figures, note that the effect of steam loss or dilution is to move the line up or down parallel to itself. Typical gas analyses of separated steam are given in Table II and calculated reservoir temperatures (from geothermometers and measured enthalpy), chloride concentrations and steam fractions are given in Table III.

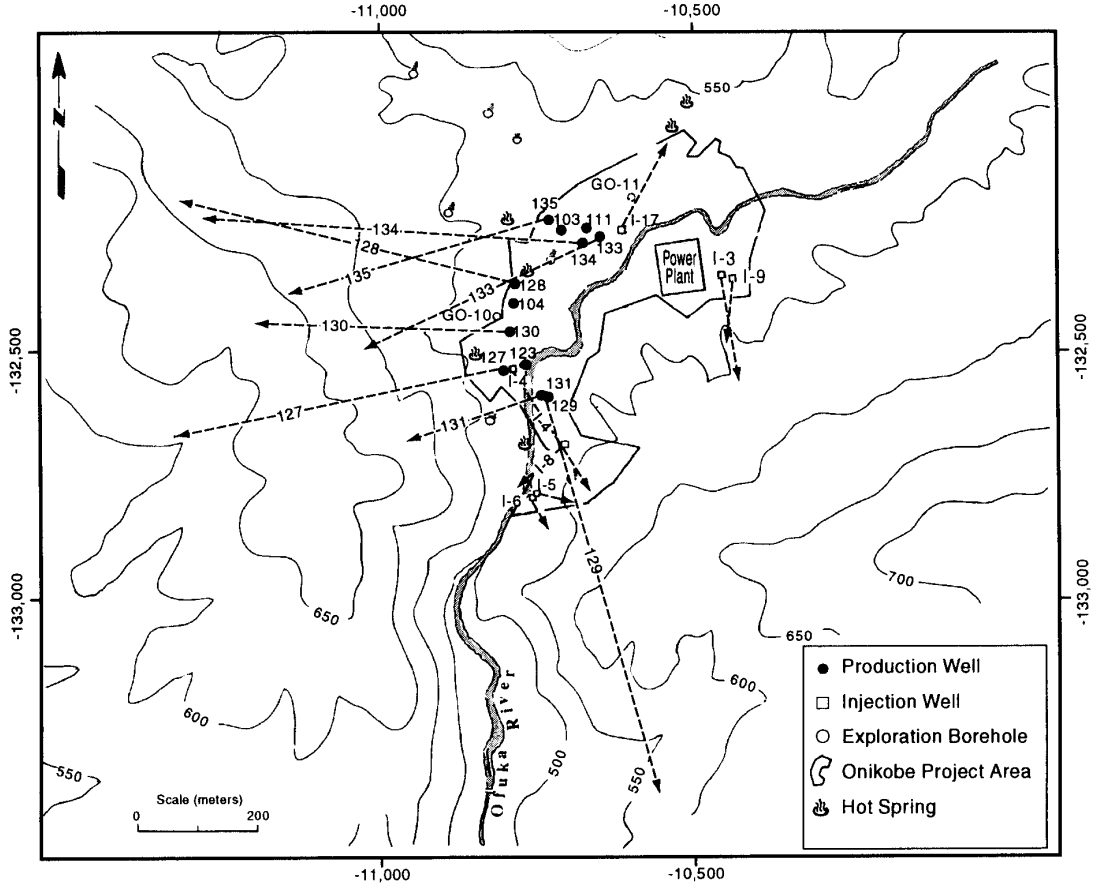

Figure 1. Map of Onikobe geothermal production field.

The Schoeller plot of the Onikobe production fluids has some interesting features. As is usual in a group of reasonably homogenous reservoir fluids, the variation in concentration of conservative (or inactive) constituents is small. In particular lithium, sodium, chloride and boron concentrations are tightly grouped and appear more so because of the logarithmic presentation. Due to relatively uniform reservoir temperatures (see Table III), potassium and silica also have small concentration ranges. Onikobe is unusual compared to other fields in the wide ranges of pH, Mg and Fe. Variations in Mg are seen in exploration well and hot spring waters elsewhere due to mixing of low Mg reservoir waters with high Mg near-surface waters. At Onikobe this variation in Mg appears to be linked to the wide range in pH and iron. The highest pH waters have the lowest magnesium and iron, and the lowest pH waters have the highest magnesium and iron. Calcium shows a similar but smaller effect. There seems to be an acid component and at least one neutral to alkaline component in these waters. The acid component is associated with relatively high concentrations of Ca, Mg and Fe, which probably are dissolved from reservoir minerals (Ca, Mg) and well casings (Fe).

Table I. Chemistry of waters collected at atmospheric pressure from deep wells of the Onikobe geothermal field.

Well	Date	Q	Psep kPag	Enth kJ/k	pH m	Li	Na	K	Ca	Mg	Fe	Mn mg/kg	Cl	SO_4	TCO_2	F	SiO_2	B
127	1984-05-14	3	312	1170	6.7	4.25	1800	320	280	9.7	0.18	-	3210	35	-	4.1	780	59.6
127	1988-10-25	4	392	1080	5.1	3.7	990	360	410	3.5	0.45	-	4060	11	9	-	674	40
127	1990-11-07	4	483	1030	5.1	3.5	1800	280	510	3.5	0.46	1.8	4000	22	-	-	640	8.8
127	1993-07-23	7	343	1060	4.6	3.15	1990	350	459	4.72	0.64	3.15	4190	18.6	15	4.74	665	60.2
127	1995-09-21	7	294	1110	4.7	4.68	1950	371	518	7.87	1.16	4.63	4270	17	10	3.45	702	64
127	1997-01-31	7	460	1170	4.9	4.27	2090	380	579	6.28	1.18	1.95	4610	12.5	10	3.26	702	56.5
127	1999-04-08	7	477	1100	5	3.63	2240	390	648	8.38	1.55	4.52	4980	19.7	10	4.56	589	71.8
128	1982-12-10	3	284	1020	8.2	-	800	120	8.4	1.7	0.1	0.05	1340	61	-	3.8	660	3.2
128	1988-06-07	4	443	1040	8.2	-	610	210	78	0.39	0.06	-	1990	38	-	-	690	-
128	1991-09-06	6	325	950	6.5	1.74	1010	170	105	2.23	0.56	5.55	1840	20.6	-	-	668	33.7
128	1993-01-13	7	216	1090	5	2.71	1230	233	145	11.3	2.72	4.27	2430	18.6	13	4.88	733	33.2
128	1996-05-15	4	448	1250	3.8	2.5	1400	240	230	15	8.5	4.5	2800	25	-	0	700	42
128	1999-04-08	7	357	1130	3.1	3.36	1850	372	474	33.5	28.2	10	4300	50	10	6.45	683	62.4
129	1983-10-20	3	492	1070	8	2.58	1280	230	260	4.8	0.15	-	2820	27	-	0.59	690	60.6
129	1986-05-26	3	503	1040	8.1	2.5	1900	3.2	280	0.89	0.01	0.92	3600	20	-	-	681	20
129	1988-04-27	5	441	1070	8	-	1260	278	111	0.9	0.35	-	3490	19	-	-	640	-
129	1990-06-18	4	582	1060	8	2.7	1100	160	360	1.2	0.01	1.6	3600	28	-	-	650	71
129	1993-01-13	7	295	901	8	2.77	1960	307	347	2	0.01	1.56	3980	21.3	62	2.62	672	58
130	1985-09-06	3	411	1130	6.2	-	1720	361	295	5.6	-	-	4040	38.1	10	-	622	-
130	1988-04-27	3	520	1100	3.5	-	1280	344	188	46	160	-	5050	19	-	-	730	-
130	1990-11-07	4	648	1170	3.2	3.2	1700	330	560	37	180	11	4400	21	-	-	690	82
130	1993-07-23	7	461	1140	3.1	2.45	1730	355	434	34.4	144	8.8	4090	16.4	10	8.15	738	55.3
130	1996-05-15	4	685	1110	3	3.3	2100	420	630	44	170	8.5	4900	14	-	6.6	710	44
130	1998-12-15	7	561	1240	2.8	2.65	2100	435	721	58.3	371	18.4	5650	29.9	10	7.49	725	77.2

Note: The code Q indicates the quality of the analyes (7=highest). Units are shown in the headings.

Table II. Isotope and Gas Analyses from Onikobe Production Wells

Well	Date	Q	Psep	Enthalpy	pH	δD	$\delta^{18}O$	G/S	CO_2	H_2S	H_2	CH_4	N_2
			kPag	kJ/kg		VSMOW o/oo		mole/mole			mole%		
127	1988-10-25	4	392	1080	5.1	-53.7	-5.5	0.0005	40.7	25.7	1.840	0.121	31.6
127	1990-11-07	4	483	1030	5.1	-49.4	-5.4	0.0005	48.2	30.6	1.690	0.157	19.2
127	1993-07-23	-	422	1090	-	-51.5	-5.3	0.0009	72.5	9.5	1.280	0.198	16.0
127	1995-10-18	4	381	1180	4.6	-50.6	-5.0	0.0014	61.8	19.9	0.942	0.062	17.3
127	1998-05-20	4	482	1120	4.9	-49.7	-5.2	0.0035	78.3	8.2	0.367	0.055	13.1
128	1988-10-25	4	424	1030	8.0	-60.4	-7.7	0.0005	51.7	30.7	1.100	0.238	16.3
128	1991-11-11	4	363	973	6.3	-55.7	-7.6	0.0006	57.0	14.2	0.789	0.196	24.8
128	1993-05-26	4	309	1030	5.0	-52.7	-6.3	0.0006	60.0	21.7	1.020	0.311	17.0
128	1996-05-15	4	449	1250	3.8	-55.4	-6.9	0.0010	66.5	20.6	0.801	0.077	12.0
128	1998-05-20	4	631	1090	3.3	-54.6	-5.9	0.0024	75.6	14.5	0.475	0.040	9.4
129	1988-06-07	4	428	1060	8.1	-53.2	-5.2	0.0047	77.7	18.2	1.920	0.233	2.0
129	1990-06-18	4	582	1060	8.0	-53.1	-5.1	0.0056	75.9	20.0	1.920	0.207	1.9
129	1993-01-13	7	296	901	8.0	-45.9	-4.8	0.0034	77.9	18.5	1.300	0.180	2.1
130	1988-06-07	4	571	1130	3.5	-56.2	-5.7	0.0011	59.5	30.6	0.376	0.062	9.5
130	1990-11-07	4	649	1170	3.2	-48.4	-5.1	0.0014	54.7	30.0	1.800	0.116	13.3
130	1993-01-13	7	508	1240	3.1	-49.4	-5.6	0.0015	67.5	19.9	0.857	0.113	11.4
130	1996-05-15	4	686	1110	3.0	-50.1	-4.9	0.0026	65.4	24.6	0.975	0.056	9.0
130	1998-10-12	4	633	1050	2.8	-49.0	-4.5	0.0036	55.8	37.0	1.230	0.029	5.9

Table III. Geothermometer temperatures (T), fluid enthalpies (E), aquifer chlorides (C), and inlet vapor fractions (IVF) calculated for Onikobe production fluids from deep wells.

Well	Date	pH	TE	TQA	TNKC	TNKW	TNKN	TNKF	TNKG	Enth	ETQA	ETNKC	ETNK	ETNK	ETNKF	CTE	CTQA	CTNKC	CNK	IVFNK	IVF-245
					degC						kJ/kg						mg/kg			Fraction	vapor
127	1984-05-14	6.7	266	264	237	259	257	272	283	1170	1160	1020	1130	1120	1190	2150	2160	2350	2200	0.0809	0.0602
127	1988-10-25	5.1	248	252	270	387	344	360	362	1080	1100	1180		1620	1760	2880	2840	2690		-0.0662	0.0091
127	1990-11-07	5.1	238	248	221	241	244	258	270	1030	1080	949	1040	1060	1120	2920	2840	3060	2900	0.0436	-0.0179
127	1993-07-23	4.6	245	251	233	258	256	271	282	1060	1090	1000	1120	1120	1190	3000	2940	3110	2880	0.0319	-0.0007
127	1995-09-21	4.7	272	256	236	269	265	279	289	1200	1110	1020	1180	1160	1230	2800	2960	3130	2830	0.0985	0.0768
127	1997-01-31	4.9	267	256	233	262	260	274	285	1170	1110	1010	1150	1130	1210	3080	3190	3410	3120	0.0912	0.0624
127	1999-04-08	5.0	253	242	231	256	255	270	281	1100	1050	994	1120	1110	1180	3480	3600	3710	3440	0.0587	0.0223
128	1982-12-10	8.2	236	251	247	236	240	254	267	1020	1090	1070	1020	1040	1110	985	943	954	985	-0.0305	-0.0254
128	1988-06-07	8.2	241	254	275	375	336	352	355	1040	1110	1210	1570	1690	1440	1380	1290			-0.106	-0.0122
128	1991-09-06	6.5	221	252	231	251	252	266	278	950	1090	995	1090	1090	1160	1410	1290	1370	1290	-0.0249	-0.0639
128	1993-01-13	5.0	251	259	240	268	264	279	289	1090	1130	1040	1180	1160	1230	1710	1660	1760	1610	0.0301	0.0165
128	1996-05-15	3.8	283	255	231	254	254	268	279	1250	1110	994	1100	1100	1170	1760	1940	2090	1950	0.144	0.111
128	1999-04-08	3.1	259	253	240	277	271	285	295	1130	1100	1040	1220	1190	1260	2950	3000	3120	2770	0.053	0.0395
129	1983-10-20	8.0	246	254	231	261	259	273	284	1070	1110	993	1140	1130	1200	2010	1960	2100	1920	0.0404	0.0027
129	1986-05-26	8.0	227	241	232	252	252	266	278	978	1040	999	1090	1100	1170	2570	2470	2530	2390	-0.0113	-0.0477
129	1988-04-27	8.0	246	248	255	292	281	296	304	1070	1080	1110	1300	1240	1320	2490	2470	2430	2130	-0.0234	0.0039
129	1990-06-18	8.0	245	249	210	232	237	251	264	1060	1080	899	998	1030	1090	2580	2540	2830	2680	0.0842	-0.0013
129	1993-01-13	8.0	211	252	228	242	245	259	271	901	1100	979	1040	1060	1130	3130	2790	2990	2880	-0.0429	-0.092
130	1985-09-06	6.2	259	246	247	284	275	290	299	1130	1070	1070	1260	1210	1290	2770	2880	2880	2540	0.0345	0.0389
130	1988-04-27	3.5	254	259	263	326	304	319	326	1100	1130	1150	1500	1370	1460	3520	3460	3410	2630	-0.0278	0.0246
130	1990-11-07	3.2	268	254	234	272	267	281	291	1170	1110	1010	1200	1170	1240	2930	3060	3250	2890	0.0925	0.0642
130	1993-07-23	3.1	261	260	241	281	273	287	297	1140	1130	1040	1240	1200	1280	2780	2800	2960	2600	0.0564	0.0452
130	1996-05-15	3.0	255	256	239	277	270	285	294	1110	1120	1030	1220	1180	1260	3400	3380	3570	3160	0.0436	0.028
130	1998-12-15	2.8	281	258	240	282	274	289	298	1240	1130	1040	1250	1200	1280	3590	3880	4100	3580	0.115	0.103
131	1988-06-07	3.4	243	251	251	318	299	314	321	1050	1090	1090	1450	1340	1420	3230	3150	3150	2430	-0.0221	-0.0059
131	1990-11-07	3.2	237	244	220	243	246	260	272	1030	1060	944	1050	1070	1140	3150	3080	3300	3090	0.0435	-0.0208
131	1993-07-23	3.3	241	245	233	264	261	275	286	1040	1060	1000	1150	1140	1210	3280	3230	3350	3050	0.0195	-0.0122
131	1996-05-15	3.5	217	236	231	258	257	271	282	929	1020	993	1120	1120	1190	3710	3520	3580	3300	-0.0352	-0.0758
131	1998-12-15	3.5	236	235	230	261	259	274	284	1020	1010	991	1140	1130	1200	3320	3330	3370	3070	0.0157	-0.0237
133	1993-02-25	4.2	293	242	230	260	258	272	283	1310	1050	990	1130	1130	1200	3010	3580	3710	3390	0.175	0.141
133	1995-02-14	3.6	221	231	228	253	253	268	279	948	996	979	1100	1100	1170	3480	3390	3420	3170	-0.0172	-0.0652
133	1997-01-31	3.2	230	236	231	263	260	274	285	990	1020	996	1150	1130	1210	3650	3590	3640	3310	-0.0038	-0.0412
133	1998-12-15	3.2	226	233	229	258	256	271	282	970	1010	987	1120	1120	1190	3920	3830	3880	3560	-0.0095	-0.0524
134	1994-03-22	8.0	250	256	240	260	258	272	283	1090	1120	1040	1130	1130	1200	1510	1490	1560	1470	0.0278	0.0148
134	1996-05-15	7.6	253	254	229	248	250	264	276	1100	1110	988	1080	1080	1150	2380	2370	2540	2410	0.0613	0.0217
134	1997-10-13	7.9	237	253	236	265	262	276	287	1020	1100	1020	1160	1140	1220	2050	1960	2060	1880	0.0028	-0.0225
134	1998-12-15	7.8	224	255	231	261	259	273	284	963	1110	997	1140	1130	1200	1640	1500	1610	1470	-0.0189	-0.0564

Note: Geothermometers used are TE, from enthalpy; TQA, Quartz adiabatic; TNKC, Na-K-Ca; TNKW, Na/K White-Ellis; TNKN, Na/K Nieva; TNKF, Na/K Fournier; TNKG, Na/K Giggenbach.

Sources of geothermometer equations: TQA Fournier and Potter, 1982; TNKC Fournier and Truesdell, 1973; TNKW Truesdell 1975; TNKN Nieva and Nieva, 1987; TNKF Fournier, 1979; TNKG Giggenbach, 1988.

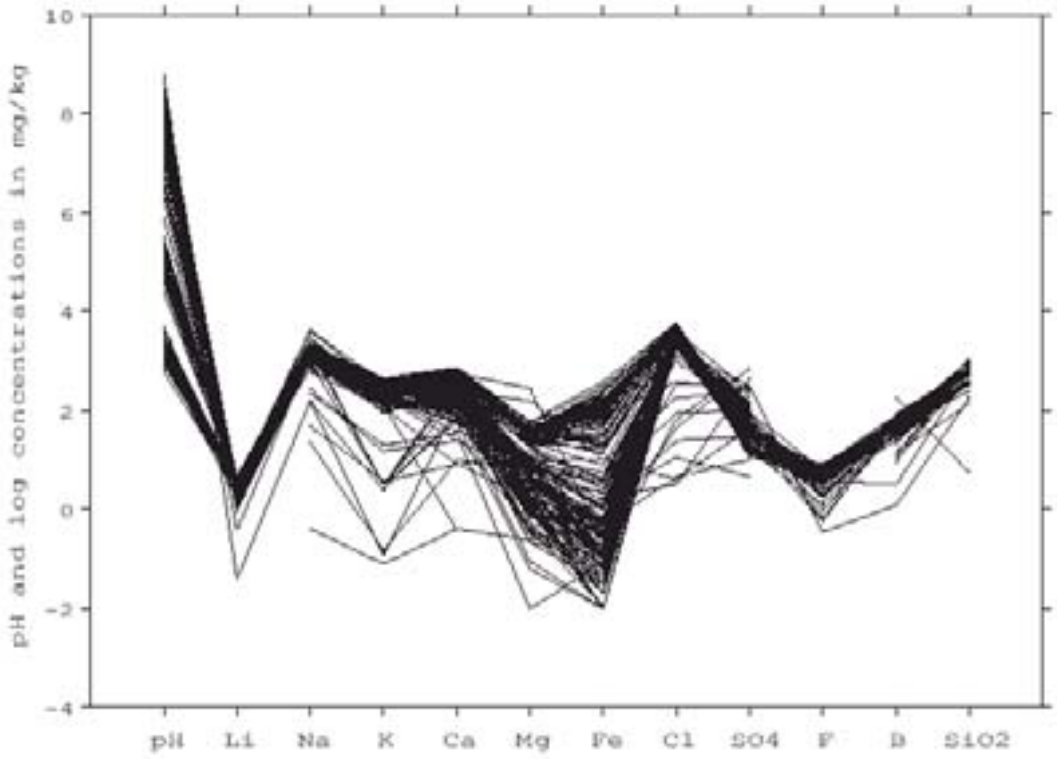

Figure 2. Schoeller plot of compositions of all production waters flashed to one atmosphere. See text for explanation.

3. Chemical behaviour of fluids from individual deep production wells

In this section, the deep wells with relatively long production records are discussed. In order to save space, shallow wells (103, 111) and wells with short histories (132, 135) are omitted and only selected data are given in Tables I–III. However, the figures in section 4 include these wells.

3.1. Production well 127

Well 127 was the first deep well. As can be seen in Figure 1, well 127 was directionally drilled slightly south of west from a pad located along the Ofuka stream. It has a total depth of 1150 m and a measured temperature of 250ºC at 960 m depth. While this well has been on line from 1984 to 1999, its flashed production fluid has varied irregularly in pH from 7.2 to 4.6. As shown in the Schoeller graph (Figure 3) the water composition is typical of this field and although the pH ranges from 4.6 to 5, iron and magnesium concentrations have stayed moderately low at 0.6 to 1.6, and 4.7 to 8.4 ppm respectively (Table I).

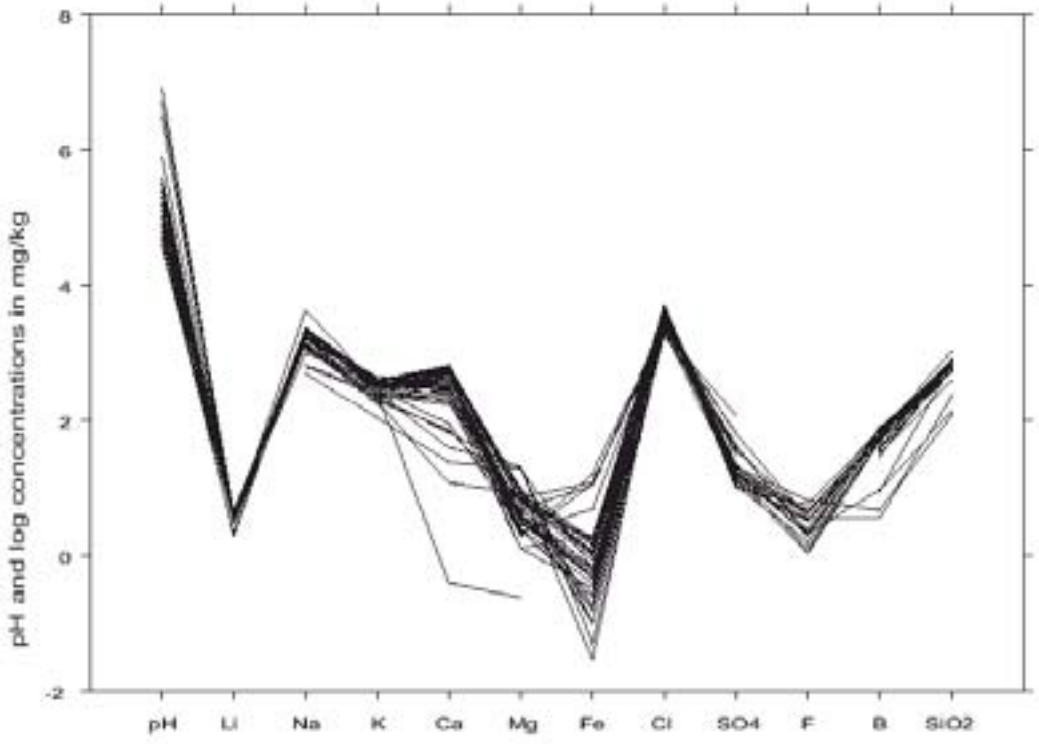

Figure 3. Schoeller plot of flashed production waters from well 127.

Temperatures calculated from cation geothermometers for Onikobe moderately acid and acid waters are not well behaved (Table III). Considering that these geothermometers are empirical and were calibrated on neutral waters, this is not surprising. Although the White-Ellis Na/K equation seems to work for Onikobe moderately acidic waters, there is no cation geothermometer that is accurate in acid waters below pH 4. Even in moderately acid waters, NaKCa geothermometer temperatures are 15 to 17 degrees too low and Na/K geothermometer temperatures are all high, the Giggenbach Na/K equation by as much as 40ºC. Possibly, the acid has altered the surface of feldspar to mica so that the cation geothermometers could not re-equilibrate. In general, it seems that greater faith should be put on the quartz saturation temperatures because they are not known to be affected by acid pH in the range observed at Onikobe (Fournier and Potter, 1982). For Onikobe neutral to alkaline waters the White-Ellis Na/K temperatures agree reasonably well with quartz temperatures (Table III).

Well 127 reservoir chloride increased from about 1250 in 1980 to near 3000 ppm from 1990 to 1996 (Table III). In 1994 there was an interruption (?) and chloride dropped to 2500 then increased rapidly to 3500 ppm in 1999. Most Onikobe production well waters (except those from wells 131 and 134) have shown similar increases in chloride, probably due in most cases to recycling of injectate. Tracer tests with KI and KBr added to injection wells have shown returns from production wells 127, 130, 131 and 133, but not from 128, 129, 134 and 135. This last group of wells have feed zones relatively far from the injection wells and most have shown constant chloride (134, 135) or special circumstances (128). For waters with acidity increasing with time (wells 128, 130, 131, 133 and possibly 127), the increase in chloride (and other solutes) may have been due in part to increased production of a more saline, acidic water. For well 128, production from more concentrated acidic waters has been shown to have occurred through a casing break (see later).

3.2. Production well 128

Well 128 was drilled from a pad 250 m due W of the power plant and deviated 800 m slightly N of W (Figure 1). Its main feed zone is at 990 m depth and 255ºC. The measured down hole temperature does not consistently agree with the temperatures calculated from enthalpy or by the use of geothermometers. The increase with time in concentrations of chloride (1800 to 3200 ppm in the reservoir) and other conservative constituents is larger than that of well 127, but the increase in acid-sensitive elements was even greater (Table I). From 1984 to 1989 the pH of flashed fluid from well 128 was between 8.0 and 8.1. After about 1990 the pH dropped progressively to 6.2 (in 1992), 5.0 and 4.7 (in 1993), 3.5 (in 1997) and 3.1 (in 1999). These changes are apparently due to increasing production from a shallow acid zone through a widening hole in the casing. As the pH decreased, iron has increased from 2.7 to 28.2 ppm and magnesium, from 11.3 to 33.5 ppm. Calcium, which is also sensitive to acidity, has increased from 145 to 474 and sulfate has increased by a similar ratio (18 to 50 ppm).

The Schoeller diagram for well 128 waters (Figure 4) shows very little change in SiO_2, probably because the temperature was nearly constant, and quartz solubility is unaffected by pH in the acid range. There are increases of about 50% in Na, Cl and other conservative constituents such as F and B, probably due to mixing with a higher salinity acid water and possibly to injection recycling as well. The change in K is limited by the near constant temperature and by charge balance constraints. Elements relatively abundant in rock minerals and casing, but at low concentrations in the reservoir water and therefore not limited by charge balance, showed the largest relative increases. The increase in SO4 is interesting because it may be a clue to the source of the acid. In reservoirs associated with active volcanoes, acidic waters may be produced by the introduction of SO_2 gas, which hydrolyses to form sulfuric acid and hydrogen sulfide. However, the concentration of SO_4 is moderate and the source of the acid is concluded in a later section to be incompletely neutralized volcanic HCl. The increase in SO4 may result from rather than cause the acidity. The decrease in pH may have caused solution of anhydrite ($CaSO_4$) as SO_4 was converted to HSO_4 at lower pH.

3.3. Production well 129

Well 129 is deviated to the SSE of the main bore-field and to the South of the power plant. This well has a temperature inversion with 259C measured at 970 m and 235ºC measured at the feed zone at 1210 m. This well has produced slightly alkaline pH 8 water throughout its 1983 to 1992 history (Table I). The Schoeller diagram (Figure 5) shows very little variation in pH, Li and Cl. Other components show moderate changes (excluding dilute samples possibly mixed with condensate) and low Mg and Fe consistent with the high pH. Well 129 was not a high producer and when its flow ceased in 1993, possibly plugged with silica, it was shut in.

It is notable that the geothermometers were very well behaved used on well 129 water (Table III). This is probably because these waters were neutral to alkaline and similar to the waters that were used to calibrate the geothermometer equations.

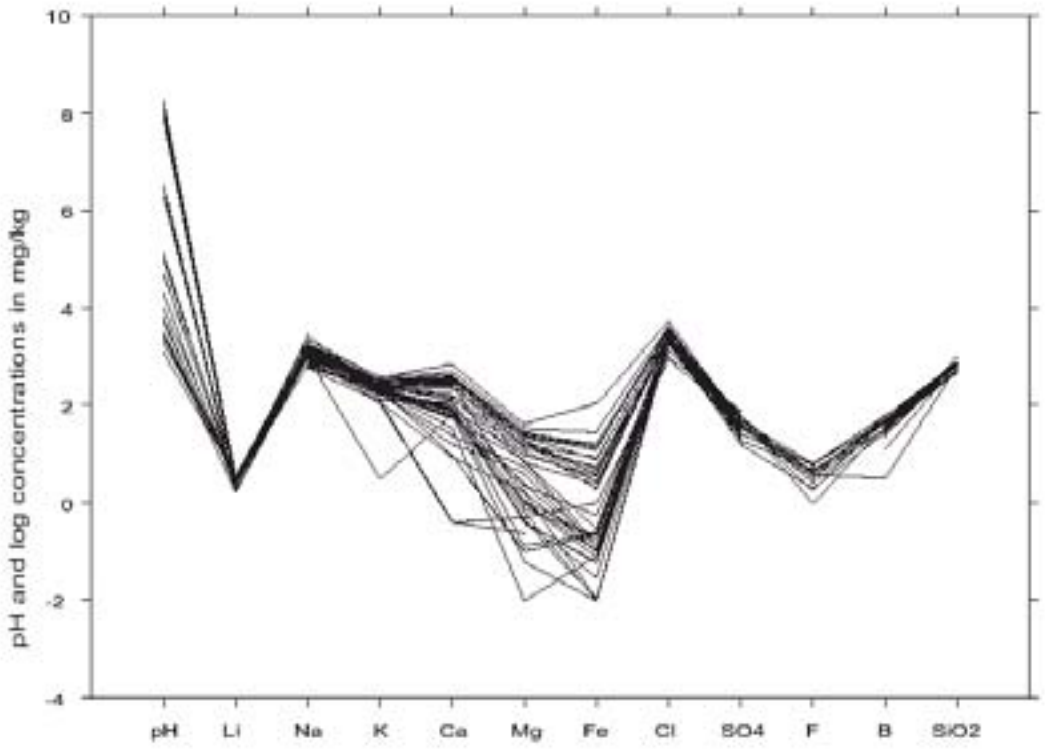

Figure 4 Schoeller plot of flashed production waters from well 128.

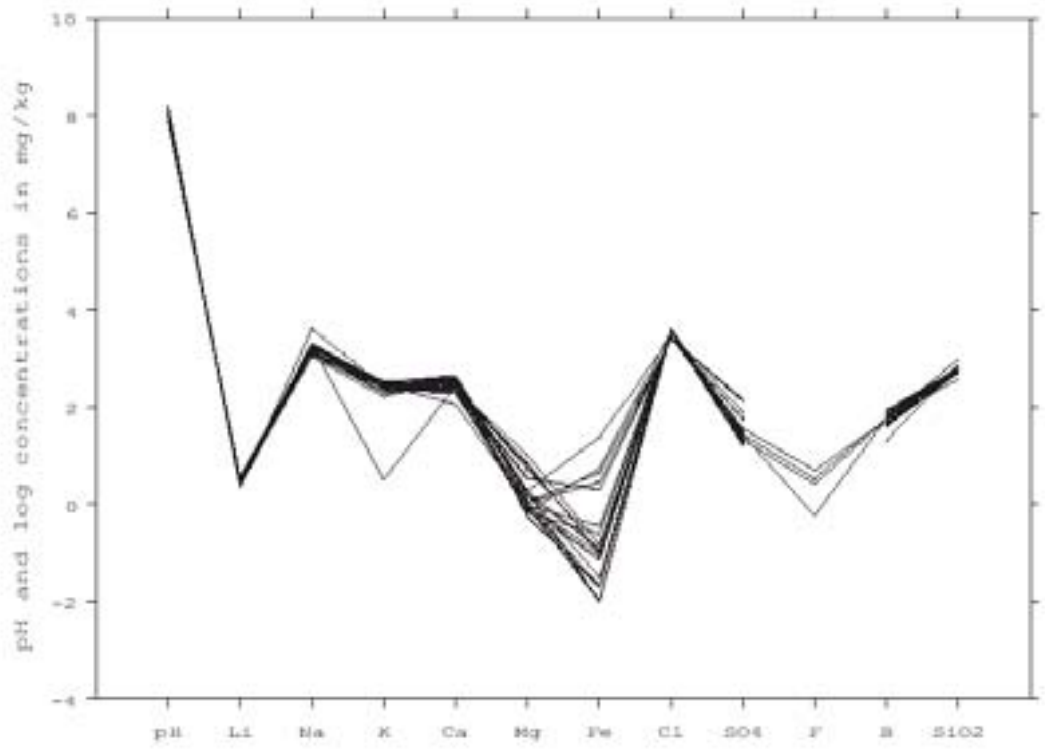

Figure 5 Schoeller plot of flashed production waters from well 129.

3.4. Production well 130

The bottom of well 130 is nearly halfway between wells 127 and 128 but somewhat nearer the power plant (Figure 1), and the feed zone at 1175 m depth was near 250ºC. This well produces the most acid waters of the field with a pH of 2.8 measured on the most recent sample (Table I). As with well 128 described earlier, the pH of the waters sampled have decreased with time, from 6.9 in 1985, 3.7 to 3.0 from 1986 to 1997, to 2.9 and 2.8 in 1998, but there is no evidence of a hole in the casing. Because of the lower pH, well 130 has Mg and Fe concentrations that are 8 times to as much as 150 times higher than those of well 127 water (Table I and Figure 6). Conservative constituents (Na, K, Cl, B) are similar to (or 10% higher than) those in well 127 waters and about 30% higher than in well 128 waters. Note that despite the higher acidity, most SO4 concentrations are similar to those of well 127 waters and lower than those of well 128 waters. This argues against the acidity originating from near-surface oxidation of H2S or from hydrolysis of volcanic SO2.

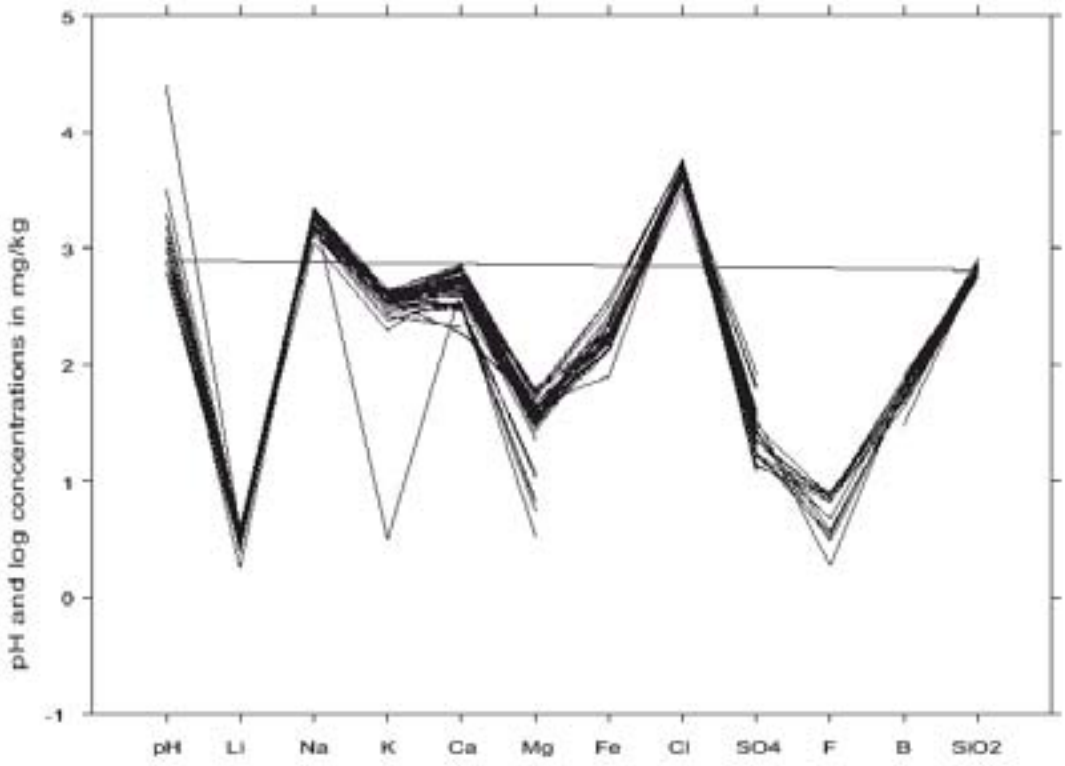

Figure 6. Schoeller plot of flashed production waters from well 130.

The application of geothermometers to well 130 waters is no more orderly than for other acid wells (Table III). Most indicated enthalpy temperatures near 253ºC are in reasonable agreement with the measured feed point temperature of 250C. Na/K temperatures tended to be very high (Giggenbach TNK over 300C) but silica ranged from about 250 to 260C in reasonable agreement with measured and enthalpy temperatures. Reservoir chloride from about 3200 mg/kg in 1993–1995 to near 4200 mg/kg in 1999. This increase is similar to that noted in other wells and probably due to both injection returns and increased production of acid, saline water.

3.5. Production Well 131

Well 131 was drilled SE of the power plant with less deviation than wells 127 and 128 (Figure 1), and its feed zone was at 900 m depth and 245ºC (Section 3). The pH of most fluids from well 131 has been reasonably constant at 3.3 ±0.1 from 1989 to 1995 and since has increased about 0.2 units (Table I). The measured enthalpy and indicated silica temperatures declined moderately from 1988 to 1998 possibly due to cooling from injectate (Table III). As with other acid waters cation geothermometer temperatures were unreliable ranging from 0 to 20ºC high (TNK White-Ellis) to 50 to 60ºC high (TNK Giggenbach).

The pH increase from 1995 to early 1998 was accompanied by a decrease in Mg, and Fe, and an increase in Cl, Na, K, Li and SO4. In the last sample in 1998, the pH decreased slightly and the other observed changes also reversed direction (Table I and Figure 7). These observations suggest that there are two waters feeding the well. One of these is hotter (higher enthalpy) with lower pH and lower Cl, Na, K, Li and SO4. This water also has higher Mg and Fe because of greater acid attack of minerals and the casing. The other water has a lower enthalpy, higher pH (with less leached Mg and Fe) and higher Cl, Na, K, Li and SO4. Reservoir chloride concentrations were nearly constant at 3300 mg/kg from 1988 to 1993, but after a gap the data diverged and rose rapidly to above 3500 kJ/kg.

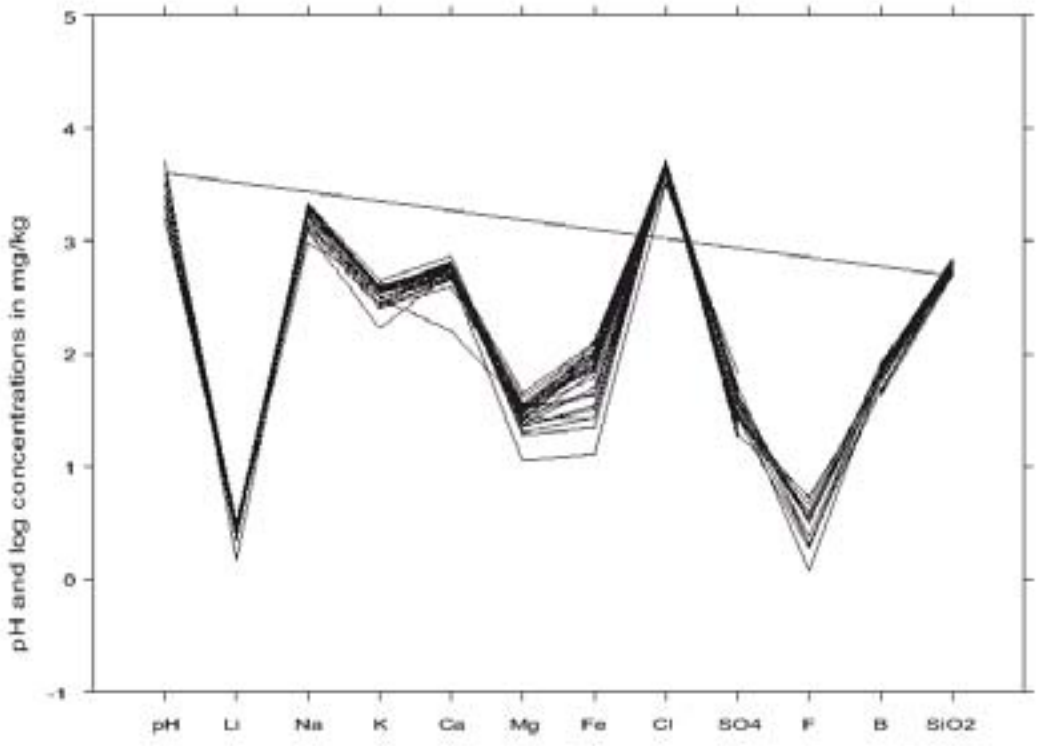

Figure 7. Schoeller plot of production waters from well 131

3.6. Production well 133

Well 133 was drilled almost parallel to well 131 and about 200 m further north (Figure 1), and its feed zone was at 900 m depth and 245ºC. This well has produced acid waters with pH values in the range of 3 to 3.6. The pH was variable in 1993 with higher (pH 3.2, 4.6) and lower values (3.0) alternating, increased to 3.6 in 1995 and has since decreased to 3.1 to 3.2 (Table I and Figure 8). The concentrations of Mg and Fe have more or less followed the pH, increasing when it decreased and vice

versa. Although not noted earlier the concentration of ammonia (NH4) in water increases when pH decreases because the NH4+ ion is less volatile than the gas. As noted above for well 131 waters, the more acid well 133 waters have higher enthalpy and are generally more saline although the range is small. Most constituents that are not pH or temperature sensitive, including Li, Na, Cl and B, have variations of less than 10%. There is some indication that F is high when Ca is low and vice versa suggesting equilibrium with fluorite (CaF2).

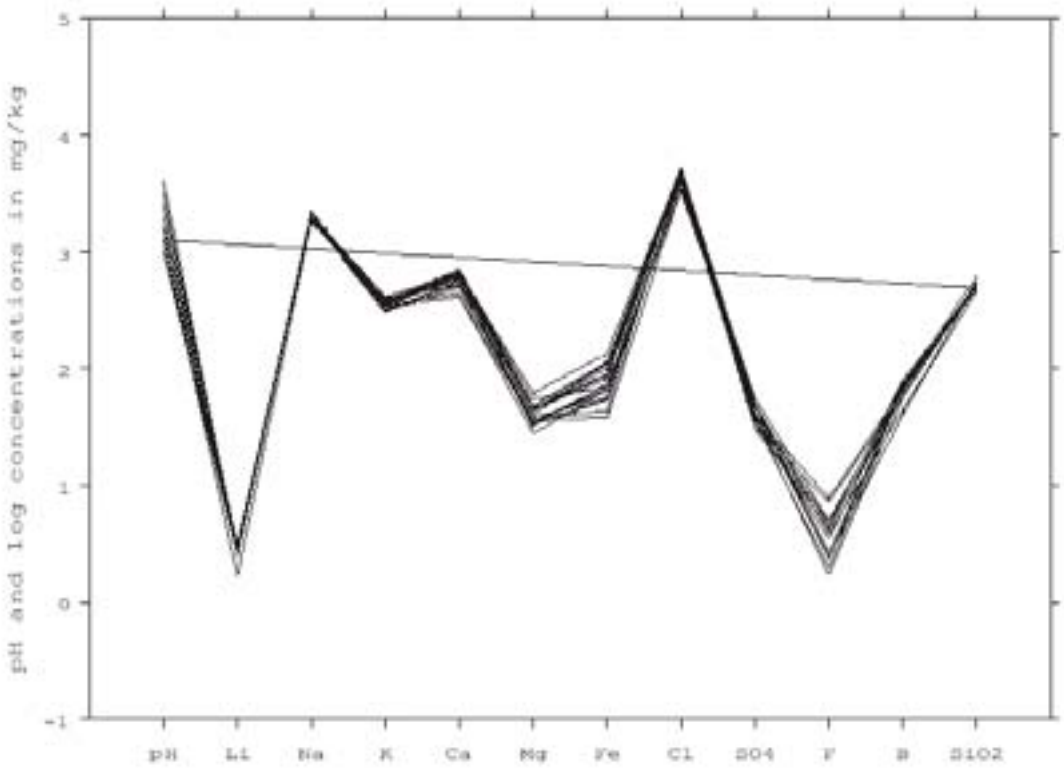

Figure 8. Schoeller plot of production waters from well 133.

As with other acid waters, reservoir temperatures (1994 and later) show good agreement between silica values and those derived from measured enthalpy, but Na/K values are high and scattered. Reservoir chloride concentrations varied from about 3500 mg/kg in late 1995 when the fluid was least acid to about 4200 mg/kg in 1998 (Table I). The chloride analyses from 1993 to early 1995 seem to vary unsystematically.

3.7. Production well 134

Well 134 was drilled from a pad across the stream from the power plant and deviated in the direction of the bottom of well 128 (Figure 1). The feed point is at 1080 m depth and the feed temperature was uncertain. Although near well 128 in plan the feed zone of well 134 is about 200 m deeper. This may explain the different chemistry of the produced water compared to earlier wells. The flashed water from this well is the most alkaline of any Onikobe production fluid with pH values from 7.2 to 8.2 (Table I and Figure 9). As a result, these waters have the lowest Ca, Mg, Fe, Mn and NH4 of any flashed production fluids. They also have the lowest Cl, B and SO4 and moderately high measured enthalpy. The only well with similar Na concentrations is well 128 and other major constituents are all

higher. These observations are counter to the correlation of higher enthalpy with lower pH and higher salinity observed in waters from wells 131 and 133.

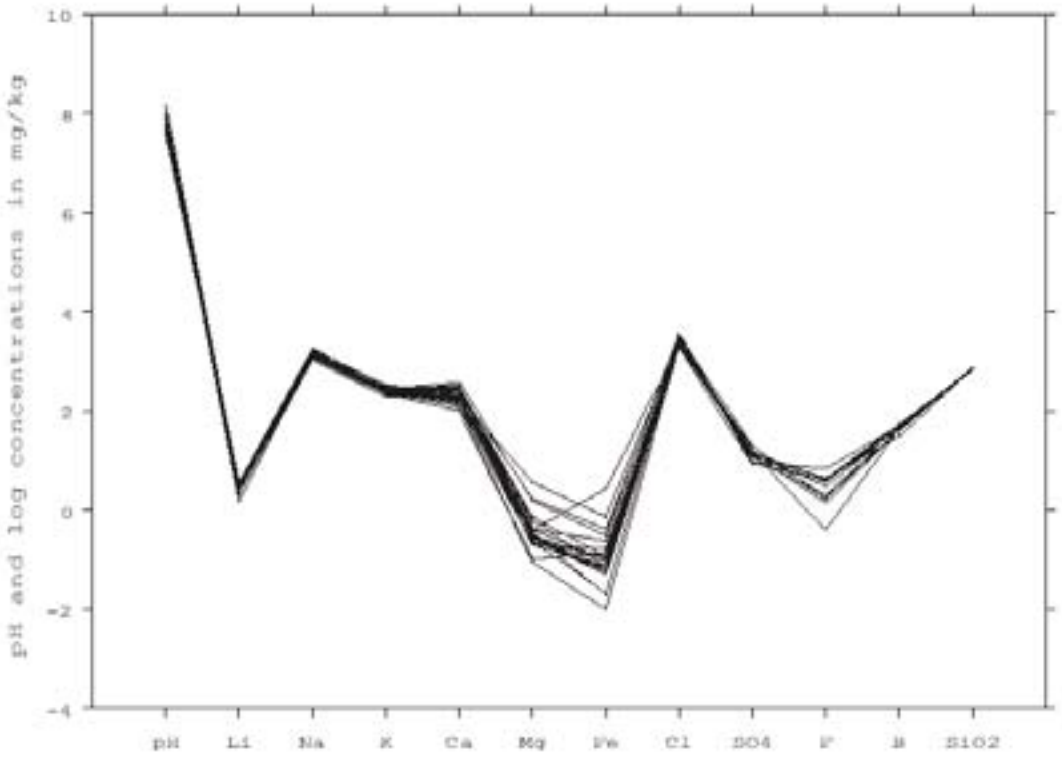

Figure 9. Schoeller plot of production waters from well 134.

As would be expected, geothermometer temperatures of well 134 waters are consistent with measured enthalpies except that Fournier and Giggenbach Na/K temperatures are consistently high by about 20 and 30ºC respectively and NKC temperatures tend to be low by 5 to 15ºC. This well is relatively far from the injection wells and its chloride has been reasonably constant with time.

4. The relations of pH, enthalpy, salinity and isotopes for deep production wells

In the discussions of individual well fluid chemistries, it has been suggested that there are systematic relationships among the salinity, acidity, enthalpy and time of production. In order to better investigate this matter, a series of graphs have been prepared that present chloride, pH and enthalpy data along with the evolution of these quantities with time for all production wells. Figure 10 shows chloride and pH. The well discharges divide into three groups: strongly acid waters with pH between 2.8 and 3.8 including all samples from wells 130, 131 and 133 and three samples from well 129; moderately acid waters including all samples from well 127 and the remaining two samples from well 129; and neutral to moderately alkaline waters including all waters from well 134 and some waters from wells 129, 132 and 135.

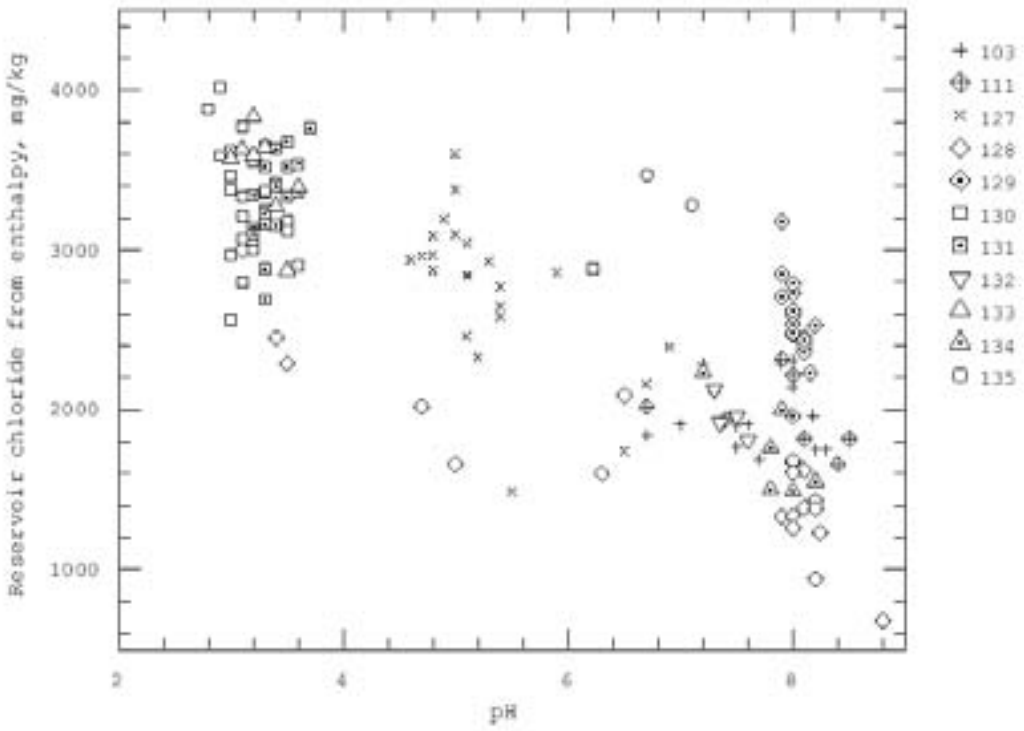

Figure 10. Reservoir chloride concentrations plotted against flashed pH values.

There is also a general correlation of chloride with pH (Figure 10). The strongly acid waters range in reservoir chloride (calculated using measured enthalpy) from 2600 ppm to 4500 ppm with most points between 3500 and 4300 ppm; That of the moderately acid group, from 1800 to 4000 ppm with most points between 3000 and 3600 ppm; And that of the neutral group, from 1500 to 3700 ppm with most points below 2500 ppm. Well 129 seems unusual in having both high pH and high chloride. The wide range in pH and chloride for samples from well 128 results from flow of shallow acid water into the well through a hole in the casing.

The overall correlation of reservoir chloride with measured enthalpy is not strong (Figure 11), but the higher chloride waters (generally those with low pH) have a wider range in enthalpy with individual wells (particularly 129, 130 and 131) showing lower enthalpy with higher chloride. Except for well 135 and shallow wells 103 and 111, the neutral wells have lower chloride and a narrower range in enthalpy.

The same separation is seen in the pH – enthalpy plot (Figure 12) with the high pH wells (except for shallow wells 103 and 111) falling between 800 and 1200 kJ/kg and acid wells between 900 and 1300.

The chloride-time plot (Figure 13) shows that for each well there is an increase in chloride with time but no single trend line for all wells. As in Figure 10, the most acid well waters (131, 133, and some 130 samples) form a group in which reservoir chloride increased from 3600 to 4200 ppm from 1991 to 1999. There is an intermediate group of waters from 127 and 135 and some from 130 that increased from 3100 to 3900 in the same period. Finally waters from well 128 (moderately acid) and most samples from well 134 (neutral) loosely form a group with increases from 1600-2000 ppm chloride in 1993–1994 to 2500-3200 in 1998–1999.

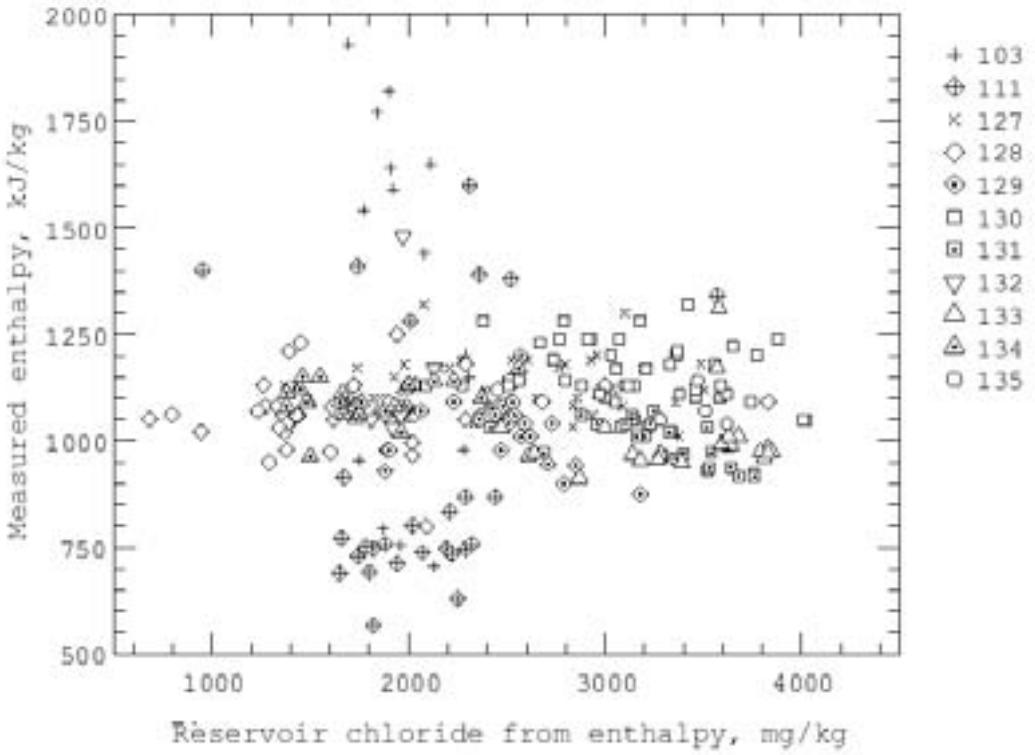

Figure 11. Measured enthalpy values plotted against reservoir chloride concentrations calculated using enthalpy.

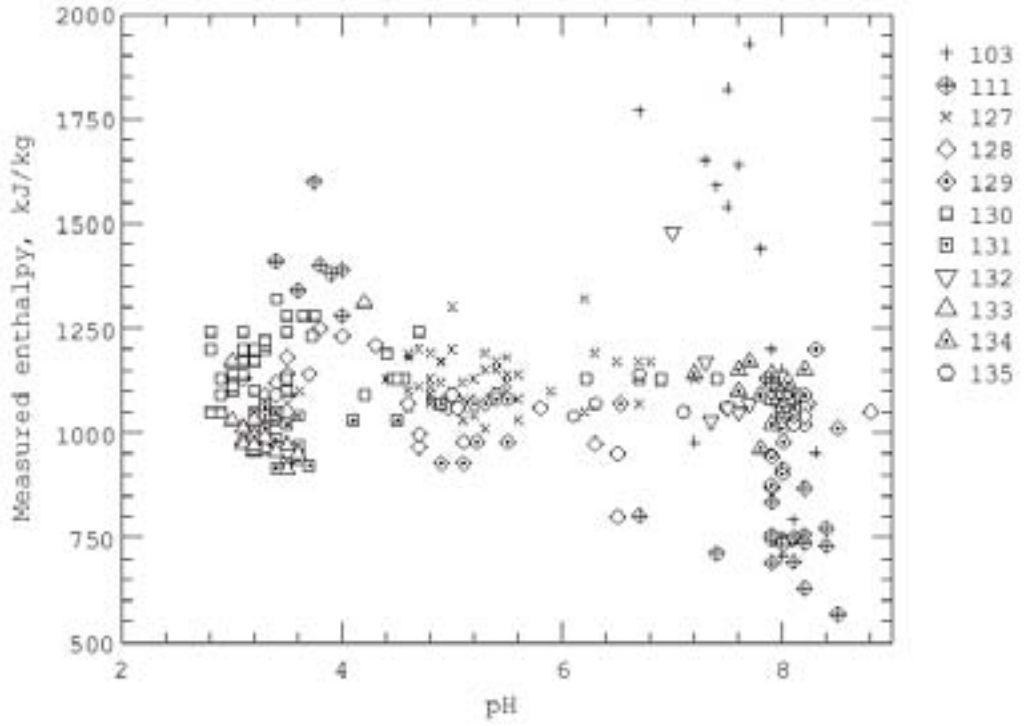

Figure 12 Measured enthalpy values against flashed water pH values.

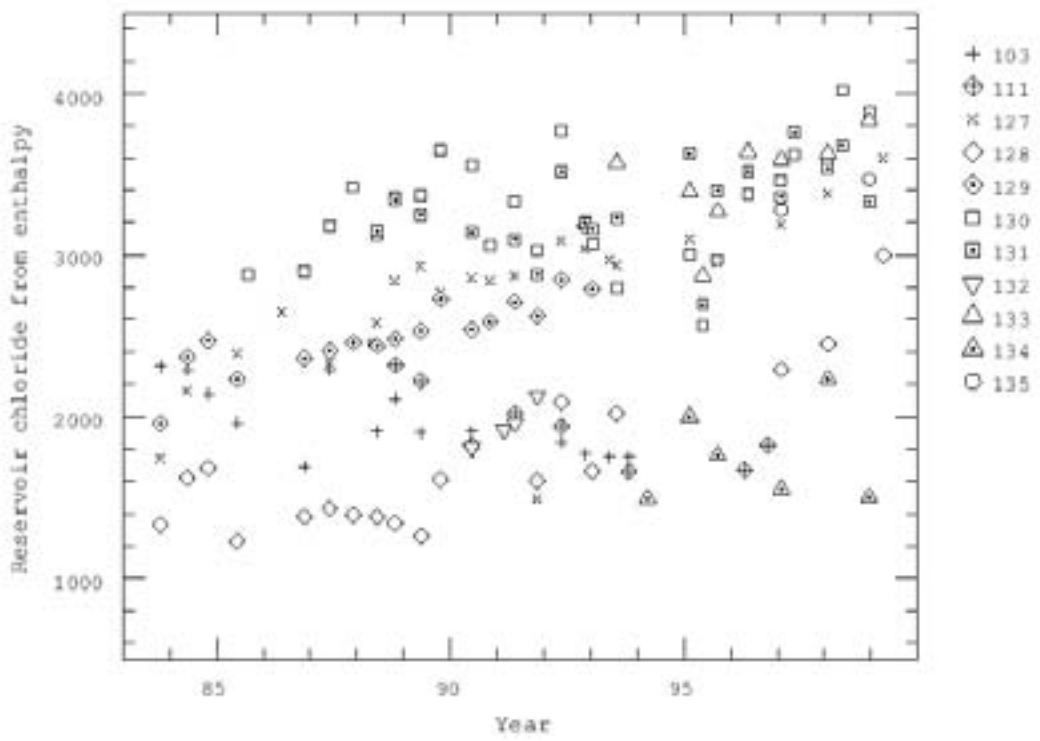

Figure 13. Changes with time of reservoir chloride concentrations (calculated using enthalpy).

These plots suggest two general processes are occurring in the reservoir but that parts of the reservoir are affected in different degrees by these processes. The general increase in chloride with time suggests that more saline water is being mixed into the original reservoir water throughout the field. This is probably from the recycling of injection water enriched in chloride from the separation of steam. This conclusion is supported by injection tests that showed connections between most injection wells and the producing wells.

In order to test whether the second reservoir water was acid, the change in pH with time is shown in Figure 14. Inspection shows that there is no large reservoir wide change in pH with time, but by different degrees several wells have decreased in pH with time. Acid fluids from wells 130 and 131 started near pH 5 and rapidly evolved to pH 3 in the early 1990s with the pH of 130 dropping and that of 131 rising slightly afterwards. The earlier discussed evolution of the pH of well 128 fluids from 8.1 in 1990 to 3.1 in 1999 can be followed in detail. The pH of well 127 fluids has changed from near 7 in 1982 to 4.6 in 1996 with a small increase thereafter. This decrease until the mid 1990s followed by a small increase occurred also with well 131 fluids. Perhaps because they are better buffered, the most acid (well 130) and most alkaline (wells 129 and 134) have shown very little change since 1990.

In a similar test to see whether the second reservoir water was higher or low in enthalpy, the measured enthalpy was plotted against time (Figure 15). Again individual wells showed patterns — most fluids from wells 127, 128, and 134 increased in enthalpy, most well 131 fluids decreased, and most well 130 and 133 fluids were nearly constant — but there was no reservoir-wide trend.

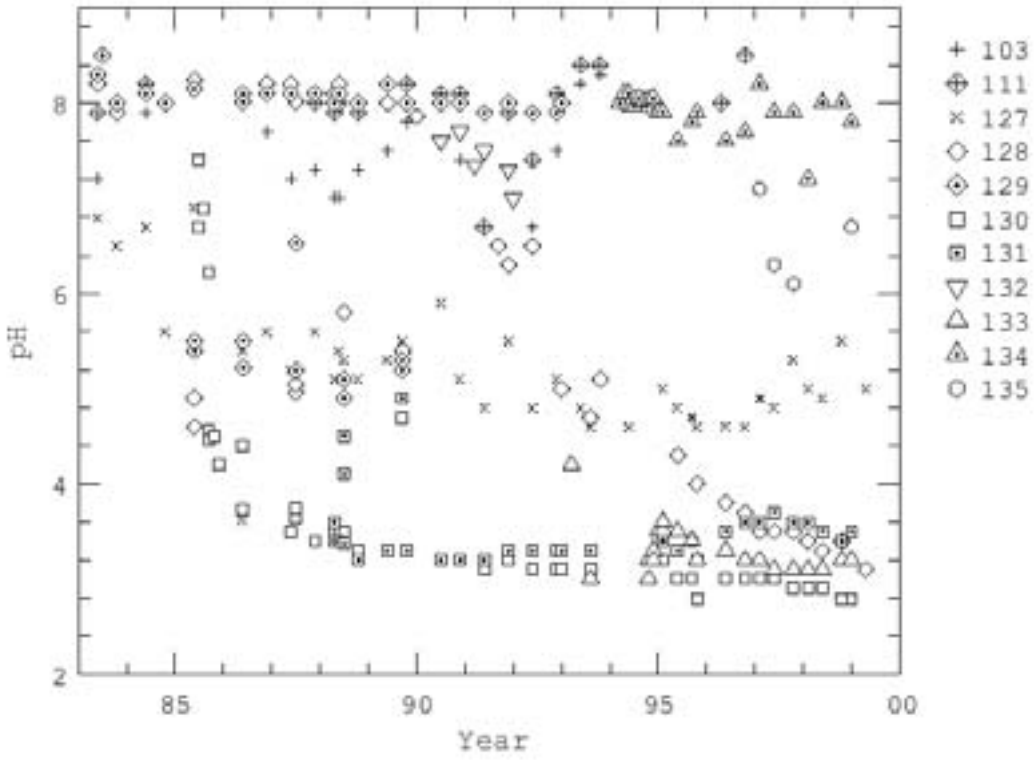

Figure 14. Changes with time of flashed water pH values.

The isotopic compositions of Onikobe production waters are shown in Figure 16. In general the acid well waters, especially those from wells 131 and 133, are isotopically heavy compared to the neutral well waters. Waters from well 130 which were near neutral in 1985, but became acid (near pH 3) before the first isotope analyses in 1988, show a wider range of isotopic compositions than other acid waters. Neutral waters from wells 128, 132, and 134 are generally isotopically light except for a few samples from 128, which have high $\delta^{18}O$ (to -4.8‰) but are similar to other neutral waters in δD. Strangely, neutral samples from wells 129 and 135 are isotopically heavy in both $\delta^{18}O$ and δD, similar to the acid waters. Waters from shallow wells 103 and 111 are neutral but occupy an isotopic middle ground (overlapping well 130 waters) between the deep acid and neutral waters. The general interpretation that the neutral waters are more closely related to meteoric waters and the acid waters to isotopically heavy volcanic water seems reasonable but the details need to be worked out.

From the data in Figures 10–16, it seems that there may be four waters involved in the Onikobe production. One is the neutral, relatively dilute, and medium to low enthalpy water produced from wells 129, 134 and 135. The second is the acid; medium enthalpy water produced from wells 131 and 133. The third is the acid, higher enthalpy water from well 130. And the last is recycled injectate that probably has somewhat different compositions depending on which wells feed which injectors, but causes an increase in salinity with time in most parts of the field. It is uncertain that the two acid waters are really distinct.

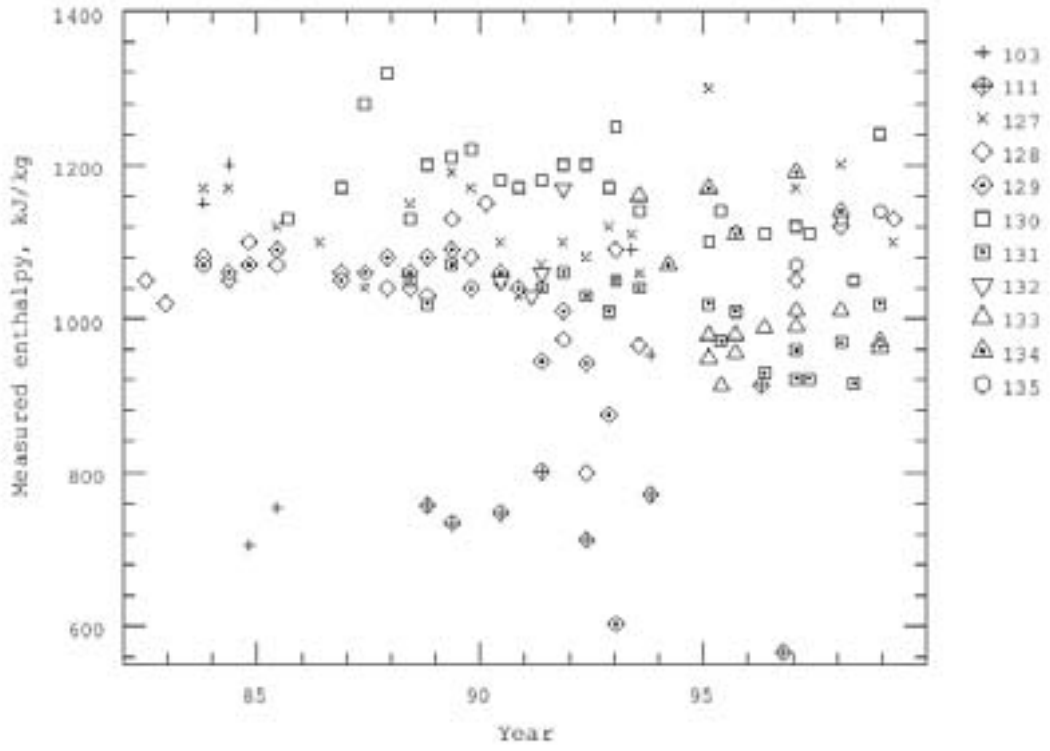

Figure 15. Changes with time of measured enthalpy values of Onikobe well waters.

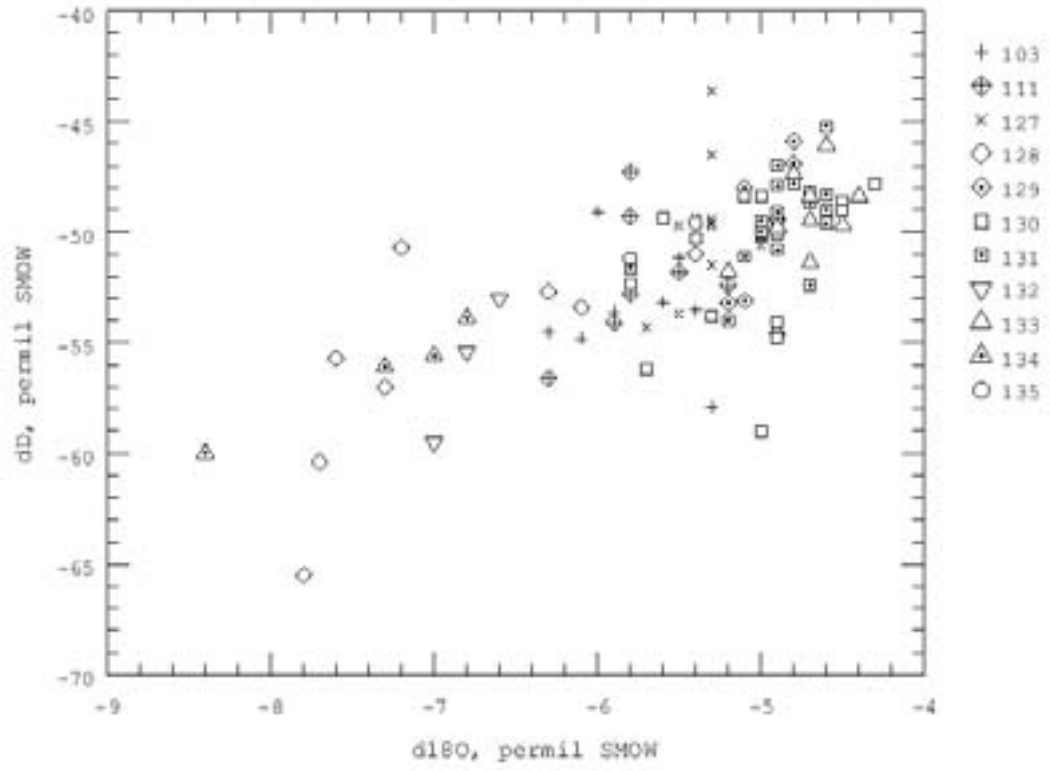

Figure 16. Total discharge isotopic composition of Onikobe well fluids.

5. Other geochemical methods applied to Onikobe fluids

Geochemical methods established in other fields have been applied to Onikobe production water and steam analyses (Tables I and II). Some of these methods use triangular graphs, which provide a way to compare the relative (but not absolute) amounts of three components. Multiplying one or more of the concentrations used in constructing these graphs moves the points but does not change their relative positions, so a line of points, possibly showing mixing, remains a line.

5.1. The Na-K-Mg geothermometer diagram

There are a number of graphical methods that have been devised to test the state of equilibration, the homogeneity and the origin of geothermal fluids. The most widely used of these methods is the Na-K-Mg triangular diagram from Werner Giggenbach (1988). Figure 17 is a version of this graph modified for Onikobe data. This diagram is intended to combine the Na/K geothermometer, which equilibrates relatively slowly with an Mg-K geothermometer (invented by Giggenbach), which should equilibrate more rapidly. When the method works as intended, compositions of equilibrated waters should fall on the line, which represents full equilibrium. Because the Giggenbach Na/K geothermometer gives unrealistically high temperatures for Onikobe (Table III), the equilibration line in Figure 17 uses the more realistic Nieva Na/K geothermometer (Nieva and Nieva, 1987). On this graph the indicated Na/K temperatures cluster around 260ºC and the points group along the 260ºC line according to their pH suggesting that Mg-K equilibrium did not occur.

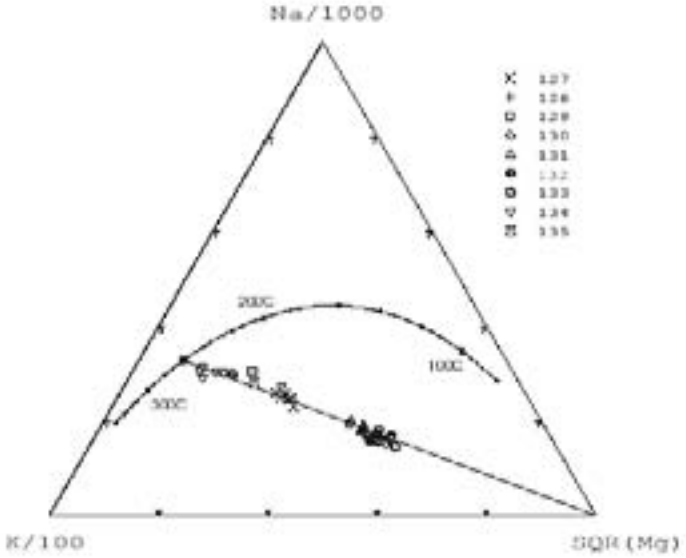

Figure 17. The combined Na/K and K-Mg geothermometer diagram using Nieva Na/K equation applied to Onikobe waters (see text for discussions).

5.2. The Cl-SO_4-HCO_3 and N_2-He-Ar diagrams

Other widely used Giggenbach graphs compare the concentrations of Cl, SO4, and HCO3 with the object of indicating the extent of alteration of volcanic and near surface waters towards mature geothermal waters and compare gas components N2, He and Ar to indicate the volcanic or atmospheric origin of reservoir gases (Giggenbach, 1991). As useful as these methods are when

applied to high temperature springs and newly produced wells, they gave very little information when applied to Onikobe fluids. All points on the Cl-SO4-HCO3 graph fell at the Cl vertex. This lack of significant SO4 and HCO3 in Onikobe waters suggests that the acidity does not originate from SO2 and confirms the generally high acidity in most waters (acidity is incompatible with HCO3).

Similarly, all points on the N2-He-Ar graph fell between the compositions of air and gases in air saturated water (ASW). The points with air composition may result from air entering the sample bottle during steam collection, but could also enter the reservoir during injection. Similarly injection of water from the cooling tower could introduce some ASW gases. It is again notable that, as with the Cl-SO4-CO2 graph, there is no evidence of volcanic components in the Onikobe fluids.

5.3. The Cl-B-SO_4 diagram

In order to show the homogeneity of the Onikobe waters, Figure 18 was constructed showing relative amounts of Cl, B and SO4 in a graph introduced by Ellis (1970). In neutral, well-mixed geothermal waters both boron and chloride are conservative elements, neither reacting with rock minerals or separating during boiling or condensation processes, so that their ratio may be used to characterize waters with the same origin. However, the wide range of Cl/B ratios in Onikobe waters shows that, at low pH, these elements do not both act conservatively. In fact boron is volatile in low pH waters because it forms boric acid, which is soluble in steam. In Figure 18 neutral to alkaline waters (from wells 134 and 132) have low Cl/B ratios near 55:1 and the acid waters (from wells 130, 131 and 133) have high ratios near 90:1, with other wells intermediate in Cl/B. Surprisingly one of the well 135 waters with neutral pH also has a high Cl/B ratio.

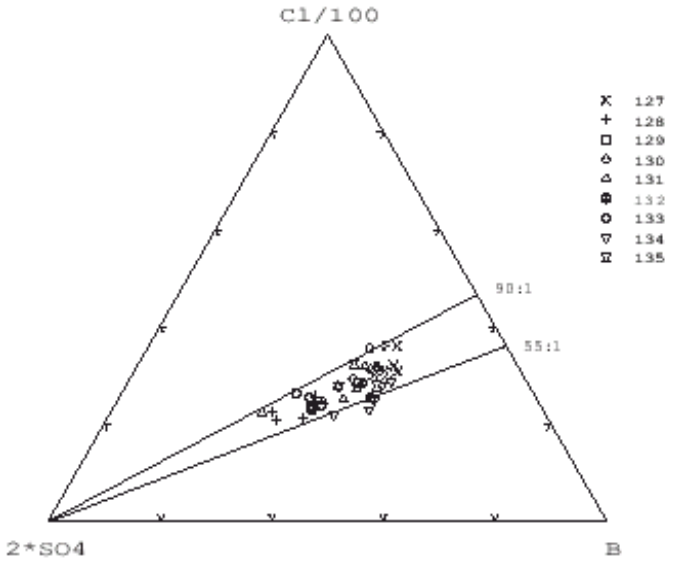

Figure 18. The Cl-SO4-B triangular diagram applied to Onikobe production waters. Note the clustering of points for wells and groups of wells.

5.4. A pH-Mg-Fe diagram

The solution of Mg and Fe by acid waters was described earlier as occurring first in the reservoir (where Mg minerals are found) and then in the well casing. Figure 19 shows that neutral waters (from wells 129, 134 and 135) have very high Mg/Fe ratios, slightly acid waters (from wells 127 and 128)

have lower Mg/Fe ratios (with Mg>Fe), and highly acid waters (from wells 130, 131 and 133) have low Mg/Fe ratios (with Fe>Mg). This graph suggests that for moderately low pH fluids reaction occurs first with rock minerals then for very low pH fluids continues in casings.

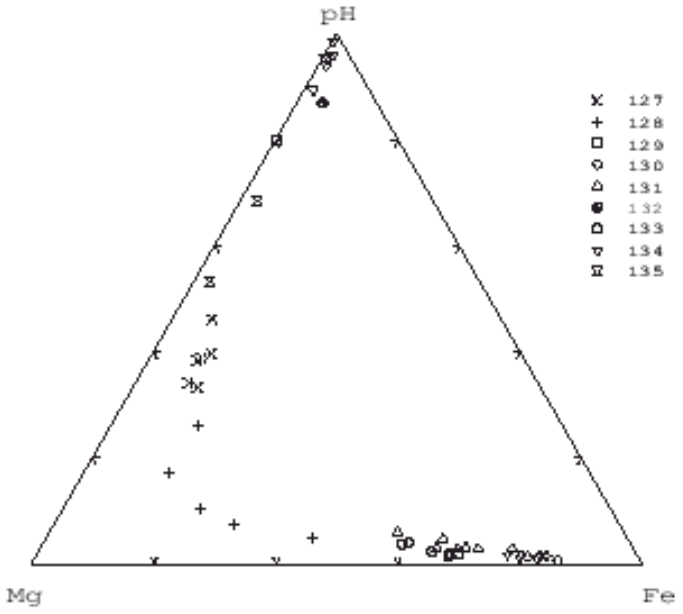

Figure 19. A pH-Mg-Fe triangular diagram applied to Onikobe production waters. Note the progressive increase in the Fe/Mg ratio with decrease in pH.

5.5. The D'Amore gas grid diagram

In Figure 20, the gas geothermometer developed by Franco D'Amore (D'Amore and Truesdell, 1985) is applied to Onikobe gases. In this diagram the "s-shaped" curves represent reservoir temperatures from 125 to 350ºC and the other curves represent values of "Y" which approximate the ratio of reservoir steam to total fluid and range from 1 to –0.01 with negative values interpreted as the fraction of gas depletion resulting from boiling. As would be expected from the good agreement of measured, geothermometer and enthalpy-derived reservoir temperatures, there is little evidence of excess steam in the Onikobe reservoir. In fact only two samples (from well 127) showed positive y values and both of these indicated only about 0.1 % excess steam. The rest of the points on the diagram have negative y values, most indicating about 1% gas loss. The temperatures, ranging from 230 to 270ºC (with a few higher temperature outliers), approximate the measured and otherwise indicated values. Not all Onikobe samples could be represented on the diagram possibly because of their very low gas content.

The gas grid diagram shows that most production fluids are highly depleted in gas. This would be expected for waters that have repeatedly passed through steam separators and been reinjected into the reservoir. Thus the gas behavior confirms the indication from the increases in salinity that one of the reservoir fluids is recycled injectate.

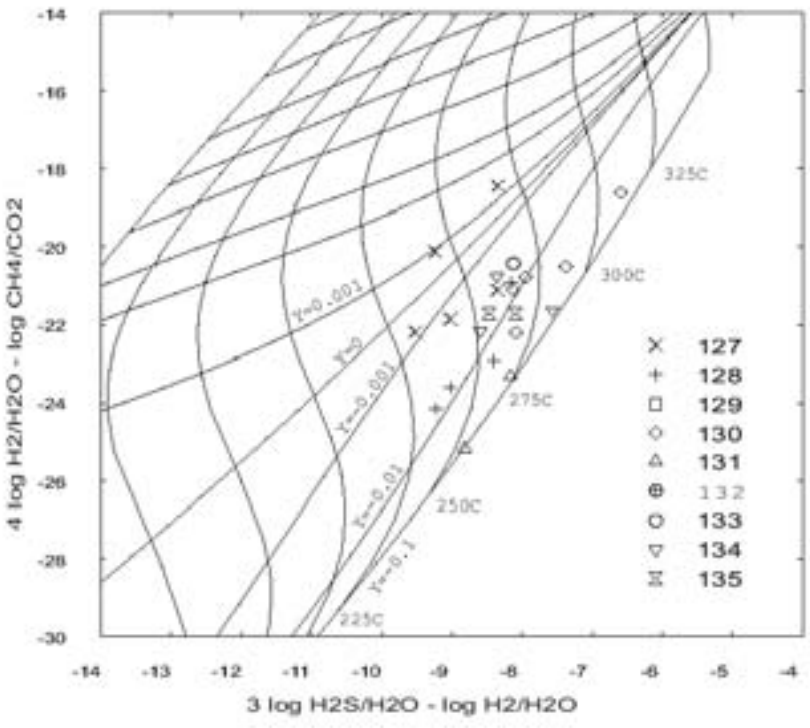

Figure 20. The Dámore gas geothermometer 'grid' diagram applied to Onikobe production steam samples. Note that almost all points indicate negative values of 'y' indicating boiling of gas-depleted waters.

6. The origin of acidity at Onikobe

Acid waters in geothermal reservoirs can come from two directions, either from below as incompletely neutralized volcanic fluids, or from above as a result of down flow of acid sulfate waters formed by atmospheric oxidation of H2S carried into the aerated zone by up flowing steam. For the andesitic volcanism that occurs behind a subduction zone as found (for example) in Japan and the Philippines, both kinds of acidity are possible. In general if the acid water has high SO4/Cl ratio and the salinity is lower than neutral waters in the same reservoir, then the most likely origin is from acid sulfate waters infiltrating the reservoir from above. If the reverse occurs and the acid waters have higher chloride (and sulfate) than the neutral waters, then the acid waters result from incomplete neutralization of HCl and H2SO4 originating from HCl and SO2 carried in superheated volcanic steam.

If HCl gas of volcanic origin enters a geothermal reservoir the reservoir water may contain "excess" chloride defined as chloride greater than that required to electrically balance all the positively charged ions in solution without counting hydrogen ion or abnormal amounts of Mg, Fe and Mn that may have been dissolved from minerals and well casing by the acid (Truesdell, 1991). In order to test this possibilities for Onikobe waters, a group of neutral and acid Onikobe waters are presented in Table IV with the calculated sum of the milliequivalents of major cations, the sums of the milliequivalents of Mg, Fe and Mn, and the milliequivalents of chloride. Clearly there is a good balance of chloride and cations in the average neutral water, but a large excess of milliequivalents of chloride in the acid waters. This is proof that at least some of the acidity entered the acid Onikobe waters as HCl. Part of the acidity may have come from sulphuric acid (of volcanic or surface origin) but not enough to affect the chloride "excess". In general the ratio of chloride to sulfate in Onikobe waters is relatively high making it unlikely that acid entered the waters as sulfuric acid of deep or shallow origin.

7. Summary of the geochemistry of Onikobe production fluids

This investigation has shown that the production fluids at Onikobe vary widely in chemical composition and concentration but have certain characteristics in common. These characteristics include a rather narrow range of reservoir temperatures from 230 to 255ºC measured temperatures; 225 to 280ºC calculated from enthalpy assuming no excess steam; 241 to 270ºC calculated from the quartz saturation geothermometer and 253 to 280ºC calculated from the most reasonable Na/K geothermometer (Table III). The agreement between enthalpy derived and other temperatures suggests that there is little excess steam as do inlet vapour fraction (IVF) values, which are less than 0.1 for almost all samples (Table III).

The largest variations in concentration are in pH and acid sensitive constituents including Fe, Mg, Ca which are dissolved from reservoir rocks and casings by low pH waters and other constituents with volatility depending on pH (NH4, HBO3). The pH varies from 2.8 to 8 and Fe varies from 0.01 to 371 ppm. The variation of other acid sensitive constituents although not as large are also significant. The source of the acid is not yet understood. The large "chloride excess" and the strong correlation of low pH with high chloride indicate that the acid enters the water as HCl, but some SO4 acidity could have been removed by reaction with plagioclase to form anhydrite.

There is a consistent increase in salinity with time along with indications that the waters are gas depleted. These observations are interpreted as showing that injected waters enriched in salts and depleted in gases are contributing to production waters. The acid reservoir seems to be limited to moderate depths in the middle of the drilled area. Drilling either to the NW where wells 134, 135 and 128 (before its casing leak) produced neutral waters or to the S where well 129 produces neutral waters would seem to be the best strategy. The relative homogeneity of the neutral waters suggests that there is a large reservoir of these fluids.

8. Discussion of the use of acid waters in geothermal exploitation

Abe (1993) has discussed the necessity of using steam flashed from acid production waters at Onikobe and the methods developed to extend service life of casings and surface facilities. Acid fluids have been used because zones with neutral fluid explored before 1993 did not have adequate permeability to maintain plant output (12.5 MW). Stainless steel is used in separators and fibreglass-reinforced plastic in surface piping. Using this equipment it is proposed that waters with pH of 3.4 and above can safely be exploited to generate electricity. Analyses in this paper show that although initial deep production waters from well 130 sampled in 1988 were somewhat less acid (pH 3.4) than that sampled later (pH 3.1 in 1993), total iron in both samples was about 150 ppm. A deposit of lead sulphide was found on the inside of casings and liners for surface pipes. It is suggested that this deposit prevented corrosion, but the consistent high concentrations of total iron and the thinning observed in the liners suggests otherwise. The increase in total iron in well 130 waters from 150 ppm in1993 when pH was 3.4 to between 215 to 370 ppm in 1998 when pH was between 2.9 and 2.8 indicates corrosion accelerated. Mineralogical studies showed that cuttings from zones producing acid waters contained pyrophyllite and those from neutral water zones contained sericite, chlorite and calcite.

Table IV. Composition (in milliequivalents) of the sums of cations (w/o H+, Mg, Fe and Mn), the sums of Mg, Fe and Mn with Chloride fro high and low pH waters.

			Milliequivalents of		
Well	Date	pH	Cations	Mg+Fe+Mn	Cl
134	1995-01-11	7.9	83.8	0.0247	81.0
134	1995-02-14	7.9	84.0	0.0608	81.2
134	1995-05-25	7.6	70.8	0.1490	59.2
134	1995-09-21	7.8	77.2	0.0706	71.9
134	1995-10-18	7.9	86.7	0.0683	87.4
134	1996-05-15	7.6	96.6	0.0668	95.9
134	1996-10-17	7.7	95.5	0.1880	104.0
134	1997-01-31	8.2	64.8	0.0285	64.0
134	1997-05-14	7.9	80.3	0.0738	79.0
134	1997-10-13	7.9	80.0	0.1730	79.0
134	1998-01-29	7.2	89.4	0.1340	90.8
134	1998-05-20	8.0	75.5	0.0659	70.5
134	1998-10-12	8.0	71.2	0.3300	67.7
134	1998-12-15	7.8	62.1	0.0579	60.9
Averages			79.9	0.1060	78.0
130	1997-10-15	2.9	131.0	9.59	150.0
130	1998-01-29	2.9	132.0	11.70	148.0
130	1998-05-20	2.9	141.0	16.10	161.0
130	1998-10-12	2.8	136.0	17.60	161.0
130	1998-12-15	2.8	139.0	18.80	159.0
131	1988-04-25	3.6	119.0	6.69	126.0
131	1988-04-27	3.4	75.9	4.31	120.0
131	1988-06-07	3.4	94.0	6.74	126.0
131	1988-07-05	4.5	88.9	1.38	93.1
131	1988-07-05	4.1	81.0	6.01	90.6
131	1988-07-12	3.3	118.0	8.18	129.0
131	1988-10-25	3.2	78.9	7.67	133.0
131	1989-05-15	3.3	105.0	6.94	129.0
131	1989-09-03	4.9	92.4	3.88	96.5
Averages			109.4	8.97	130.2

Other geothermal developments have used acid waters to produce steam. PNOC in the Philippines has used waters with pH as low as 3.4 to generate steam with good results although surface pipes have needed periodic replacement (M. Ramos-Candelaria, pers. com.1995). As more volcanic geothermal fields are exploited for power, the necessity of developing technology for utilizing acidic fluids will grow. Research into materials and techniques for safe utilization of acid waters should be pursued.

REFERENCES

[1] ABE, M., (1993) Long term use of acidic reservoir at Onikobe geothermal power plant: Proc. 15th NZ Geothermal Workshop, p. 5–10.

[2] ELLIS, A.J., (1970) Quantitative interpretation of chemical characteristics of hydrothermal systems: Geothermics v. 2, p.516–528.

[3] FOURNIER, R.O. (1979) A revised equation for the Na-K geothermometer. Geothermal Res. Council Trans., 3, 221–224.

[4] FOURNIER, R.O. and POTTER, R.W. II. (1982) An equation correlating the solubility of quartz in water from 25°C to 900°C at pressures up to 10,000 bars. *Geochim. Cosmochim. Acta, 46,* 1969–1974.

[5] FOURNIER, R.O. and TRUESDELL, A. H. (1973) An empirical Na-K-Ca geothermometer for natural waters. *Geochim. Cosmochim. Acta, 37,* 1255–1275.

[6] GIGGENBACH, W.F. (1988) Geothermal solute equilibria. Derivation of Na-K-Ca-Mg geoindicators. Geochim. Cosmochim. Acta, 52, 2749–2765.

[7] GIGGENBACH, W.F. (1991) Chemical techniques in geothermal exploration. Chapter 5 in Application of Geochemistry in Geothermal Reservoir Development. F. D'Amore, ed., UNITAR/UNDP Rome 1991, p. 119–144.

[8] NIEVA, D. and NIEVA, R. (1987) Developments in geothermal energy in Mexico, part 12. A cationic geothermometer for prospecting of geothermal resources. Heat Recovery Systems Chapt. 7, p. 243–258.

[9] TRUESDELL, A.H. (1975) Summary of section III - Geochemical techniques in exploration. Proceedings, Second U.N. Symp. on the Development and Use of Geothermal Resources, San Francisco v.1 liii–lxxix

[10] TRUESDELL, A.H., 1991, Origins of acid fluids in geothermal systems: Geothermal Resources Council Trans., v. 15, p. 289–296.

LIST OF PRINCIPAL SCIENTIFIC INVESTIGATORS

Abidin, Z.
Center for Application of Isotopes & Radiation
National Atomic Energy Agency
Jln.Cinere Pasar Jumat
P.O.Box 7002, JKSKL, Jakarta 12070
Indonesia

Ferrer, H.
PNOC Energy Development Corporation
PNPC Complex, Merritt Road, Fort Bonifacio,
Makati City
Philippines

Karpov, G.
Institute of Volcanology
Piyp Blvd 9, Petropavlovsk-Kamchatsky 683006
Russian Federation

Matsuda, K.
West Japan Engineering Consultants, Inc.
Geothermal Dept.
2-1-82 Watanabe-dori, Chuo-ku
Fukuoka
Japan

Pang, Z.
Institute of Geology and geophysics
Chinese Academy of Sciences
Beijing, 100029
China

Panichi, C.
Istituto Inaternazionale per le Ricerche Geotermiche
Piazza Solferino 2, 56128 Pisa
Italy

Simsek, S.
Hacettepe University
International Research & Application Center for
Karst Water Resources
06532 Beytepe, Ankara
Turkey

Tello H. E.
Gerencia de Proyectos Geotermoelectricos
Alejandro Volta No.655
Col.Electricistas C.P. 58290
Morelia, Michoacan
Mexico

Truesdell, A.
Center for Isotope Geochemistry
MS 70A-4418
Lawrence Berkeley National Laboratory
Berkeley, CA 94720
United States of America

Zhou, W.
East China Geological Institute
Linchuan, Jiangxi Province, 344000
China

IAEA PUBLICATIONS
ON THE HYDROLOGICAL AND GEOCHEMICAL STUDIES
OF GEOTHERMAL SYSTEMS

1992 Geothermal Investigations with Isotope and Geochemical Techniques in Latin America (IAEA-TECDOC-641)

1995 Isotope and Geochemical Techniques Applied to Geothermal Investigations (IAEA-TECDOC-788)

2000 Isotopic and Chemical Techniques in Geothermal Exploration, Development and Use

2004 Application of Radiotracers in Industry – A Guidebook (Technical Reports Series No. 423)